

Antibody-based approaches to modulate immune response

Aina Segués Cisteró

© 2023 Aina Segués Cisteró

All rights reserved. Published papers were reprinted in this publication under CC license. No parts of this thesis may be reproduced or transmitted in any form or by any means without prior permission of the author.

ISBN: 978-94-6469-320-1

The research described in this thesis was performed at Aduro Biotech Europe B.V., Oss, The Netherlands; School of Biology, University of Edinburgh, United Kingdom; Department of Immunology and Infection, School of Biological Sciences, University of Edinburgh, United Kingdom and *Centro de Investigación Médica Aplicada (CIMA)* and *Universidad de Navarra*, Pamplona, Spain.

Cover design: Aina Segués Cisteró conceives the idea and makes the final layout drawing the elements. Curve lines, in a minimalist design, mean the standard structure of an immunoglobulin. The antibody is the leading element of this thesis. The circles represent T cells, with special regard with T regulatory cells.

Layout and design: Aina Segués Cisteró

Printing: Proefschrift Maken | www.proefschriftmaken.nl/en/

Printing of this thesis was financially supported by Infection & Immunity Utrecht and by the Immunology Section, Department of Biomolecular Health Science, Faculty of Veterinary Medicine, Utrecht University.

Antibody-based approaches to modulate immune response

Antistof-gebaseerde benaderingen om de immuunrespons te moduleren

(met een samenvatting in het Nederlands)

Proefschrift

ter verkrijging van de graad van doctor aan de
Universiteit Utrecht
op gezag van de
rector magnificus, prof.dr. H.R.B.M. Kummeling,
ingevolge het besluit van het college voor promoties
in het openbaar te verdedigen op 13 juni 2023 des middags te 2.15 uur

door

Aina Segués Cisteró

geboren op 29 december 1995
te SANT RAMON (LLEIDA), Spanje

Promotoren:

Prof. dr. E.J.A.M. Sijts

Prof. dr. F. Broere

Beoordelingscommissie:

Dr. ir. B.J. Bosch

Prof. dr. W. van Eden

Prof. dr. C. van Els

Prof. dr. J. Garssen

Prof. dr. J. de Vries

This thesis was accomplished with financial support from the European Union's Horizon 2020 research and innovation programme under the Marie Skłodowska-Curie grant agreement [grant numbers 765394, 2018].

Table of contents

Chapter 1:	General introduction	7
Chapter 2:	Opportunities and challenges of bi-specific antibodies	33
Chapter 3:	Shortened hinge design of Fab x sdAb-Fc bispecific antibodies enhances redirected T-cell killing of tumor cells	65
Chapter 4:	Mouse IgG2a isotype therapeutic antibodies elicit superior tumor growth control compared to mIgG1 or mIgE	99
Chapter 5:	Generation and characterization of novel co-stimulatory anti-mouse TNFR2 antibodies	130
Chapter 6:	TNFR2 antibodies target Tregs and CD4 ⁺ T effector cells <i>in vivo</i>	173
Chapter 7:	General discussion	198
Chapter 8:	Summary in English	214
	Nederlandse Samenvatting	217
Appendix		221
	<i>Acknowledgements</i>	222
	<i>Curriculum Vitae</i>	227
	<i>List of publications</i>	228



1

General introduction

Preface

Over the recent years, the possibilities for immune therapy of cancer patients have considerably improved. For example, adoptive transfer of tumor-specific CD8⁺ T cells, and anti-tumor immunizations were shown to have the potency to prolong patients' life. However, it was also found that the intra-tumoral immune suppressive environment may hamper the efficacy of tumor immune therapy. Treatment with "check-point inhibitors", such as with the T regulatory cells (Tregs) targeting Cytotoxic T-Lymphocyte Associated Protein 4 (CTLA-4) antagonist Ipilimumab, successfully counteracts these immune-suppressive mechanisms, but is accompanied by severe side effects.

To this end, one of the major strategies gaining importance in clinical trials are monoclonal antibodies. They achieve their therapeutic effect through different mechanisms such as ligand competition, interfering with the downstream signal upon binding, and also differential mediated effector response through isotype choice. Furthermore, bispecific antibodies, binding simultaneously to two different types of antigen or different epitopes might circumvent off-target specificity issues in healthy tissues that monoclonal antibodies arise.

Tregs are a key cell population modulating and suppressing the effector immune response. Current checkpoint-targeted therapies have severe side effects, due to a relative lack of specificity of administered antibodies for the targeted T cell populations. For example, Tregs suppress intratumoral immune effector functions and therefore are an excellent target for tumor therapies. However, there are no unique Treg markers, since receptors expressed on Tregs can also be expressed by other leukocytes. Consequently, Treg-targeted monoclonals also affect other immune cell populations. In order to diminish therapy-associated side effects, we focused on a novel antibody-based approach to target Tumor Necrosis Factor Receptor 2 (TNFR2), a receptor which has recently gained importance in Treg biology due to its expression role on Tregs.

The general aim of this thesis was to evaluate the potential roles of targeting different receptors and different Fc-isotypes while focusing on the generation and development of novel antibodies aiming to target Tregs.

Monoclonal antibodies and isotype formats:

Antibodies (Abs) are glycoproteins of the immunoglobulin (Ig) superfamily. They can be anchored on the B cell membrane and act as a B cell receptor, or they can be released into the circulation and lymph by mature B cells known as plasma cells. Secreted antibodies provide humoral immunity by recognising and promoting killing of pathogens^{1,2}. The shared structure the different antibodies is a basic structure consisting of two heavy and two light chains connected by interchain disulfide bonds. In humans, there are two types of light chain - κ and λ – whereas heavy chains can be classified into five: μ , δ , γ , ϵ and α . The type of heavy chain defines the class of immunoglobulin: IgM, IgD, IgG, IgE and IgA³.

In 1975, Kohler and Milstein were the first to describe the production of murine mAbs from hybridomas¹. The concept of hybridomas, antibody producing B-cell fused with immortal myeloma cells, revolutionized the production and development of mAbs. The first therapeutic mAb OrthoClone OKT3 was generated in 1984 and approved in clinical use in 1986 for the treatment of transplant rejection⁴. Since then, more than 570 therapeutic mAbs have been studied in clinical trials and FDA has approved more than 80 mAbs for clinical application⁵.

Therapeutic monoclonal antibodies (mAbs) are often of the IgG isotype. IgG antibodies are the most prevalent in human serum. IgGs are large molecules (approximately 150kDa) composed of two heavy and two light chains. Each heavy chain has two regions: constant (C_H) and variable (V_H). The light chain has two domains: constant (C_L) and variable (V_L)⁶. The fragment antigen binding domain (Fab) is formed by the V_H , C_{H1} and V_L , C_L regions combined to produce the antigen binding site, whereas the fragment crystallizable (Fc) domain responsible for effector action is made up of two constant domains. The Y-shape of an immunoglobulin can be cleaved into three fragments by

papain resulting into three pieces: two Fab fragments and one Fc fragment⁷ (Fig. 1).

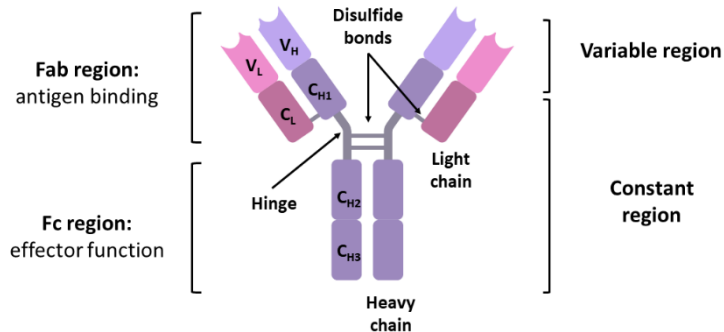


Figure 1. Scheme of IgG structure. Antibody consisting of two heavy chains (purple) and two light chains (pink) folded into constant and variable domains. Each light chain and the variable heavy and constant heavy chain 1 form an antigen binding site (Fab regions). Antigen binding sites are each formed by the variable regions of a light chain and a heavy chain (Fab regions). The tail (Fc region) is formed by the constant regions of the heavy chains. A flexible hinge region links the two Fab regions and Fc improving the ability of the Ab to bind antigen. Chains are bonded with disulfide bonds. Fab: fragment binding site, Fc: fragment crystallizable, V_L: variable light, C_L: constant light V_H: variable heavy, C_H: constant heavy. Created with Biorender.

While the variable domains of a mAb dictate its specificity and selectivity, the Fc region provides significant functionality to the molecule. Upon binding to Fc receptors, an effector response might be mediated depending on the isotype: antibody-dependent cell-mediated cytotoxicity (ADCC), antibody-dependent cell-mediated phagocytosis (ADCP), and/or complement dependent cytotoxicity (CDC). Furthermore, the Fc region can interact with the neonatal Fc receptor (FcRn), resulting in a longer half-life⁸.

IgG Fc portion binds to Fc gamma receptor (FcγR). FcγRs are functionally categorized into activating or inhibitory receptors based on the presence of an intracellular immunoreceptor tyrosine-based activation or inhibitory motif, ITAM or ITIM respectively. IgG immune complexes that engage activating or inhibitory FcγRs trigger immunostimulatory or immunosuppressive signals, which influence the outcome of IgG-mediated inflammation and immunity, respectively. The immune response is influenced by the FcγR activating/inhibitory ratio⁹.

In humans, there are three classes of activating FcγR depending on the affinity of the receptor. The high-affinity receptor is FcγRI (CD64), and the low-affinity receptors are FcγRIIa/c (CD32) and FcγRIIIa/b (CD16). These are expressed in diverse combinations on the surface membrane of different immune cells¹⁰. FcγRI is found on macrophages, neutrophils, eosinophils and dendritic cells¹¹. FcγRII is expressed by macrophages, neutrophils, eosinophils, platelets, Langerhans cells and conventional but not plasmacytoid dendritic cells. FcγRIII is found on natural killer (NK) cells and macrophages. The inhibitory FcγRIIb is located on B cells, mast cells, macrophages, eosinophils and dendritic cells¹². Similarly, mice have three activating receptors with an ITAM motif (FcγRIa, FcγRIII, and FcγRIV) and one inhibitory FcγR with an ITIM motif (FcγRIIb). These receptors are orthologs of the human FcγRI, FcγRIIa, FcγRIIIa, and FcγRIIb, respectively¹³ (Table 1).

Table 1. Human and mice FcγR. Type of FcγR categorized into activating or inhibitory signalling and cell populations with the respective expression. A/I: Activating or inhibitory receptor, NK: Natural killer.

Human FcγR	A/I	Cell types	Mouse FcγR
I (CD64)	A	macrophages, neutrophils, eosinophils and dendritic cells	I
IIa/c (CD32a/c)	A	Myeloid cells, neutrophils, eosinophils, platelets, Langerhans cells, NK cells	III
IIb (CD32b)	I	B cells, mast cells, myeloid cells, dendritic cells	IIb
IIIa/b (CD16)	A	NK cells, macrophages	IV

While the Fc region of mAb mediates immune effector functions for therapeutic applications, in some therapeutic approaches a mechanism of action (MOA) exclusively mediated by the Fab fragment might be beneficial. In these approaches, a silent Fc is essential to abrogate Fc – FcγR binding¹¹. Other strategies where the Fc is not present have been explored, however, they might be less advantageous due to a significant reduction in half-life when antibodies are not recycled via FcRn. Various Fc mutations have been

described to reduce the immune effector functions mediated by the Fc fragment. Among the different variants studied, one with a “LALA” double mutation (Leu234Ala together with Leu235Ala) was first described as a molecule with diminished effector functions¹⁵. Addition of a “PG” mutation (P329G) led to further reduction of FcγR-mediated effector function and complement activity^{14,16}.

Bispecific antibodies:

Despite the great progress with mAbs therapy, several limitations such as development of drug resistance or failure to respond to treatment have been described together with undesired side effects¹⁷. To overcome the drawback, new approaches have been developed aimed to target distinct cell types with more specificity. The creation of bispecific antibodies (BsAbs) is one strategy that permits these treatments. Nisonoff first described the BsAb concept in the 1960s¹⁸. A BsAb is a protein that can bind to two different types of antigens or two separate epitopes on the same antigen at the same time. While mAbs have a typical MOA of binding to a single receptor expressed in a single cell type, by dual targeting, BsAbs could improve biological efficacy by minimising antigen escape and increasing target selectivity by concurrently binding to two non-selective antigens that can be selectively present on the surface of target cells¹⁹.

Although Nisonoff et al. developed the concept of BsAbs in the 1960s, the first therapeutic BsAb was licenced in 2009, over 50 years later, owing to manufacturing problems and clinical failure^{18,20}. The hybrid hybridoma approach (the fusion of two hybridomas also known as quadroma) for BsAb production was invented in 1983^{21,22}. However, the theoretical yield of desirable BsAbs produced by this method was just 12.5%. The purification of the correct BsAb construct is extremely difficult because there are heavy/light chain randomly formed molecules during assembly, known as chain association issue²². As a result, the primary challenge for BsAb development from the start was to manufacture pure BsAbs free of unwanted by-products.

The MOA provided by BsAbs is wider than mAbs, either targeting two receptors on the same cell type or targeting two receptors expressed on different cellular types, consequently bridging two different cell types such as immune and tumoral cells. Simultaneously, upon binding, inhibition or stimulation of multiple signal pathways might occur. BsAb might target multiple epitopes whereas mAb are designed to target a single epitope. Thus, bsAbs could present very high specificity. BsAbs have been studied for cancer immunotherapy, medication delivery, and the treatment of Alzheimer's disease.

When mAbs are compared to that of BsAbs, a number of distinctions emerge. mAbs are easier to produce on a big scale and are more stable than BsAbs. This is mostly because modified sequences of BsAbs, which are utilised to improve the coupling of two distinct arms, are more sensitive to physical and chemical circumstances. Furthermore, large-scale production processes for mAbs are simpler than for BsAbs, and there is less variability between batches, increasing the dependability of mAbs over BsAbs during clinical use²³. However, the use of BsAbs compared to combination therapy with two monospecific antibodies makes it possible to optimize expenses by reducing the cost of development and clinical trials^{24,25}.

Currently over 100 different BsAb formats have become available for researchers to take advantage of for different scenario of applications^{26,27}. The varied BsAb formats are usually divided into two classes: IgG-like and non-IgG-like. IgG-like BsAbs retain the full Y-shape of a standard IgG antibody whereas non-IgG-like BsAbs no longer have the Fc region. Thus, IgG-like BsAbs often have a long serum half-life, display relatively good solubility and stability and are able to induce secondary immune functions (ADCC, ADCP and CDC). While non-IgG-like BsAbs are advantageous over IgG-like ones in immunogenicity, tissue-penetrating capacity and yield²⁸.

BsAb therapeutics currently represent one of the fastest-growing classes of drugs on the market with four BsAb drugs approved and more than 193 BsAbs in clinical phase²⁹.

T regulatory cells biology:

Among all the milestones achieved by immunotherapy strategies, targeting immune checkpoint Cytotoxic T-Lymphocyte Associated Protein 4 (CTLA-4) became an appealing approach to target Tregs³⁰.

Tregs are a discrete subpopulation of CD4⁺ T cells defined by the expression of the transcription factor forkhead-box protein P3 (Foxp3), which is a key and essential element for maintaining homeostasis of the immune system by triggering full suppressive function and maturation of Tregs throughout their development^{31,32}. Mutations in the Foxp3 gene are associated with Treg defectivity and deficiency, resulting in immune dysregulation, autoimmune lymphoproliferative diseases and allergies. The lack of Foxp3 expression also leads to immune dysregulation, polyendocrinopathy, and enteropathy X-linked (IPEX) syndrome, a severe autoimmune lymphoproliferative disease that is fatal without bone marrow transplant³⁴⁻³⁶.

Treg cells develop either in the thymus (natural Tregs (nTregs)) or in the periphery from naïve CD4⁺ T cells (induced Tregs (iTregs)). Thymocytes undergo positive and negative selection during TCR rearrangement. Throughout these selections, a precursor Treg cell population arises which is phenotypically characterized as CD4⁺ CD25^{high}. In this population Foxp3 expression is triggered through stimulation of IL-2 and IL-15 resulting in nTregs³⁷. iTregs are derived in the periphery from conventional T cells by environmental antigens such as microbial antigens or food antigens via mucosal tissue-resident dendritic cells (DCs)³⁸. The generation of an immunosuppressive environment with transforming growth factor beta (TGF-β), retinoic acids and short chain fatty acids promotes iTregs differentiation³⁸⁻⁴⁰. Both types of Tregs must achieve a balance between peripheral tolerance maintenance by suppressing potential autoimmune responses, while also controlling the effector response to pathogens.

Tregs lack a unique identifying cell surface marker. CD25, the high affinity IL-2 receptor α (IL-2Rα), was identified as a marker for Tregs. However, conventional T cells express CD25 upon activation. In humans, CD127 has been inversely correlated with Foxp3 expression and suppressive capacity,

therefore, Tregs are commonly defined as a CD4⁺ CD25^{high} CD127^{low} T cell subset^{41,42}.

Tregs modulate the innate and adaptive immune system by suppressing different immune cells such as B cells, CD4⁺ T cells, CD8⁺ cytotoxic T cells, NK cells, NKT cells, macrophages, DCs and neutrophils⁴³ (Fig. 2).

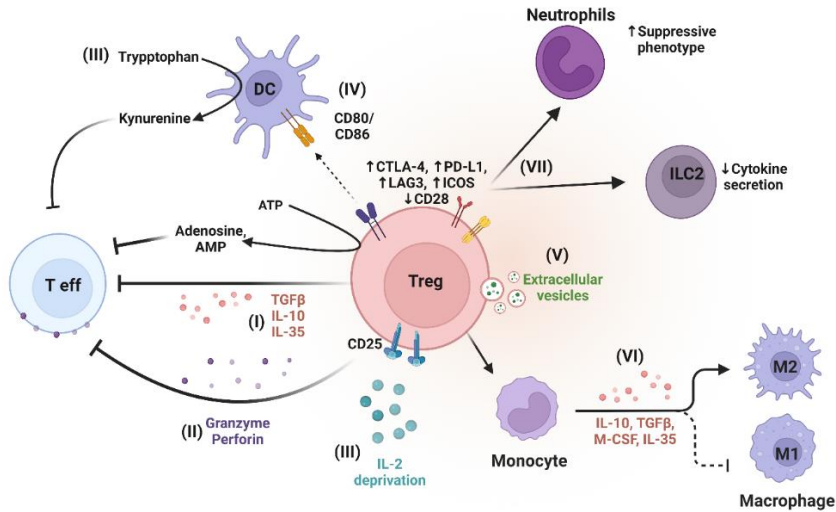


Figure 2. Mechanisms of Treg suppression. The direct and indirect mechanisms used by Tregs to promote immunosuppressive activity are: (i) immunosuppressive cytokines release including TGF-β, IL-10 and IL-35^{44–46}, (ii) granzyme and perforin mediated cytotoxicity^{18,19}, (iii) metabolic alterations to promote pro-inflammatory cytokine deprivation such as IL-2 starvation or generation of adenosine, adenosine monophosphate (AMP) and kynurenine^{49,50}, (iv) interaction with antigen presenting cells (APC) to modulate CD80 and CD86 expression, maturation and functional stage through immune checkpoint regulation^{51,52}, (v) generation of extracellular vesicles (EVs)⁵³, (vi) promoting differentiation towards anti-inflammatory macrophages M2^{54,55}, (vii) induction of suppressive phenotype in neutrophils and reduction of ILC2 cytokine secretion⁵⁶. Treg: T regulatory cells, T eff: T effector cells, DC: dendritic cell, ILC2: innate lymphoid cells, M1/2: macrophage, TGFβ: transforming growth factor beta, M-CSF: macrophage colony-stimulating factor, IL: interleukin, CTLA-4: Cytotoxic T-Lymphocyte Associated Protein 4, PD-L1: Programmed death-ligand 1, LAG3: Lymphocyte Activating 3, ICOS: Inducible T Cell Costimulator. Created with Biorender.

Tregs are involved in the maintenance of the tolerance to self-antigens by preventing autoimmune and inflammatory diseases and in controlling an effector immune response upon pathogen elimination by antigen-specific immune response. Therefore, immunosuppressive activity carried out by Tregs plays pivotal role in autoimmune and inflammatory disorders such as

type 1 diabetes, multiple sclerosis, and cancer disease, making the Tregs an important target for therapeutic applications⁵⁷⁻⁵⁹.

In autoimmune diseases, a disbalance towards effector T cell activity is observed. Autoreactive effector T cells expand when self-tolerance is lost. A reduction of Foxp3⁺ Tregs in number or function has been reported in different autoimmune diseases. The most evident case is observed in patients with IPEX where a mutation in the Foxp3 gene leads to impaired Treg function which triggers multi-organ autoimmunity³⁶. In addition, alterations in the IL-2R α pathway or immune checkpoints have been described as factor involved in autoimmune disorders⁶⁰.

Several therapies aiming to target Tregs are under investigation. Rapamycin, an m-TOR inhibitor, as well as other biologicals such as IL-10, low-dose IL-2, TNF receptor 2 (TNFR2) agonists, or FMS-like tyrosine kinase 3 ligand (Flt3L), have been explored^{29,30-34}.

In cancer disease, Tregs that are present in the tumor microenvironment (TME) limit inflammation and effector responses leading to immune evasion and tumor growth. Increased presence of Tregs has been associated with poor prognosis in several cancers⁶⁷⁻⁷⁵. Nevertheless, elevated intratumoral Treg levels are not always associated with poor prognosis^{76,77}. These opposing results show that the function of Treg cells in the growth of cancer is greatly influenced by the type and location of the tumor.

Although it is still not completely clear what drives the preferential migration of Tregs to the tumor microenvironment, chemokine synthesis by the tumor most likely triggers chemotaxis. The binding of CCL22, which is released by a variety of tumor cell types, to the chemokine receptor CCR4 expressed on Treg cells, promotes Treg infiltration into the tumor microenvironment^{78,79}. Similarly, CCR8 and its ligand CCL1 have been reported to drive Treg infiltration^{80,81}. Thus, different factors are likely to elevate the number of Treg cells in the TME.

To directly or indirectly modulate Treg-mediated immune suppression in cancer, several therapeutic options are available or in clinical trials. Most treatment options are based on targeting Treg cell-expressed

molecules^{47,48,77–80}, but also other strategies have been reported^{81–87}. As previously mentioned, CTLA-4 targeting suggested that anti-CTLA-4 mAbs could selectively deplete intratumoral Tregs in mice and thus, would have a potentially relevant activity in humans as well. However, despite the increase of intratumoral CD4⁺ and CD8⁺ cells infiltration, a significant reduction of Tregs within the TME is not observed in humans^{30,93}. CTLA-4 is a transmembrane protein which competes with CD28 for interaction with common ligands CD80 (B7.1) and CD86 (B7.2)⁹⁴. The immunoregulatory role of CTLA-4 is to dampen the T cell response, while CD28 signalling stimulates T cell activation⁹⁵. The greater affinity of CTLA-4 for both ligands is countered by its predominately intracellular location, as opposed to CD28, which is constitutively expressed at the T cell surface. When CTLA-4 is expressed, less CD80 and CD86 is available for CD28 favouring the inhibition of the T cell response^{96,97}. CTLA-4 is expressed by conventional T cells upon activation and it is constitutively expressed on the Treg cell surface⁹⁸. CTLA-4 is essential for Treg-mediated suppression, albeit partially, via controlling CD80/CD86 expression by APCs⁹⁹. Consequently, the role of CTLA-4 in supporting the suppressing function of Treg makes it a suitable molecule for targeting and eliminating intratumoral Tregs which ultimately boosts the CD8 antitumor response. Despite the promising results obtained with anti-CTLA-4 mAbs *in vivo* in mouse tumor models, severe immunotherapy-related adverse events have been reported in humans¹⁰⁰. Thus, although CTLA-4 targeting became one of the best-explored strategies to deplete Tregs, other receptors present on the surface of Tregs are being explored as well.

Overall, Tregs represent an attractive target for different therapeutic approaches, but optimal tools for Treg targeting require further exploration.

One novel Treg target is the TNFR2:

Tumor Necrosis factor receptor 2 (TNFR2) expression has been associated with costimulatory effects in Tregs, and may represent an optimal Treg target in autoimmune diseases, neuroinflammation and cancer¹⁰¹. This receptor mediates most of the metabolic effects of Tumor Necrosis factor alpha (TNF α).

TNF α is a cytokine which plays a role in immune responses, cell growth and proliferation, and tumor progression. There are two main isoforms depending on TNF α cleavage: soluble TNF α (sTNF α) and membrane-bound TNF α (mTNF α)^{102,103}. In addition, there are two receptors of TNF α : TNF receptor 1 (TNFR1) and TNFR2. TNF α can bind both receptors, but sTNF α presents a higher affinity for TNFR1 while mTNF α triggers a response upon TNFR2 binding^{104,105}.

While TNFR1 is widely expressed on different cell types, TNFR2 expression is more limited to some immune cells such as Tregs and myeloid-derived suppressing cells, but also different types of tumors and malignant cells¹⁰⁶. Its role in the tumor microenvironment and as immune modulator turns it into an attractive target.

Binding of sTNF α to TNFR1 induces receptor trimerization and recruitment of TNFR1-associated death domain (TRADD). TRADD recruitment leads to mixed lineage kinase domain-like (MLKL) and caspase 8 activation resulting in inflammation, apoptosis or necroptosis, ultimately mediating cell death^{107,108}. TNFR1, parallelly, leading to a formation of a complex formed by TNF receptor-associated factor 2 (TRAF2), RIPK1 and cIAP1/2 engaging the signalling pathways that activate transcription factors of the nuclear factor of kappa B (NF- κ B) family or kinases of the MAP kinase family^{109,110}.

TNFR2, mainly triggered by mTNF α and lacking a death domain downstream, recruits a complex composed of TNF receptor-associated factor 2 (TRAF2), TRAF2-associated proteins and cIAP1/2. Downstream signals activate the NF- κ B pathway through PI3K/Akt resulting in cell survival and proliferation¹¹¹. Furthermore, Tumor necrosis factor-alpha converting enzyme (TACE) enzymes can cleave mTNFR2 to sTNFR2 when TNFR2 trimerizes with TNF and forms a densely packed complex¹¹². Depending on the cell type, mTNFR2 is both immunosuppressive on Tregs and immunostimulatory on T effector cells (Teffs)¹¹³. However, sTNFR2 consistently has an immunosuppressive effect¹¹⁴.

Different TNFR2-mediated signalling pathways appear to have different functions in different cell types. On Teffs, TNFR2 induces co-stimulation and

cell death through the upregulated expression of the inhibitory receptor Tim3¹¹³. On Tregs, cell proliferation and maintenance is enhanced via IKK/NF- κ B, mTOR and MAPK^{76,85,86}. On myeloid-derived suppressor cells (MDSCs), cell survival, cell recruitment and increased suppression is mediated by FLICE-inhibitory protein (c-FLIP) upregulation and inhibition of caspase-8¹¹⁸. On regulatory B-cells, suppression activity is regulated by formation of IL-10⁸⁸. On macrophages, TNFR2 increases the production of pro-inflammatory factors via activation of p38 MAPK and NF- κ B pathways¹²⁰. On mesenchymal stem cells (MSCs), proliferation and functional properties are promoted by the expression of immunosuppressive proteins^{122,123}. On endothelial progenitor cells (EPCs), survival, differentiation and immunosuppression are triggered by angiogenesis and production of different anti-inflammatory cytokines such as IL-10, TGF- β ¹²⁴.

TNFR2 was previously assumed to be a T-cell stimulator, like other TNFRSF receptors¹²⁵. T cells have long been regarded as an important target for cancer treatment. Immunosuppressive tumor infiltrating Tregs play an important function in the immunosuppressive tumor microenvironment's stability^{126,127}. Tregs can not only aid tumor cells in avoiding apoptosis, but they can also help tumor cells survive by suppressing a subset of CD8⁺ Teffs³⁶. According to reports, TNFR2 expression on Treg cells is extremely suppressive^{102,115} and is associated with a bad prognosis in patients¹²⁸. Furthermore, activated Tregs are able to shed large amounts of TNFR2 turning the sTNFR2 into a soluble mediator that can inhibit any of the above mentioned effects, thus enhancing the immunosuppressive mechanism of Tregs¹¹⁴. In addition, these TNFR2⁺ Tregs express more immunosuppressive markers, such as CTLA-4 and CD73. TNFR2⁺ Tregs can also produce more inhibitory immune cytokines, such as IL-10 or TGF- β , allowing them to suppress the immune system more effectively¹²⁹. It was speculated that targeting this subset of highly suppressive TNFR2⁺ Treg cells will lead to the breakdown of various immune regulatory circuits in the tumor microenvironment¹³⁰. TNFR2 expression has also been described on other conventional T cells which promotes a costimulatory effect^{131,132}. Increased TNFR2 expression on Teffs after TCR stimulation is required not only for Teff

proliferation and activation, but also for the induction of activation-induced cell death (AICD)^{113,133}.

Hence, TNFR2 becomes an alternative target for immunotherapy strategies aiming to target Tregs.

Scope of this thesis

The research described in this thesis aimed to improve the current understanding of the bispecific antibodies and their potential to improve current therapeutic strategies. In parallel, the impact of different antibody isotypes on treatment outcome has been explored. The field of antibody therapeutics prompted us to generate novel antibodies targeting TNFR2 which could be a useful tool to target Treg cells.

In **Chapter 1**, a brief theoretical crucial background for understanding the importance of the research described in this thesis.

In **Chapter 2**, a review of the recent progress in BsAb design, their opportunities, current limitations and challenges in their design has been given. In addition, BsAbs are presented as an attractive approach to target Tregs based on the cell surface markers expressed in this specific population. Therefore, Treg-targeting BsAbs that are currently being developed are listed.

In **Chapter 3**, following with the BsAbs therapeutic potential, the effect of the hinge length in a T cell redirecting bispecific antibody (TbsAb) targeting mouse EGFR and mouse CD3 has been studied. The data show that the short hinge design improved ADCC against tumor cells, probably by closer proximity of CD8⁺ cells and target cells. Furthermore, the shorter TbsAb promoted higher T cell activation. These findings point out that hinge modifications could be implemented in other antibody-based constructs as well in order to optimize the therapeutic effect.

In **Chapter 4**, we studied the therapeutic effect of different mouse isotypes targeting the same tumor-associated antigen. Anti-Thy1.1 antibodies were generated with the same specificity but different isotypes and were used to target B16-OVA-Thy1.1 tumors in a syngeneic mouse model. The results



indicate that mouse IgG2a isotype is superior to mIgG1 or mIgE in controlling the tumor growth.

In **Chapter 5**, the main focus remains on the generation and characterization of novel anti-mouse TNFR2 antibodies. A wide panel of anti-TNFR2 antibodies with different features has been developed and might be a useful tool to assess the therapeutic effect of targeting TNFR2-expressing cells, such as Treg cells.

In **Chapter 6**, further exploration of two novel anti-mTNFR2 antibodies was assessed *in vitro*, *ex vivo* and *in vivo*. The Fc-effector function of these antibodies was tested in a CDC assay, confirming that silent Fc abrogates the effector activity. We hypothesized that TNFR2 antibodies were targeting Tregs in an *in vivo* setup, blocking and/or depleting them, leading to assess naïve CD4 proliferation in a Rag 1 KO mice model.

In **Chapter 7**, a general discussion of all findings in this thesis is presented, together with future perspectives and potential applications.

Finally, in **Chapter 8** as an appendix, the acknowledgements, the curriculum vitae and the list of publications are given.

References

1. Köhler G, Milstein C. Continuous cultures of fused cells secreting antibody of predefined specificity. *Nature*. 1975;256(5517):495-497. doi:10.1038/256495a0
2. Meffre E, Casellas R, Nussenzweig MC. Antibody regulation of B cell development. *Nat Immunol*. 2000;1(5):379-385. doi:10.1038/80816
3. Chothia C, Lesk AM. Canonical structures for the hypervariable regions of immunoglobulins. *J Mol Biol*. 1987;196(4):901-917. doi:10.1016/0022-2836(87)90412-8
4. Wauwe JPV, Mey JRD, Goossens JG. OKT3: a monoclonal anti-human T lymphocyte antibody with potent mitogenic properties. *J Immunol*. 1980;124(6):2708-2713.
5. Lu RM, Hwang YC, Liu IJ, et al. Development of therapeutic antibodies for the treatment of diseases. *J Biomed Sci*. 2020;27(1):1. doi:10.1186/s12929-019-0592-z
6. Schroeder HW, Cavacini L. Structure and function of immunoglobulins. *J Allergy Clin Immunol*. 2010;125(2, Supplement 2):S41-S52. doi:10.1016/j.jaci.2009.09.046
7. Charles A Janeway J, Travers P, Walport M, Shlomchik MJ. The structure of a typical antibody molecule. *Immunobiol Immune Syst Health Dis 5th Ed*. Published online 2001. Accessed October 21, 2022. <https://www.ncbi.nlm.nih.gov/books/NBK27144/>
8. Daëron M. Fc RECEPTOR BIOLOGY. *Annu Rev Immunol*. 1997;15(1):203-234. doi:10.1146/annurev.immunol.15.1.203
9. Nimmerjahn F, Ravetch JV. Fcγ receptors as regulators of immune responses. *Nat Rev Immunol*. 2008;8(1):34-47. doi:10.1038/nri2206
10. Bruhns P. Properties of mouse and human IgG receptors and their contribution to disease models. *Blood*. 2012;119(24):5640-5649. doi:10.1182/blood-2012-01-380121
11. Boruchov AM, Heller G, Veri MC, Bonvini E, Ravetch JV, Young JW. Activating and inhibitory IgG Fc receptors on human DCs mediate opposing functions. *J Clin Invest*. 2005;115(10):2914-2923. doi:10.1172/JCI24772
12. Hayes JM, Wormald MR, Rudd PM, Davey GP. Fc gamma receptors: glycobiology and therapeutic prospects. *J Inflamm Res*. 2016;9:209-219. doi:10.2147/JIR.S121233
13. Bruhns P, Jönsson F. Mouse and human FcR effector functions. *Immunol Rev*. 2015;268(1):25-51. doi:10.1111/imr.12350
14. Schlothauer T, Herter S, Koller CF, et al. Novel human IgG1 and IgG4 Fc-engineered antibodies with completely abolished immune effector functions. *Protein Eng Des Sel PEDS*. 2016;29(10):457-466. doi:10.1093/protein/gzw040

15. Chappel MS, Isenman DE, Everett M, Xu YY, Dorrington KJ, Klein MH. Identification of the Fc gamma receptor class I binding site in human IgG through the use of recombinant IgG1/IgG2 hybrid and point-mutated antibodies. *Proc Natl Acad Sci U S A*. 1991;88(20):9036-9040.
16. Hessel AJ, Hangartner L, Hunter M, et al. Fc receptor but not complement binding is important in antibody protection against HIV. *Nature*. 2007;449(7158):101-104. doi:10.1038/nature06106
17. Regales L, Gong Y, Shen R, et al. Dual targeting of EGFR can overcome a major drug resistance mutation in mouse models of EGFR mutant lung cancer. *J Clin Invest*. 2009;119(10):3000-3010. doi:10.1172/JCI38746
18. Nisonoff A, Wissler FC, Lipman LN. Properties of the Major Component of a Peptic Digest of Rabbit Antibody. *Science*. 1960;132(3441):1770-1771. doi:10.1126/science.132.3441.1770
19. Mazor Y, Hansen A, Yang C, et al. Insights into the molecular basis of a bispecific antibody's target selectivity. *mAbs*. 2015;7(3):461-469. doi:10.1080/19420862.2015.1022695
20. Garber K. Bispecific antibodies rise again. *Nat Rev Drug Discov*. 2014;13(11):799-801. doi:10.1038/nrd4478
21. Milstein C, Cuello AC. Hybrid hybridomas and their use in immunohistochemistry. *Nature*. 1983;305(5934):537-540. doi:10.1038/305537a0
22. Klein C, Sustmann C, Thomas M, et al. Progress in overcoming the chain association issue in bispecific heterodimeric IgG antibodies. *mAbs*. 2012;4(6):653-663. doi:10.4161/mabs.21379
23. Byrne H, Conroy PJ, Whisstock JC, O'Kennedy RJ. A tale of two specificities: bispecific antibodies for therapeutic and diagnostic applications. *Trends Biotechnol*. 2013;31(11):621-632. doi:10.1016/j.tibtech.2013.08.007
24. Kontermann RE. Dual targeting strategies with bispecific antibodies. *mAbs*. 2012;4(2):182-197. doi:10.4161/mabs.4.2.19000
25. Zhang X, Yang Y, Fan D, Xiong D. The development of bispecific antibodies and their applications in tumor immune escape. *Exp Hematol Oncol*. 2017;6:12. doi:10.1186/s40164-017-0072-7
26. Brinkmann U, Kontermann RE. The making of bispecific antibodies. *mAbs*. 2017;9(2):182-212. doi:10.1080/19420862.2016.1268307
27. Godar M, de Haard H, Blanchetot C, Rasser J. Therapeutic bispecific antibody formats: a patent applications review (1994-2017). *Expert Opin Ther Pat*. 2018;28(3):251-276. doi:10.1080/13543776.2018.1428307
28. Fan G, Wang Z, Hao M, Li J. Bispecific antibodies and their applications. *J Hematol Oncol J Hematol Oncol*. 2015;8(1):130. doi:10.1186/s13045-015-0227-0

29. Zhang Z, Luo F, Cao J, et al. Anticancer bispecific antibody R&D advances: a study focusing on research trend worldwide and in China. *J Hematol Oncol/J Hematol Oncol*. 2021;14(1):124. doi:10.1186/s13045-021-01126-x
30. Ha D, Tanaka A, Kibayashi T, et al. Differential control of human Treg and effector T cells in tumor immunity by Fc-engineered anti-CTLA-4 antibody. *Proc Natl Acad Sci U S A*. 2019;116(2):609-618. doi:10.1073/pnas.1812186116
31. Fontenot JD, Gavin MA, Rudensky AY. Foxp3 programs the development and function of CD4+CD25+ regulatory T cells. *Nat Immunol*. 2003;4(4):330-336. doi:10.1038/ni904
32. McMurphy AN, Gillies J, Gizzi MC, et al. A novel function for FOXP3 in humans: intrinsic regulation of conventional T cells. *Blood*. 2013;121(8):1265-1275. doi:10.1182/blood-2012-05-431023
33. Deng G, Xiao Y, Zhou Z, et al. Molecular and biological role of the FOXP3 N-terminal domain in immune regulation by T regulatory/suppressor cells. *Exp Mol Pathol*. 2012;93(3):334-338. doi:10.1016/j.yexmp.2012.09.013
34. Chatila TA, Blaeser F, Ho N, et al. JM2, encoding a fork head-related protein, is mutated in X-linked autoimmunity-allergic dysregulation syndrome. *J Clin Invest*. 2000;106(12):R75-81. doi:10.1172/JCI11679
35. Wildin RS, Ramsdell F, Peake J, et al. X-linked neonatal diabetes mellitus, enteropathy and endocrinopathy syndrome is the human equivalent of mouse scurfy. *Nat Genet*. 2001;27(1):18-20. doi:10.1038/83707
36. Bennett CL, Christie J, Ramsdell F, et al. The immune dysregulation, polyendocrinopathy, enteropathy, X-linked syndrome (IPEX) is caused by mutations of FOXP3. *Nat Genet*. 2001;27(1):20-21. doi:10.1038/83713
37. Lio CWJ, Hsieh CS. A Two-Step Process for Thymic Regulatory T Cell Development. *Immunity*. 2008;28(1):100-111. doi:10.1016/j.immuni.2007.11.021
38. Coombes JL, Siddiqui KRR, Arancibia-Cárcamo CV, et al. A functionally specialized population of mucosal CD103+ DCs induces Foxp3+ regulatory T cells via a TGF- β - and retinoic acid-dependent mechanism. *J Exp Med*. 2007;204(8):1757-1764. doi:10.1084/jem.20070590
39. Sun CM, Hall JA, Blank RB, et al. Small intestine lamina propria dendritic cells promote de novo generation of Foxp3 T reg cells via retinoic acid. *J Exp Med*. 2007;204(8):1775-1785. doi:10.1084/jem.20070602
40. Benson MJ, Pino-Lagos K, Roseblatt M, Noelle RJ. All-trans retinoic acid mediates enhanced T reg cell growth, differentiation, and gut homing in the face of high levels of co-stimulation. *J Exp Med*. 2007;204(8):1765-1774. doi:10.1084/jem.20070719

41. Liu W, Putnam AL, Xu-Yu Z, et al. CD127 expression inversely correlates with FoxP3 and suppressive function of human CD4+ T reg cells. *J Exp Med*. 2006;203(7):1701-1711. doi:10.1084/jem.20060772
42. Seddiki N, Santner-Nanan B, Martinson J, et al. Expression of interleukin (IL)-2 and IL-7 receptors discriminates between human regulatory and activated T cells. *J Exp Med*. 2006;203(7):1693-1700. doi:10.1084/jem.20060468
43. Schmidt A, Oberle N, Krammer PH. Molecular mechanisms of treg-mediated T cell suppression. *Front Immunol*. 2012;3:51. doi:10.3389/fimmu.2012.00051
44. Hawrylowicz CM, O'Garra A. Potential role of interleukin-10-secreting regulatory T cells in allergy and asthma. *Nat Rev Immunol*. 2005;5(4):271-283. doi:10.1038/nri1589
45. Annacker O, Asseman C, Read S, Powrie F. Interleukin-10 in the regulation of T cell-induced colitis. *J Autoimmun*. 2003;20(4):277-279. doi:10.1016/s0896-8411(03)00045-3
46. Joetham A, Takeda K, Takada K, et al. Naturally occurring lung CD4(+)CD25(+) T cell regulation of airway allergic responses depends on IL-10 induction of TGF-beta. *J Immunol Baltim Md 1950*. 2007;178(3):1433-1442. doi:10.4049/jimmunol.178.3.1433
47. Gondek DC, Lu LF, Quezada SA, Sakaguchi S, Noelle RJ. Cutting Edge: Contact-Mediated Suppression by CD4+CD25+ Regulatory Cells Involves a Granzyme B-Dependent, Perforin-Independent Mechanism. *J Immunol*. 2005;174(4):1783-1786. doi:10.4049/jimmunol.174.4.1783
48. Cao X, Cai SF, Fehniger TA, et al. Granzyme B and Perforin Are Important for Regulatory T Cell-Mediated Suppression of Tumor Clearance. *Immunity*. 2007;27(4):635-646. doi:10.1016/j.immuni.2007.08.014
49. Deaglio S, Dwyer KM, Gao W, et al. Adenosine generation catalyzed by CD39 and CD73 expressed on regulatory T cells mediates immune suppression. *J Exp Med*. 2007;204(6):1257-1265. doi:10.1084/jem.20062512
50. Kobie JJ, Shah PR, Yang L, Rebhahn JA, Fowell DJ, Mosmann TR. T Regulatory and Primed Uncommitted CD4 T Cells Express CD73, Which Suppresses Effector CD4 T Cells by Converting 5'-Adenosine Monophosphate to Adenosine. *J Immunol*. 2006;177(10):6780-6786. doi:10.4049/jimmunol.177.10.6780
51. Fallarino F, Grohmann U, Hwang KW, et al. Modulation of tryptophan catabolism by regulatory T cells. *Nat Immunol*. 2003;4(12):1206-1212. doi:10.1038/ni1003
52. Mellor AL, Munn DH. Ido expression by dendritic cells: tolerance and tryptophan catabolism. *Nat Rev Immunol*. 2004;4(10):762-774. doi:10.1038/nri1457

53. Clayton A, Mitchell JP, Court J, Mason MD, Tabi Z. Human Tumor-Derived Exosomes Selectively Impair Lymphocyte Responses to Interleukin-2. *Cancer Res.* 2007;67(15):7458-7466. doi:10.1158/0008-5472.CAN-06-3456
54. Taams LS, van Amelsfort JMR, Tiemessen MM, et al. Modulation of monocyte/macrophage function by human CD4+CD25+ regulatory T cells. *Hum Immunol.* 2005;66(3):222-230. doi:10.1016/j.humimm.2004.12.006
55. Tiemessen MM, Jagger AL, Evans HG, van Herwijnen MJC, John S, Taams LS. CD4+CD25+Foxp3+ regulatory T cells induce alternative activation of human monocytes/macrophages. *Proc Natl Acad Sci.* 2007;104(49):19446-19451. doi:10.1073/pnas.0706832104
56. Rigas D, Lewis G, Aron JL, et al. Type 2 innate lymphoid cell suppression by regulatory T cells attenuates airway hyperreactivity and requires inducible T-cell costimulator–inducible T-cell costimulator ligand interaction. *J Allergy Clin Immunol.* 2017;139(5):1468-1477.e2. doi:10.1016/j.jaci.2016.08.034
57. Tang Q, Adams JY, Penaranda C, et al. Central Role of Defective Interleukin-2 Production in the Triggering of Islet Autoimmune Destruction. *Immunity.* 2008;28(5):687-697. doi:10.1016/j.immuni.2008.03.016
58. Jamshidian A, Shaygannejad V, Pourazar A, Zarkesh-Esfahani SH, Gharagozloo M. Biased Treg/Th17 balance away from regulatory toward inflammatory phenotype in relapsed multiple sclerosis and its correlation with severity of symptoms. *J Neuroimmunol.* 2013;262(1-2):106-112. doi:10.1016/j.jneuroim.2013.06.007
59. Togashi Y, Shitara K, Nishikawa H. Regulatory T cells in cancer immunosuppression — implications for anticancer therapy. *Nat Rev Clin Oncol.* Published online January 31, 2019. doi:10.1038/s41571-019-0175-7
60. Grant CR, Liberal R, Mieli-Vergani G, Vergani D, Longhi MS. Regulatory T-cells in autoimmune diseases: challenges, controversies and--yet--unanswered questions. *Autoimmun Rev.* 2015;14(2):105-116. doi:10.1016/j.autrev.2014.10.012
61. Abbas AK, Trotta E, R Simeonov D, Marson A, Bluestone JA. Revisiting IL-2: Biology and therapeutic prospects. *Sci Immunol.* 2018;3(25):eaat1482. doi:10.1126/sciimmunol.aat1482
62. Battaglia M, Stabilini A, Roncarolo MG. Rapamycin selectively expands CD4+CD25+FoxP3+ regulatory T cells. *Blood.* 2005;105(12):4743-4748. doi:10.1182/blood-2004-10-3932
63. Battaglia M, Stabilini A, Draghici E, et al. Rapamycin and interleukin-10 treatment induces T regulatory type 1 cells that mediate antigen-specific transplantation tolerance. *Diabetes.* 2006;55(1):40-49.
64. Zeiser R, Leveson-Gower DB, Zambricki EA, et al. Differential impact of mammalian target of rapamycin inhibition on CD4+CD25+Foxp3+ regulatory T cells compared

- with conventional CD4+ T cells. *Blood*. 2008;111(1):453-462. doi:10.1182/blood-2007-06-094482
65. Biswas M, Sarkar D, Kumar SRP, et al. Synergy between rapamycin and FLT3 ligand enhances plasmacytoid dendritic cell-dependent induction of CD4+CD25+FoxP3+ Treg. *Blood*. 2015;125(19):2937-2947. doi:10.1182/blood-2014-09-599266
66. Chen X, Baumel M, Mannel DN, Howard OMZ, Oppenheim JJ. Interaction of TNF with TNF Receptor Type 2 Promotes Expansion and Function of Mouse CD4+CD25+ T Regulatory Cells. *J Immunol*. 2007;179(1):154-161. doi:10.4049/jimmunol.179.1.154
67. Bates GJ, Fox SB, Han C, et al. Quantification of Regulatory T Cells Enables the Identification of High-Risk Breast Cancer Patients and Those at Risk of Late Relapse. *J Clin Oncol*. 2006;24(34):5373-5380. doi:10.1200/JCO.2006.05.9584
68. Ladoire S, Arnould L, Apetoh L, et al. Pathologic Complete Response to Neoadjuvant Chemotherapy of Breast Carcinoma Is Associated with the Disappearance of Tumor-Infiltrating Foxp3+ Regulatory T Cells. *Clin Cancer Res*. 2008;14(8):2413-2420. doi:10.1158/1078-0432.CCR-07-4491
69. Woo EY, Chu CS, Goletz TJ, et al. Regulatory CD4+CD25+ T Cells in Tumors from Patients with Early-Stage Non-Small Cell Lung Cancer and Late-Stage Ovarian Cancer. *Cancer Res*. 2001;61(12):4766-4772.
70. Tao H, Mimura Y, Aoe K, et al. Prognostic potential of FOXP3 expression in non-small cell lung cancer cells combined with tumor-infiltrating regulatory T cells. *Lung Cancer*. 2012;75(1):95-101. doi:10.1016/j.lungcan.2011.06.002
71. Soo RA, Chen Z, Yan Teng RS, et al. Prognostic significance of immune cells in non-small cell lung cancer: meta-analysis. *Oncotarget*. 2018;9(37):24801-24820. doi:10.18632/oncotarget.24835
72. Jie HB, Schuler PJ, Lee SC, et al. CTLA-4+ Regulatory T Cells Increased in Cetuximab-Treated Head and Neck Cancer Patients Suppress NK Cell Cytotoxicity and Correlate with Poor Prognosis. *Cancer Res*. 2015;75(11):2200-2210. doi:10.1158/0008-5472.CAN-14-2788
73. Fu J, Xu D, Liu Z, et al. Increased Regulatory T Cells Correlate With CD8 T-Cell Impairment and Poor Survival in Hepatocellular Carcinoma Patients. *Gastroenterology*. 2007;132(7):2328-2339. doi:10.1053/j.gastro.2007.03.102
74. Boucek J, Mrkvan T, Chovanec M, et al. Regulatory T cells and their prognostic value for patients with squamous cell carcinoma of the head and neck. *J Cell Mol Med*. 2010;14(1-2):426-433. doi:10.1111/j.1582-4934.2008.00650.x
75. Shang B, Liu Y, Jiang S, Juan, Liu Y. Prognostic value of tumor-infiltrating FoxP3+ regulatory T cells in cancers: a systematic review and meta-analysis. *Sci Rep*. 2015;5(1):15179. doi:10.1038/srep15179

76. Frey DM, Droeser RA, Viehl CT, et al. High frequency of tumor-infiltrating FOXP3+ regulatory T cells predicts improved survival in mismatch repair-proficient colorectal cancer patients. *Int J Cancer*. 2010;126(11):2635-2643. doi:10.1002/ijc.24989
77. West NR, Kost SE, Martin SD, et al. Tumour-infiltrating FOXP3+ lymphocytes are associated with cytotoxic immune responses and good clinical outcome in oestrogen receptor-negative breast cancer. *Br J Cancer*. 2013;108(1):155-162. doi:10.1038/bjc.2012.524
78. Iellem A, Mariani M, Lang R, et al. Unique chemotactic response profile and specific expression of chemokine receptors CCR4 and CCR8 by CD4(+)CD25(+) regulatory T cells. *J Exp Med*. 2001;194(6):847-853. doi:10.1084/jem.194.6.847
79. Gobert M, Treilleux I, Bendriss-Vermare N, et al. Regulatory T cells recruited through CCL22/CCR4 are selectively activated in lymphoid infiltrates surrounding primary breast tumors and lead to an adverse clinical outcome. *Cancer Res*. 2009;69(5):2000-2009. doi:10.1158/0008-5472.CAN-08-2360
80. Barsheshet Y, Wildbaum G, Levy E, et al. CCR8+FOXP3+ Treg cells as master drivers of immune regulation. *Proc Natl Acad Sci*. 2017;114(23):6086-6091. doi:10.1073/pnas.1621280114
81. Kuehnemuth B, Piseddu I, Wiedemann GM, et al. CCL1 is a major regulatory T cell attracting factor in human breast cancer. *BMC Cancer*. 2018;18(1):1278. doi:10.1186/s12885-018-5117-8
82. Mitchell DA, Cui X, Schmittling RJ, et al. Monoclonal antibody blockade of IL-2 receptor α during lymphopenia selectively depletes regulatory T cells in mice and humans. *Blood*. 2011;118(11):3003-3012. doi:10.1182/blood-2011-02-334565
83. Rech AJ, Mick R, Martin S, et al. CD25 Blockade Depletes and Selectively Reprograms Regulatory T Cells in Concert with Immunotherapy in Cancer Patients. *Sci Transl Med*. 2012;4(134):134ra62-134ra62. doi:10.1126/scitranslmed.3003330
84. Doi T, Muro K, Ishii H, et al. A Phase I Study of the Anti-CC Chemokine Receptor 4 Antibody, Mogamulizumab, in Combination with Nivolumab in Patients with Advanced or Metastatic Solid Tumors. *Clin Cancer Res*. 2019;25(22):6614-6622. doi:10.1158/1078-0432.CCR-19-1090
85. Zappasodi R, Sirard C, Li Y, et al. Rational design of anti-GITR-based combination immunotherapy. *Nat Med*. 2019;25(5):759-766. doi:10.1038/s41591-019-0420-8
86. Jochems C, Fantini M, Fernando RI, et al. The IDO1 selective inhibitor epacadostat enhances dendritic cell immunogenicity and lytic ability of tumor antigen-specific T cells. *Oncotarget*. 2016;7(25):37762-37772. doi:10.18632/oncotarget.9326
87. Eschweiler S, Ramírez-Suástegui C, Li Y, et al. Intermittent PI3K δ inhibition sustains anti-tumour immunity and curbs irAEs. *Nature*. 2022;605(7911):741-746. doi:10.1038/s41586-022-04685-2

88. Wachstein J, Tischer S, Figueiredo C, et al. HSP70 Enhances Immunosuppressive Function of CD4+CD25+FoxP3+ T Regulatory Cells and Cytotoxicity in CD4+CD25- T Cells. *PLOS ONE*. 2012;7(12):e51747. doi:10.1371/journal.pone.0051747
89. Ali K, Soond DR, Pineiro R, et al. Inactivation of PI(3)K p110 δ breaks regulatory T-cell-mediated immune tolerance to cancer. *Nature*. 2014;510(7505):407-411. doi:10.1038/nature13444
90. Finke JH, Rini B, Ireland J, et al. Sunitinib reverses type-1 immune suppression and decreases T-regulatory cells in renal cell carcinoma patients. *Clin Cancer Res Off J Am Assoc Cancer Res*. 2008;14(20):6674-6682. doi:10.1158/1078-0432.CCR-07-5212
91. Chen ML, Yan BS, Lu WC, et al. Sorafenib relieves cell-intrinsic and cell-extrinsic inhibitions of effector T cells in tumor microenvironment to augment antitumor immunity. *Int J Cancer*. 2014;134(2):319-331. doi:10.1002/ijc.28362
92. Gulley JL, Heery CR, Schlom J, et al. Preliminary results from a phase 1 trial of M7824 (MSB0011359C), a bifunctional fusion protein targeting PD-L1 and TGF- β , in advanced solid tumors. *J Clin Oncol*. 2017;35(15_suppl):3006-3006. doi:10.1200/JCO.2017.35.15_suppl.3006
93. Sharma A, Subudhi SK, Blando J, et al. Anti-CTLA-4 Immunotherapy Does Not Deplete FOXP3+ Regulatory T Cells (Tregs) in Human Cancers. *Clin Cancer Res*. 2019;25(4):1233-1238. doi:10.1158/1078-0432.CCR-18-0762
94. Sansom DM. CD28, CTLA-4 and their ligands: who does what and to whom? *Immunology*. 2000;101(2):169-177. doi:10.1046/j.1365-2567.2000.00121.x
95. Lenschow DJ, Walunas TL, Bluestone JA. CD28/B7 system of T cell costimulation. *Annu Rev Immunol*. 1996;14:233-258. doi:10.1146/annurev.immunol.14.1.233
96. Collins AV, Brodie DW, Gilbert RJC, et al. The interaction properties of costimulatory molecules revisited. *Immunity*. 2002;17(2):201-210. doi:10.1016/s1074-7613(02)00362-x
97. Linsley PS, Bradshaw J, Greene J, Peach R, Bennett KL, Mittler RS. Intracellular trafficking of CTLA-4 and focal localization towards sites of TCR engagement. *Immunity*. 1996;4(6):535-543. doi:10.1016/s1074-7613(00)80480-x
98. Takahashi T, Tagami T, Yamazaki S, et al. Immunologic self-tolerance maintained by CD25(+)CD4(+) regulatory T cells constitutively expressing cytotoxic T lymphocyte-associated antigen 4. *J Exp Med*. 2000;192(2):303-310. doi:10.1084/jem.192.2.303
99. Qureshi OS, Zheng Y, Nakamura K, et al. Trans-endocytosis of CD80 and CD86: a molecular basis for the cell-extrinsic function of CTLA-4. *Science*. 2011;332(6029):600-603. doi:10.1126/science.1202947

100. Fecher LA, Agarwala SS, Hodi FS, Weber JS. Ipilimumab and Its Toxicities: A Multidisciplinary Approach. *The Oncologist*. 2013;18(6):733-743. doi:10.1634/theoncologist.2012-0483
101. Chen X, Subleski JJ, Kopf H, Howard OMZ, Mannel DN, Oppenheim JJ. Cutting Edge: Expression of TNFR2 Defines a Maximally Suppressive Subset of Mouse CD4⁺CD25⁺FoxP3⁺ T Regulatory Cells: Applicability to Tumor-Infiltrating T Regulatory Cells. *J Immunol*. 2008;180(10):6467-6471. doi:10.4049/jimmunol.180.10.6467
102. Nguyen DX, Ehrenstein MR. Anti-TNF drives regulatory T cell expansion by paradoxically promoting membrane TNF-TNF-RII binding in rheumatoid arthritis. *J Exp Med*. 2016;213(7):1241-1253. doi:10.1084/jem.20151255
103. Kruglov A, Drutskaya M, Schlienz D, et al. Contrasting contributions of TNF from distinct cellular sources in arthritis. *Ann Rheum Dis*. 2020;79(11):1453-1459. doi:10.1136/annrheumdis-2019-216068
104. Jones EY, Stuart DI, Walker NPC. Structure of tumour necrosis factor. *Nature*. 1989;338(6212):225-228. doi:10.1038/338225a0
105. Faustman D, Davis M. TNF receptor 2 pathway: drug target for autoimmune diseases. *Nat Rev Drug Discov*. 2010;9(6):482-493. doi:10.1038/nrd3030
106. Diaz-Montero CM, Finke J, Montero AJ. Myeloid derived suppressor cells in cancer: therapeutic, predictive, and prognostic implications. *Semin Oncol*. 2014;41(2):174-184. doi:10.1053/j.seminoncol.2014.02.003
107. Wang H, Sun L, Su L, et al. Mixed lineage kinase domain-like protein MLKL causes necrotic membrane disruption upon phosphorylation by RIP3. *Mol Cell*. 2014;54(1):133-146. doi:10.1016/j.molcel.2014.03.003
108. Oberst A, Dillon CP, Weinlich R, et al. Catalytic activity of the caspase-8-FLIP(L) complex inhibits RIPK3-dependent necrosis. *Nature*. 2011;471(7338):363-367. doi:10.1038/nature09852
109. Wajant H, Scheurich P. TNFR1-induced activation of the classical NF- κ B pathway. *FEBS J*. 2011;278(6):862-876. doi:10.1111/j.1742-4658.2011.08015.x
110. Brenner D, Blaser H, Mak TW. Regulation of tumour necrosis factor signalling: live or let die. *Nat Rev Immunol*. 2015;15(6):362-374. doi:10.1038/nri3834
111. Pimentel-Muiños FX, Seed B. Regulated commitment of TNF receptor signaling: a molecular switch for death or activation. *Immunity*. 1999;11(6):783-793. doi:10.1016/s1074-7613(00)80152-1
112. Black RA, Rauch CT, Kozlosky CJ, et al. A metalloproteinase disintegrin that releases tumour-necrosis factor- α from cells. *Nature*. 1997;385(6618):729-733. doi:10.1038/385729a0

113. Ye LL, Wei XS, Zhang M, Niu YR, Zhou Q. The Significance of Tumor Necrosis Factor Receptor Type II in CD8+ Regulatory T Cells and CD8+ Effector T Cells. *Front Immunol*. 2018;9. doi:10.3389/fimmu.2018.00583
114. van Mierlo GJD, Scherer HU, Hameetman M, et al. Cutting edge: TNFR-shedding by CD4+CD25+ regulatory T cells inhibits the induction of inflammatory mediators. *J Immunol Baltim Md 1950*. 2008;180(5):2747-2751. doi:10.4049/jimmunol.180.5.2747
115. He T, Liu S, Chen S, et al. The p38 MAPK Inhibitor SB203580 Abrogates Tumor Necrosis Factor-Induced Proliferative Expansion of Mouse CD4+Foxp3+ Regulatory T Cells. *Front Immunol*. 2018;9:1556. doi:10.3389/fimmu.2018.01556
116. Yang S, Wang J, Brand DD, Zheng SG. Role of TNF-TNF Receptor 2 Signal in Regulatory T Cells and Its Therapeutic Implications. *Front Immunol*. 2018;9:784. doi:10.3389/fimmu.2018.00784
117. Buchan S, Manzo T, Flutter B, et al. OX40- and CD27-mediated co-stimulation synergize with anti-PD-L1 blockade by forcing exhausted CD8+ T cells to exit quiescence. *J Immunol Baltim Md 1950*. 2015;194(1):125-133. doi:10.4049/jimmunol.1401644
118. Zhao X, Rong L, Zhao X, et al. TNF signaling drives myeloid-derived suppressor cell accumulation. *J Clin Invest*. 2012;122(11):4094-4104. doi:10.1172/JCI64115
119. Ticha O, Moos L, Wajant H, Bekeredjian-Ding I. Expression of Tumor Necrosis Factor Receptor 2 Characterizes TLR9-Driven Formation of Interleukin-10-Producing B Cells. *Front Immunol*. 2017;8:1951. doi:10.3389/fimmu.2017.01951
120. Ruspi G, Schmidt EM, McCann F, et al. TNFR2 increases the sensitivity of ligand-induced activation of the p38 MAPK and NF- κ B pathways and signals TRAF2 protein degradation in macrophages. *Cell Signal*. 2014;26(4):683-690. doi:10.1016/j.cellsig.2013.12.009
121. Ivagnès A, Messaoudene M, Stoll G, et al. TNFR2/BIRC3-TRAF1 signaling pathway as a novel NK cell immune checkpoint in cancer. *Oncoimmunology*. 2018;7(12):e1386826. doi:10.1080/2162402X.2017.1386826
122. Djouad F, Fritz V, Apparailly F, et al. Reversal of the immunosuppressive properties of mesenchymal stem cells by tumor necrosis factor alpha in collagen-induced arthritis. *Arthritis Rheum*. 2005;52(5):1595-1603. doi:10.1002/art.21012
123. Miettinen JA, Pietilä M, Salonen RJ, et al. Tumor necrosis factor alpha promotes the expression of immunosuppressive proteins and enhances the cell growth in a human bone marrow-derived stem cell culture. *Exp Cell Res*. 2011;317(6):791-801. doi:10.1016/j.yexcr.2010.12.010
124. Naserian S, Abdelgawad ME, Afshar Bakshloo M, et al. The TNF/TNFR2 signaling pathway is a key regulatory factor in endothelial progenitor cell

- immunosuppressive effect. *Cell Commun Signal CCS*. 2020;18(1):94. doi:10.1186/s12964-020-00564-3
125. Kim EY, Teh HS. TNF type 2 receptor (p75) lowers the threshold of T cell activation. *J Immunol Baltim Md 1950*. 2001;167(12):6812-6820. doi:10.4049/jimmunol.167.12.6812
126. Speiser DE, Ho PC, Verdeil G. Regulatory circuits of T cell function in cancer. *Nat Rev Immunol*. 2016;16(10):599-611. doi:10.1038/nri.2016.80
127. Facciabene A, Motz GT, Coukos G. T-Regulatory Cells: Key Players in Tumor Immune Escape and Angiogenesis. *Cancer Res.*:10.
128. Yan F, Du R, Wei F, et al. Expression of TNFR2 by regulatory T cells in peripheral blood is correlated with clinical pathology of lung cancer patients. *Cancer Immunol Immunother Cll*. 2015;64(11):1475-1485. doi:10.1007/s00262-015-1751-z
129. Govindaraj C, Tan P, Walker P, Wei A, Spencer A, Plebanski M. Reducing TNF receptor 2+ regulatory T cells via the combined action of azacitidine and the HDAC inhibitor, panobinostat for clinical benefit in acute myeloid leukemia patients. *Clin Cancer Res Off J Am Assoc Cancer Res*. 2014;20(3):724-735. doi:10.1158/1078-0432.CCR-13-1576
130. He J, Li R, Chen Y, Hu Y, Chen X. TNFR2-expressing CD4+Foxp3+ regulatory T cells in cancer immunology and immunotherapy. In: *Progress in Molecular Biology and Translational Science*. Vol 164. Elsevier; 2019:101-117. doi:10.1016/bs.pmbts.2019.03.010
131. Aspalter RM, Eibl MM, Wolf HM. Regulation of TCR-mediated T cell activation by TNF-RII. *J Leukoc Biol*. 2003;74(4):572-582. doi:10.1189/jlb.0303112
132. Reiner SL. Development in motion: helper T cells at work. *Cell*. 2007;129(1):33-36. doi:10.1016/j.cell.2007.03.019
133. Chen X, Hamano R, Subleski JJ, Hurwitz AA, Howard OMZ, Oppenheim JJ. Expression of costimulatory TNFR2 induces resistance of CD4+FoxP3- conventional T cells to suppression by CD4+FoxP3+ regulatory T cells. *J Immunol Baltim Md 1950*. 2010;185(1):174-182. doi:10.4049/jimmunol.0903548



2

Opportunities and challenges of bi-specific antibodies

Aina Segués^{a,b,†}, Shuyu Huang^{a,b,†}, Alice Sijts^b, Pedro Berraondo^{c,d,e}, and Dietmar M. Zaiss^{a,f,g,h,*}

- a. *Institute of Immunology and Infection Research, School of Biological Sciences, University of Edinburgh, Edinburgh, United Kingdom*
- b. *Faculty of Veterinary Medicine, Department of Infectious Diseases and Immunology, Utrecht University, Utrecht, The Netherlands*
- c. *Program of Immunology and Immunotherapy, CIMA Universidad de Navarra, Pamplona, Spain*
- d. *Centro de Investigación Biomédica en Red de Cáncer (CIBERONC), Madrid, Spain*
- e. *Navarra Institute for Health Research (IDISNA), Pamplona, Spain*
- f. *Department of Immune Medicine, University Regensburg, Regensburg, Germany*
- g. *Institute of Clinical Chemistry and Laboratory Medicine, University Hospital Regensburg, Regensburg, Germany*
- h. *Institute of Pathology, University Regensburg, Regensburg, Germany*

*Corresponding author: e-mail address: dietmar.zaiss@ukr.de

† Authors contributed equally.

International Review of Cell and Molecular Biology, Volume 369.

<https://doi.org/10.1016/bs.ircmb.2022.05.001>

Contribution statement: Aina Segués Cisteró conceived the presented idea. Aina Segués Cisteró did bibliographic research and she took the lead in writing the manuscript.

Contents

Introduction

Cis- versus trans-targeting bispecific antibodies

Technical challenges in the design and production of bispecific antibodies

Examples of BsAbs approved for clinical application

 Catumaxomab (Removab, Fresenius Biotech and Trion Pharma)

 Emicizumab (HEMLIBRA, Genentech, Inc.)

 Blinatumomab (Blincyto, Amgen Inc.)

 Amivantamab (Rybrevant, Janssen Biotech, Inc.)

Further opportunities for bispecific antibodies on the example of regulatory T-cells

 Regulatory T-cell expressed cell surface markers

Current bi-specific antibodies targeting regulatory T-cells

 ATOR-1015

 ATOR-1144

 KY1055

Concluding remarks

Funding

Disclosure statement

References

Abstract

Over the last years, bi-specific antibodies (BsAbs) have revealed great therapeutic potential. For one, the clinical approval of the first bispecific T-cell engager (BiTE), Blinatumomab, has revealed the therapeutic potential of an antibody construct to selectively link T-cells with tumor cells *in trans* and to thereby induce tumor cell removal. For the other, by the clinical approval of Amivantamab, a BsAb targeting the EGFR and cMet *in cis*, it was revealed that the concomitant targeting of two tumor antigens on the same tumor cell can substantially improve the efficacy of treatment beyond the efficacy of each monoclonal antibody alone or in combination. *Cis*-targeting BsAbs furthermore allow for a more selective targeting of cell populations which concurrently express two antigens, for which each antigen expression pattern in itself might not be selective. In this way, BsAbs harbor the great prospect of being more specific and to show fewer side effects than monoclonal antibodies. Nevertheless, BsAbs have also faced major obstacles, for instance, in ensuring reliable assembly and clinical grade purification. In this review, we summarize the different available antibody platforms currently used for the generation of IgG-like and non-IgG-like BsAbs and explain which approaches have been used to assemble those BsAbs which are currently approved for clinical application. By focusing on the example of regulatory T-cells (Tregs) and the different, ongoing approaches to develop BsAbs specifically targeting Tregs within the tumor microenvironment, our review highlights the huge potential as well as the pitfalls BsAbs face in order to emerge as one of the most effective therapeutic biologicals targeting desired cell populations in a highly selective way. Such BsAbs may improve treatment efficacy and reduce side effects, thereby opening novel treatment opportunities for a range of different diseases, such as cancer or autoimmune diseases.

Introduction

The clinical application of monoclonal antibodies has transformed the treatment of a wide range of diseases. Prominent successes have been the use of TNF-inhibitors for therapy of inflammatory diseases¹, and so-called immune check-point inhibitors in the field of tumor immunotherapy². Nonetheless, the clinical success of monoclonal antibody-based therapeutic approaches has slowed in recent years. In many cases, treatment turned out to be associated with severe side-effects as the effects of injected antibodies are often not focused on the site of inflammation or the tumor itself but may mediate systemic effects. Furthermore, many attractive target antigens are expressed in a more ubiquitous way, thus their expression is not limited to for instance specific tumor cells or leukocyte subpopulations, such as regulatory T-cells. One rather appealing approach to increase the specificity of antibody-based treatment is the generation of bispecific antibodies (BsAbs), whereby one antibody is recognizing two different antigens at the same time. Already in the 1960s, the very first BsAb targeting two different antigens with one antibody was described by Nisonoff *et al.*³. At that stage, two rabbit antigen-binding fragments were combined from two different polyclonal sera through mild re-oxidation³. However, the advent of recombinant antibody design has dramatically enhanced the development of BsAbs. Since the marketing of Blinatumomab, a fragment based BsAb targeting CD19 and CD3 in trans, and of Emicizumab, a BsAb that mimics the function of the coagulation factor VIII, their sales have increased continuously. In 2019, Blinatumomab's sales reached \$312 million and the sales of Emicizumab \$1.49 billion⁴. It is currently estimated that the BsAb market scale will surpass \$8 billion by 2025. Accordingly, the growth rate of the number of BsAb in the developmental pipeline has been estimated to reach three times that of conventional monoclonal antibody drugs in the next few years.

In this review, we will discuss the progress that bispecific antibody design has made in recent years, their opportunities and, in particular, the current limitations their design is facing.

Cis- versus trans-targeting bispecific antibodies

Compared to monospecific antibodies (mAbs), BsAbs potentially harbour several advantages. In particular, BsAbs have the capability to target cells either in a *cis*- or in a *trans*- binding orientation. During *trans*-binding, the antibody recognizes two different antigens, each expressed on a different cell population. Thus, such BsAbs can link two different cell populations with each other. One of the most prominent examples of such *trans*-binding BsAbs are the bispecific T-cell engagers (BiTE). For the construction of these cell-engaging BsAbs, a T-cell or NK-cell specific antibody fragment is linked with a tumor antigen recognizing antibody⁵ (Fig. 1). In this way, within a tumor the cell engager cross-links tumor cells with T- or NK-cells, thereby targeting their cellular cytotoxicity towards the tumor cell and, thus, inducing the killing of the recognized tumor cell. Following the clinical success of Blinatumomab, the first BiTE approved for clinical application, cell engagers constructs have reached much attention with a wide range of different constructs targeting different tumor antigens⁶.

In contrast to the *trans*-binding, *cis*-binding BsAbs are targeted to antigens expressed on the very same cell. By dual targeting, BsAbs could increase target selectivity by concurrent binding to two antigens. Given the affinity for each antigen were low enough for the antibody to bind only weakly to target cells that express only one of the antigens but strongly to cells that express both antigens, then such a BsAb could be highly selective for target cells presenting both antigens on their cell surface⁷.

In this way, these *cis*-binding BsAbs could be particularly attractive for clinical application, as specific tumor antigens could be included in the repertoire of clinically targeted antigens, despite the fact that also other cell types may occasionally express one of the two targeted antigens. In a similar way, bispecific, depleting antibodies could then be specifically targeted towards selected leukocyte populations, such as regulatory T-cells, based on the combined expression of antigens. Such a selectivity of treatment mediated by bi-specific antibodies could then substantially improve the efficacy of treatment and diminish the side-effects currently observed by the use of several monoclonal antibodies.

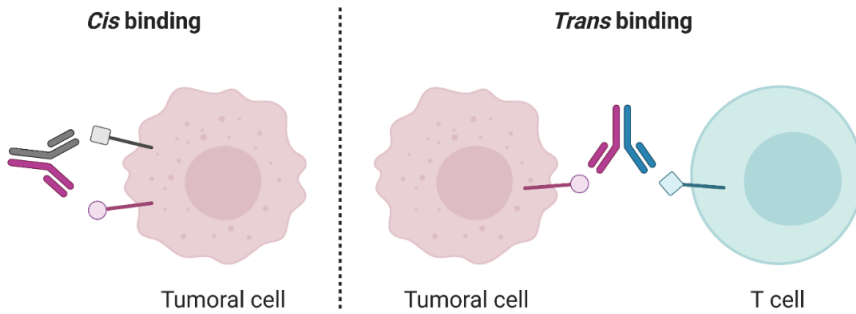


Figure 3. Scheme illustrating Bi-specific Antibodies binding in a cis- and a trans-mode. Bi-specific antibodies recognize two antigens. If both antigens are expressed on the same cell surface, then a cis-binding antibody recognizes both antigens on the same, the cis-side. However, if both antigens are expressed on two different cells, then a trans-binding antibody can form a link in between two cells, with the second antigen being expressed on the other, the trans-side.

Technical challenges in the design and production of bispecific antibodies

Although Nisonoff et al. had already demonstrated the feasibility of the concept of bispecific antibodies in the 1960s, the first market approval for a therapeutic BsAb was almost 50 years later, in 2009. This delay was due to a number of challenges that the design of such BsAbs is facing. Main challenges that emerged were the specificity of cis-targeting constructs and the manufacturing of the constructs³. When comparing the mechanism of action of monospecific with that of bispecific antibodies, a number of differences become apparent (Table 1). mAbs are relatively easy to produce in large scale and tend to be more stable than BsAbs. This is mainly due to the fact that the modified sequences of BsAbs, which are used to enhance combination of two different arms, are more sensitive to physical and chemical conditions. Also, the large-scale production methods for mAbs are easier compared to BsAbs and less differences are present between batches which increases the reliability of mAbs over BsAbs during clinical application⁸.

Faced with these challenges, several different technical approaches were established that would allow the reliable production of highly pure and stable BsAbs⁹.

Table 1. Comparison between monospecific and bispecific antibodies.

	Monospecific antibody	Bispecific antibody
MOA	Target one single population expressing the antigen of interest, inhibit/stimulate one signal pathway, Fc mediated effect	Emerging MOAs only for BsAbs: bridging immune cells and tumor cells; inhibit/stimulate multiple signal pathways simultaneously
Antigen	Single epitope	Multiple epitopes
Specificity	High	Very high
Stability	Medium	Relatively low; more sensitive to physical/chemical conditions
Standardized production	Relatively easy; little batch difference	Relatively difficult; potential batch difference
Production	Medium	Relatively high

Abbreviations: MOA: mechanism of action

In 1983, the hybrid hybridoma (quadroma) technology was invented for bispecific antibody production¹⁰. In this approach, two hybridoma cell lines, expressing a different monoclonal antibody each, were fused. In this fused hybridoma randomly formed heavy/light chain pairs are formed during assembly. The theoretical yield of desired bispecific antibodies produced by this approach was assumed to be around an eighth of all produced antibodies. Nevertheless, during purification the different sets of BsAbs turned out to be extremely difficult to separate, and the production of pure BsAbs without the presence of non-desired by-products remained a major obstacle¹¹. Over the last decades, paralleled by advances in protein engineering, several different approaches and production platforms have been developed that enforce the correct association of two different antibody pairs. Thereby one has to differentiate between so-called “IgG-like” and “non-IgG-like” BsAb, whereby the IgG-like BsAbs in principle retain the

classical heavy and light chain structure, while the non-IgG-like BsAbs leave that structure entirely and combine two or more antigen-binding domains, which could be antigen-binding fragment (Fab), single-chain variable fragment (scFv) or single-domain antibody (sdAb), also known as a nanobody. The IgG-like BsAbs have the substantial advantage that by interacting with the FcR expressed on different types of immune cells they are able to induce secondary immune functions, such as antibody-dependent cellular cytotoxicity (ADCC), antibody-dependent cellular phagocytosis (ADCP) and complement-dependent cytotoxicity (CDC). By enhanced engineering, such as interfering with the glycosylation of the heavy chain, the interaction of these BsAbs with specific FcRs can be altered and, consequently, the clinical efficacy of the used antibody substantially improved¹².

In contrast, non-IgG-like BsAbs have the edge over IgG-like ones with regard to immunogenicity and tissue-penetrating capacity¹³. The T-cell engager Blinatumomab is a prominent example of an approved non-IgG-like BsAb. The bispecific T cell engager (BiTE) platform used for its construction consists of two scFv parts, one targeting CD3 and a second the cell surface-expressed tumor-associated antigen (TAA) CD19, which are linked by a G4S linker (Fig. 2A). The resulting 55 kDa BsAb, Blinatumomab showed an impressive efficacy at very low doses in patients with non-Hodgkin lymphoma (NHL) and relapsed and/or refractory (r/r) acute lymphoblastic leukemia (ALL)^{14,15}. Most interestingly, clinical trials using a similar antibody targeting CD3 and CD19 (MGD-011 / Duvortuxizumab) had to be ceased due to safety concerns over neurological events occurring in some patients during treatment for ALL in phase I studies (NCT02848911) and r/r NHL (NCT02106091)¹⁶. This antibody was based on the dual-affinity retargeting (DART) platform, which is similar to the BiTE platform but covalently links two Fab-fragments through C-terminal cysteine residues (Fig. 2B).

A number of additional non-IgG-like antibodies are currently in clinical trial. Prominently, the company Ablynx uses its nanobody platform to construct Bi-Nanobodies. This platform connects three nanobody moieties into a trivalent molecule linked by two flexible poly-Glycine/Serine linkers. Two of

these nanobody moieties specifically recognize therapeutic targets with the third nanobody targeting human serum albumin (HSA) in order to extend the half-life of the BsAb (Fig. 2C). BI-836880 is a BsAb developed using this platform, which targets vascular endothelial growth factor (VEGF) and angiopoietin-2 (ANG2). It is currently in clinical trial in patients with different solid tumors (NCT02674152). A similar approach is used to generate tri-specific T-cell activating constructs (TriTAC) platform from Harpoon Therapeutics. These are composed of two single-domain antibodies and an scFv which specifically bind to a TAA, HSA, and CD3, respectively (Fig. 2D). Based on this platform, the BsAb HPN424 was developed to target CD3 and PSMA. Early results from clinical trials showed a promising efficacy in patients with metastatic castration-resistant prostate cancer (mCRPC)¹⁷.

Compared to non-IgG-like BsAb, IgG-like BsAbs show a substantially longer serum half-life. Furthermore, the IgG-like BsAb tend to display a relatively good solubility and stability. Nevertheless, the IgG-like BsAbs face the problem of the unspecific pairing of the two heavy chains with each other or of the heavy and light chains. A number of different approaches have been developed to address this issue. The predominant approaches applied to ensure a reliable hetero-heavy chain assembly are leucine zipper induced heterodimerization (LUZ-Y)¹⁸, bispecific engagement by antibodies based on T-cell receptor (BEAT) and strand-exchange engineered domain CH3 heterodimers (SEEDbody) approaches. In the leucine zipper induced heterodimerization (LUZ-Y)¹⁸ approach additional leucine zippers are fused to the C terminus of each heavy chain. Following transfection, these leucine zippers then force the newly formed antibodies into a hetero heavy-heavy chain association. Following purification, the leucine zipper can be readily removed. In contrast, in the bispecific engagement by antibodies based on T-cell receptor (BEAT)¹⁹ approach a hetero heavy chain interface is created, which mimics the natural dimerization of the T-cell surface receptors α and β and thus forces hetero chain formation between two heavy chains. Finally, in the strand-exchange engineered domain heterodimers (SEEDbody)²⁰ approach, complementary human IgG and IgA heavy chain domains are fused with each other on the different heavy chains. Once expressed, these hetero-domains allow for the formation of desired AG/GA heterodimers and

prevent the formation of homodimers between AG and GA. Nevertheless, the currently by far most common approach used is the so-called “knobs-into-holes” (KiH)^{21,22} approach. In this approach, mutations are introduced in different domains to create either a “knob” structure or a “hole” structure in each heavy chain. These complementary mutations very efficiently prevent homodimerization and promote the heterodimerization of newly expressed antibodies.

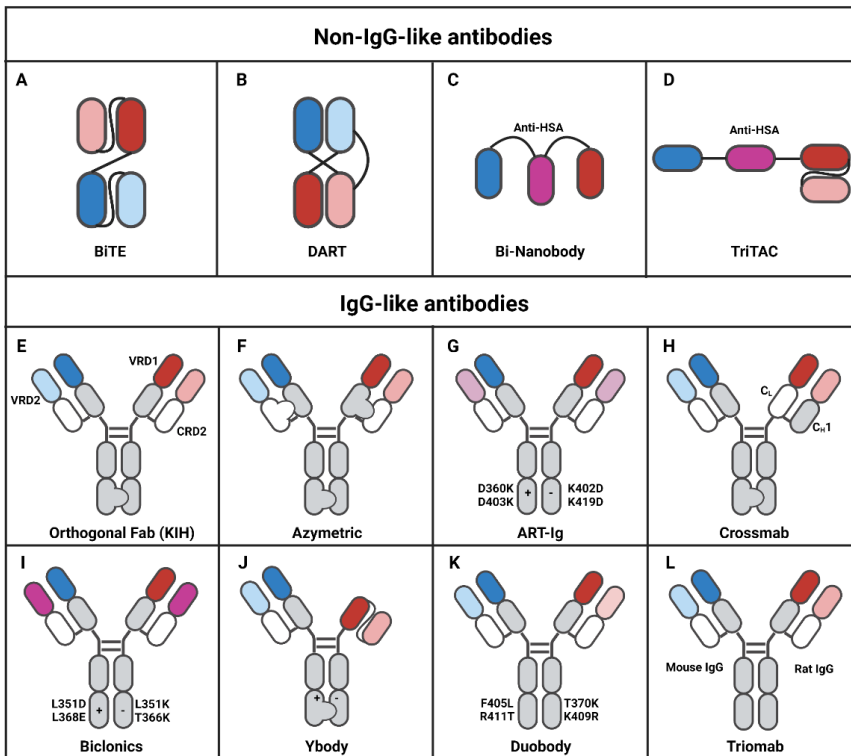


Figure 2. Currently common platforms for the expression of Bi-specific Antibodies.

Bi-specific antibodies can be expressed in the form of a loose connection of antigen-binding domains lacking an Fc-part (non-IgG-like platforms, A-D) or in forms of a more classical antibody structure with Fc-part (IgG-like platforms, E-L). The bispecific T cell engager (BiTE) platform (A) consists of a protein encompassing two scFv, one targeting CD3 and another specific for a tumor-associated antigen (TAA), connected via a linker. In contrast, the Dual-Affinity Re-Targeting (DART) platform (B) is based on 2 separate polypeptides, consisting of a cognate heavy and light chain variable domain each. These two proteins are assembled and stabilized via a disulfide bridge.

The Bi-Nanobody platform (C) connects three nanobody moieties into trivalent molecules by two flexible linkers. Of this trimer, one nanobody is specific for human serum albumin (HSA), in order to extend serum half-life of the construct, while the other two are specific for therapeutic targets, such as tumor antigens.

The trispecific T-cell activating construct (TriTAC) (D) is composed of two single-domain antibodies and an scFv. Of the IgG-like platforms, the Orthogonal Fab platform (E) solves heavy-light chain (H-LC) mis-pairing issue by introducing mutations to generate an “orthogonal interface” that enables preferential alignment of the different Fab domains combined with Knob-into-Hole (KiH) heavy-heavy chain (H-HC) heterodimerization method. The Azymetric platform (F) also uses KiH for H-HC heterodimerization and introduces mutations into CH3 to ensure the correct H-LC heterodimerization. In contrast, the Asymmetric Reengineering Technology-immunoglobulin (ART-Ig) platform (G) facilitates H-HC heterodimer formation by introducing electrostatic steering mutations and uses a common, shared light chain to ensure correct H-LC pairing. The CrossMab platform (H) overcomes H-LC mispairing by exchanging the CH1 of the heavy chain with the CL of the light chain within the Fab of one half of the BsAb, while correct H-HC heterodimer formation is ensured by typical heterodimer technologies, such as KiH. The Biclomics platform (I) also utilizes a shared, common light chain strategy and electrostatic steering to ensure correct H-HC heterodimer formation. The Y-Body platform (J) is an asymmetric bsAb platform which composes of a Fab-Fc and a scFv-Fc, in this way overcoming H-LC mis-pairing issue. The Duobody platform (K) uses a controlled Fab-arm exchange (cFAE) of two parental antibodies that prefer heterodimer over homodimer formation. Of the Triomab platform (L) heavy and light chain constant regions are of different isotypes, preventing mis-assembly.

Subsequently, heavy-light chain mis-pairing issues had to be overcome. In order to prevent heavy-light chain mis-pairing, several different strategies emerged. For instance, a common light chain approach was used, in which identical light chains are shared by two different heavy chains²³⁻²⁵. Alternatively, similar to heterodimerization methods applied for heavy-heavy chain association, some approaches engineered the contact points between the specific light and heavy chain by structure-based design to enhance correct heavy-light chain association²⁶⁻²⁸. Furthermore, some approaches exchanged domains between the heavy and light chain²⁹, ensuring that the engineered light chain can only associate to its corresponding domain-swapped heavy chain.

Based on a combination of different of the above named approaches, several companies developed their own platforms to efficiently purify highly pure BsAbs from transfected cells. One example using some of the above-named approaches is the Orthogonal Fab platform Lilly²⁷. This platform prevents heavy-light chain mis-pairing issues by introducing mutations to generate an “orthogonal interface” that enables preferential alignment of the different Fab domains with correct assembly. Additional KiH mutations in the heavy chain (Fig. 2E) allow for the very efficient and reliable formation of BsAbs. This platform has been used for the construction of several BsAbs. Nevertheless, the BsAb LY3164530, produced by this platform, simultaneously targeting EGFR and c-MET, had completed a phase I trial (NCT012221882) but further development was stopped due to significant toxicities that were observed in several treated patients³⁰. Nevertheless, more successful appears an antibody constructed based on a similar platform, the so called Azymetric platform by Zymeworks³¹. This platform also uses a KiH heavy-heavy chain heterodimerization method (Fig. 2F). Based on the Azymetric platform, the BsAb ZW25 was designed to biparatopically bind domain 2 and 4 in the extracellular region of HER2 simultaneously in order to increase avidity and to inhibit HER2/HER3 heterodimer formation. This BsAb demonstrated potent silencing of HER2 signalling and efficient removal of HER2 from the cell surface. In a phase I study (NCT02892123), this BsAb showed promising clinical efficacy³². Similar to the above described KiH approach, also the Asymmetric Reengineering Technology-immunoglobulin (ART-Ig) platform facilitates H-HC heterodimer formation. Nevertheless, in this approach electrostatic steering mutations are introduced in complementary domain interfaces of each heavy chain, providing them with different charges. Consequently, heavy chain homodimers are prevented from forming due to repulsive charge, while heterodimer formation is favored (Fig. 2G). The Emicizumab BsAb by Genentech has been developed based on this platform and was approved in 2018 to treat patients with hemophilia A. Also, the CrossMab from Roche and the Biclonis platform from Merus utilize combinations of the above explained approaches to construct and express BsAbs. The CrossMab platform overcomes heavy-light chain mispairing by exchanging heavy with

light chain domains within the Fab of one-half of the BsAb. Combined with another Fc heterodimer technology such as KiH, BsAb can be produced in a rather reliable way (Fig. 2H). There are a considerable number of BsAbs developed by this platform. Current BsAbs in clinical study are for example EM801 (CD3xBCMA), RG6026 (CD3xCD20), RG7802 (CD3xCEA), Vanucizumab (ANG2xVEGF), and RG7769 (PD-1xTim3)³³. In contrast, the Biclomics platform utilizes both a common light chain strategy and electrostatic steering effects which introduces positively charged mutations in one heavy chain and negatively charged mutations in the second heavy chain (Fig. 2I). Based on this platform, MCLA-128, an ADCC enhanced HER2 × HER3 BsAb, is undergoing clinical evaluation for patients with solid tumors harboring Neuroregulin1 (NRG1) fusion³⁴.

Nevertheless, in order to entirely prevent any possibility for mismatching, fundamentally alternative approaches and manufacturing platforms have been developed. Some platforms only use heavy chain heterodimerization methods in which they combine a Fab with an scFv or nanobody to avoid the heavy-light chain mis-pairing issue. For instance, the Y-body platform³⁵ from ZYBio, combines a Fab-Fc and an scFv-Fc to overcome heavy-light chain (H-LC) mis-pairing. Both Knobs-in-Holes (KiH) and electrostatic steering effects or “salt-bridge” technologies are applied on an Fc-CH3 interface to overcome heavy chain misassembly (Fig. 2J). M802 (anti-HER2×anti-CD3), developed by this platform, was approved for clinical trials to treat advanced HER2-positive solid tumors³⁵. Similarly, the Immune-therapy antibody (ITab™) platform (36) developed by Shanghai Generon uses two scFv-Fc to overcome heavy-light chain mis-pairing. Based on this platform, A-319, a T-cell activating BsAb designed to target CD19 and CD3 is under clinical evaluation for the treatment of patients with refractory/relapsed B cell lymphoma³⁶. Finally, a fundamentally different and very successful approach is used by Genmab in the DuoBody technology. The DuoBody technology does not rely on the formation of BsAb in transfected cells but basically mimics the *in vivo* naturally occurring process of human IgG4 Fab-arm exchange which results in generation of bispecific antibodies^{37,38}. Two parental IgG1s, each containing destabilizing mutations in their heavy chain domain, are produced separately. Subsequently, the purified antibodies are

dissociated and mixed with their pairing partner and then reassembled in vitro. This so-called “controlled Fab-arm exchange” (cFAE) allows for the formation of a wide range of different BsAbs (Fig. 2K). This platform has been licensed-out to many pharmaceutical companies such as BioNTech, Janssen Biotech, Inc., Novo Nordisk and led to several BsAbs in clinical trials such as JNJ-64007957 (CD3 x BCMA), JNJ-63709178 (CD3 x CD123), GEN3013 (CD3 x CD20), JNJ-64407564 (CD3 x GPRC5D) and one, Amivantamab (EGFR x c-Met), recently approved for clinical application.

Examples of BsAbs approved for clinical application

Due to the technical success in the assembly of BsAb over the last years, BsAb therapeutics currently represented one of the fastest-growing classes of drugs on the market with four BsAb drugs approved and more than 193 BsAbs in clinical study³⁹. Recently, FDA published the Bispecific Antibody Development Programs, the Guidance for Industry⁴⁰ indicative of increasing interest in the production of these reagents. Below, the four BsAbs which have so far been approved by FDA and made it into the market are described. Currently, only three of them are available.

- Catumaxomab (*Removab*, Fresenius Biotech and Trion Pharma)

Approved in 2009 but retracted in 2017, Catumaxomab was a trifunctional rat-mouse hybrid IgG2 monoclonal antibody with two different fragment antigen-binding (Fab) domains. This BsAb bound with one arm to EpCAM on tumor cells and with the other arm to CD3 on T cells in trans. Furthermore, via its Fc-part, the BsAb engaged with antigen-presenting cells⁴¹. In this way, the BsAbs formed a trifunctional connection between tumor cells, T-cells and antigen-presenting cells. The generation of this BsAb was based on a Triomab IgG-like platform (Fig. 2L). The Fc segment enhanced an effector response after engaging T-cells and mediated antibody-dependent cell-mediated cytotoxicity (ADCC) against tumoral cells. Catumaxomab was indicated for intraperitoneal treatment of malignant ascites in patients with epithelial cell adhesion molecule (EpCAM)-positive carcinomas⁴². But, in 2017, it was withdrawn from the market due to the insolvency of the manufacturer of the drug substance. Nevertheless, the company has

recently initiated a new phase III study for Catumaxomab to treat patients with advanced gastric carcinoma with peritoneal metastasis (NCT04222114).

- Emicizumab (HEMLIBRA, Genentech, Inc.)

Approved in 2018, Emicizumab is a humanized modified asymmetric bispecific IgG4 antibody that binds to blood clotting factor IXa and factor X. Its generation is based on the Art-Ig IgG-like platform (Fig. 2G). It is used to treat patients with hemophilia A, a hereditary bleeding disorder caused by a lack of blood clotting factor VIII. This BsAb mimics the function of the coagulation factor VIII by enhancing the formation of the prothrombinase complex and downstream clot formation^{43,44}. Compared to original factor VIII drug, Emicizumab displays an excellent subcutaneous bioavailability and a relative long half-life in vivo, and therefore currently dominates the market of hemophilia A treatment⁴⁵.

- Blinatumomab (*Blinicyto*, Amgen Inc.)

Approved in 2018, Blinatumomab is a fragment-based BsAb, lacking an Fc region, that targets CD19 and CD3 in trans to treat relapsed B-precursor acute lymphoblastic leukemia (ALL)^{46,47}. Its generation is based on BiTE non-IgG-like platform (Fig. 2A). The unspecific binding of this BsAb with the TCR receptor on CD8 T-cells induces an antigen-independent cross-linking of the TCR on T-cells, thereby inducing a targeted cellular cytotoxicity towards the tumor cell, leading to the deletion of the tumor cell recognized by the BiTE. Blinatumomab has been the first BsAb drug approved by FDA to treat leukaemia. Due to their impressive clinical efficacy (NCT01209286 and NCT01466179), the development of T- and NK-cell bispecific engagers have gained extensive attention and investment by pharmaceutical companies⁶.

- Amivantamab (*Rybrevant*, Janssen Biotech, Inc.)

Approved in 2021, Amivantamab is a fully-humanized IgG1-based bispecific antibody targeting both epidermal growth factor receptor (EGFR) and mesenchymal-epithelial transition factor (MET). Its generation is based on the Duobody IgG-like platform (Fig. 2K) described above and was shown to bind the EGFR independently of the diverse primary and acquired resistance

mutations the EGFR develops in advanced cancers and has been shown to downregulate EGFR expression on tumor cells^{48,49}. It blocks both EGFR and MET signalling via receptor inactivation. Amivantamab showed substantially enhanced clinical efficacy over EGFR blockade monotreatment and is indicated for the treatment of adult patients with locally advanced or metastatic NSCLC harbouring EGFR Exon 20 insertion mutations, whose disease has progressed on, or after platinum-based chemotherapy⁵⁰. As many tumors overexpress MET in order to escape EGFR blockade⁵¹, it is assumed that Amivantamab prevents this escape and, consequently, enhances treatment efficacy. Nevertheless, owing to a low-fucose-containing Fc-part, this BsAb is also more adept at inducing ADCC than antibodies with traditional Fc-parts^{48,52}. Hence, a combination of both effects may have contributed to the clinical success of this BsAb⁵².

Further Opportunities for bispecific antibodies on the example of regulatory T-cells:

The clinical success of the currently approved BsAbs encouraged the development of even more BsAbs. Furthermore, bsAbs are currently tested as potential therapy in fields like autoimmune and inflammatory disease⁵³ or as treatment for infectious diseases, such as SARS-CoV2⁵⁴. In this review, as a representative example, we will further focus on the generation of cis-binding BsAb, with a special outlook on Tregs targeting in cancer (Table 2).

- Regulatory T-cell biology:

Regulatory T-cells (Tregs) populations play a pivotal role in preserving an immune balance between self-tolerance and effector responses⁵⁵. Their dysfunction causes severe autoimmune disease⁵⁶. The concept of suppressor T cells was first described in 1970 by Gershon and Kondo⁵⁷. After several years of research and the discovery of CD25 as a Treg marker in 1995, Treg populations became substantially better characterized⁵⁶. Currently, Tregs are defined as a highly immunosuppressive subset of CD4⁺ T cells that dampen excessive immune responses and maintain immune homeostasis by inhibiting effector T cells (Teff) proliferation and cytokine production, hence preventing the development of autoimmune diseases and tissue

destruction⁵⁸. FOXP3 was defined as the hallmark transcription factor of Tregs. Genetic alterations of FOXP3 expression induce Treg cell deficiency, causing severe autoimmune disorders, allergy and inflammation⁵⁹⁻⁶¹. Hence, enhancing Treg function is currently seen as an attractive approach for the treatment of autoimmune diseases⁶². On the other hand, Tregs have also been identified as a critical cell type interfering with anti-tumor immune responses and several studies have shown that a high frequency of tumor-infiltrating Tregs in combination with low frequency of T effector cells, resulting in a low Teff/Treg ratio, is correlated with a poor prognosis for cancer patients and tumor immunotherapy^{63,64}. In particular, in the context of CTLA-4 and PD-1 immune checkpoint inhibitor (ICI) treatments, it became apparent that Tregs play an important role in ICI resistance^{65,66}. Therefore, there is a need to find Treg targeting strategies. However, an exclusive Treg cell surface marker is currently not known. Several monoclonal antibodies described to specifically target intra-tumoral Tregs in mice, failed to be effective in a clinical setting. This failure is based in part on the difference in biology of these receptors between species. In mice, anti-CTLA-4 antibodies preferentially deplete tumor-infiltrating Tregs by activating FcγR binding^{67,68}. In contrast, in humans, anti-CTLA-4 treatment shows controversial results: a reduction of Treg intratumorally but collateral effects in secondary lymphoid organs^{69,70}. Other monoclonal antibodies have been described to target Tregs in mice but fail to show effects in clinical trials. For instance, Daclizumab (an anti-CD25 mAb aimed to target Tregs) had to be withdrawn from the market for MS treatment following induction of severe liver failure in some treated patients⁷¹.

Therefore, it has become a rather appealing approach to target specifically intra-tumoral Treg populations with BsAb with the aim to enhance the specificity of Treg targeting with an appropriate combination of two independent antigens expressed on Treg cell surfaces.

Regulatory T-cell expressed cell surface markers:

Tregs express a number of different cell surface markers. Most of these are shared by other activated T-cells. Nevertheless, the most promising



approaches for BsAbs targeting specifically Tregs have been focused on a combination of the following receptors:

- CTLA-4 (CD152): CTLA-4 is an inhibitory receptor relative of the T cell costimulatory molecule CD28⁷². However, in contrast to CD28, CTLA-4 suppresses T cell responses upon binding of CD80/CD86⁷³. CTLA-4 is an activation marker transiently expressed on all activated T-cells, but it is constitutively expressed on the Treg cell surface⁷⁴. Mice selectively deficient in CTLA-4 in Treg cells develop systemic lymphoproliferation and fatal autoimmune disease, indicative of its importance for Treg-mediated maintenance of immunological self-tolerance⁷⁵.
- GITR (TNFRSF18/CD357): glucocorticoid-induced tumor necrosis factor receptor-related protein belongs to the costimulatory receptors tumor necrosis factor receptor superfamily (TNFRsf). Also GITR is an activation marker transiently expressed to some extent on all activated T-cells. Nevertheless, GITR is crucial during Treg maturation and mature Tregs highly express it on its surface⁷⁶. It was shown that anti-GITR Ab abrogates the suppressive activity of Tregs^{77,78} and that GITR triggering costimulates Tregs⁷⁹.
- OX-40 (TNFRSF4/CD132): OX-40 belongs to the costimulatory receptors TNFRsf. Similar to GITR, OX-40 is transiently expressed by recently activated T-cells. In Tregs, OX-40 mediated costimulation is important for Treg proliferation and, in contrast to effector T-cells, its expression is maintained in Tregs⁷⁶.
- CD25: There is a constitutively high expression of the IL-2 receptor CD25 on Tregs, allowing Tregs to respond to IL-2 as a requirement for their growth and survival. IL2 binding facilitates immune tolerance in Tregs⁸⁰ and upregulates FOXP3 expression and drive their immunosuppressive phenotype. Due to a lack of Treg function, IL-2 deficient mice die due to the early onset of auto-immune diseases⁸¹. However, CD25 is also a critical activation marker expressed on activated T-cells. Expression level on activated T-cells is lower than on Tregs, but it mediates essential IL-2 induced signals that facilitate effector T-cell survival and proliferation.
- PD-1 (CD279): PD-1 is expressed by T and B cells and has a role in regulating immune responses. It is an immune checkpoint which

downregulates the immune system. In this way, it plays an essential role in the regulation between protective immunity and immunopathology. Consequently, PD-1 deficient mice are prone to develop auto-immune diseases. Its expression on Tregs is critical to maintaining the immunosuppressive activity of these cells⁸².

- CCR4 (CD194): CCR4 is a chemokine receptor expressed on cutaneous T-cells. However, also recently activated, effector Treg cells express elevated levels of it, making it an attractive target for Treg specific depletion⁸³.

Taken together, none of the above-mentioned cell surface markers is uniquely expressed on Tregs. Thus, targeting either of these cell surface markers using monoclonal antibodies has been associated with sometimes rather severe side effects. Therefore, several BsAbs candidates have been designed and undergone first clinical trials. In the following, the currently generated BsAbs against Tregs which are being developed and under study are described.

- ATOR-1015:

ATOR-1015 is a human CTLA-4 x OX40 bispecific IgG1 antibody from Alligator Bioscience. Its BsAb format consists of an appended IgG (anti-OX-40) with single-chain variable fragments (scFv) (anti-CTLA-4) fused to a light chain. CTLA-4 and OX40 are both expressed on activated T cells, however, are expressed to a substantially higher level on Tregs in the tumor microenvironment (TME)^{70,84}. Hence, this antibody was designed to target and deplete Tregs in the TME. It combines a simultaneous blockade of CTLA-4 and an agonistic OX40 binding. The use of an IgG1 isotype enhances ADCC, and this BsAb shows superior ADCC activity compared to the combination of monoclonal antibodies⁸⁵. Thanks to its encouraging results in preclinical studies⁸⁶, a first-in-human phase I clinical trial was performed, indicated for solid tumors and neoplasms (NCT03782467).

- ATOR-1144:

Similar to ATOR-1015, also ATOR-1144 is a humanized bispecific IgG1 antibody. Its BsAb format consists of an appended IgG (anti-GITR) with



single-chain scFv (anti-CTLA-4) fused to the light chain. CTLA-4 and GITR are upregulated on activated T cells, however, yet again, to a substantially higher level on Tregs in the TME⁸⁷. In order to target and deplete Tregs in TME a simultaneous blockade of CTLA-4 was combined with GITR agonistic binding. ATOR-1144 was developed for treatment of solid tumors and hematological malignancies. In preclinical testing, ATOR-1144 showed Treg depletion via ADCC and the activation of effector T and NK cells within the tumor^{88,89}.

- KY1055:

It is a human ICOS x PD-L1 bispecific IgG1 antibody produced by Kymab. a human IgG1 format that consists of fully human Fab arms targeting ICOS and a modified Fc (Fcab) targeting PD-L1. ICOS is a co-stimulatory molecule transiently expressed on activated T cells and constitutively by Tregs in the TME⁹⁰. Via a simultaneous PD-L1 and ICOS binding, KY1055 showed higher anti-tumor activity in several syngeneic pre-clinical tumor models compared to the treatment combining both monoclonal antibodies. In these models, KY1055 depleted Tregs and improved Teff/Treg ratio⁹¹.

Table 2. BsAb antibodies generated against Tregs.

Reagent trademark	Compounds (administration)	Indications	NCT (phase) / status	Sponsor	Ref.
ATOR-1015	CTLA-4 x OX40 bispecific (iv)	Solid tumors and neoplasms	NCT03782467 (I) / completed	Alligator Bioscience	(85)
ATOR-1144	CTLA-4 x GITR	Solid tumors and hematological malignancies	-	Alligator Bioscience	(88)
KY1055	ICOS x PD-L1		-	Kymab	(91)

Concluding remarks

The above mentioned BsAb appear rather promising in specifically targeting intra-tumoral Treg populations. All Treg targeting BsAbs for tumor malignancies treatment currently share one common goal: to block or deplete Tregs, specifically within the TME. Given the increased specificity of a combination of two selective targets, the use of BsAbs with isotypes that bind and activate stimulating Fc receptors may potentially have fewer side effects than the use of similar monoclonal antibodies. The BsAbs may trigger an effector response specifically within the TME and might hence enhance the efficacy of treatment. For example, high ADCC with anti-CTLA-4 mAb achieves predominant depletion of Treg cells without many off-target effects on Teff cells as the level of CTLA-4 expression on Treg cells is substantially higher on Tregs than on Teff cells⁶⁹. Nevertheless, developing a BsAb with increased selectivity over two individual mAbs turned out to be rather challenging. In particular, it turned out to be very difficult to lower the binding affinity of an individual antibody moiety sufficiently to prevent unspecific binding to cells that express one antigen only, while at the same time achieving the specific binding of the BsAb to cells that express both antigens. Introducing mutations in the target binding site of an antibody is often complicated and unpredictable, easily leading to entire loss of binding rather than in just lowering it. Furthermore, in particular the selective expression levels of specific receptors expressed on the target cell population is critical for the selection of relevant BsAbs targets^{16,92}. However, the exact prediction of cell surface expression of each target on different cell types within distinct organs and places within the body of patients remains also rather unpredictable. This aspect always raises the possibility of inducing unexpected side-effects in treated patients during clinical trials. Therefore, a number of formidable obstacles remain for BsAb prior to us being able to explore the full potential of their efficacy in clinical settings. Nevertheless, BsAbs are becoming more and more relevant for medical scientists due to the newly provided insights into the huge impact these antibodies can have. This provides new opportunities in the treatment of various diseases. These could include even rather unexpected diseases, as

for instance, most recently, BsAbs have shown surprisingly promising efficacy in the treatment of SARS-CoV-2 infected patients⁵⁴.

Thus, taken together, BsAb may have the great potential to improve treatment efficacy and to reduce side effects in treated patients. This may then open entirely novel treatment opportunities for diseases, such as cancer or autoimmune diseases. Nevertheless, for each BsAb also, daunting challenges may have to be overcome prior to any planned clinical rollout.

Funding

This work was supported by the European Union's Horizon 2020 research and innovation programme under the Marie Skłodowska-Curie grant agreement [grant numbers 765394, 2018].

Disclosure statement

The authors declare no competing interests. Figures created by Biorender.

References

1. Zhang H, Shi N, Diao Z, Chen Y, Zhang Y. Therapeutic potential of TNFalpha inhibitors in chronic inflammatory disorders: Past and future. *Genes Dis.* 2021;8(1):38-47.
2. Chen AY, Wolchok JD, Bass AR. TNF in the era of immune checkpoint inhibitors: friend or foe? *Nat Rev Rheumatol.* 2021;17(4):213-23.
3. Nisonoff A, Wissler FC, Lipman LN. Properties of the major component of a peptic digest of rabbit antibody. *Science.* 1960;132(3441):1770-1.
4. Hosseini SS, Khalili S, Baradaran B, Bidar N, Shahbazi MA, Mosafer J, et al. Bispecific monoclonal antibodies for targeted immunotherapy of solid tumors: Recent advances and clinical trials. *Int J Biol Macromol.* 2021;167:1030-47.
5. DiLillo DJ, Olson K, Mohrs K, Meagher TC, Bray K, Sineshchekova O, et al. A BCMAxCD3 bispecific T cell-engaging antibody demonstrates robust antitumor efficacy similar to that of anti-BCMA CAR T cells. *Blood Adv.* 2021;5(5):1291-304.
6. Tian Z, Liu M, Zhang Y, Wang X. Bispecific T cell engagers: an emerging therapy for management of hematologic malignancies. *J Hematol Oncol.* 2021;14(1):75.
7. Mazor Y, Hansen A, Yang C, Chowdhury PS, Wang J, Stephens G, et al. Insights into the molecular basis of a bispecific antibody's target selectivity. *MAbs.* 2015;7(3):461-9.
8. Byrne H, Conroy PJ, Whisstock JC, O'Kennedy RJ. A tale of two specificities: bispecific antibodies for therapeutic and diagnostic applications. *Trends Biotechnol.* 2013;31(11):621-32.
9. Labrijn AF, Janmaat ML, Reichert JM, Parren P. Bispecific antibodies: a mechanistic review of the pipeline. *Nat Rev Drug Discov.* 2019;18(8):585-608.
10. Milstein C, Cuello AC. Hybrid hybridomas and their use in immunohistochemistry. *Nature.* 1983;305(5934):537-40.
11. Klein C, Sustmann C, Thomas M, Stubenrauch K, Croasdale R, Schanzer J, et al. Progress in overcoming the chain association issue in bispecific heterodimeric IgG antibodies. *MAbs.* 2012;4(6):653-63.
12. Vukovic N, van Elsas A, Verbeek JS, Zaiss DMW. Isotype selection for antibody-based cancer therapy. *Clin Exp Immunol.* 2021;203(3):351-65.
13. Fan G, Wang Z, Hao M, Li J. Bispecific antibodies and their applications. *J Hematol Oncol.* 2015;8:130.
14. Loffler A, Kufer P, Lutterbuse R, Zettl F, Daniel PT, Schwenkenbecher JM, et al. A recombinant bispecific single-chain antibody, CD19 x CD3, induces rapid and high lymphoma-directed cytotoxicity by unstimulated T lymphocytes. *Blood.* 2000;95(6):2098-103.

15. Rogala B, Freyer CW, Ontiveros EP, Griffiths EA, Wang ES, Wetzler M. Blinatumomab: enlisting serial killer T-cells in the war against hematologic malignancies. *Expert Opin Biol Ther.* 2015;15(6):895-908.
16. Reusch U, Duell J, Ellwanger K, Herbrecht C, Knackmuss SH, Fucek I, et al. A tetravalent bispecific TandAb (CD19/CD3), AFM11, efficiently recruits T cells for the potent lysis of CD19(+) tumor cells. *MAbs.* 2015;7(3):584-604.
17. Bono JSD, Fong L, Beer TM, Gao X, Geynisman DM, III HAB, et al. Results of an ongoing phase 1/2a dose escalation study of HPN424, a tri-specific half-life extended PSMA-targeting T-cell engager, in patients with metastatic castration-resistant prostate cancer (mCRPC). 2021;39(15_suppl):5013-.
18. Wranik BJ, Christensen EL, Schaefer G, Jackman JK, Vendel AC, Eaton D. LUZ-Y, a novel platform for the mammalian cell production of full-length IgG-bispecific antibodies. *J Biol Chem.* 2012;287(52):43331-9.
19. Brinkmann U, Kontermann RE. The making of bispecific antibodies. *MAbs.* 2017;9(2):182-212.
20. Davis JH, Aperlo C, Li Y, Kurosawa E, Lan Y, Lo KM, et al. SEEDbodies: fusion proteins based on strand-exchange engineered domain (SEED) CH3 heterodimers in an Fc analogue platform for asymmetric binders or immunofusions and bispecific antibodies. *Protein Eng Des Sel.* 2010;23(4):195-202.
21. Merchant AM, Zhu Z, Yuan JQ, Goddard A, Adams CW, Presta LG, et al. An efficient route to human bispecific IgG. *Nature Biotechnology.* 1998;16(7):677-81.
22. Huang S, Segues A, Hulsik DL, Zaiss DM, Sijs A, van Duijnhoven SMJ, et al. A novel efficient bispecific antibody format, combining a conventional antigen-binding fragment with a single domain antibody, avoids potential heavy-light chain mispairing. *J Immunol Methods.* 2020;483:112811.
23. Merchant AM, Zhu Z, Yuan JQ, Goddard A, Adams CW, Presta LG, et al. An efficient route to human bispecific IgG. *Nat Biotechnol.* 1998;16(7):677-81.
24. Jackman J, Chen Y, Huang A, Moffat B, Scheer JM, Leong SR, et al. Development of a two-part strategy to identify a therapeutic human bispecific antibody that inhibits IgE receptor signaling. *J Biol Chem.* 2010;285(27):20850-9.
25. Krah S, Schroter C, Eller C, Rhiel L, Rasche N, Beck J, et al. Generation of human bispecific common light chain antibodies by combining animal immunization and yeast display. *Protein Eng Des Sel.* 2017;30(4):291-301.
26. Igawa T, Tsunoda H, Kikuchi Y, Yoshida M, Tanaka M, Koga A, et al. VH/VL interface engineering to promote selective expression and inhibit conformational isomerization of thrombopoietin receptor agonist single-chain diabody. *Protein Eng Des Sel.* 2010;23(8):667-77.

27. Lewis SM, Wu X, Pustilnik A, Sereno A, Huang F, Rick HL, et al. Generation of bispecific IgG antibodies by structure-based design of an orthogonal Fab interface. *Nat Biotechnol.* 2014;32(2):191-8.
28. Bonisch M, Sellmann C, Maresch D, Halbig C, Becker S, Toleikis L, et al. Novel CH1:CL interfaces that enhance correct light chain pairing in heterodimeric bispecific antibodies. *Protein Eng Des Sel.* 2017;30(9):685-96.
29. Schanzer JM, Wartha K, Croasdale R, Moser S, Kunkele KP, Ries C, et al. A novel glycoengineered bispecific antibody format for targeted inhibition of epidermal growth factor receptor (EGFR) and insulin-like growth factor receptor type I (IGF-1R) demonstrating unique molecular properties. *J Biol Chem.* 2014;289(27):18693-706.
30. Shim H. Bispecific Antibodies and Antibody-Drug Conjugates for Cancer Therapy: Technological Considerations. *Biomolecules.* 2020;10(3).
31. Von Kreudenstein TS, Escobar-Carbrera E, Lario PI, D'Angelo I, Brault K, Kelly J, et al. Improving biophysical properties of a bispecific antibody scaffold to aid developability: quality by molecular design. *MAbs.* 2013;5(5):646-54.
32. MERIC-BERNSTAM F, HAMILTON EP, BEERAM M, HANNA DL, EL-KHOUEIRY AB, KANG Y-K, et al. Zanidatamab (ZW25) in HER2-expressing gastroesophageal adenocarcinoma (GEA): Results from a phase I study. *Journal of Clinical Oncology.* 2021;39(3_suppl):164-.
33. Yoon A, Lee S, Lee S, Lim S, Park YY, Song E, et al. A Novel T Cell-Engaging Bispecific Antibody for Treating Mesothelin-Positive Solid Tumors. *Biomolecules.* 2020;10(3).
34. Wu Y, Yi M, Zhu S, Wang H, Wu K. Recent advances and challenges of bispecific antibodies in solid tumors. *Exp Hematol Oncol.* 2021;10(1):56.
35. Zhou P, Zhang J, Yan Y, inventors; WUHAN YZY BIOPHARMA CO Ltd, assignee. Bispecific antibody2012 2017-02-07.
36. Cui Y, Huang Z, Chen H, Zhang X, Qi B, Yan X, inventors; Itabmed Hk Ltd, assignee. Multispecific fab fusion proteins and use thereof. United States2016.
37. van der Neut Kofschoten M, Schuurman J, Losen M, Bleeker WK, Martinez-Martinez P, Vermeulen E, et al. Anti-inflammatory activity of human IgG4 antibodies by dynamic Fab arm exchange. *Science.* 2007;317(5844):1554-7.
38. Labrijn AF, Meesters JI, de Goeij BE, van den Bremer ET, Neijssen J, van Kampen MD, et al. Efficient generation of stable bispecific IgG1 by controlled Fab-arm exchange. *Proc Natl Acad Sci U S A.* 2013;110(13):5145-50.
39. Zhang Z, Luo F, Cao J, Lu F, Zhang Y, Ma Y, et al. Anticancer bispecific antibody R&D advances: a study focusing on research trend worldwide and in China. *J Hematol Oncol.* 2021;14(1):124.

40. FDA. Bispecific Antibody Development Programs Guidance for Industry. In: Services USDoHaH, Administration FaD, (CDER) CfDEaR, (CBER) CfBEaR, editors. 2021.
41. Chelius D, Ruf P, Gruber P, Ploscher M, Liedtke R, Gansberger E, et al. Structural and functional characterization of the trifunctional antibody catumaxomab. *MABs*. 2010;2(3):309-19.
42. Seimetz D. Novel monoclonal antibodies for cancer treatment: the trifunctional antibody catumaxomab (removab). *J Cancer*. 2011;2:309-16.
43. Uchida N, Sambe T, Yoneyama K, Fukazawa N, Kawanishi T, Kobayashi S, et al. A first-in-human phase 1 study of ACE910, a novel factor VIII-mimetic bispecific antibody, in healthy subjects. *Blood*. 2016;127(13):1633-41.
44. Kitazawa T, Esaki K, Tachibana T, Ishii S, Soeda T, Muto A, et al. Factor VIIIa-mimetic cofactor activity of a bispecific antibody to factors IX/IXa and X/Xa, emicizumab, depends on its ability to bridge the antigens. *Thromb Haemost*. 2017;117(7):1348-57.
45. Kitazawa T, Igawa T, Sampei Z, Muto A, Kojima T, Soeda T, et al. A bispecific antibody to factors IXa and X restores factor VIII hemostatic activity in a hemophilia A model. *Nat Med*. 2012;18(10):1570-4.
46. Löffler A, Kufer P, Lutterbüse R, Zettl F, Daniel PT, Schwenkenbecher JM, et al. A recombinant bispecific single-chain antibody, CD19 × CD3, induces rapid and high lymphoma-directed cytotoxicity by unstimulated T lymphocytes. *Blood*. 2000;95(6):2098-103.
47. Goebeler ME, Bargou R. Blinatumomab: a CD19/CD3 bispecific T cell engager (BiTE) with unique anti-tumor efficacy. *Leuk Lymphoma*. 2016;57(5):1021-32.
48. Moores SL, Chiu ML, Bushey BS, Chevalier K, Luistro L, Dorn K, et al. A Novel Bispecific Antibody Targeting EGFR and cMet Is Effective against EGFR Inhibitor-Resistant Lung Tumors. *Cancer Res*. 2016;76(13):3942-53.
49. Castoldi R, Ecker V, Wiehle L, Majety M, Busl-Schuller R, Asmussen M, et al. A novel bispecific EGFR/Met antibody blocks tumor-promoting phenotypic effects induced by resistance to EGFR inhibition and has potent antitumor activity. *Oncogene*. 2013;32(50):5593-601.
50. Vijayaraghavan S, Lipfert L, Chevalier K, Bushey BS, Henley B, Lenhart R, et al. Amivantamab (JNJ-61186372), an Fc Enhanced EGFR/cMet Bispecific Antibody, Induces Receptor Downmodulation and Antitumor Activity by Monocyte/Macrophage Trophocytosis. *Molecular Cancer Therapeutics*. 2020;19(10):2044.
51. Kalyankrishna S, Grandis JR. Epidermal Growth Factor Receptor Biology in Head and Neck Cancer. *Journal of Clinical Oncology*. 2006;24(17):2666-72.

52. Grugan KD, Dorn K, Jarantow SW, Bushey BS, Pardinas JR, Laquerre S, et al. Fc-mediated activity of EGFR x c-Met bispecific antibody JNJ-61186372 enhanced killing of lung cancer cells. *MAbs*. 2017;9(1):114-26.
53. Zhao Q. Bispecific Antibodies for Autoimmune and Inflammatory Diseases: Clinical Progress to Date. *BioDrugs*. 2020;34(2):111-9.
54. De Gasparo R, Pedotti M, Simonelli L, Nickl P, Muecksch F, Cassaniti I, et al. Bispecific IgG neutralizes SARS-CoV-2 variants and prevents escape in mice. *Nature*. 2021;593(7859):424-8.
55. Sakaguchi S, Miyara M, Costantino CM, Hafler DA. FOXP3+ regulatory T cells in the human immune system. *Nat Rev Immunol*. 2010;10(7):490-500.
56. Sakaguchi S, Sakaguchi N, Asano M, Itoh M, Toda M. Immunologic self-tolerance maintained by activated T cells expressing IL-2 receptor alpha-chains (CD25). Breakdown of a single mechanism of self-tolerance causes various autoimmune diseases. *J Immunol*. 1995;155(3):1151-64.
57. Gershon RK, Kondo K. Cell interactions in the induction of tolerance: the role of thymic lymphocytes. *Immunology*. 1970;18(5):723-37.
58. Yang S, Wang J, Brand DD, Zheng SG. Role of TNF-TNF Receptor 2 Signal in Regulatory T Cells and Its Therapeutic Implications. *Front Immunol*. 2018;9:784.
59. Brunkow ME, Jeffery EW, Hjerrild KA, Paepfer B, Clark LB, Yasayko SA, et al. Disruption of a new forkhead/winged-helix protein, scurfy, results in the fatal lymphoproliferative disorder of the scurfy mouse. *Nat Genet*. 2001;27(1):68-73.
60. Wildin RS, Ramsdell F, Peake J, Faravelli F, Casanova J-L, Buist N, et al. X-linked neonatal diabetes mellitus, enteropathy and endocrinopathy syndrome is the human equivalent of mouse scurfy. *Nature Genetics*. 2001;27(1):18-20.
61. Bennett CL, Christie J, Ramsdell F, Brunkow ME, Ferguson PJ, Whitesell L, et al. The immune dysregulation, polyendocrinopathy, enteropathy, X-linked syndrome (IPEX) is caused by mutations of FOXP3. *Nat Genet*. 2001;27(1):20-1.
62. Eggenhuizen PJ, Ng BH, Ooi JD. Treg Enhancing Therapies to Treat Autoimmune Diseases. *Int J Mol Sci*. 2020;21(19).
63. Shang B, Liu Y, Jiang SJ, Liu Y. Prognostic value of tumor-infiltrating FoxP3+ regulatory T cells in cancers: a systematic review and meta-analysis. *Sci Rep*. 2015;5:15179.
64. Sato E, Olson SH, Ahn J, Bundy B, Nishikawa H, Qian F, et al. Intraepithelial CD8+ tumor-infiltrating lymphocytes and a high CD8+/regulatory T cell ratio are associated with favorable prognosis in ovarian cancer. *Proc Natl Acad Sci U S A*. 2005;102(51):18538-43.

65. Maj T, Wang W, Crespo J, Zhang H, Wang W, Wei S, et al. Oxidative stress controls regulatory T cell apoptosis and suppressor activity and PD-L1-blockade resistance in tumor. *Nat Immunol.* 2017;18(12):1332-41.
66. Jie HB, Schuler PJ, Lee SC, Srivastava RM, Argiris A, Ferrone S, et al. CTLA-4(+) Regulatory T Cells Increased in Cetuximab-Treated Head and Neck Cancer Patients Suppress NK Cell Cytotoxicity and Correlate with Poor Prognosis. *Cancer Res.* 2015;75(11):2200-10.
67. Simpson TR, Li F, Montalvo-Ortiz W, Sepulveda MA, Bergerhoff K, Arce F, et al. Fc-dependent depletion of tumor-infiltrating regulatory T cells co-defines the efficacy of anti-CTLA-4 therapy against melanoma. *J Exp Med.* 2013;210(9):1695-710.
68. Selby MJ, Engelhardt JJ, Quigley M, Henning KA, Chen T, Srinivasan M, et al. Anti-CTLA-4 Antibodies of IgG2a Isotype Enhance Antitumor Activity through Reduction of Intratumoral Regulatory T Cells. *Cancer Immunology Research.* 2013;1(1):32.
69. Ha D, Tanaka A, Kibayashi T, Tanemura A, Sugiyama D, Wing JB, et al. Differential control of human Treg and effector T cells in tumor immunity by Fc-engineered anti-CTLA-4 antibody. *Proc Natl Acad Sci U S A.* 2019;116(2):609-18.
70. Arce Vargas F, Furness AJS, Litchfield K, Joshi K, Rosenthal R, Ghorani E, et al. Fc Effector Function Contributes to the Activity of Human Anti-CTLA-4 Antibodies. *Cancer Cell.* 2018;33(4):649-63 e4.
71. Stettner M, Gross CC, Mausberg AK, Pul R, Junker A, Baba HA, et al. A fatal case of daclizumab-induced liver failure in a patient with MS. *Neurology - Neuroimmunology Neuroinflammation.* 2019;6(2):e539.
72. Lenschow DJ, Walunas TL, Bluestone JA. CD28/B7 system of T cell costimulation. *Annu Rev Immunol.* 1996;14:233-58.
73. Pentcheva-Hoang T, Egen JG, Wojnoonski K, Allison JP. B7-1 and B7-2 selectively recruit CTLA-4 and CD28 to the immunological synapse. *Immunity.* 2004;21(3):401-13.
74. Takahashi T, Tagami T, Yamazaki S, Uede T, Shimizu J, Sakaguchi N, et al. Immunologic self-tolerance maintained by CD25(+)CD4(+) regulatory T cells constitutively expressing cytotoxic T lymphocyte-associated antigen 4. *J Exp Med.* 2000;192(2):303-10.
75. Wing K, Onishi Y, Prieto-Martin P, Yamaguchi T, Miyara M, Fehervari Z, et al. CTLA-4 control over Foxp3+ regulatory T cell function. *Science.* 2008;322(5899):271-5.
76. Mahmud SA, Manlove LS, Schmitz HM, Xing Y, Wang Y, Owen DL, et al. Costimulation via the tumor-necrosis factor receptor superfamily couples TCR signal strength to the thymic differentiation of regulatory T cells. *Nat Immunol.* 2014;15(5):473-81.

77. Shimizu J, Yamazaki S, Takahashi T, Ishida Y, Sakaguchi S. Stimulation of CD25(+)CD4(+) regulatory T cells through GITR breaks immunological self-tolerance. *Nat Immunol.* 2002;3(2):135-42.
78. McHugh RS, Whitters MJ, Piccirillo CA, Young DA, Shevach EM, Collins M, et al. CD4(+)CD25(+) immunoregulatory T cells: gene expression analysis reveals a functional role for the glucocorticoid-induced TNF receptor. *Immunity.* 2002;16(2):311-23.
79. Ronchetti S, Zollo O, Bruscoli S, Agostini M, Bianchini R, Nocentini G, et al. GITR, a member of the TNF receptor superfamily, is costimulatory to mouse T lymphocyte subpopulations. *Eur J Immunol.* 2004;34(3):613-22.
80. Malek TR. The biology of interleukin-2. *Annu Rev Immunol.* 2008;26:453-79.
81. Zeiser R, Negrin RS. Interleukin-2 receptor downstream events in regulatory T cells: implications for the choice of immunosuppressive drug therapy. *Cell Cycle.* 2008;7(4):458-62.
82. Sharpe AH, Pauken KE. The diverse functions of the PD1 inhibitory pathway. *Nat Rev Immunol.* 2018;18(3):153-67.
83. Kurose K, Ohue Y, Wada H, Iida S, Ishida T, Kojima T, et al. Phase Ia Study of FoxP3+ CD4 Treg Depletion by Infusion of a Humanized Anti-CCR4 Antibody, KW-0761, in Cancer Patients. *Clin Cancer Res.* 2015;21(19):4327-36.
84. Montler R, Bell RB, Thalhofer C, Leidner R, Feng Z, Fox BA, et al. OX40, PD-1 and CTLA-4 are selectively expressed on tumor-infiltrating T cells in head and neck cancer. *Clin Transl Immunology.* 2016;5(4):e70.
85. Kvarnhammar AM, Veitonmaki N, Hagerbrand K, Dahlman A, Smith KE, Fritzell S, et al. The CTLA-4 x OX40 bispecific antibody ATOR-1015 induces anti-tumor effects through tumor-directed immune activation. *J Immunother Cancer.* 2019;7(1):103.
86. Yachnin J, Ullenhag GJ, Carneiro A, Nielsen D, Rohrberg KS, Kvarnhammar AM, et al. A first-in-human phase I study in patients with advanced and/or refractory solid malignancies to evaluate the safety of ATOR-1015, a CTLA-4 x OX40 bispecific antibody. *Journal of Clinical Oncology.* 2020;38(15_suppl):3061-.
87. Pedroza-Gonzalez A, Verhoef C, Ijzermans JN, Peppelenbosch MP, Kwekkeboom J, Verheij J, et al. Activated tumor-infiltrating CD4+ regulatory T cells restrain antitumor immunity in patients with primary or metastatic liver cancer. *Hepatology.* 2013;57(1):183-94.
88. Fritzell S, Levin M, Åberg I, Johansson M, Winnerstam M, Smith KE, et al. Abstract 4077: ATOR-1144 is a tumor-directed CTLA-4 x GITR bispecific antibody that acts by depleting Tregs and activating effector T cells and NK cells. *Cancer Research.* 2019;79(13 Supplement):4077.

89. Millan-Perez Pena L, Martin PS, Herrera-Camacho I, Bandala C, Anaya-Ruiz M. Colon carcinoma treatment using bispecific anti-GITR/CTLA-4 antibodies: a patent evaluation of WO2018091739. *Expert Opin Ther Pat.* 2020;30(5):307-11.
90. Nagase H, Takeoka T, Urakawa S, Morimoto-Okazawa A, Kawashima A, Iwahori K, et al. ICOS(+) Foxp3(+) TILs in gastric cancer are prognostic markers and effector regulatory T cells associated with *Helicobacter pylori*. *Int J Cancer.* 2017;140(3):686-95.
91. Sainson RC, Parveen N, Borhis G, Kosmac M, Okell T, Taggart E, et al. Abstract LB-153: KY1055, a novel ICOS-PD-L1 bispecific antibody, efficiently enhances T cell activation and delivers a potent anti-tumour response in vivo. *Cancer Research.* 2018;78(13 Supplement):LB-153.
92. Chen K-J, Lin S-Z, Zhou L, Xie H-Y, Zhou W-H, Taki-Eldin A, et al. Selective Recruitment of Regulatory T Cell through CCR6-CCL20 in Hepatocellular Carcinoma Fosters Tumor Progression and Predicts Poor Prognosis. *PLOS ONE.* 2011;6(9):e24671.



3

Shortened hinge design of Fab x sdAb-Fc bispecific antibodies enhances redirected T-cell killing of tumor cells

Shuyu Huang^{1,2,†}, Aina Segués^{1,2,†}, Martin Waterfall¹, David Wright¹, Charlotte Vayssiere¹, Sander M. J. van Duijnhoven³, Andrea van Elsas⁴, Alice J. A. M. Sijts² and Dietmar M. Zaiss^{1,5,6,7,*}

¹ *Institute of Immunology and Infection Research, School of Biological Sciences, University of Edinburgh, Edinburgh EH9 3FL, UK; s.huang@uu.nl (S.H.); asegues@ed.ac.uk (A.S.); mwaterfa@ed.ac.uk (M.W.); david.wright@ed.ac.uk (D.W.); ch.6.phenix@icloud.com (C.V.)*

² *Faculty of Veterinary Medicine, Department of Infectious Diseases and Immunology, Utrecht University, 3584 CS Utrecht, The Netherlands; e.j.a.m.sijts@uu.nl (A.J.S)*

³ *ImmunoPrecise Antibodies Ltd., 5349 AB Oss, The Netherlands; svanduijnhoven@ipatherapeutics.com*

⁴ *Third Rock Ventures, San Francisco, CA 94158, USA; avanelzas@thirdrockventures.com*

⁵ *Department of Immune Medicine, University Regensburg, 93053 Regensburg, Germany*

⁶ *Institute of Clinical Chemistry and Laboratory Medicine, University Hospital Regensburg, 93053 Regensburg, Germany*

⁷ *Institute of Pathology, University Regensburg, 93053 Regensburg, Germany*

* *Correspondence: dietmar.zaiss@ukr.de*

† *These authors contributed equally to this work.*

Biomolecules 2022, 12, 1331.

<https://doi.org/10.3390/biom12101331>

Contribution statement: *Aina Segués Cisteró designed and performed the experiments. Aina Segués Cisteró contributed to the analysis of the flow cytometry data and the interpretation of the results.*

Abstract

T cell engager (TCE) antibodies have emerged as promising cancer therapeutics that link cytotoxic T-cells to tumor cells by simultaneously binding to CD3E on T-cells and to a tumor-associated antigen (TAA) expressed by tumor cells. We previously reported a novel bispecific format, the IgG-like Fab x sdAb-Fc (also known as half-Ig_VH-h-CH2-CH3), combining a conventional antigen-binding fragment (Fab) with a single domain antibody (sdAb). Here, we evaluated this Fab x sdAb-Fc format as a T-cell redirecting bispecific antibody (TbsAbs) by targeting mEGFR on tumor cells and mCD3E on T cells. We focused our attention specifically on the hinge design of the sdAb arm of the bispecific antibody. Our data show that a TbsAb with a shorter hinge of 23 amino acids (TbsAb.short) showed a significantly better T cell redirected tumor cell elimination than the TbsAb with a longer, classical antibody hinge of 39 amino acids (TbsAb.long). Moreover, the TbsAb.short form mediated better T cell-tumor cell aggregation and increased CD69 and CD25 expression levels on T cells more than the TbsAb.long form. Taken together, our results indicate that already minor changes in the hinge design of TbsAbs can have significant impact on the anti-tumor activity of TbsAbs and may provide a new means to improve their potency.

Keywords: bispecific antibody; cancer immunotherapy; mCD3E; mEGFR; hinge

Introduction

T-cell engager antibodies (TCEs) redirect cytotoxic T-cells to tumor cells by simultaneously binding to a component of the TCR complex (commonly CD3E) and a tumor associated antigen (TAA) on tumor cells¹. Due to the clinical success of the bispecific T-cell engager (BiTE) blinatumomab, approved by the FDA in 2014^{2,3}, the majority of bispecific antibodies (BsAbs) in clinical development are currently TCEs⁴. TCEs can further be classified into two broad classes according to their formats: IgG-like or fragment-based TCEs. Currently, the IgG-like T cell redirecting bispecific antibodies (TbsAbs) being the most widely used form, largely due to their longer in vivo serum half-life due to the presence of an Fc region⁵.

Although the concept of BsAbs has a long history, due to challenges in BsAb manufacturing, they only began to stimulate the interest of pharmaceutical companies in the past decade. The production of IgG-like BsAbs requires the correct assembly of antibody's light and heavy chain fragments. A random assembly of four distinctive polypeptide chains may result in 16 combinations⁶. Therefore, in order to manufacture IgG-like BsAb that can reliably be assembled, it is required to ensure the selective formation of the heterodimerized heavy chains (HCs) and the proper pairing of the light chains of each arm with the cognate HC⁷. Multiple recombinant technologies have been developed to ensure the correct formation of IgG-like bispecific antibodies. In our previous study, we developed a novel Fab x sdAb-Fc format which combined a single domain antibody (sdAb) with a conventional antigen-binding fragment (Fab)⁸. Both arms were linked to an Fc domain optimized for heavy-heavy chain heterodimerization by the introduction of matched amino acid mutations, thus ensuring both correct heavy-chain and heavy-light chain assembly⁸. However, the hinge between sdAb and Fc can be designed in various ways, dependent on different applications. Previous studies demonstrated a direct role of the distance between TAA and CD3E binding sites of TbsAbs on T-cell mediated tumor cell lysis^{9,10}. In these applications, the authors modulated their format using various approaches with the common objective of shortening the distance between the two arms of TbsAbs which resulted in improved tumor cell lysis¹¹⁻¹⁴. Additional

studies looked at the correlation between the length of effector/target cell synapse distance and T-cell mediated tumor killing by alternative strategies, such as tumor antigen epitope distance to the cancer cell membrane or the overall size of the antigen, which can increase the distance between the effector and target cell⁹. Thereby, it has become apparent that TbsAbs that bind to membrane-distal epitopes extend the intermembrane spacing resulting in decreased tumor killing compared to TbsAbs that bind membrane-proximal epitopes¹⁵⁻¹⁹. Additionally, the size of the targeted antigen can also effectively increase the distance within the synapse between the T-cell and target cell and has been shown to affect TbsAb potency^{15,16}. In particular, it was noticed that the IgG hinge region in different IgG subclasses was a major modulator of antibody function. IgG3 molecules have an extended hinge region of 62 amino acids. This long hinge provides superior flexibility and leads to improved phagocytosis. In contrast, other IgG molecules have shorter and less flexible hinge regions, which was associated with improved antibody-dependent cellular cytotoxicity²⁰. These findings suggested that the size of the hinge between the heavy chain and the Fab arm may determine the flexibility of the antibody and therefore the cytotoxic effector functions of it. Therefore, we hypothesized that TbsAbs in the Fab x sdAb-Fc format may benefit from a short hinge design.

To address this hypothesis, we constructed and evaluated TbsAbs targeting mouse EGFR and mouse CD3E with two different hinge region lengths connecting the mEGFR binding domain and its cognate constant region. The longer hinge TbsAb (TbsAb.long) format was designed to mimic the distance between two binding sites of conventional IgG format TbsAb, while the shorter hinge TbsAb (TbsAb.short) was designed to minimize the distance between two binding sites. Our results demonstrated that the efficiency of T cell redirected tumor cell killing directly correlated with the proximity of mEGFR and mCD3E binding regions in Fab x sdAb-Fc TbsAbs.

Results

Designing and preparation of mCD3E x mEGFR TbsAbs with different hinges

In order to avoid potential heavy-light chain mispairing during BsAb expression, we previously suggested a novel Fab x sdAb-Fc bispecific antibody format⁸. To further investigate this novel antibody format, we designed and expressed TbsAbs, using a mCD3E Fab-Fc combined with an mEGFR sdAb-Fc with two different hinges. The design of the shorter hinge (23 amino acids in total) was based on the natural mouse IgG2a hinge sequence, with the exception of an Arginine residue at position 3 which we replaced with a lysine residue in order to stabilize the sdAb²¹. The longer hinge (39 amino acids in total) was designed as a chimer hinge based on a combination between a mouse IgG2a hinge and a part of the llama hinge. This resulted in 16 additional amino acids compared with the shorter hinge and mimicked the length of an entire CH1 domain (starts at the end of the hinge and ends with VDKKI, approximately 32.6 Å, Fig. S2)²², in this way, extending the length of the sdAb arm to a similar length of a conventional Fab (Fig. 1A).

To abrogate Fc-FcR mediated effector functions without affecting affinity, LALAPG mutations were introduced to each parental antibody (anti-mCD3E, clone 2c11; anti-mEGFR, clone RR359)²³. The mCD3E x mEGFR TbsAb with a long hinge (TbsAb.long) and mCD3E x mEGFR TbsAb with a short hinge (TbsAb.short) were then constructed by performing controlled Fab-arm exchange (cFAE) based on the duobody platform (Fig. 1B,C).

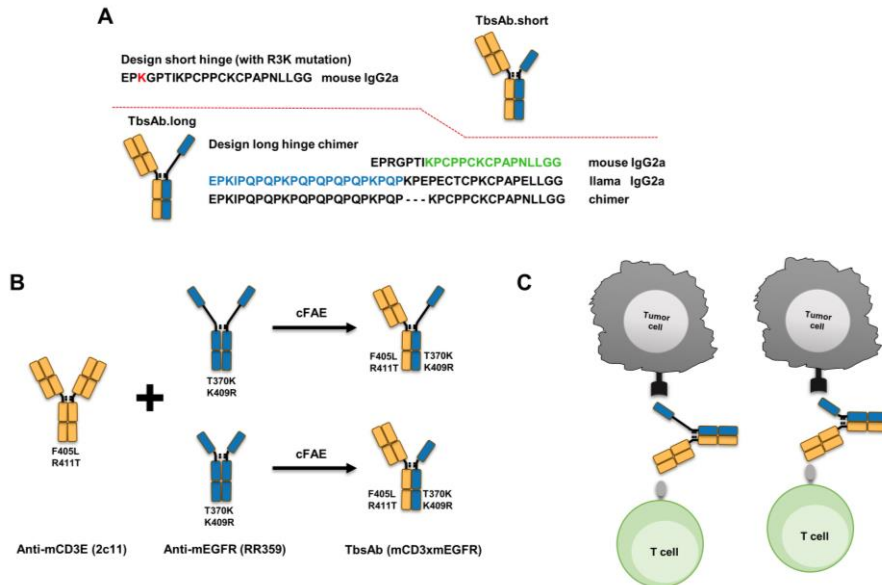


Figure 1. Preparation of Fab x sdAb-Fc TbsAbs with different hinge designs. (A) Schematic diagrams of two types of Fab x sdAb-Fc TbsAbs: TbsAb.long, TbsAb.short. (B) Schematic illustration of mCD3E x mEGFR TbsAbs generated by the duobody platform. (C) Schematic diagrams of tumor cell eliminated by mCD3E x mEGFR TbsAbs.

The purity of each expressed TbsAb was analyzed by size-exclusion chromatography (SEC) and sodium dodecyl sulfate–polyacrylamide gel electrophoresis (SDS-PAGE). The monomericity of each parental antibody was >97% (HcAb.RR359.long), >97% (HcAb.RR359.short), and >98% (2c11), respectively (Fig. S1). Following cFAE, a single peak was observed in the resulting SEC for each TbsAb and monomericity evaluated was $\geq 96\%$ (TbsAb.long) and $\geq 99\%$ (TbsAb.short), respectively (Fig. 2A). Under non-reducing SDS-PAGE conditions, the desired TbsAbs showed a predominant band with an MW of ~ 125 kDa, whereas parental antibodies showed predominant bands with an MW of ~ 95 kDa or ~ 165 kDa, respectively (Fig. 2B). For TbsAb.long and TbsAb.short, additional minor bands were detected at the same size as of parental antibodies, which indicated minor contamination of the parental mEGFR HcAb and mCD3E mAb in the TbsAb.

The purity of TbsAb.long and TbsAb.short were evaluated as ~80.7% and 82.8%, respectively. Under reducing conditions, one band for mEGFR HcAb, two bands for mCD3E mAb and three bands for TbsAbs were detected, as expected (Fig. 2C). The bands just below 63 kDa detected in TbsAbs and mCD3E mAb represent the heavy chain of the mCD3E mAb, while the MW bands just above 48 kDa which are detected in mEGFR HcAb and TbsAbs represent the heavy chain of the mEGFR HcAb. The bands at ~35 kDa detected in TbsAbs and mCD3E mAb represent the light chain of the mCD3E mAb. Taken together, these results demonstrate the successful generation of TbsAbs with long and short hinges.

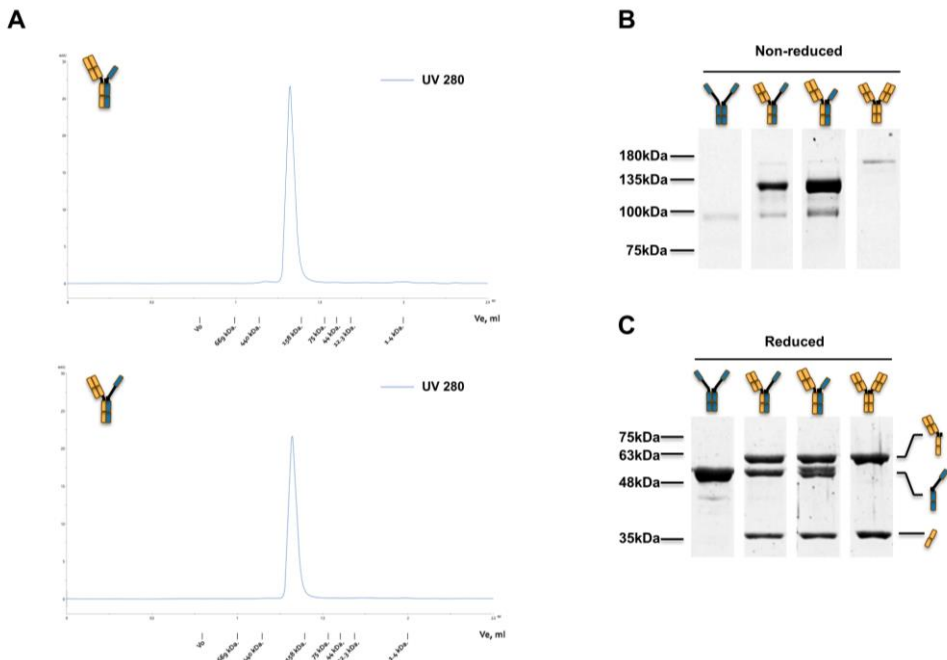


Figure 2. Analysis of the expressed mCD3E x mEGFR TbsAbs. (A) Size exclusion chromatography (SEC) analysis of TbsAb.long and TbsAb.short proteins. Ten μL of each respective sample (TbsAb.long and TbsAb.short), at 0.5 mg/mL were eluted by DPBS buffer at a flow rate of $50 \mu\text{L}\cdot\text{min}^{-1}$. (B,C) SDS-PAGE analysis of TbsAb.long and TbsAb.short proteins under non-reducing and reducing conditions, respectively.

Generation of TbsAb negative control antibody

In order to express an appropriate negative control TbsAb²⁴, we disrupted the binding ability of the mEGFR arm of the TbsAb to mEGFR through site-directed mutagenesis. We started out by evaluating the structure of mEGFR sdAb (RR359) using ColabFold (Fig. 3A and S3)²⁵. By aligning the sequence of mEGFR sdAb to the PDB database, the molecule with PDB ID 5IMMB was found to be the most similar sdAb to mEGFR sdAb, which facilitated the identification of CDR1,2,3 of mEGFR sdAb (Fig. 3B). Given that the CDR3 of the mEGFR sdAb differs most from 5IMMB, we considered it was very likely the region that determined the antibody specificity. Consequently, we performed targeted mutagenesis on this region. Based on the computational analysis of the interactions between sdAb and mEGFR protein by using Discovery Studio software, several amino acids (e.g., Y101, D105, D107, L110, H115 etc.) appeared to be critical for antigen binding. A set of HcAbs containing site-specific mutations were expressed and subsequently affinity to mEGFR recombinant protein was measured by biolayer interferometry using Octet (Fig. S4). The HcAbs with Y101S, D105A or H115K mutation showed no detectable binding to mEGFR protein based on the Octet results (Fig. 3C). Considering the mEGFR recombinant protein might differ in structure from the natural mEGFR, the binding activity of the HcAbs with either Y101S, D105A or H115K mutation were further examined by FACS, using a CHO cell line overexpressing the mEGFR. No binding of the HcAb with D105A mutation in CDR3 was confirmed with CHO/mEGFR cells (Fig. 3D). This version of HcAb was subsequently incorporated into a mCD3E × mEGFR TbsAb by cFAE and used as negative control bispecific antibody (TbsAb.con). The expressed TbsAb.con showed similar purity to the other TbsAbs (Fig. S5) and retained its binding capacity to mCD3E (Fig. 3E).

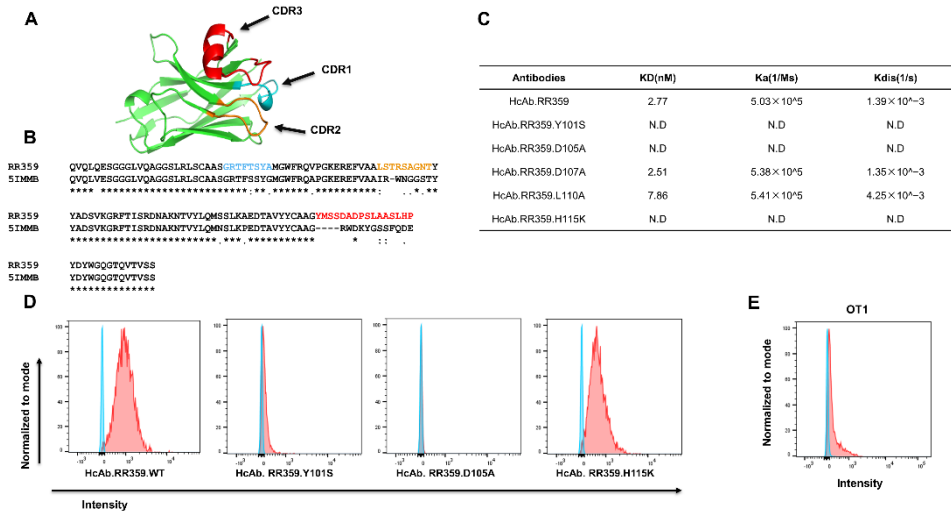


Figure 3. Generation of bispecific negative control antibody by CDR3 mutagenesis. (A) Structure of anti-mEGFR sdAb (RR359) predicted by ColabFold. (B) The sequence of anti-mEGFR sdAb (RR359) aligned to sdAb (5IMMB). The sequence of CDR1 (blue), CDR2 (orange), CDR3 (red) was indicated. (C) The affinity of mutated anti-mEGFR HcAbs measured by Octet. (D) The binding of mutated mEGFR HcAbs to CHO/mEGFR cell line. (E) TbsAb.con (mCD3E x mEGFR.D105A) binds to OT-1 cells detected by flow cytometry. N.D, not detectable. The “*” (asterisk) indicates positions with conserved residues. The “:” (colon) indicates conservation between groups of amino acids with similar properties. The “.” (period) indicates amino acids with weakly similar properties.

mCD3E x mEGFR TbsAb.short molecule mediated enhanced T cell redirected killing in vitro

To investigate the capacity of the purified TbsAb for mEGFR+ cell killing, Lactate dehydrogenase (LDH) release cytotoxicity assays were performed. As target cells in the cytotoxicity assays, different mEGFR+ cell lines were used. In order to determine mEGFR expression level on target cells, ID8, CHO/mEGFR, and CHO/K1 were stained with RR359 and antibody binding was measured by FACS (Fig. 4A). In order to generate an mEGFR-deficient control cell line, CRISPR/Cas9 was performed to disrupt the mEGFR gene on ID8 cells (Fig. 4A). As effector T cells, OT-1s were derived from the spleens

of OT-1 \times *Rag1*^{-/-} mice. OT-1 CD8 T-cells were derived from a C57BL/6 mouse strain, transgenic for a T-cell receptor (TCR) which recognizes an immunodominant ovalbumin-derived epitope. These T-cells can be activated with their cognate antigen, the ovalbumin-derived peptide SIINFEKL. Following a 48 h incubation with the SIINFEKL peptide, activated OT-1 s and target cells were mixed and incubated with each TbsAb for 24 h. At the concentration of 0.02688 nM (0.0032 μ g/mL) of each group, significantly more and bigger T cell clumps were observed in the TbsAb.short-treated group compared to TbsAb.long and TbsAb.con treated groups, which suggested stronger proliferation (T-cell blast) of T cells induced by the TbsAb.short form than by the other two TbsAbs (Fig. 4B,C). Furthermore, the LDH release assay showed higher LDH release in the presence of the TbsAb.short molecules, suggesting that the TbsAb.short form induced better T-cell mediated cytotoxicity towards ID8 and CHO/mEGFR cells than the TbsAb.long form. The TbsAb.con form appeared not to induce any specific cell lysis. In addition, mEGFR negative cell lines, ID8/mEGFR^{-/-} and CHO.K1, showed no specific cell lysis induced in the presence of either the TbsAb.long, the TbsAb.short or the TbsAb.con form (Fig. 4D).

To corroborate these findings, an alternative approach was used to measure tumor cell killing. To this end, ID8 cells and ID8 mEGFR^{-/-} cells were labeled by eFluo 450 or eFluor 670, respectively, and incubated with OT-1 cells at a concentration of 0.02688 nM (0.0032 μ g/mL) for each TbsAb or PBS for 24 h. OT-1 cells were carefully washed off by PBS and adherent ID8 cells were then harvested using trypsin detachment. Flow cytometry was performed to detect live ID8 and ID8 mEGFR^{-/-} cells (Fig. 4E). As shown in Fig. 4F, the TbsAb.short form depleted mEGFR-expressing ID8 cells significantly better than the TbsAb.long form (Fig. 4F).

Taken together, using two different approaches, these data strongly suggest that mCD3E \times mEGFR TbsAb.short molecules mediate better T cell redirected killing than the TbsAb.long form.

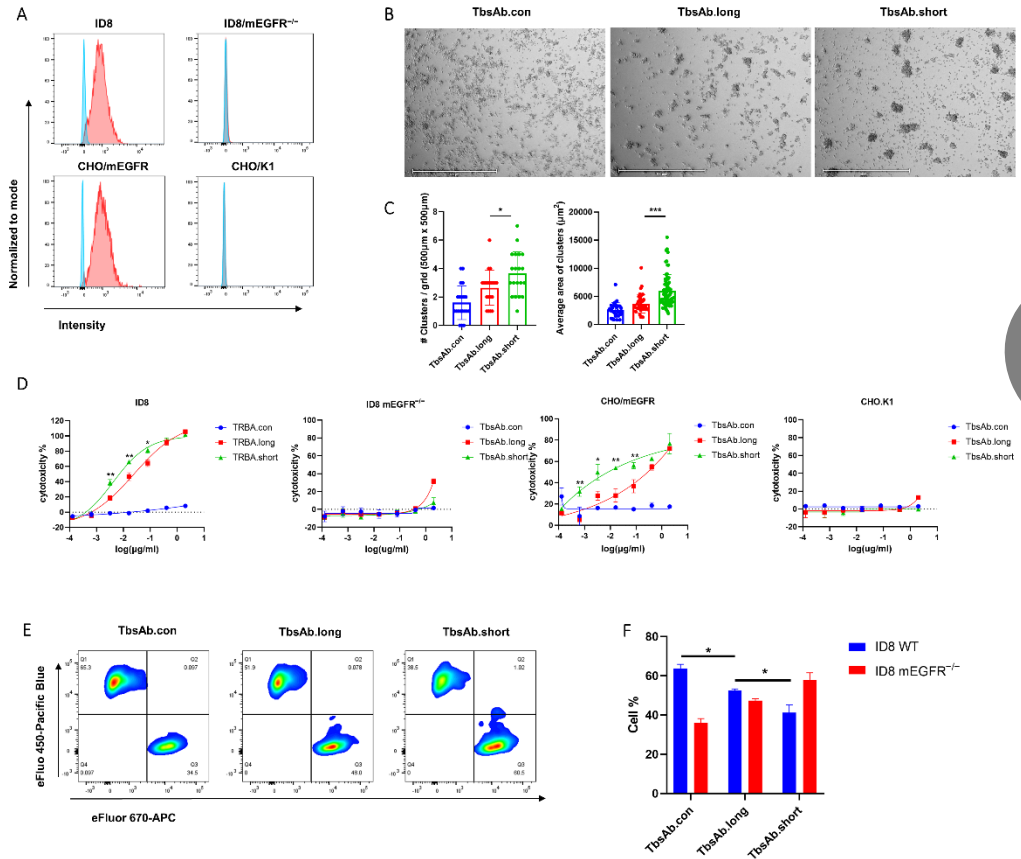


Figure 4. The TbsAb.short form mediates superior T cell mediated cytotoxic. (A) Expression of mEGFR on ID8, ID8/mEGFR^{-/-}, CHO/mEGFR and CHO/K1 cell lines were measured by flow cytometry. (B) OT-1 T cell blasts with CHO/mEGFR cells in the presence of 0.02688 nM (0.0032 µg/mL) of either mCD3E x mEGFR TbsAb.long or TbsAb.short at an E: T ratio of 5:1 following 24 h incubation. Images were obtained under 4 × magnification, and scale bars 650 µm. (C) Quantified number of T cell blasts per grid and average area per T cell blasts by EVOS analysis software. (D) In vitro cytotoxicity assay of mCD3E x mEGFR TbsAbs using LDH release assay. Curves were fitted using a four-parameter logistic fitting with GraphPad Prism 8. (E) In vitro cytotoxicity assay of mCD3E x mEGFR TbsAbs (0.02688 nM, equal to 0.0032 µg/mL) using FACS. (F). Data points represent the mean of three samples; error bars, SD. *: $p < 0.05$; **: $p < 0.01$; ***: $p < 0.001$.

mCD3E × mEGFR TbsAb.short mediated enhanced cell–cell association in vitro

To investigate the underlying mechanisms, which may lead to the improved redirected T cell killing observed with the mCD3E × mEGFR TbsAb.short molecules, we evaluated the ability of the different TbsAbs to induce ID8/OT-1 cell association. Non-activated, naïve OT-1 cells and ID8 cells were used for association and cell aggregation, as measured by FACS. ID8 and OT-1 cells were stained with two different cell-staining dyes and subsequently mixed and incubated with TbsAb.long, TbsAb.short or TbsAb.con. The flow cytometry results showed that a clear cell–cell association was observed with both TbsAb.long and TbsAb.short molecules, but not with the TbsAb.con control construct (Fig. 5A,B). Furthermore, the TbsAb.short molecules could induce more cell aggregates than the TbsAb.long form (up to ~8% of the total cell population in the presence of TbsAb.short molecules compared to ~4% of the cell aggregates in the presence of the TbsAb.long molecules). Such an enhanced level of cell–cell association mediated by TbsAb.short molecules was observed consistently across a range of concentrations of the bispecific antibodies. As expected, the TbsAb.con molecule did not induce the cell–cell association of ID8 and OT-1 cells at any concentration tested (Fig. 5B). Taken together, these data show that the TbsAb.short form has a higher capacity to form cell aggregates than the TbsAb.long form. Compared to ~30% cell aggregates we reported in our previous study and ~5–17% cell aggregates that others have typically reported^{8,18}, the relatively lower percentage of cell aggregates induced in our experiments might be for several reasons. So far, we have not yet followed up on these, nevertheless, several aspects such as the expression level of antigens, the affinity of antibodies used or the geometry of the specific antigens could all influence the efficiency with which such TbsAb molecules can link two different cell populations.

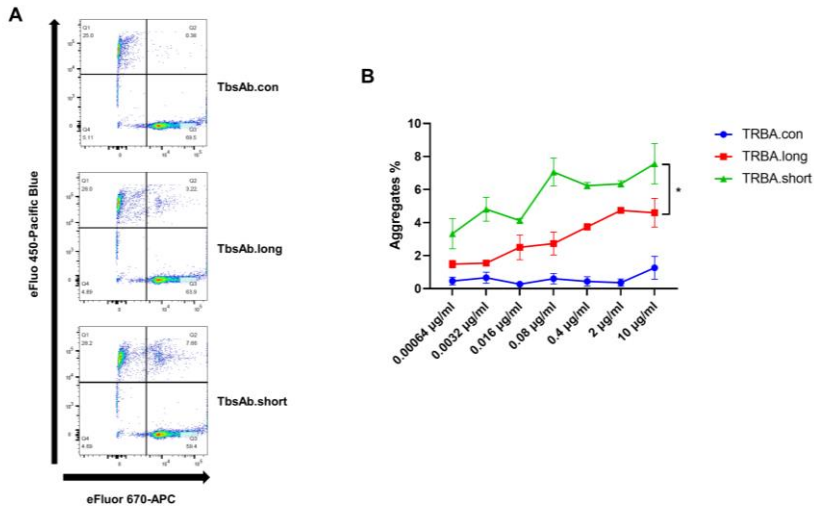


Figure 5. The TbsAb.short form shows better cell aggregate formation than the TbsAb.long form. OT-1 cells were labeled with eFluor 670 dye, and ID8 cells were labeled with the eFluor 450 dye. (A) Cells were incubated for 30 min at room temperature with TbsAb.con, TbsAb.long or TbsAb.short molecules at 0.672 nM (0.08 µg/mL). The OT-1-ID8 cell-cell association was determined using flow cytometry and quantified as the percentage of eFluor 450 and eFluor 670 double positive cells in the upper right quadrant. (B) The experiment was repeated using increasing concentrations for each of the molecules. Each experimental point was set up in duplicate and the mean SD was plotted. *: $p < 0.05$.

mCD3E × mEGFR TbsAb.short mediated enhanced T cell activation in vitro

To investigate to what extent either form of the mCD3E × mEGFR TbsAb could induce T cell activation, splenocytes were mixed with ID8 cells in the presence or absence of the different TbsAb forms and the expression levels of the early activation marker CD69 and of the late activation marker CD25 were determined by flow cytometry on CD4⁺ and CD8⁺ T cells after 24 h of in vitro incubation. Our data show that in the presence of ID8 cells, the expression levels of activation marker CD69 and CD25 were considerably upregulated by the TbsAb.long form as well as by the TbsAb.short form. However, in comparison to the TbsAb.long form, the TbsAb.short form

3

activated a significantly higher fraction of CD4 T cells (Fig. 6A,F). Furthermore, on a single cell level, the TbsAb.short form activated a significantly higher expression levels of CD69 and CD25 per cell (Fig. 6D,I). For CD8 T cells, both TbsAb forms activated a similar fraction of CD8 T-cells (Fig. 6B,G), but the TbsAb.short form induced significantly higher expression levels of CD69 and CD25 than the TbsAb.long form (Fig. 6E,J). Gating strategy is shown in Fig. S6. These data strongly suggest that while both TbsAb can induce T cell activation, the TbsAb with the shorter hinge induced a stronger T cell activation than the TbsAb with the longer hinge.

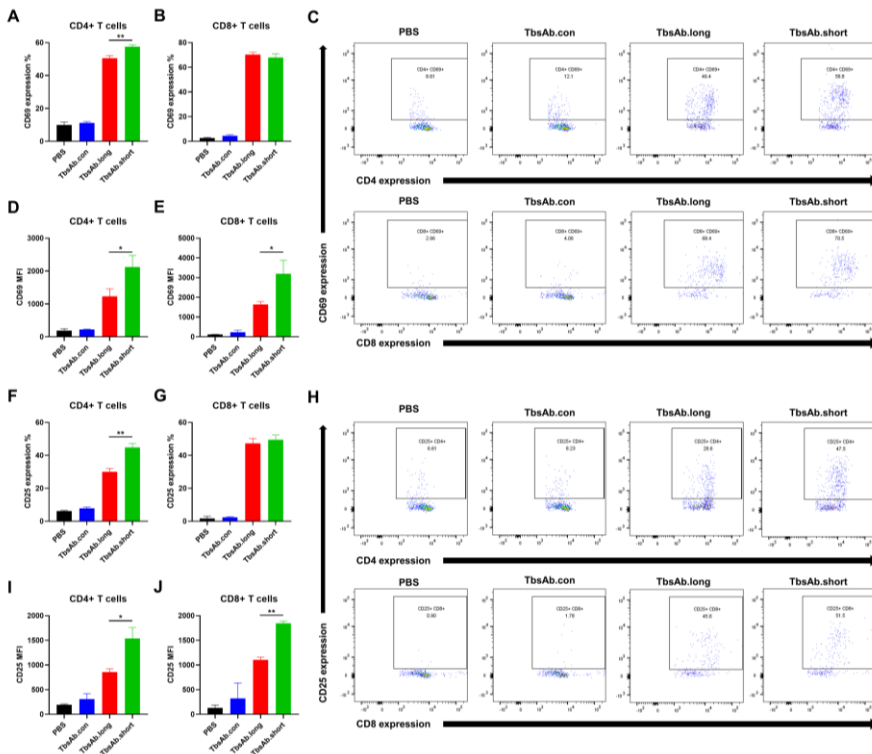


Figure 6. The TbsAb.short form induces superior T cell activation. (A–E) The expression level of CD69 on CD4⁺ and CD8⁺ T cells was detected after incubating with each TbsAb for 24 h (E:T = 5:1). (F–J) The expression level of CD25 on CD4⁺ and CD8⁺ T cells was detected after incubating with each TbsAb for 24 h (E:T = 5:1). *: $p < 0.05$; **: $p < 0.01$.

Discussion

Several different factors have been described that can affect the potency of bispecific T-cell engagers. These include the copy number of the targeted antigen, the size of the antigen, and the distance of the target epitope to the membrane, as well as antibody formats with different sizes, valences, and geometries^{9,10}. In this study, we focused on modulating the distance between T cells and tumor cells, by modulating the hinge region between the heavy chain backbone of the antibody molecule and the Fab arm. To this end, two mCD3E × mEGFR bispecific antibodies with different hinge designs in the Fab x sdAb-Fc format were generated; one with a shorter hinge and one with a longer hinge design. As our results show, the TbsAb.short molecule exhibited significantly greater potency than the TbsAb.long molecule in T-cell redirected killing (Fig. 4D). Furthermore, the TbsAb.short form linked T cells to mEGFR-expressing tumor cells more efficiently than the TbsAb.long form by forming more T cell-tumor cell aggregates. In addition, as measured by CD69 and CD25 expression, T cells appeared to be more strongly activated by the TbsAb.short than by the TbsAb.long format. Since the same antigen recognition specificities were used, the enhancement observed with the TbsAb.short molecule was presumably due to the hinge difference in the molecules. Such a finding is consistent with previous studies. Bluemel and colleagues designed TbsAbs to target different epitopes on human melanoma chondroitin sulfate proteoglycan (hMCSP) and found that the distance of the binding domain to the target cell membrane had a significant impact on the potency of T cell redirecting bispecific antibodies¹⁶. Additionally, several more recent studies, targeting other TAAs such as FcRH5, ROR1, and CD3E, further confirmed that targeting membrane-proximal epitopes, which also shortened the distance between T cells and tumor cells, could improve the in vitro potency of their antibody constructs to facilitate T cell mediated target cell lysis^{15,19,26}. In yet another study, TbsAbs in conventional IgG2 format were compared to a Diabody-Fc (DbFc) format in in vitro tumor cell cytotoxicity assays. The DbFc format shortened the distance between antigen-binding arms and turned out to be more potent²⁷. With TbsAbs in all these cases, also in the one we have described here, several factors may contribute to the enhanced tumor

elimination potency by using a short hinge format. For instance, we found that the TbsAb.short molecule induced significantly more T cell-tumor cell aggregation than the TbsAb.long molecule (Fig. 5). Such improved aggregation could facilitate the T cell mediated attack of tumor cells. It has been reported that immunological synapse formation requires an optimal distance between T cells and tumor cells¹⁰. This optimal distance might be influenced by the geometric configurations of the different antibody constructs. In line with such an assumption, it was reported previously, that targeting membrane-proximal epitope by TbsAbs could facilitate efficient T cell synapse formation leading to enhanced tumor cell elimination¹⁵. Based on this finding, one could argue that possibly by forming tight immunological synapses the TbsAb.short form might be more potent in T cell redirected tumor cell elimination than the TbsAb.long form. Alternatively, efficient T cell-tumor cell engagement might form multiple TbsAbs mediated connections at the immune synapse. In such a situation, the property of individual TbsAbs, such as the flexibility of the binding sites, could be an important factor in forming efficient T cell-tumor cell aggregation^{14,15}. In line with such an assumption, it has been reported by Kapelskia *et al.* that the different flexibility shown in the hinge region of human IgG subclasses (IgG1 > IgG4 > IgG2, IgG1 being the most flexible) significantly impacted the T cell redirected tumor cell elimination²⁸. Compared to the TbsAb.long molecule, the TbsAb.short molecule has a shorter and relatively rigid hinge, which results in a relatively fixed distance and orientation between the two binding domains. Consequently, given the same specific concentration of each TbsAb, the binding arm of randomly free-floating TbsAb.long molecules would require more time to adjust the preferable orientation to bridging T cells and tumor cells than the more rigid TbsAb.short molecules. In addition, due to the dynamic and reversible binding property of TbsAbs, once the T cell-tumor cell aggregation has been formed, TbsAb.short could keep the distance between T cells and tumor cells shorter. This might facilitate other free TbsAb.short molecules to support and further enhance this originally brief interaction between T cells and tumor cells; consequently, resulting in a tighter T cell-tumor cell aggregation than the TbsAb.long molecule might be able to establish. In line with such an assumption, the TbsAb.short

construct induced in comparison to the TbsAb.long construct increased CD69 and CD25 expression on T cells, suggesting a more extensive activation of the T cells. T cell activation is generally considered to be sensitive to consistent TCR signaling, which is triggered by constant antigen/receptor interaction²⁹. Therefore, the higher expression level of CD69 and CD25 could be assumed to be a direct result of a tighter T cell: tumor cell aggregation induced and maintained by the TbsAb.short molecule.

In summary, we investigated the potential application of the Fab x sdAb-Fc bispecific format for T-cell mediated tumor cell killing. We demonstrated that a TbsAb with a shorter distance between the two arms allows for a tighter bridging between the tumor cells and the effector T cells, subsequently leading to a more robust T cell activation and in turn greater tumor cell killing. Instead of comparing different bispecific formats^{14,30-36}, here, we demonstrated that by already changing a dozen of the amino acids in the hinge region in the same bispecific format could induce a substantial impact on its cytotoxic activity. So far, our data have been limited to mouse antibody constructs. However, the hinge length of human antibodies differs from that of mouse antibodies. Therefore, additional research might be needed to apply our findings to human antibody constructs. Nonetheless, our data strongly suggest that the development of human Fab x sdAb-Fc TbsAb for the treatment of cancers could potentially benefit from a shortened hinge design. Therefore, our data indicate that the modulation of the 'hinge region length' parameter could potentially also be applied to other IgG-like TbsAb formats in order to optimize their efficacy.

3

Materials and Methods

Cell lines

CHO.K1 and CHO/mEGFR cell lines were described in our previous study⁸. Mouse ovarian cancer surface epithelial cell line (ID8) was kindly provided by Professor Rose Zamoyska, the cells were cultured in IMDM (ThermoFisher Scientific, UK #I3390-500ML) supplemented with 10% FBS (Gibco, UK #10500-064), 1% L-glutamine (ThermoFisher Scientific, UK #25030-081), 0.1% 2-mercaptoethanol (Sigma-Aldrich) in 10-cm-Petri dishes and

incubated at 37 °C. ID8/mEGFR^{-/-} cell line was generated by CRISPR/Cas9 gene-editing system. Cloning was performed using Truecut V2 cas9 (ThermoFisher Scientific). ID8 cells were transfected with CRISPR plasmid-containing gRNA for mEGFR-KO by electroporation (1600V, 10ms, 3 pulses) using the Invitrogen™ Neon™ Transfection System (ThermoFisher Scientific). TRACR RNA was obtained from Integrated DNA technologies and the gRNA sequence is 5' CCTCATTGCCCTCAACACCG 3'. The transfected cells were cultured with IMDM (ThermoFisher Scientific, UK #I3390-500ML) for 4 days before sorting. Cells were stained with HcAb anti-mouse EGFR (clone RR359), followed by anti-mouse IgG2a-PE (1:100). Using the BD FACSARIA™ II sorter, the mEGFR⁻ ID8 population was bulk-sorted based on mEGFR expression. Sorted ID8 clones without mEGFR expression were isolated and expanded.

OT-1 cells were derived from spleens of OT-1 Rag1^{-/-} (C57BL/6) mice. Spleens were gently dissociated mechanically through a 70 µm filter. The suspension was then centrifuged at 300× g at 4 °C for 5 min, the supernatant discarded, and RBC lysis buffer (Sigma-Aldrich, UK #R7757-100ML) was added. The suspension was incubated for 5 min at room temperature, cells were then centrifuged again and the pellet was resuspended in IMDM. Cells were counted and cultured in IMDM (ThermoFisher Scientific, UK #I3390-500ML) supplemented with 10% FBS (Gibco, UK #10500-064), 1% L-glutamine (ThermoFisher Scientific, UK #25030-081), 0.1% 2-mercaptoethanol (Sigma-Aldrich, USA #M6250) in 10 cm petri dishes and incubated at 37 °C.

Designation and construction of expression vectors for bispecific antibodies

By using the established duobody platform, we designed IgG2a-mCD3E × mEGFR TbsAbs in a Fab × sdAb-Fc format previously developed by Huang *et al.* with two different hinge lengths. These comprised (i) the variable light chain (VL) and variable heavy chain (VH) domains of 2c11, an anti-mCD3E monoclonal antibody, (ii) VH domain of anti-mEGFR single domain antibody RR359, and (iii) a mouse IgG2a Fc module with duobody mutations for heterodimerization.

The anti-mEGFR sdAb (RR359) was described previously and the amino acid sequence of anti-mCD3E (2c11) was obtained from the IMGT database^{8, 37}. The amino acid mutations introduced to each vector to allow heavy-heavy chain heterodimerization are depicted in Fig. 3C. T370K and K409R point mutations were introduced to the CH3 region of heavy chain only anti-mEGFR antibody RR359. F405L and R411T point mutations were introduced to the CH3 region of the conventional anti-mCD3E antibody 2c11. In addition, L234A, L235A, and P329G (LALA-PG) mutations were introduced to the Fc domain of each 2c11 and RR359 sequence to silence their Fc-mediated effector functions. The amino acid sequences of the expressed constructs are shown in Supplementary Table S1. The parental mAb expression vectors were constructed by de novo synthesis (GeneArt, ThermoFisher Scientific).

Two different hinge constructs were produced by introducing different linkers in the parental anti-mEGFR plasmids. For the short hinge design, a full mouse IgG2a linker was introduced (EPKGP_TIKPCPPCKCPAPNLLGG) between the sdAb part and the Fc part of RR359 antibody. For the long hinge design, a camelid/mouse chimeric linker (EPKIPQPQPKPQPQPQPKPQKPCPPCKCPAPNLLGG) was introduced between the sdAb part and Fc domain of the RR359 antibody (Fig. 1). The expression vectors of these antibodies were constructed by de novo synthesis (GeneArt, ThermoFisher Scientific Scientific).

Generation of bispecific antibodies

FreeStyle™ 293-F cells (Invitrogen, UK # R79007) were grown in FreeStyle 293 Expression medium (Invitrogen, UK #12338-018). Each relevant heavy and light chain expression vector was co-transfected into FreeStyle™ 293-F cells (Invitrogen, UK # R79007), using 293fectin™ reagent (Invitrogen, UK #12347-019) according to the manufacturer's recommended conditions. At 7-days post-transfection, the antibodies were purified by protein A affinity chromatography (Peptide Synthetics), dialyzed overnight to PBS (Gibco, UK #D8537-500ML), and filter-sterilized over 0.22-µm filters. Antibody concentration was calculated based on the Beer-Lambert Law, $A = \epsilon \times b \times c$, (A is the A280 absorbance, b is the path length, c is the analyte

concentration, and ϵ is the wavelength-dependent molar absorptivity coefficient with units of $M^{-1} \text{ cm}^{-1}$). A280 absorbance was measured by spectrophotometry using a Nanodrop ND-1000 system (ThermoFisher Scientific). Equimolar amounts of relevant parental antibodies were mixed and incubated with 2-mercaptoethylamine (2-MEA; Sigma, Switzerland #30078-25G) at a final concentration of 1 mg/mL total antibody in PBS (Gibco, UK #D8537-500ML). The final concentration of 2-MEA was 75 mM. The mixtures were incubated for 5 h at 31 °C. The mixtures were then buffer-exchanged against PBS using Slide-A-Lyzer cassettes (ThermoFisher Scientific, USA #66380) to remove 2-MEA. Samples were stored overnight at 4 °C to allow for the re-oxidation of the disulfide bonds. Bispecific antibody concentration was calculated as previously described. The purity of TbsAbs was evaluated by SDS-PAGE in reducing and non-reducing conditions.

Generation of control TbsAb by mutagenesis

The three-dimensional structure model of mEGFR sdAb was predicted by ColabFold, which combines a protein homolog search MMseqs2 with AlphaFold2 (<https://colab.research.google.com/github/sokrypton/ColabFold/blob/main/AlphaFold2.ipynb>, accessed on 1 June 2021). The mutations were introduced into the mEGFR binding CDR3 of the RR359.short antibody sequence by site-directed mutagenesis by PCR. mEGFR-His recombinant protein (R&D systems) was diluted to 50 mM in 10 mM acetate pH 5.0 (ForteBio, USA #18-1069) and loaded on NHS/EDC activated AR2G biosensors (ForteBio, USA #18-5088). HcAb.mEGFR antibodies with different mutations were diluted to 20 $\mu\text{g}/\text{mL}$ in 10 \times kinetic buffer (ForteBio, USA #18-1092) and associated to mEGFR-His protein and 10 \times kinetic buffer was used as negative control. Binding kinetics were measured by the Octet system according to the manufacturer's instructions (ForteBio). Data was analyzed using data analysis software HT V10.0 (ForteBio). Signal of negative control was subtracted in the BLI experiment. cFAE was performed as described above, using parental antibodies HcAb.mEGFR with short hinge and D105A mutation and mCD3E mAb to generate the TbsAb.con.

Size-exclusion chromatography (HP-SEC)

Aggregation and degradation of TbsAbs were quantified by SEC. Ten μL of each respective sample (TbsAb.long and TbsAb.short), at 0.5 mg/mL were loaded (20 μL load volume) onto a calibrated Superdex-200 Increase 3.2/300 GL (Cytiva, UK #28990946) size exclusion column pre-equilibrated in PBS, pH 7.4, at 8 °C and run with a flow rate of 50 $\mu\text{L}\cdot\text{min}^{-1}$ on an ÄKTA PURE Micro™ LC system (Cytiva, UK # 29302479). Elution was monitored at 220 nm, 256 nm, and 280 nm, with 2.5 s integration. The concentration of protein in respective peaks was calculated using the peak analysis software (with a morphological baseline with a skim value of 7.0) provided with the instrument (UNICORN v7.7™; Cytiva) and the relative purity was calculated as a percentage of all integrated peaks.

In vitro cytotoxicity assays

Naïve OT-1 cells (enriched from spleens of OT-1 Rag1^{-/-} mice) were activated by exposure to ovalbumin peptide SIINFEKL (2 ng/mL, Peptide Synthetics) for 48 h. LDH method: Target cells were seeded in IMDM (ThermoFisher Scientific, UK #I3390-500ML) with 10% FBS (ThermoFisher Scientific, UK #10500-064) at a density of 1×10^4 cells/well on a 96-well flat-bottom cell culture plate. Five-fold serial gradient dilution of either TbsAb.long, TbsAb.short, or TbsAb.con was performed in a complete medium, starting with a 16.8 nM (2 $\mu\text{g}/\text{mL}$) concentration and incubated for 0.5 h. Samples were added to corresponding wells at a final volume of 150 μL . Subsequently, in IMDM with 10% inactivated FBS medium, OT-1 cells were adjusted to 5×10^4 cells/well added into the plate at an effector cell:tumor cell (E:T) ratio of 5:1. The cytotoxicity assay was detected after plates were incubated at 37 °C for 24 h from supernatant samples using CytoTox96® Non-Radioactive LDH Kit (Promega, USA #G1781). The cytotoxicity percentages were calculated following the manufacturer's instructions as shown here:

$$\text{Cytotoxicity \%} = \frac{\text{signal (Experimental)} - \text{Effector spontaneous}}{\text{signal (Target maximum)} - \text{signal(target spontaneous)}} \times 100\%$$



Flow cytometry method: ID8 cells and ID8 mEGFR^{-/-} cells were labeled by eFluo 450 or eFluo 670, respectively. ID8 cells and ID8 mEGFR^{-/-} were seeded in IMDM (ThermoFisher Scientific, UK #I3390-500ML) with 10% FBS (ThermoFisher Scientific, UK #10500-064) at a density of 2×10^4 cells/well on a 96-well flat-bottom cell culture plate. Five-fold serial gradient dilution of either TbsAb.long, TbsAb.short, or TbsAb.con was performed in a complete medium, starting with a 16.8 nM (2 µg/mL) concentration and incubated for 0.5 h. PBS treated samples were used as negative control. Samples were added to corresponding wells at a final volume of 150 µL. Subsequently, in IMDM with 10% inactivated FBS medium, OT-1 cells were adjusted to 1×10^5 cells/well added into the plate at an effector cell:tumor cell (E:T) ratio of 5:1. The OT-1 cells were washed off by PBS after 24 h incubation. Remaining attached ID8 and ID8 mEGFR^{-/-} cells were detected by flow cytometry. The ID8 lysis percentages were calculated following the formula as shown here:

$$ID8 \text{ lysis } \% = \left[1 - \frac{\text{number of Pacific blue positive cells}(TRBA \text{ treated})}{\text{number of Pacific blue positive cells}(PBS \text{ treated})} \right] \times 100\%$$

All tests were repeated in triplicates and linear or nonlinear regression analysis to fit dose-response curves were assayed with GraphPad Prism Version 8.0.

Microscopy

Ovalbumin peptide SIINFEKL activated OT-1s were incubated with CHO/mEGFR cells in the presence of TbsAb.con, TbsAb.long or TbsAb.short respectively for 24 h. Images of activated OT-1s were taken with an EVOS M7000 microscope under $4 \times$ magnification. T cell blasts analysis was performed using EVOS analysis software to count the number and calculate the area of T cell blasts in each group. T cell blasts in randomly selected 20 grids (500 µm × 500 µm) of each photo were counted and calculated for analyzing.



Cell-cell association assays

OT-1 cells were labelled with fixable viability dye eFluor 670 (eBiosciences, USA #65-0840-85) as effector cells and ID8 cells were labelled with fixable viability dye eFluor 450 (eBiosciences, USA #65-0842-85) as target cells, according to the manufacturer's instructions. Mixtures of 5×10^4 cells of each labelled cell line were incubated together at 4 °C for 45 min in a 96-round bottom plate, with 5-fold serially diluted TbsAb.long, TbsAb.short, or TbsAb.con in FACS buffer (PBS supplemented with 1% BSA + 1% EDTA, Gibco), starting with a 84 nM (10 µg/mL) concentration. All tests were repeated in duplicates. Cells were then washed in FACS buffer and resuspended in 200 µL for analysis on a FACSCanto II flow cytometer (BD Biosciences). Data were analyzed using FlowJo v.10.8.0 software (BD Biosciences), and GraphPad Prism Version 9.0 software. Ten thousand events were collected.

T cell activation assays

Freshly isolated splenocytes from the WT C57BL/6 mice (1×10^5 cells/mL) were treated with either TbsAb.long, TbsAb.short or TbsAb.con at 3.36 nM (0.4 µg/mL) and incubated with ID8 target cells (2×10^4 cells/mL) in 96-well plates for 18 h. The splenocytes were collected and stained with CD8-APC (eBioscience, USA #17-0081-83), CD4-Pacific blue (eBioscience, USA, #57004282) and CD69-PE (PharMingen, USA #553237)/CD25-PE (PharMingen, USA #09985B). Cells were counted by flow cytometry on a FACSCanto II system (BD Biosciences) and data were analyzed with FlowJo v.10.8.0 software (BD Biosciences). Percentage of PE positive cells and mean fluorescence intensities (MFI) were used for statistical analysis using GraphPad Prism version 9.0 software.

Statistical analysis

Statistical analyses were performed using Prism software version 9.0 (GraphPad). P values were determined for comparisons between TbsAb.long and TbsAb.short-mediated T-cell cytotoxicity by paired T-test and T-cell activation by unpaired *t*-test. *p* values for comparisons between TbsAb.long

and TbsAb.short-mediated cell-cell association were determined by 2-way ANOVA test. For all statistical tests, results with a p value <0.05 were considered significant. *: $p < 0.05$; **: $p < 0.01$; ***: $p < 0.001$.

Supplementary Materials: The following supporting information can be downloaded at: <https://www.mdpi.com/article/10.3390/biom12101331/s1> Figure S1: Monomericity of each parental antibody (RR359.long, RR359.short and 2c11) analyzed by size-exclusion chromatography (SEC); Figure S2: Length of antibody CH1 evaluated by Discovery Studio; Figure S3: Prediction quality judged by visualizing multiple sequence alignments (MSA) depth and showing the AlphaFold2 confidence measures ; Figure S4: Raw data binding kinetics of HcAb.RR359 with different mutations to AR2G-sensor bound mEGFR-His protein as measured by BLI on an Octet machine; Figure S5: Purity of TRBA.con evaluated by SDS-Page at non-reducing condition; Figure S6: The gating strategy for the T-cells shown in Figure 6; Table S1: The amino acid sequences of the expressed constructs.

Author contributions: S.H., A.S. and C.V. prepared BsAb samples. S.H. and A.S. performed the experiments with support by D.W. M.W. helped with the analysis of flow cytometry data. S.H. and C.V. drafted the manuscript. S.M.J.v.D. designed BsAb constructs. D.M.Z., A.J.S., S.M.J.v.D., and A.v.E. designed and discussed the study. All authors have read and agreed to the published version of the manuscript.

Funding: This research was funded by the European Union, Horizon 2020 research and innovation programme under the Marie Skłodowska-Curie Innovative Training Networks [grant number 765394, 2018]. Further support came from the Edinburgh Protein Production Facility (EPPF) and the Centre Core Grants (092076 and 203149) to the Wellcome Centre for Cell Biology at the University of Edinburgh.

Institutional review board statement: Not applicable.

Informed consent statement: Not applicable.

Data availability statement: Original data sets will be made available upon request.

Conflicts of interest: The authors declare no conflict of interest.

Supplementary material

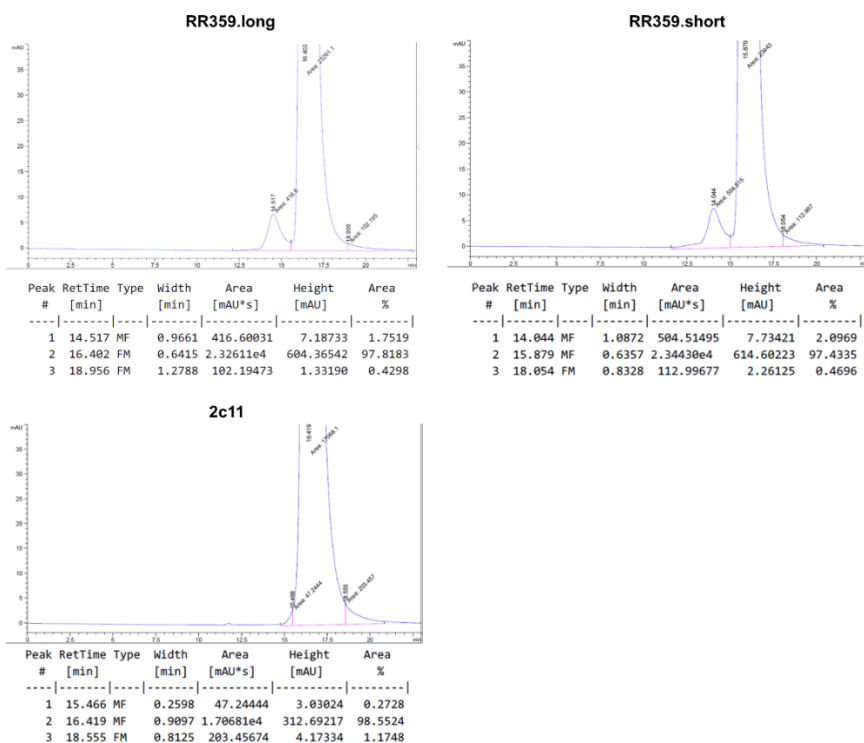


Figure S1. Monomericity of each parental antibody (RR359.long, RR359.short and 2c11) analyzed by size-exclusion chromatography (SEC).

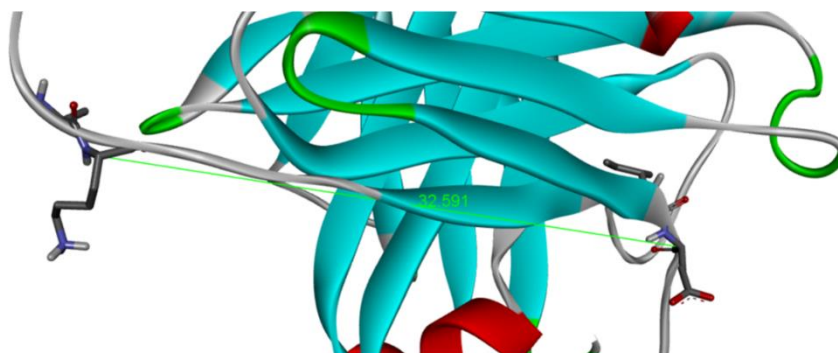


Figure S2. Length of antibody CH1 evaluated by Discovery Studio (used PDB ID 3R06 as template).

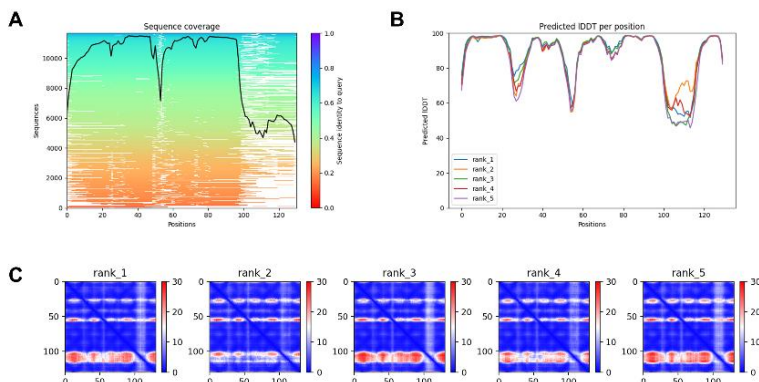


Figure S3. Prediction quality judged by visualizing multiple sequence alignments (MSA) depth and showing the AlphaFold2 confidence measures. (A) Multiple sequence alignments. Number of sequences per position, the higher the better. (B) Predicted local distance difference test (IDDT) per position. Model confidence (out of 100) at each position. The higher the better. (C) Predicted alignment error (PAE). A useful metric to assess how confident the model is about the interface. The lower the better. Rank 1 structure was used in this study.

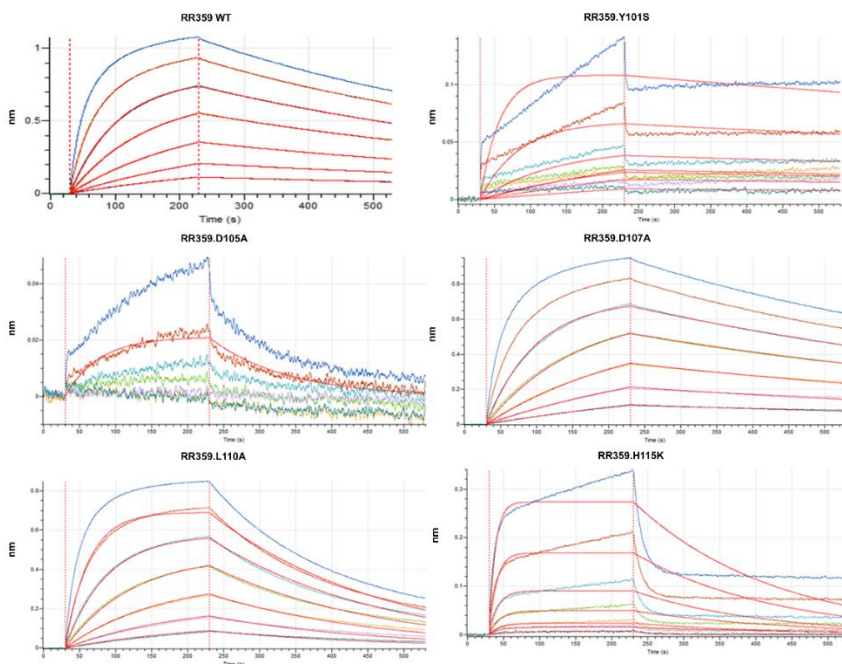


Figure S4. Raw data binding kinetics of HcAb.RR359 with different mutations to AR2G-sensor bound mEGFR-His protein as measured by BLI on an Octet machine.

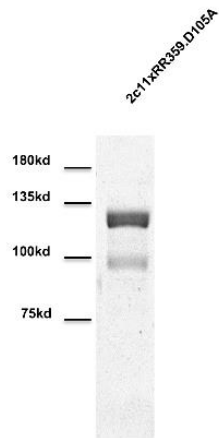


Figure S5. Purity of TRBA.con evaluated by SDS-Page at non-reducing condition.

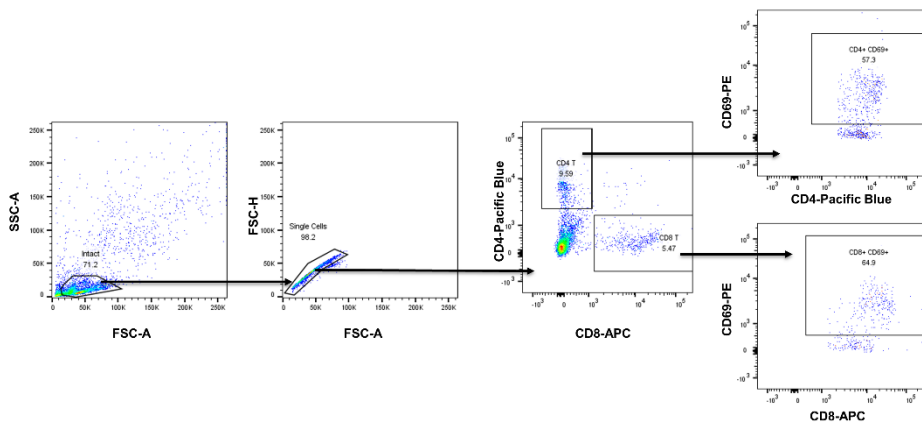


Figure S6. The gating strategy for the T-cells shown in Figure 6.

Supplementary Table 1.

RR359(anti-EGFR)-long-migg2a.LALAPG.T370K.K409R
QVQLQESGGGLVQAGGSLRLSCAASGRFTFSYAMGWFRQVPGKEREFVAALSTRSAGNT YYADSVKGRFTISRDNAKNTVYLQMSSLKAEDTAVYYCAAGYMSSDADPSLAASLHPYDY WGQGTQVTVSSEPKIPQPKPQPKPQPKPQPKPCKPCPAPNAAGGPSVFIFPPKI KDVLMISLSPMVTCTVVDVSEDDPDVQISWVFNNEVLTAQTQTHREDYNSTLRVVSAL PIQHQDWMSGKEFKCKVNNKALGAPIERTISKPKGSVRAPQVYVLPPEEEMTKKQVTLT CMVKDFMPEDIYVEWTNNGKTELNYKNTEPVLDSGDSYFMYSLRVEKKNWVERNSYS CSVVHEGLHNHHTTKFSRTPGK
RR359(anti-EGFR)-sh-migg2a.LALAPG.T370K.K409R
QVQLQESGGGLVQAGGSLRLSCAASGRFTFSYAMGWFRQVPGKEREFVAALSTRSAGNT YYADSVKGRFTISRDNAKNTVYLQMSSLKAEDTAVYYCAAGYMSSDADPSLAASLHPYDY WGQGTQVTVSSEPKGPTIKPCPPCKPCPAPNAAGGPSVFIFPPKIKDVLMISLSPMVTCTVV DVSEDDPDVQISWVFNNEVLTAQTQTHREDYNSTLRVVSALPIQHQDWMSGKEFKCK VNNKALGAPIERTISKPKGSVRAPQVYVLPPEEEMTKKQVTLTCMVKDFMPEDIYVEWT NNGKTELNYKNTEPVLDSGDSYFMYSLRVEKKNWVERNSYSCSVVHEGLHNHHTTKSFS RTPGK
RR359(anti-EGFR)-sh-migg2a.D105A.LALAPG.T370K.K409R
QVQLQESGGGLVQAGGSLRLSCAASGRFTFSYAMGWFRQVPGKEREFVAALSTRSAGNT YYADSVKGRFTISRDNAKNTVYLQMSSLKAEDTAVYYCAAGYMSSAADPSLAASLHPYDY WGQGTQVTVSSEPKGPTIKPCPPCKPCPAPNAAGGPSVFIFPPKIKDVLMISLSPMVTCTVV DVSEDDPDVQISWVFNNEVLTAQTQTHREDYNSTLRVVSALPIQHQDWMSGKEFKCK VNNKALGAPIERTISKPKGSVRAPQVYVLPPEEEMTKKQVTLTCMVKDFMPEDIYVEWT NNGKTELNYKNTEPVLDSGDSYFMYSLRVEKKNWVERNSYSCSVVHEGLHNHHTTKSFS RTPGK
2c11(anti-CD3)-migg2a.LALAPG.F405L.R411T
EVQLVESGGGLVQPGLSLKLSCEASGFTFSYGMHWVRQAPGRGLESVAYITSSINIKYA DAVKGRFTVSRDNANKLLFLQMNILKSEDTAMYYCARFDWDKNYWGQGTMTVTVSSAK TTAPSVYPLAPVCGDGTGSSVTLGCLVKGYFPEPVTLTWNSGSLSSGVHTFPAVLQSDLYTL SSSVTVTSSTWPSQITCNVAHPASSTKVDKKIEPRGPTIKPCPPCKPCPAPNAAGGPSVFIFP PKIKDVLMISLSPMVTCTVVDVSEDDPDVQISWVFNNEVLTAQTQTHREDYNSTLRVVS ALPIQHQDWMSGKEFKCKVNNKALGAPIERTISKPKGSVRAPQVYVLPPEEEMTKKQVTL LTCMVTDMPEDIYVEWTNNGKTELNYKNTEPVLDSGDSYLMYSLTVEKKNWVERNSY SCSVVHEGLHNHHTTKFSRTPGK
2c11(anti-CD3), light chain
DIQMTQSPSSLPASLGDRVTINCPASQDISNYLNWYQQKPKGAPKLLIYYTNKLADGVPSR FSGSGSGRDSFTISLSEEDIGSYCCQQYNYPWTFGPGTKLEIKRADAAPTIVSIFPPSSEQ LTSGGASVVCFLNFFPKDINVKWKIDGSERQNGVLSWTDQDSKSTYSMSSTLTLTKD EYERHNSYTCETHKSTSPIVKSFNRNEC

References

1. Blanco, B.; Compte, M.; Lykkemark, S.; Sanz, L.; Alvarez-Vallina, L. T Cell-Redirecting Strategies to 'STAb' Tumors: Beyond CARs and Bispecific Antibodies. *Trends Immunol.* 2019, *40*, 243–257. <https://doi.org/10.1016/j.it.2019.01.008>.
2. Seimetz, D.; Lindhofer, H.; Bokemeyer, C. Development and Approval of the Trifunctional Antibody Catumaxomab (Anti-EpCAM× anti-CD3) as a Targeted Cancer Immunotherapy. *Cancer Treat. Rev.* 2010, *36*, 458–467. <https://doi.org/10.1016/j.ctrv.2010.03.001>.
3. Przepiorka, D.; Ko, C.-W.; Deisseroth, A.; Yancey, C.L.; Candau-Chacon, R.; Chiu, H.-J.; Gehrke, B.J.; Gomez-Broughton, C.; Kane, R.C.; Kirshner, S.; et al. FDA Approval: Blinatumomab. *Clin. Cancer Res.* 2015, *21*, 4035–4039. <https://doi.org/10.1158/1078-0432.CCR-15-0612>.
4. Huang, S.; van Duijnhoven, S.M.J.; Sijts, A.J.A.M.; van Elsas, A. Bispecific Antibodies Targeting Dual Tumor-Associated Antigens in Cancer Therapy. *J. Cancer Res. Clin. Oncol.* 2020, *146*, 3111–3122. <https://doi.org/10.1007/s00432-020-03404-6>.
5. Strohl, W.R.; Naso, M. Bispecific T-Cell Redirection versus Chimeric Antigen Receptor (CAR)-T Cells as Approaches to Kill Cancer Cells. *Antibodies* 2019, *8*, 41. <https://doi.org/10.3390/antib8030041>.
6. Wang, Q.; Chen, Y.; Park, J.; Liu, X.; Hu, Y.; Wang, T.; McFarland, K.; Betenbaugh, M.J. Design and Production of Bispecific Antibodies. *Antibodies* 2019, *8*, 43. <https://doi.org/10.3390/antib8030043>.
7. Schaefer, W.; Regula, J.T.; Böhner, M.; Schanzer, J.; Croasdale, R.; Dürr, H.; Gassner, C.; Georges, G.; Kettenberger, H.; Imhof-Jung, S.; et al. Immunoglobulin Domain Crossover as a Generic Approach for the Production of Bispecific IgG Antibodies. *Proc. Natl. Acad. Sci. USA* 2011, *108*, 11187–11192. <https://doi.org/10.1073/pnas.1019002108>.
8. Huang, S.; Segué, A.; Hulsik, D.L.; Zaiss, D.M.; Sijts, A.J.A.M.; van Duijnhoven, S.M.J.; van Elsas, A. A Novel Efficient Bispecific Antibody Format, Combining a Conventional Antigen-Binding Fragment with a Single Domain Antibody, Avoids Potential Heavy-Light Chain Mis-Pairing. *J. Immunol. Methods* 2020, *483*, 112811. <https://doi.org/10.1016/j.jim.2020.112811>.
9. Ellerman, D. Bispecific T-Cell Engagers: Towards Understanding Variables Influencing the in Vitro Potency and Tumor Selectivity and Their Modulation to Enhance Their Efficacy and Safety. *Methods* 2019, *154*, 102–117. <https://doi.org/10.1016/j.ymeth.2018.10.026>.
10. Dickopf, S.; Georges, G.J.; Brinkmann, U. Format and Geometries Matter: Structure-Based Design Defines the Functionality of Bispecific Antibodies. *Comput. Struct. Biotechnol. J.* 2020, *18*, 1221–1227. <https://doi.org/10.1016/j.csbj.2020.05.006>.
11. Klein, D.; Jacobs, S.; Sheri, M.; Anderson, M.; Attar, R.; Barnakov, A.; Brosnan, K.; Bushey, B.; Chevalier, K.; Chin, D.; et al. Abstract LB-312: Bispecific Centyrin Simultaneously Targeting EGFR and c-Met Demonstrates Improved Activity

- Compared to the Mixture of Single Agents. *Cancer Res.* 2013, 73, LB-312. <https://doi.org/10.1158/1538-7445.AM2013-LB-312>.
12. Wuellner, U.; Klupsch, K.; Buller, F.; Attinger-Toller, I.; Santimaria, R.; Zbinden, I.; Henne, P.; Grabulovski, D.; Bertschinger, J.; Brack, S. Bispecific CD3/HER2 Targeting FynomAb Induces Redirected T Cell-Mediated Cytolysis with High Potency and Enhanced Tumor Selectivity. *Antibodies* 2015, 4, 426–440. <https://doi.org/10.3390/antib4040426>.
 13. Santich, B.H.; Park, J.A.; Tran, H.; Guo, H.-F.; Huse, M.; Cheung, N.-K.V. Interdomain Spacing and Spatial Configuration Drive the Potency of IgG-[L]-ScFv T Cell Bispecific Antibodies. *Sci. Transl. Med.* 2020, 12, eaax1315. <https://doi.org/10.1126/scitranslmed.aax1315>.
 14. Moore, P.A.; Zhang, W.; Rainey, G.J.; Burke, S.; Li, H.; Huang, L.; Gorlatov, S.; Veri, M.C.; Aggarwal, S.; Yang, Y.; et al. Application of Dual Affinity Retargeting Molecules to Achieve Optimal Redirected T-Cell Killing of B-Cell Lymphoma. *Blood* 2011, 117, 4542–4551. <https://doi.org/10.1182/blood-2010-09-306449>.
 15. Li, J.; Stagg, N.J.; Johnston, J.; Harris, M.J.; Menzies, S.A.; DiCara, D.; Clark, V.; Hristopoulos, M.; Cook, R.; Slaga, D.; et al. Membrane-Proximal Epitope Facilitates Efficient T Cell Synapse Formation by Anti-FcRH5/CD3 and Is a Requirement for Myeloma Cell Killing. *Cancer Cell* 2017, 31, 383–395. <https://doi.org/10.1016/j.ccell.2017.02.001>.
 16. Bluemel, C.; Hausmann, S.; Fluhr, P.; Sriskandarajah, M.; Stallcup, W.B.; Baeuerle, P.A.; Kufer, P. Epitope Distance to the Target Cell Membrane and Antigen Size Determine the Potency of T Cell-Mediated Lysis by BiTE Antibodies Specific for a Large Melanoma Surface Antigen. *Cancer Immunol. Immunother.* 2010, 59, 1197–1209. <https://doi.org/10.1007/s00262-010-0844-y>.
 17. James, S.E.; Greenberg, P.D.; Jensen, M.C.; Lin, Y.; Wang, J.; Till, B.G.; Raubitschek, A.A.; Forman, S.J.; Press, O.W. Antigen Sensitivity of CD22-Specific Chimeric TCR Is Modulated by Target Epitope Distance from the Cell Membrane. *J. Immunol.* 2008, 180, 7028–7038. <https://doi.org/10.4049/jimmunol.180.10.7028>.
 18. Root, A.R.; Cao, W.; Li, B.; LaPan, P.; Meade, C.; Sanford, J.; Jin, M.; O’Sullivan, C.; Cummins, E.; Lambert, M.; et al. Development of PF-06671008, a Highly Potent Anti-P-Cadherin/Anti-CD3 Bispecific DART Molecule with Extended Half-Life for the Treatment of Cancer. *Antibodies* 2016, 5, 6. <https://doi.org/10.3390/antib5010006>.
 19. Qi, J.; Li, X.; Peng, H.; Cook, E.M.; Dadashian, E.L.; Wiestner, A.; Park, H.; Rader, C. Potent and Selective Antitumor Activity of a T Cell-Engaging Bispecific Antibody Targeting a Membrane-Proximal Epitope of ROR1. *Proc. Natl. Acad. Sci. USA* 2018, 115, E5467–E5476. <https://doi.org/10.1073/pnas.1719905115>.
 20. Chu, T.H.; Patz, E.F.; Ackerman, M.E. Coming Together at the Hinges: Therapeutic Prospects of IgG3. *mAbs* 2021, 13, 1882028. <https://doi.org/10.1080/19420862.2021.1882028>.
 21. Wang, F.; Tsai, J.C.; Davis, J.H.; Chau, B.; Dong, J.; West, S.M.; Hogan, J.M.; Wheeler, M.L.; Bee, C.; Morishige, W.; et al. Design and Characterization of Mouse IgG1 and

- IgG2a Bispecific Antibodies for Use in Syngeneic Models. *mAbs* 2019, *12*, 1685350. <https://doi.org/10.1080/19420862.2019.1685350>.
22. Griffin, L.M.; Snowden, J.R.; Lawson, A.D.G.; Wernery, U.; Kinne, J.; Baker, T.S. Analysis of Heavy and Light Chain Sequences of Conventional Camelid Antibodies from *Camelus Dromedarius* and *Camelus Bactrianus* Species. *J. Immunol. Methods* 2014, *405*, 35–46. <https://doi.org/10.1016/j.jim.2014.01.003>.
 23. Bailey, M.J.; Duehr, J.; Dulin, H.; Broecker, F.; Brown, J.A.; Arumemi, F.O.; Bermúdez González, M.C.; Leyva-Grado, V.H.; Evans, M.J.; Simon, V.; et al. Human Antibodies Targeting Zika Virus NS1 Provide Protection against Disease in a Mouse Model. *Nat. Commun.* 2018, *9*, 4560. <https://doi.org/10.1038/s41467-018-07008-0>.
 24. Choi, B.D.; Gedeon, P.C.; Kuan, C.-T.; Sanchez-Perez, L.; Archer, G.E.; Bigner, D.D.; Sampson, J.H. Rational Design and Generation of Recombinant Control Reagents for Bispecific Antibodies through CDR Mutagenesis. *J. Immunol. Methods* 2013, *395*, 14–20. <https://doi.org/10.1016/j.jim.2013.06.003>.
 25. Mirdita, M.; Schütze, K.; Moriwaki, Y.; Heo, L.; Ovchinnikov, S.; Steinegger, M. ColabFold: Making Protein Folding Accessible to All. *Nat. Methods* 2022, *19*, 679–682. <https://doi.org/10.1038/s41592-022-01488-1>.
 26. Nair-Gupta, P.; Diem, M.; Reeves, D.; Wang, W.; Schulingkamp, R.; Sproesser, K.; Mattson, B.; Heidrich, B.; Mendonça, M.; Joseph, J.; et al. A Novel C2 Domain Binding CD33×CD3 Bispecific Antibody with Potent T-Cell Redirection Activity against Acute Myeloid Leukemia. *Blood Adv.* 2020, *4*, 906–919. <https://doi.org/10.1182/bloodadvances.2019001188>.
 27. Chen, W.; Yang, F.; Wang, C.; Narula, J.; Pascua, E.; Ni, I.; Ding, S.; Deng, X.; Chu, M.L.-H.; Pham, A.; et al. One Size Does Not Fit All: Navigating the Multi-Dimensional Space to Optimize T-Cell Engaging Protein Therapeutics. *mAbs* 2021, *13*, 1871171. <https://doi.org/10.1080/19420862.2020.1871171>.
 28. Kapelski, S.; Cleiren, E.; Attar, R.M.; Philippar, U.; Häslner, J.; Chiu, M.L. Influence of the Bispecific Antibody IgG Subclass on T Cell Redirection. *mAbs* 2019, *11*, 1012–1024. <https://doi.org/10.1080/19420862.2019.1624464>.
 29. Aleksic, M.; Dushek, O.; Zhang, H.; Shenderov, E.; Chen, J.-L.; Cerundolo, V.; Coombs, D.; van der Merwe, P.A. Dependence of T Cell Antigen Recognition on T Cell Receptor-Peptide MHC Confinement Time. *Immunity* 2010, *32*, 163–174. <https://doi.org/10.1016/j.immuni.2009.11.013>.
 30. Ellwanger, K.; Reusch, U.; Fucek, I.; Knackmuss, S.; Weichel, M.; Gantke, T.; Molkenthin, V.; Zhukovsky, E.A.; Tesar, M.; Treder, M. Highly Specific and Effective Targeting of EGFRvIII-Positive Tumors with TandAb Antibodies. *Front. Oncol.* 2017, *7*, 100.
 31. Kipriyanov, S.M.; Moldenhauer, G.; Schuhmacher, J.; Cochlovius, B.; Von der Lieth, C.-W.; Matys, E.R.; Little, M. Bispecific Tandem Diabody for Tumor Therapy with Improved Antigen Binding and Pharmacokinetics. Edited by J. Karn. *J. Mol. Biol.* 1999, *293*, 41–56. <https://doi.org/10.1006/jmbi.1999.3156>.

32. Hoseini, S.S.; Guo, H.; Wu, Z.; Hatano, M.N.; Cheung, N.-K.V. A Potent Tetravalent T-Cell-Engaging Bispecific Antibody against CD3 in Acute Myeloid Leukemia. *Blood Adv.* 2018, *2*, 1250–1258. <https://doi.org/10.1182/bloodadvances.2017014373>.
33. Harwood, S.L.; Alvarez-Cienfuegos, A.; Nuñez-Prado, N.; Compte, M.; Hernández-Pérez, S.; Merino, N.; Bonet, J.; Navarro, R.; Van Bergen en Henegouwen, P.M.P.; Lykkemark, S.; et al. ATTACK, a Novel Bispecific T Cell-Recruiting Antibody with Trivalent EGFR Binding and Monovalent CD3 Binding for Cancer Immunotherapy. *Onc Immunology* 2018, *7*, e1377874. <https://doi.org/10.1080/2162402X.2017.1377874>.
34. Kipriyanov, S.M.; Moldenhauer, G.; Strauss, G.; Little, M. Bispecific CD3 × CD19 Diabody for T Cell-Mediated Lysis of Malignant Human B Cells. *Int. J. Cancer* 1998, *77*, 763–772. [https://doi.org/10.1002/\(SICI\)1097-0215\(19980831\)77:5<763::AID-IJC16>3.0.CO;2-2](https://doi.org/10.1002/(SICI)1097-0215(19980831)77:5<763::AID-IJC16>3.0.CO;2-2).
35. Feldmann, A.; Stamova, S.; Bippes, C.C.; Bartsch, H.; Wehner, R.; Schmitz, M.; Temme, A.; Cartellieri, M.; Bachmann, M. Retargeting of T Cells to Prostate Stem Cell Antigen Expressing Tumor Cells: Comparison of Different Antibody Formats. *Prostate* 2011, *71*, 998–1011. <https://doi.org/10.1002/pros.21315>.
36. Durben, M.; Schmiedel, D.; Hofmann, M.; Vogt, F.; Nübling, T.; Pysz, E.; Bühring, H.-J.; Rammensee, H.-G.; Salih, H.R.; Große-Hovest, L.; et al. Characterization of a Bispecific FLT3 X CD3 Antibody in an Improved, Recombinant Format for the Treatment of Leukemia. *Mol. Ther.* 2015, *23*, 648–655. <https://doi.org/10.1038/mt.2015.2>.
37. Zaiss, D.M.W.; van Loosdregt, J.; Gorlani, A.; Bekker, C.P.J.; Gröne, A.; Sibilía, M.; van Bergen en Henegouwen, P.M.P.; Roovers, R.C.; Coffey, P.J.; Sijts, A.J.A.M. Amphiregulin Enhances Regulatory T Cell-Suppressive Function via the Epidermal Growth Factor Receptor. *Immunity* 2013, *38*, 275–284. <https://doi.org/10.1016/j.immuni.2012.09.023>.



4

Mouse IgG2a isotype therapeutic antibodies elicit superior tumor growth control compared to mIgG1 or mIgE

Natasa Vukovic^{1†}, Aina Segué^{1,2,†}, Shuyu Huang^{1,2,†}, Martin Waterfall¹, Alice J.A.M. Sijts², Dietmar M. Zaiss^{1,3,4,5*}

¹ *Institute of Immunology and Infection Research, School of Biological Sciences, University of Edinburgh, Edinburgh, United Kingdom;*

² *Faculty of Veterinary Medicine, Department of Infectious Diseases and Immunology, Utrecht University, Utrecht, The Netherlands;*

³ *Department of Immune Medicine, University Regensburg, Regensburg, Germany;*

⁴ *Institute of Clinical Chemistry and Laboratory Medicine, University Hospital Regensburg, Regensburg, Germany;*

⁵ *Institute of Pathology, University Regensburg, Regensburg, Germany*

* *Correspondence: e-mail address: dietmar.zaiss@ukr.de (D.M.Z)*

† *Authors contributed equally.*

Cancer Research Communications CRC-22-0356.

<https://doi.org/10.1158/2767-9764.CRC-22-0356>

Contribution statement: *Aina Segué Cisteró contributed to the design and implementation of the research, to the analysis of the results and to the writing of the manuscript.*

Running title: Tumor-targeting IgG2a is superior to IgG1 and IgE in mice

Abbreviations list:

ADCC, antibody-dependent cell-mediated cytotoxicity

CDC, complement-dependent cytotoxicity

Fc, fragment crystallizable

FcRs, fragment crystallizable receptors

LALA-PG, L234A/L235A/P329G mutations

mAbs, monoclonal antibodies

mIg, mouse immunoglobulin

NK, natural killer

Keywords: antibody isotype, IgG2a, IgG1, IgE, LALA-PG, tumor therapy

Declaration of competing interest

None.

Abstract

In the last decades, antibody based tumor therapy has fundamentally improved the efficacy of treatment for cancer patients. Currently, almost all tumor-antigen targeting antibodies approved for clinical application are of IgG1 Fc-isotype. Similarly, the mouse homolog mIgG2a is the most commonly used in tumor mouse models. However, in mice the efficacy of antibody based tumor therapy is largely restricted to a prophylactic application. Direct isotype comparison studies in mice in a therapeutic setting are scarce. In this study, we assessed the efficacy of mouse tumor-targeting antibodies of different isotypes in a therapeutic setting using a highly systematic approach. To this end, we engineered and expressed antibodies of the same specificity but different isotypes, targeting the artificial tumor antigen CD90.1 / Thy1.1 expressed by B16 melanoma cells. Our experiments revealed that in a therapeutic setting mIgG2a was superior to both mIgE and mIgG1 in controlling tumor growth. Furthermore, the observed mIgG2a anti-tumor effect was entirely Fc-mediated as the protection was lost when an Fc silenced mIgG2a isotype (LALA-PG mutations) was used. These data confirm mIgG2a superiority in a therapeutic tumor model.

Significance

Direct comparisons of different antibody isotypes of the same specificity in cancer settings are still scarce. Here, it is shown that mIgG2a has a greater effect compared with mIgG1 and mIgE in controlling tumor growth in a therapeutic setting.

Introduction

Monoclonal antibodies (mAbs) are among the fastest-growing class of drugs, with more than 100 mAbs with marketing approval since 1986¹. Most of them belong to cancer therapeutics², where their introduction critically contributed to better outcomes and increased survival for different types of cancer. However, many patients are still unresponsive to such tumor-targeting antibody therapy, underlying the need for further optimisation of antibody-based approaches.

Most of the mAbs used in cancer therapy target tumor antigens which are, to varying extent, involved in tumor survival, growth and invasiveness. Interfering with tumor cell signalling pathways can induce tumor cell death on its own (e.g. anti-HER2, anti-EGFR)^{3,4}. However, it has become increasingly apparent that Fc-mediated activation of the immune system substantially contributes to tumor cell destruction and the efficacy of treatment^{4,5}. With their Fc tail, antibodies can engage the complement system and different effector cells such as natural killer cells and macrophages, mediating antibody-dependent cell-mediated cytotoxicity (ADCC), antibody-dependent cell-mediated phagocytosis (ADCP) and complement-dependent cytotoxicity (CDC) against tumor cells^{5,6}. Since different antibody isotypes bind to different FcRs on immune cells and differ in their potential to activate the complement system, they can induce diverse immune responses. Thus, the downstream effector function is determined by antibody isotype.

For murine IgG antibodies, it has been established that mIgG2a offers superior activity to mIgG1, mostly due to differential affinity for activating and inhibitory FcRs, also defined as activating-to-inhibitory (A/I) ratio. Similar to human IgG1, mIgG2a has high A/I ratio reflecting its high affinity for activating FcRs and low affinity for the inhibitory one. In contrast, mIgG1 shows very low A/I ratio⁷. Based on the seminal publication by Nimmerjahn *et al.*⁸, mIgG2a has been dominantly used as the most active antibody isotype in mouse tumor models. Here, the tumor-targeting mIgG2a showed superior tumor control to mIgG1 in B16 lung metastasis model. However, the antibody treatment in this study was prophylactic, as it started on the

same day when the tumor cells were injected. On the other hand, the same antibody typically failed to control the tumor growth in a therapeutic setting once the tumors were established⁹.

Therefore, the aim of this study was to compare the *in vivo* efficacy of tumor-targeting antibodies of different isotypes in a therapeutic setting. To this end, we followed a similar approach as in the prophylactic setting⁸ and compared the therapeutic efficacy of one specific monoclonal antibody with either a mIgG2a, mIgG1 or mIgE isotype. Our results show that mIgG2a was superior to both mIgE and mIgG1 in controlling tumor growth in a therapeutic setting. Furthermore, the observed mIgG2a anti-tumor effect was entirely Fc-mediated as the protection was lost when an Fc-silenced mIgG2a isotype (via LALA-PG mutations) was used.

Materials and methods

Antibody design, production and purification

Amino acid sequences of all anti-Thy1.1 antibodies are provided in Supplementary Table 1. The design and production of murine anti-Thy1.1 IgG1 and IgE has been done as described before¹⁰. In short, the starting point was OX7 hybridoma (anti-Thy1.1 IgG1) which was sequenced in order to obtain heavy and light chain variable domain sequences (VH, VL). Next, we designed chimeric anti-Thy1.1 mIgE and mIgG1 heavy chains by combining the VH with the known sequences of the constant domains of murine IgE or IgG1 (CHs). Just between VH and CH domains, a unique restriction site (AfeI) was introduced, allowing us to change the isotypes by cloning. The IgG2a HC and the IgG2a HC featuring silencing LALA-PG mutations were cloned using standard cloning techniques from plasmids available in house (anti-Siglec and anti-TNFR2, respectively) into the pcDNA3.1(+) encoding for anti-Thy1.1_VH (Fig.1 A, B). Correct clones were confirmed by Sanger sequencing (GENEWIZ). The plasmid encoding for the anti-Thy1.1 light chain was *de novo* synthesized (GeneArt).

Anti-Thy1.1 IgG2a and anti-Thy1.1 IgG2a-LALA-PG were produced in ExpiCHO-S™ cells and FreeStyle293 cells, respectively, as described before¹⁰. Purification was done with MabSelect SuRe LX resin. Anti-Thy1.1 IgG2a had

to be polished with preparative size-exclusion chromatography (SEC) (data not shown). Preparative SEC and the quality control consisting of UPLC-SEC, CE-SDS and SDS-PAGE were performed as described previously¹⁰.

Thy1.1 plasmids

Full-length Thy1.1 was cloned from pCR4-Blunt-TOPO into pcDNA3.1(+) with EcoRI and Apal two-step digestion, using a standard cloning procedure. In short, digested bands of interest were excized from the gel and extracted with Qiagen Gel Extraction Kit, according to manufacturer's protocol. Dephosphorylation of the vector and subsequent ligation were done with Rapid DNA Dephos & Ligation Kit (Roche) in 1:3 vector:insert molar ratio. DH5 α competent cells were transformed with the ligation reaction and plated on LBampicillin plates. Colonies were picked, expanded and submitted to plasmid isolation with MidiPrep Kit (GenElute HP, Sigma). The correct clone was confirmed by Sanger sequencing with T7 promoter and BGH-R universal primers (Macrogen).

GPI anchor of Thy1 was replaced with MHC-1 transmembrane domain in the following way. Thy1.1 propeptide, which is removed when GPI is attached to Cys130 in the endoplasmic reticulum, was replaced with a part of MHC-1 molecule (Uniprot ID P01900) consisting of the connecting peptide, transmembrane domain and cytoplasmic region. pcDNA3.1(+)_Thy1.1-MHC-1 plasmid was *de novo* synthesized (Biomatik). Thy1.1-MHC-1 was cloned into a pSG5 vector using standard cloning techniques described above with EcoRI and BglII restriction enzymes in two-step digestion. The correct clone was confirmed by Sanger sequencing (University of Dundee). The amino acid sequence of the designed construct is given in Supplementary Table 2.

Cell culture

The B16-OVA cells with intracellular ovalbumin (OVA) were a kind gift from Ton Schumacher (The Netherlands Cancer Institute)¹¹. Cell line authentication was not performed, except confirming OVA expression with Western blot analysis. They were cultured in Iscove's modified Dulbecco's medium (IMDM; Gibco) supplemented with 10% heat-inactivated Fetal Bovine Serum FBS (Gibco), 1% penicillin/streptomycin (Gibco), 2mM L-

glutamine (Gibco) and 50 μ M 2-mercaptoethanol (Gibco; IMDM complete). CHO.K1 cells (ATCC CCL-61) were cultured in DMEM/F12 medium (Gibco) supplemented with 5% New Born Calf Serum (Biowest) and 1% penicillin/streptomycin (Gibco). No regular Mycoplasma testing was performed.

Generation of B16-OVA-Thy1.1 stable cell line

B16-OVA cells were co-transfected with 1.5 μ g of pSG5-Thy1.1-MHC-1 plasmid and 0.5 μ g of pLXSP plasmid coding for puromycin resistance with FuGENE HD reagent (Promega) in 6:1 FuGENE: DNA ratio. Briefly, the DNA was diluted in OptiMEM medium, after which FuGENE HD was added, and the mixture was incubated for 10 min at room temperature. The transfection mixture was added dropwise to the cells at 80% confluency. 24 h after transfection, 3 μ g/mL of puromycin was added to the culture medium, and the cells were grown under puromycin pressure for 10-14 days. Selected cells were stained with 2 μ g/mL of PE anti-Thy1.1 antibody (OX7 clone, Biolegend #202524) and single-cell sorted into 96-well plates containing the selection medium with puromycin. Thy1.1 expression was regularly monitored by flow cytometry with the antibody mentioned above on FACSCanto. Positive clones were expanded and the one showing stable Thy1.1 expression even after puromycin retrieval was selected for the *in vivo* study.

Thy1.1 transient transfection and cell ELISA

An amount of 24 μ g of pcDNA3.1(+)-Thy1.1 plasmid was transfected into CHO.K1 cells (10 mm Petri dish, 80% confluent) using the lipofectamine 2000 reagent (Invitrogen) according to the manufacturer's recommendation. The following day, cells were plated into a 96-well plate (5×10^5 cells/well). Two days after transfection, an antibody binding ELISA was performed. The cell supernatant was discarded, and either anti-Thy1.1 IgE, IgG2a or IgG1 were added in serial dilutions. After incubation at room temperature for 1 h, goat anti-mouse IgE-HRP conjugate (Southern Biotech, 1:4000) or goat anti-mouse IgG Fc-HRP (Jackson Immuno Research 1:5000) in 1:1 1% BSA PBS/PBST were added for 45 min at room temperature. Immunoreactivity

was visualized with TMB Stabilized Chromogen (Invitrogen). Reactions were stopped after 15 min with 0.5M H₂SO₄, and absorbances were read at 450 nm and 620 nm. All samples were tested in duplicate.

OT-1 activation

Fresh spleens from OT-1 mice were used for splenocyte isolation. The spleens were mashed through a 70 µm cell strainer, after which the Red Blood Cell Lysing Buffer (Hybri-Max, Sigma) was used to remove any erythrocytes. The splenocytes were plated at the density of 0.5 million cells/ml in 12-well plates (1ml/well). They were cultured in IMDM medium (Gibco) supplemented with 10% heat-inactivated Fetal Bovine Serum (Gibco), 1% penicillin/streptomycin (Gibco), 2mM L-glutamine (Gibco), 50 µM 2-mercaptoethanol (Gibco) and 2µg/mL OVA peptide (SIINFEKL). 48h later (day 2), the cells were subcultured 1:2. On day 3, the activated OT-1 cells were washed with PBS and injected intravenously via tail. OT-1 activation was confirmed by flow cytometry based on CD8 (BD Biosciences) and CD25 (Biolegend) expression using FACS analysis. Consistently we found that about 90% of the cells injected were fully activated OT-1 (CD8⁺ CD25⁺) (Fig. S3A).

Mice

OT-1 mice were maintained in the animal facility at the University of Edinburgh. Age-matched, 6–10-week-old female mice on a C57BL/6 background were purchased from Charles River. Experiments were carried out under the project license PPL: PP7488818. All animal experiments were approved by The University of Edinburgh.

Tumor rejection studies

After thawing, B16-OVA-Thy1.1-MHC1 cells were cultured for about a week (~3 passages) before injecting into mice. 5 x 10⁵ B16-OVA-Thy1.1-MHC-1 cells were subcutaneously injected into the right flank. Antibody treatment consisted of either 200 µg anti-Thy1.1 IgG2a or 200 µg anti-Thy1.1 Ig1 or 10 µg anti-Thy1.1 IgE (all in house produced as described above). IgGs were

administered intraperitoneally, whereas IgE was administered intravenously. The antibodies were injected on days 7, 13, 17 and 24. Some mice received the adoptive cell transfer of 2.5×10^5 activated OT-1 cells in PBS intravenously on day 13. The tumor size was measured regularly with a calliper. The mice were sacrificed when the tumors reached 10 mm in diameter or at the first sign of ulceration or if significant weight loss was observed ($> 20\%$ of initial weight). Tumor volume was calculated by the modified ellipsoidal formula: $V = \frac{1}{2} (\text{Length} \times \text{Width}^2)$.

CDC assay

B16-OVA and B16-OVA-Thy1.1 cells were detached with 2mM Ethylenediamine tetraacetic acid (EDTA) (Gibco) and were pre-stained with eF450 and eF670 (eBioscience) respectively, following manufacturers' instructions. The stained cells were then mixed in 1:1 ratio in 96-well round bottom plate (5×10^5 cells per well). Cells were washed three times with FACS buffer (1% FBS in PBS) at 400g for 3min at 4 °C and incubated with indicated antibodies at 50 µg/ml (50 µl per well) for 30min at 4 °C in the dark. Next, the cells were washed three times and were incubated with pre-warmed Rabbit Complement (RC) (Cedarlane) diluted 1:8 in IMDM complete media (50µl of RC/well). The cells were incubated for 1 hour at 37 °C, after which DNase (Promega) (1 U/µl) diluted in FACS buffer was added and the cells were washed three times. Finally, the cells were resuspended in 150 µl FACS buffer with 1 mg/ml Propidium iodide (PI) (Sigma Aldrich). 100 µl of the stained cells were analysed on a FACS LSRFortessa (BD) using the software program BD FACSDiva. Further analysis was performed with FlowJo and shown results plotted in GraphPad.

Generation of NK cells

Spleens from Rag1 KO mice were homogenized and submitted to red blood cell lysis using the RBC lysis buffer (Sigma Aldrich). The splenocytes were seeded at 2×10^6 cells/ml in 24-wells plates with RPMI (Sigma) supplemented with 10% heat-inactivated Fetal Bovine Serum (Gibco), 1% penicillin/streptomycin (Gibco), 2mM L-glutamine (Gibco), 50 µM 2-mercaptoethanol (Gibco), 20 ng/ml of IL-2 (BD Pharmingen) and 20 ng/ml of

IL-15 (PeproTech). Cells were used at day 5 when ~95% of intact cell population was identified as NK cells based on the expression of NKp46 (eBioscience) and NK1.1 (eBioscience) and lack of expression of CD3 (BD Pharmingen) by flow cytometry (CD3⁻ NKp46⁺ NK1.1⁺) using FACS LSRFortessa (BD).

Antibody-dependent cell cytotoxicity (ADCC) assay

B16-OVA and B16-OVA-Thy1.1 target cells were detached with 2mM EDTA (Gibco) and added to 96-well round bottom plates at 1×10^4 cells/well. The indicated anti-Thy1.1 antibodies were added at 10 µg/ml per well in FACS buffer and incubated for 30min at 4 °C, followed by two washing steps with FACS buffer at 400g for 3min at 4 °C. The live effector NK cells were counted using trypan blue staining and a viability of about 95% was consistently observed. NK cells were then added in pre-warmed media at 3-fold decreasing concentrations starting at 9:1 effector:target ratio. The cells were centrifuged at 400g for 2min to concentrate them at the bottom of the wells and ADCC assay was run for 4 hours at 37 °C. After 4 hours of incubation, the cells were centrifuged at 300g for 5min, and the supernatant was used to assess the cell toxicity with CytoTox 96® Non-Radioactive Cytotoxicity Assay LDH cytotoxicity Assay kit (Promega) following manufacturer's instructions. The LDH activity of medium alone was subtracted from the LDH activity of test conditions to obtain the corrected values. These corrected values were then used to calculate the percentage of cellular cytotoxicity using the following formula: percentage specific lysis = $\frac{(E+T+mAb)-(E+T)}{T_{max\ lysis} - T} \times 100$, where E are the effector cells, T are the target cells and T_{max} the lysed target cells alone.

Statistical analysis

Statistical analysis was performed in GraphPad Prism software. Survival was evaluated with the Mantel-Cox test. P-values of ≤0.05 were considered statistically significant. ns = P>0.05, * = P≤0.05. CDC assay was evaluated by one-way ANOVA applied to subtracted values (no RC – with RC) of each condition. ADCC assay was evaluated by multiple t-test at each specific ratio.

Indicated * mean the significant difference between B16-OVA-Thy1.1 IgG1 and IgG2a versus all the other conditions.

Data availability

Data were generated by the authors and included in the article. The data generated in this study are available within the article and its supplementary data files. Raw data is available upon request from the corresponding author.

Results

Expression of anti-Thy1.1 antibodies with different Fc-isotypes

To compare different isotypes in a therapeutic setting, we repeated an approach used by Nimmerjahn and colleagues⁸ and expressed antibodies with the same specificity but different isotypes (Fig. 1A). For our study, we chose an antibody, which recognises CD90.1 / Thy1.1, a congenic marker often used for immunological studies. This antibody binds to lymphocytes expressing Thy1.1, which is expressed by some mouse lines, such as AKR mice, but does not bind to Thy1.2, which is expressed by other mouse lines, such as C57BL/6. To this end, we sequenced the heavy and light chain variable domain sequences (VH, VL) of the OX7 hybridoma (anti-Thy1.1). OX7 expresses antibodies with an IgG1 isotype and is known to lack cell depleting activity once injected into mice. We therefore designed chimeric anti-Thy1.1 mIgG2a heavy chains by combining the VH with the known sequences of the constant domains of murine IgG2a (CHs). In addition, we expressed antibodies with the same anti-Thy1.1 specificity but an IgE isotype. This was mainly due to the fact that in some preclinical models, IgE antibodies have been shown to exhibit superior tumor control in comparison to their IgG homologs^{12,13}.

The anti-Thy1.1 antibodies with different Fc-isotypes were expressed *in vitro* and purified using MabSelect SuRe LX resin. Preparative size-exclusion chromatography (SEC) and quality control consisting of ultra-performance liquid chromatography (UPLC)-SEC, capillary electrophoresis sodium dodecyl sulphate (CE-SDS) and SDS-PAGE were performed. Size-exclusion ultra-performance liquid chromatography (SE-UPLC) showed that all three



antibodies (anti-Thy1.1 IgG1, IgG2a and IgE) reached monomericity levels of >95% (Fig. S1A). Next, the purity was tested by CE-SDS. Since CE-SDS was not optimized for IgE, we also included SDS-PAGE to confirm the correct molecular weights and purity of IgE. The analysis under non-reducing conditions confirmed the expected molecular weights and indicated that a high purity (>90%) was reached in all samples (Fig. S1B (left) and S1C). Furthermore, only heavy chain (HC) and light chain (LC) were observed under reducing conditions, confirming the correct sample composition (Fig. S1B (right) and S1C).

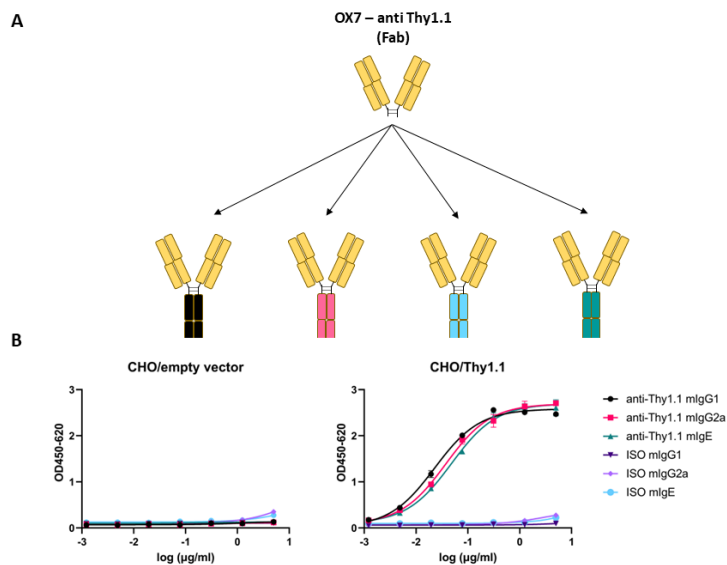


Figure 1. Panel of the different OX-7 antibodies targeting Thy1.1 used. (A) Schematic summary of the different isotypes of OX7 antibodies used. Fab (Fragment antigen-binding). (B) Cell binding ELISA of anti-Thy1.1 antibodies. The binding of anti-Thy1.1 IgG1, IgG2a and IgE was tested on CHO cells transiently transfected with an empty vector (left) or Thy1.1 (right). Isotype controls were used for each antibody isotype. Mean + SD of duplicates are shown.

Taken together, the produced antibodies complied with high-quality standards regarding monomericity and purity. In addition, we confirmed that the antigen binding was preserved in binding ELISA with Thy1.1 expressing CHO cells (Fig. 1B). Importantly, no difference in binding was observed between different isotypes.

Stable Thy1.1 expression by B16-OVA cells

CD90 (Thy1) is a glycosylphosphatidylinositol (GPI) anchored cell surface protein, and it is, therefore, susceptible to the cleavage of GPI anchor by Phospholipase-C¹⁴ (Fig. 2A). To overcome a possible loss of expression, as it has been reported before¹⁵, we replaced the GPI anchor of Thy1.1 with a murine MHC-1 transmembrane domain (Fig. 2B). Transfected B16-OVA cells were tested for their expression stability for about five weeks. B16-OVA-Thy1.1 clone showed no changes in Thy1.1 expression even after removal of puromycin used for selection, confirming stable expression by this clone (Fig. 2C-E). The replacement of the Thy1.1 transmembrane domain did not affect the binding capacity of anti-Thy1.1 antibodies, as Thy1.1-MHC-1 expression levels were measured using the same anti-Thy1.1 antibody clone (OX7).

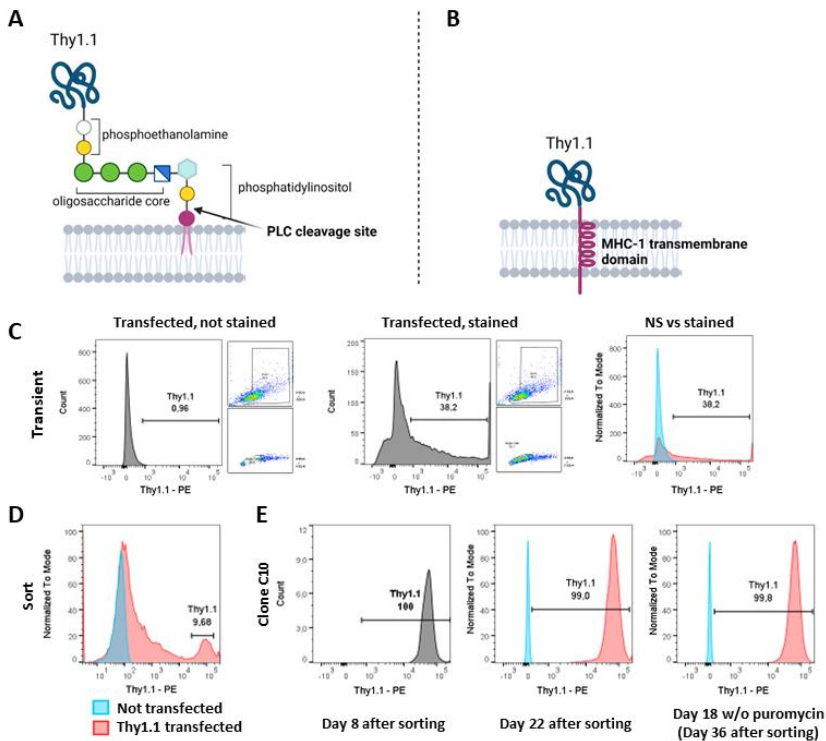


Figure 2. Thy1.1-MHC-1 expression on B16-OVA cell. B16-OVA cells were co-transfected with pSG5-Thy1.1-MHC-1 and pLXSP, selection agent (puromycin) was

added 24h after transfection and single-cell sorting was performed after at least 10 days of growing the cells in the selection medium. Thy1.1 expression was regularly tested by FACS. Schematic representation of (A) Thy1.1 with its GPI anchor and (B) the designed construct in which the GPI anchor has been replaced with MHC-1 transmembrane domain. (C-E) FACS analysis of Thy1.1 expression on B16-OVA cells after transfection with pSG5-Thy1.1_MHC-1. (C) Transient expression 24h after transfection. (D) Expression at single-cell sorting. (E) Expression on the selected clone on the indicated days.

Different CDC and ADCC profiles for IgG2a, IgG1 and IgE antibodies

To assess the capacity of the different antibodies to induce complement-mediated CDC and NK cell-mediated ADCC, *in vitro* cytotoxicity assays were performed. In order to detect on-target CDC killing, we mixed B16-OVA-Thy1.1 target cells with B16-OVA control cells in 1:1 ratio and tested how the ratio changes after antibody-mediated complement activation. As expected, only IgG2a significantly reduced the ratio (Fig. 3A-B), suggesting that only the IgG2a isotype successfully mediated CDC against target cells. Furthermore, as a control, the introduction of the Fc silencing LALA-PG mutations into IgG2 isotype abrogated the complement mediated activity (Fig 3B). In parallel, different antibody isotypes were evaluated in an ADCC assay where NK cells were used as effector cell population (Fig. S2). Here, both IgG2a and IgG1 showed high cytotoxicity towards B16-OVA-Thy1.1 cells (Fig. 3C), whereas IgE and IgG2a-LALA-PG did not induce NK cell-mediated cell killing. Finally, no cytotoxicity was observed with B16-OVA control cells not expressing Thy1.1 antigen with any of the tested isotypes.

Taken together, these data show that the expressed antibodies retained their described effector function. Although our data showed the highest complement-mediated activity for IgG2a, the ADCC effect was similar for both IgG2a and IgG1. This is to be expected as NK cells were used as effector cells in the ADCC assay. NK cells only express FcγRIII^{16,17}, which shows similar binding profiles for IgG1 and IgG2a¹⁸. Nonetheless, IgG2a presents higher affinity for the activating FcγRIV, which is absent on NK cells, but present on macrophages. Therefore, *in vivo*, where macrophages may also contribute as effector cells, superior effector function of IgG2a expressing antibodies could be postulated¹⁹⁻²¹.

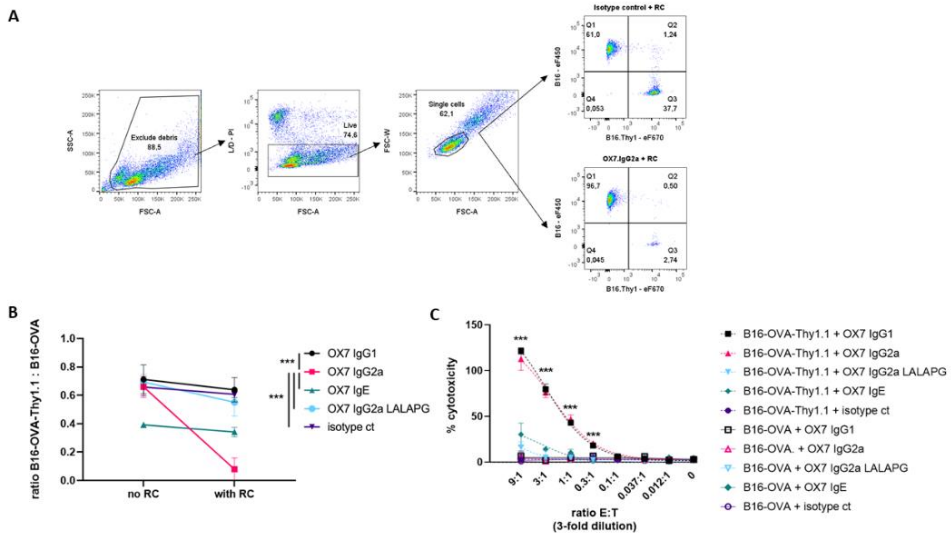


Figure 3. CDC and ADCC profiles of anti-Thy1.1 IgG1, IgG2a, IgE and IgG2a-LALAPG. (A) Representative plots used to calculate B16-OVA-Thy1.1:B16-OVA ratio. First, B16 cells were gated based on FSC-A / SSC-A properties. Next, Live cells were based on FSC-A / PI staining. Live cells were gated for single cells based FSC-A / FSC-W. Target cells B16-OVA-Thy1.1 are found in Q3 as eF670⁺ and B16 are found as Q1 as eF450⁺. Data representative from samples incubated isotype control or OX7.IgG2a and with RC. (B) B16-OVA-Thy1.1 target cells and B16-OVA control cells were previously stained, then co-incubated with 50 µg/mL of anti-Thy1.1 antibodies at 4 °C for 30 min and finally incubated with RC for 1h at 37 °C. Cells were analyzed by FACS and B16-OVA-Thy1:B16-OVA ratio was calculated. (C) B16-OVA-Thy1.1 target cells and B16-OVA control cells were incubated independently with 10 µg/mL of anti-Thy1.1 antibodies and then co-incubated at various effector-to-target ratios with NK cells for 4 h at 37 °C. CytoTox 96® Non-Radioactive Cytotoxicity Assay LDH cytotoxicity Assay kit was used to assess cytotoxic effect mediated by the antibodies. Mean + SD of triplicates are shown of a representative biological replicate out of n=3 biological replicates. (Statistics: CDC assay - one-way ANOVA on subtracted values (no RC – with RC); ADCC assay – multiple t-test, ***P < 0.001)



IgG2a antibodies show superior therapeutic tumor control to their IgG1 and IgE homologues

To test the therapeutic capacity of different antibody isotypes to control tumor growth in a syngeneic mouse model, C57BL/6 mice were subcutaneously injected with B16-OVA-Thy1.1 cells and treated with either anti-Thy1.1 IgG2a, IgG1 or IgE antibodies, starting on day 7 after tumor cells transfer (Fig. 4A). Similar to the prophylactic setting, in this therapeutic setting antibody treatment with an IgG2a isotype showed superior tumor growth control compared with antibodies with an IgG1 or IgE isotype (Fig. 4B-C). Whereas all IgG1 (10/10) or IgE (12/12) treated animals reached the human defined endpoint by day 49, 50% (6/12) of IgG2a antibody treated mice showed very small or no tumor growth at all, at day 60. Median survival was 24 days for IgG1 and 26 days for IgE, compared to 48 days for IgG2a (Fig. 4D).

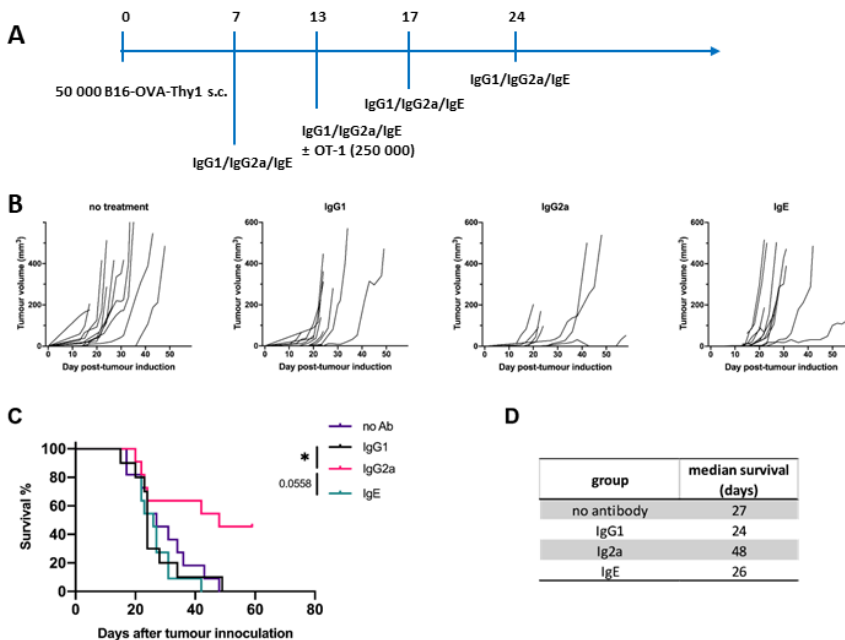


Figure 4. Superior tumor growth control of anti-Thy1.1 IgG2a in vivo. C57BL/6 mice were subcutaneously injected with 50 000 B16-OVA-Thy1.1 cells in the flank and were treated with anti-Thy1.1 IgG1, IgG2a or IgE antibodies. (A) Experimental scheme of the antibody isotype comparison in the B16-OVA-Thy1.1 model. (B) Tumor

growth curves. (C) Survival analysis. (D) Median survival in days. Statistical significance was calculated with the Mantel-Cox test. * = $P \leq 0.05$ B, C and D: $n=10-12$, combined data of two independent experiments.

To confirm that the superior tumor control is mediated via the IgG2a interaction with the immune system, we introduced LALA-PG mutations in the constant domain of the IgG2a heavy chain. LALA-PG mutations have been shown to significantly reduce the binding of both human and murine IgG antibodies to Fc γ receptors²². In the case of mIgG2a, the binding to Fc γ R1, II and IV is completely interrupted, while the binding to Fc γ RIII is reduced more than 50-fold. In addition, LALA-PG mutants show decreased C1q binding and C3 fixation in murine serum and, consequently, lose the capacity to mediate complement mediated cell lysis. When we compared the anti-Thy1.1 IgG2a and IgG2a-LALA-PG *in vivo*, we observed a complete loss of efficacy with the Fc-silenced antibody (Fig. 5A).

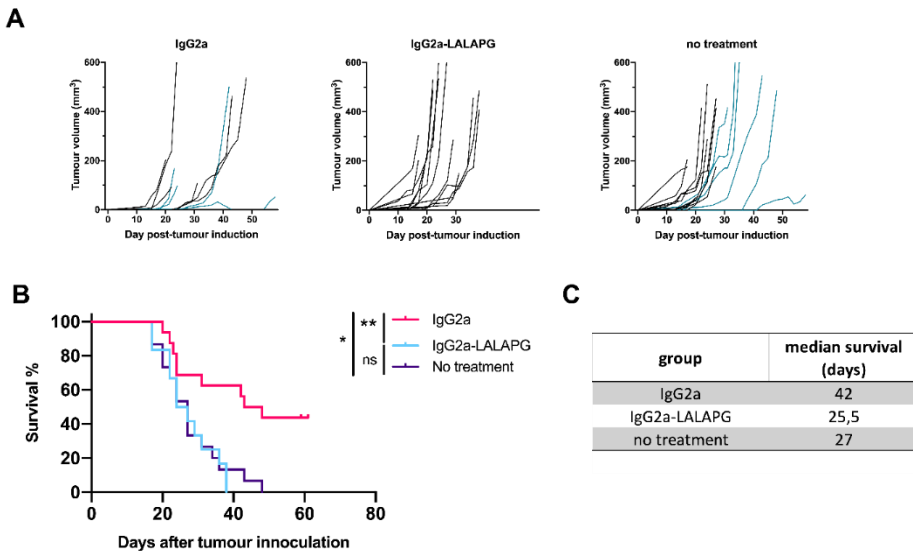


Figure 5. *In vivo* tumor control is lost when IgG2a Fc tail is silenced. C57BL/6 mice were subcutaneously injected with 50 000 B16-OVA-Thy1.1 cells in the flank and were treated with anti-Thy1.1 IgG2a (active) or anti-Thy1.1 IgG2a-LALA-PG (Fc silent) antibody. (A) Tumor growth curves. (B) Survival analysis. (C) Median survival in days. Combined data of three independent experiments are shown ($n=12-16$). Blue lines in Fig. 5A are indicative of data from figure 4 in IgG2a and control group. Statistical significance was calculated with the Mantel-Cox test. (* $P < 0.1$, ** $P < 0.01$)

Whereas IgG2a survival rate was around 50% at day 60, all mice treated with IgG2a-LALA-PG reached the endpoint by day 39 (Fig. 5B). Median survival was 42 days for IgG2a compared to 25,5 days for IgG2a-LALAPG and 27 days for the untreated group (Fig. 5C). These results clearly show that the observed anti-tumor effect of the anti-Thy1.1 IgG2a antibody was Fc mediated and isotype dependent.

Antibody treatment is not synergising with T-cell based adoptive cell transfer (ACT)

In addition, the antibodies were also tested in combination with the adoptive cell transfer of activated OT-1 cells. B16-OVA tumors are characterized by an immune-suppressive tumor microenvironment dominated by T regulatory cells (Tregs). It has been shown that depletion of intratumoral Tregs offers tumor protection when combined with the GVAX vaccine due to enhanced activation of CD8⁺ T cells^{23,24}. These data suggest that, in this setup, OT-1 efficacy can be inversely correlated with T_{reg} function. With the B16-OVA cell line that we used, OT-1 monotherapy is usually ineffective when given after day seven post tumor implantation. Therefore, we injected the OT-1 cells at a later stage of tumor development when they can no longer control the tumor growth due to an established immune-suppressive tumor microenvironment. This allowed us to test whether our antibodies attenuate this immune-suppressive tumor microenvironment (TME) and may rescue OT-1 efficacy. Nonetheless, our results show that OT-1 treated mice had similar outcomes to those that did not receive OT-1 adoptive cell transfer (Fig. S4A). These data suggest that none of the IgG2a, IgG1, or IgE treatments synergized with ACT treatment.

Discussion

In mice, the efficacy of antibody-based treatments is largely restricted to a prophylactic application, but lack efficacy in a therapeutic setting, once the tumor has been established. In this study, we directly compared the therapeutic activity of murine IgG2a, IgG1 and IgE antibodies of the same specificity, targeting a surface tumor antigen (Thy1.1). Wild type mice bearing syngeneic B16-OVA-Thy1.1 tumors were used for this purpose. Our

results show that in this setting antibodies with an IgG2a isotype offer superior tumor control in comparison to antibodies with an IgG1 or IgE isotype. The observed effect was entirely Fc-mediated as it was completely lost using IgG2a featuring Fc silencing LALA-PG mutations.

IgG2a is known as the most active IgG subclass in mice due to its high A/I ratio. Nevertheless, direct comparisons of different antibody isotypes of the same specificity in cancer settings are still scarce, although the first mechanistic basis for different activity of IgG subclasses was provided in 2005⁸. By using the B16-F10 lung metastasis model and a prophylactic treatment with TA99 antibody of different IgG subclasses (targeting Trp1 expressed on B16-F10 cells), the authors showed in that study that IgG2a offers superior tumor control to IgG1, IgG2b and IgG3⁸. However, these TA99 antibodies lack activity in a therapeutic setting⁹. Furthermore, Dahan *et al.* showed that an anti-PD-L1 IgG2a antibody is superior to IgG1 in MC38 and B16-OVA tumor models²⁵. However, PD-L1 expression is not restricted to tumor cells and has a substantial influence on local immune responses within tumors, making it challenging to extrapolate these results to exclusively tumor antigen-targeting mAbs.

Here, we sought to further our understanding of the therapeutic capacity of IgG2a expressing antibodies. To this end, we focused our study exclusively on therapeutic setting and started antibody-based treatment on day 7 after tumor cell injection. Furthermore, we focused our study on an artificial and well-characterized model antigen exclusively presented by tumor cells. For this purpose, Thy1.1 was chosen as a target antigen. As wild type C57BL/6 mice express only Thy1.2, the anti-Thy1.1 antibody treatment is tumor-selective. Furthermore, in contrast to other model tumor antigens, Thy1.1 has not functional importance for the tumor cell as such. Therefore, the anti-tumor effect observed is solely due to Fc-mediated effects, making it an ideal model system for comparing the therapeutic efficacy of different antibody isotypes.

In addition, we also included antibodies expressing the IgE isotype in this study. In multiple preclinical studies, antibodies with the IgE isotype have been shown to mediate superior anti-tumor effects in comparison to

antibodies expressing commonly used IgG isotypes^{12,13,26}. However, these studies have not addressed the potential outcome of IgE-mediated activation of mast cells (MCs) and basophils on tumor development. Since IgE can induce extremely potent immune reactions through these cell types, diverting them against tumor cells could have therapeutic benefits. Mice represent a good model for addressing this question, as their FcεRI expression is limited to MCs and basophils²⁷. Nonetheless, our results show that IgE treatment did not have any effect on tumor growth, as the growth curves and survival rate of IgE antibody treated mice were not significantly different compared to untreated mice. A similar approach has been recently used by a group at Massachusetts Institute of Technology (MIT) that showed that IgE targeting a surface tumor antigen could not successfully control the tumor growth in B16-OVA and MC-38 models in C57BL/6 wild type mice²⁸. In many studied types of tumor, mast cells have been detected to be located mainly in the peritumoral and less so in the intra-tumoral space²⁹. Therefore, a lack of effect as we observed it with IgE based antibody treatment could potentially be explained by a poor presence of IgE effector populations within B16-OVA tumors. Thus, targeting a surface tumor antigen with an IgE antibody may not be optimal for MC/basophil activation. Such limitations could potentially be overcome by using soluble tumor antigens, as they may have a higher probability of reaching MCs at the tumor edges. In line with such an assumption, our data may suggest that a tumor resident cell surface antigen, such as Thy1.1 we used in our model system, might not be an optimal IgE target for inducing MC and basophil activation at the site of solid tumors. Therefore, in order to perform a proper comparison between the therapeutic capacity of antibodies with an IgG2a and an IgE isotype, studies using mice with a humanised expression pattern of the IgεR^{12,13,26} appear warranted.

Finally, we combined antibody treatment with OT-1 adoptive cell transfer, which, as monotherapy, is usually not effective in rejecting already established B16-OVA tumors due to the immune-suppressive TME of the tumor¹¹. To our knowledge, such combination therapies consisting of tumor-targeting antibodies and adoptively transferred CTLs have not been previously tested. However, they could potentially have a beneficial effect,

if the antibody treatment could attenuate the immune-suppressive state of the TME. We were particularly interested, if IgE could mediate such an effect by inducing the T_{reg} suppression via histamine released from degranulating MCs³⁰. Nonetheless, none of the tested antibody isotypes was able to improve the efficacy of OT-1 treatment, not even treatment with the IgG2a antibody which showed substantial efficacy in monotherapy. Such findings indicate that the immune-suppressive tumor microenvironment within the transferred B16 tumors may not have been substantially altered by the antibody treatment.

Nonetheless, one should keep in mind that such a lack of response as we have observed it in our study might not necessarily be generalisable. We purposely chose the well-established B16 melanoma model system for our study, as it allowed us to keep all other factors stable, but selectively manipulate exactly one variable, i.e. the isotype of the heavy chain of the used antibodies. However, using such a highly artificial model system also has its limitations, as other tumor models might potentially be more susceptible to antibody mediated shifts in the TME. B16 melanoma, for instance, are not particularly susceptible to PD-1 targeted antibody treatment, while the colon carcinoma cell line MC38 is highly responsive to such treatment. Therefore, it might be worthwhile to investigate susceptibilities of different tumor models to ACT in combination with therapeutic antibody treatment in future studies. Furthermore, it appears necessary to aim for a better understanding of how such combined treatment might influence immune cell influx. Due to technical limitations, we could not assess such differences following the treatment with different antibodies in this study. However, there has been substantial progress in the field of highly sensitive techniques that might allow to explore this aspect in future studies. As mentioned before, in particular with respect to IgE antibodies such studies might be able to open entire novel fields of research and, potentially, therapeutic treatment opportunities. Alternatively, synergisms between tumor targeting antibody treatment and regulatory T-cell (Treg) depleting antibodies might want to be explored in more detail. In the B16 melanoma model system, it has been shown that targeting intratumoral Tregs, using CTLA-4 antibodies, offers tumor protection when

combined with CD8 T-cell inducing vaccination^{23,24}. Therefore, at this stage, it remains tempting to speculate that in future experiments a combination of T_{reg}-depleting or TGF β -neutralising antibody treatments with tumor antigen targeting antibodies may show synergistic effects in reverting an immunosuppressive TME and, hence, in enhancing the efficacy of treatment.

Therefore, in conclusion, while this study provides *in vivo* evidence that tumor antigen-targeting IgG2a is superior to its IgG1 and IgE homologs in controlling the tumor growth in a therapeutic setting in wild type C57BL/6 mice, future studies may have to dissect how these different isotypes influence immune cell influx into tumors and gauge their capacity to influence the immunosuppressive micro-environment within tumors.

Authors' Disclosures

N. Vukovic reports grants and personal fees from European Union's Horizon 2020 research and innovation programme during the conduct of the study. M. Waterfall reports there are no relationships etc. that M. Waterfall believes are a conflict of interest. However, your form will not allow the selection of the NO check box. D.M. Zaiss reports grants and personal fees from European Union's Horizon 2020 during the conduct of the study. No disclosures were reported by the other authors.

Authors' Contributions

N. Vukovic: Investigation, visualization, methodology, writing-original draft, writing-review and editing. **A. Segués:** Investigation, visualization, methodology, writing-original draft, writing-review and editing. **S.Huang:** Investigation, visualization, methodology, writing-original draft, writing-review and editing. **M. Waterfall:** Methodology, writing-review and editing. **A.J.A.M. Sijts:** Supervision, writing-review and editing. **D.M. Zaiss:** Writing-original draft, writing-review and editing.

Acknowledgements

This work was supported by the European Union's Horizon 2020 research and innovation programme under the Marie Skłodowska-Curie grant agreement [grant numbers 765394, 2018]. We thank Nicola Logan (University of Edinburgh) for her technical assistance in animal experiments. We are grateful to Aduro Biotech Europe team, especially Andrea van Elsas and Sander van Duijnhoven, for their support in antibody production and quality control.

Note

Supplementary data for this article are available at Cancer Research Communications Online (<https://aacrjournals.org/cancerrescommun/>). Received September 06, 2022; revised November 25, 2022; accepted January 01, 2023; published first January 12, 2023.

Supplementary material

Supplementary Table 1. Amino acid sequences of anti-Thy1.1 antibodies. Signal peptides are highlighted in grey, and LALA-PG mutations in cyan.

Anti-Thy1.1 IgG2a HC
MAVLGLLFCLVTFPSCVLSEIQLQQSGPELMKPGASVKISCKASGYSFTSYMDWVKQSH GKNLEWIGYIDPFNGDTSYNQKFKDKATLTVDKSSSTAYMHLSSLTSEDSAVYYCARGIYY GYGGYFDYWGGQTTLTVSSAKTTAPSVYPLAPVCGDTTGSSVTLGCLVKGYFPEPVTLTW NSGSLSSGVHTFPAVLQSDLYTLSSSVTVSSTWPSQSITCNVAHPASSTKVDDKIEPRGPTI KPCPPCKCPAPNLLGGPSVFIFPPKIKDVLMSLSPIVTCVVVDVSEDDPDVQISWVFNVE VHTAQTQTHREDYNSTLRVVSALPIQHQQDWMSGKEFKCKVNNKDLPAPIERTISKPKGSV RAPQVYVLPPEEEMTKKQVTLTCMVTDFMPEDIYVEWTNNGKTELNYKNTEPVLDSGD SYFMYSKLRVEKKNWVERNSYSCSVVHEGLHNHHTTKFSRTPGK
Anti-Thy1.1 IgG2a LALA-PG HC
MAVLGLLFCLVTFPSCVLSEIQLQQSGPELMKPGASVKISCKASGYSFTSYMDWVKQSH GKNLEWIGYIDPFNGDTSYNQKFKDKATLTVDKSSSTAYMHLSSLTSEDSAVYYCARGIYY GYGGYFDYWGGQTTLTVSSAKTTAPSVYPLAPVCGDTTGSSVTLGCLVKGYFPEPVTLTW NSGSLSSGVHTFPAVLQSDLYTLSSSVTVSSTWPSQSITCNVAHPASSTKVDDKIEPRGPTI KPCPPCKCPAPNAAAGGPSVFIFPPKIKDVLMSLSPIVTCVVVDVSEDDPDVQISWVFNVE EVHTAQTQTHREDYNSTLRVVSALPIQHQQDWMSGKEFKCKVNNKDLGAPIERTISKPKGS VRAPQVYVLPPEEEMTKKQVTLTCMVTDFMPEDIYVEWTNNGKTELNYKNTEPVLDSGD GSYFMYSKLRVEKKNWVERNSYSCSVVHEGLHNHHTTKFSRTPGK
Anti-Thy1.1 IgG1 HC
MAVLGLLFCLVTFPSCVLSEIQLQQSGPELMKPGASVKISCKASGYSFTSYMDWVKQSH GKNLEWIGYIDPFNGDTSYNQKFKDKATLTVDKSSSTAYMHLSSLTSEDSAVYYCARGIYY GYGGYFDYWGGQTTLTVSSAKTTAPSVYPLAPGSAQTNSMVTGCLVKGYFPEPVTVT WNSGSLSSGVHTFPAVLQSDLYTLSSSVTVPSSTWPSETVTCNVAHPASSTKVDDKIVPRD CGCKPCICTVPEVSSVFIFPPKPKDVLITLTPKVTVCVVVDISKDDPEVQFSWFVDDDEVHT AQTQPREEQFNSTFRSVSELPIMHQDWLNGKEFKCRVNSAAFPAPIEKTISKTKGRPKAPQ VYTIPPPKEQMAKDKVSLTCMITDFFPEDITVEWQWNGQPAENYKNTQPIMDTDGSYFV YSKLNQKSNWEAGNTFTCSVLHEGLHNHHTTEKLSLHSPGK
Anti-Thy1.1 IgE HC
MAVLGLLFCLVTFPSCVLSEIQLQQSGPELMKPGASVKISCKASGYSFTSYMDWVKQSH GKNLEWIGYIDPFNGDTSYNQKFKDKATLTVDKSSSTAYMHLSSLTSEDSAVYYCARGIYY GYGGYFDYWGGQTTLTVSSASIRNPQLYPLKPKGTASMTLGCLVKDYFPNPVTVTWYSD SLNMSTVNFPALGSELKVTTSQVTSWGSAKNFTCHVTHPPSFNESRTILVRPNITEPTLE LLHSSCDPNAFHSTIQLYCFIYGHILNDVSVSWLMDDREITDTLAQTVLIKEEGKLASTCSKL NITEQQW/MSESTFTCKVTSQGVLDYLAHTRRPCDHEPRGVITYLIPPSPLDLYQNGAPKLTC LVVDLESEKVNVTWNQEKKTSVSASQWYTKHHNNATTSITSILPVVAKDWIEGYGYQCI VDHPDFPKPIVRISITKTPGQRSAPVYVFPPEEESDKRTLTCLIQNFPEPDISVQWLGDG KLISNSQHSSTTTLKSNQGNQGGFFFSRLEVAKTLWTQRKQFTCQVIHEALQKPRKLEKTIST SLGNTSLRPS

Anti-Thy1.1 LC
MSVLTQVLALLLWLTGARCDIVLTQSPASLAVSLGQRATISCRASDSVDSFGNSFMHWF QQKPGQPPKLLIYRASTPESGIPARFSGSGSRTDFTLTISPVEADDVATYYCQQSIEDPFTFG GGTKLEIKRADAAPTVSIFPPSSEQLTSGGASVVCFLNMFYPKDINVKWKIDGSRQNGVL NSWTDQDSKDYMSSTLTLTKDEYERHNSYTCEATHKTSTSPIVKSFNRNEC

Supplementary Table 2. Amino acid sequence of designed Thy1.1-MHC-1 construct

Thy1.1-MHC-1
MNPVISITLLLSVLQMSRGQRVISLTAQLVNQNLRLDCRHENNTNLPQHEFSLTREKKKHV LSGTLGVPEHTYRSRVNLFSDRFIKVLTLANFTTKDEGDYMCELRVSGQNPTSSNKTINVIR DKLVKCGKEEPPSSTKTNTVIIAVPVVLGAVVILGAVMAFVMKRRRNTGGKGGDYALAPG SQSSDMSLPDCKV

Legend: Signal peptide – Thy1.1 without its propeptide – connecting peptide –
transmembrane domain of MHC-1 – cytoplasmic domain of MHC-1



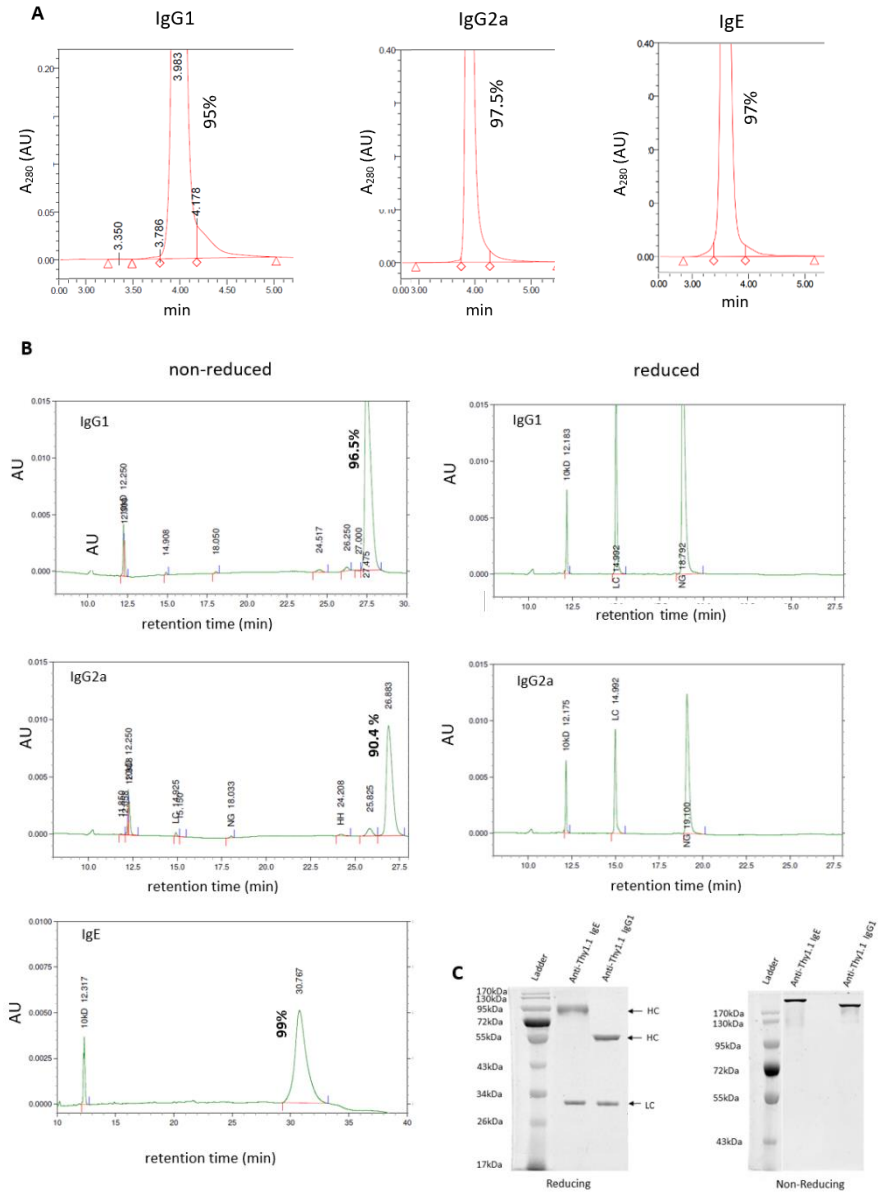


Figure S1. Quality control of anti-Thy1.1 antibodies. (A) Monomericity was evaluated with UPLC-SEC, monomer percentage is shown; (B) CE-SDS under non-reducing conditions and purity percentage (left) and under reducing conditions (right); (C) SDS-PAGE was used for IgE evaluation as a complementary method, since CE-SDS was not optimised for IgE. The data for IgE has been previously published¹⁰.

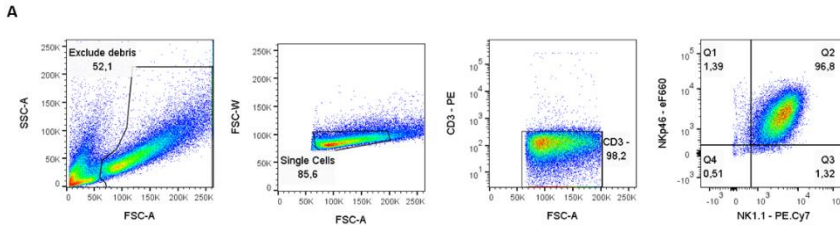


Figure S2. Flow cytometry data used for ADCC. (A) Characterization of NK population at day 5 derived from ex vivo material. Gating was done on unstained splenocytes at day 5 and its respective fluorescence-minus-one sample. First, NK cells were gated based on FSC-A / SSC-A properties. Next, single cells were gated based FSC-A / FSC-W. NK population were gated as CD3 negative. Next to the CD3⁻ population, NK population are found at NKp46⁺ NK1.1⁺ gate.

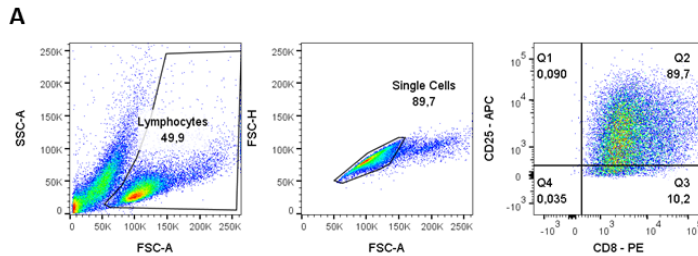


Figure S3. Confirmation of OT-1 cells activation by flow cytometry. (A) Characterization of OT-1 cells at day 3 before injection. Gating was done based on FSC-A / SSC-A properties. Next, single cells were gated based FSC-A / FSC-H. OT-1 cells were gated as CD8 positive and activated cells as CD25 positive. CD8 and CD25 quadrants based on non-stained sample.

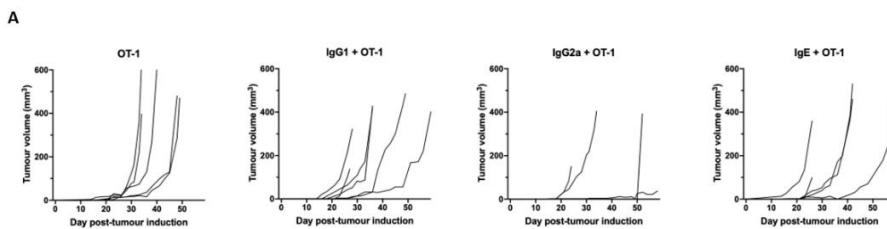


Figure S4. No synergistic effected is achieved combining anti-thy1.1 antibodies with adoptive cell transfer of activated OT-1s. C57BL/6 mice were subcutaneously injected with 50 000 B16-OVA-Thy1.1 cells in the flank and were treated with anti-Thy1.1 IgG1, IgG2a or IgE antibodies. Mice received the combination treatment consisting of anti-Thy1.1 antibodies and adoptive cell transfer of activated OT-1 cells. (A) Tumor growth curves. n=5-6, the experiment was done once.



References

1. Antibody therapeutics approved or in regulatory review in the EU or US. The Antibody Society. Accessed April 4, 2022. <https://www.antibodysociety.org/resources/approved-antibodies/>
2. Grilo AL, Mantalaris A. The Increasingly Human and Profitable Monoclonal Antibody Market. *Trends in Biotechnology*. 2019;37(1):9-16. doi:10.1016/j.tibtech.2018.05.014
3. Hudis CA. Trastuzumab — Mechanism of Action and Use in Clinical Practice. *New England Journal of Medicine*. 2007;357(1):39-51. doi:10.1056/NEJMra043186
4. Weiner GJ. Monoclonal antibody mechanisms of action in cancer. *Immunol Res*. 2007;39(1):271-278. doi:10.1007/s12026-007-0073-4
5. Chenoweth AM, Wines BD, Anania JC, Mark Hogarth P. Harnessing the immune system via FcγR function in immune therapy: A pathway to next-gen mAbs. *Immunol Cell Biol*. Published online March 11, 2020:imcb.12326. doi:10.1111/imcb.12326
6. Bordron A, Bagacean C, Tempescul A, et al. Complement System: a Neglected Pathway in Immunotherapy. *Clinic Rev Allerg Immunol*. 2020;58(2):155-171. doi:10.1007/s12016-019-08741-0
7. Vukovic N, van Elsas A, Verbeek JS, Zaiss DMW. Isotype selection for antibody-based cancer therapy. *Clin Exp Immunol*. Published online November 5, 2020. doi:10.1111/cei.13545
8. Nimmerjahn F. Divergent Immunoglobulin G Subclass Activity Through Selective Fc Receptor Binding. *Science*. 2005;310(5753):1510-1512. doi:10.1126/science.1118948
9. Ly LV, Sluijter M, Burg SH van der, Jager MJ, Hall T van. Effective Cooperation of Monoclonal Antibody and Peptide Vaccine for the Treatment of Mouse Melanoma. *The Journal of Immunology*. 2013;190(1):489-496. doi:10.4049/jimmunol.1200135
10. Vukovic N, Harraou S, van Duijnhoven SMJ, Zaiss DM, van Elsas A. Purification of murine immunoglobulin E (IgE) by thiophilic interaction chromatography (TIC). *J Immunol Methods*. 2021;489:112914. doi:10.1016/j.jim.2020.112914
11. de Witte MA, Coccoris M, Wolkers MC, et al. Targeting self-antigens through allogeneic TCR gene transfer. *Blood*. 2006;108(3):870-877. doi:10.1182/blood-2005-08-009357
12. Pellizzari G, Bax HJ, Josephs DH, et al. Harnessing Therapeutic IgE Antibodies to Re-educate Macrophages against Cancer. *Trends in Molecular Medicine*. 2020;26(6):615-626. doi:10.1016/j.molmed.2020.03.002
13. Daniels-Wells TR, Helguera G, Leuchter RK, et al. A novel IgE antibody targeting the prostate-specific antigen as a potential prostate cancer therapy. *BMC Cancer*. 2013;13:195. doi:10.1186/1471-2407-13-195

14. Bütikofer P, Malherbe T, Boschung M, Roditi I. GPI-anchored proteins: now you see 'em, now you don't. *The FASEB Journal*. 2001;15(2):545-548. doi:10.1096/fj.00-0415hyp
15. Ferris ST, Durai V, Wu R, et al. cDC1 prime and are licensed by CD4+ T cells to induce anti-tumour immunity. *Nature*. 2020;584(7822):624-629. doi:10.1038/s41586-020-2611-3
16. Mandelboim O, Malik P, Davis DM, Jo CH, Boyson JE, Strominger JL. Human CD16 as a lysis receptor mediating direct natural killer cell cytotoxicity. *Proc Natl Acad Sci U S A*. 1999;96(10):5640-5644. doi:10.1073/pnas.96.10.5640
17. Bryceson YT, March ME, Ljunggren HG, Long EO. Synergy among receptors on resting NK cells for the activation of natural cytotoxicity and cytokine secretion. *Blood*. 2006;107(1):159-166. doi:10.1182/blood-2005-04-1351
18. Dekkers G, Bentlage AEH, Stegmann TC, et al. Affinity of human IgG subclasses to mouse Fc gamma receptors. *MAbs*. 2017;9(5):767-773. doi:10.1080/19420862.2017.1323159
19. Uccellini MB, Aslam S, Liu STH, Alam F, García-Sastre A. Development of a Macrophage-Based ADCC Assay. *Vaccines*. 2021;9(6):660. doi:10.3390/vaccines9060660
20. Beum PV, Lindorfer MA, Taylor RP. Within Peripheral Blood Mononuclear Cells, Antibody-Dependent Cellular Cytotoxicity of Rituximab-Opsonized Daudi cells Is Promoted by NK Cells and Inhibited by Monocytes due to Shaving. *The Journal of Immunology*. 2008;181(4):2916-2924. doi:10.4049/jimmunol.181.4.2916
21. Beum PV, Kennedy AD, Williams ME, Lindorfer MA, Taylor RP. The Shaving Reaction: Rituximab/CD20 Complexes Are Removed from Mantle Cell Lymphoma and Chronic Lymphocytic Leukemia Cells by THP-1 Monocytes. *The Journal of Immunology*. 2006;176(4):2600-2609. doi:10.4049/jimmunol.176.4.2600
22. Lo M, Kim HS, Tong RK, et al. Effector-attenuating Substitutions That Maintain Antibody Stability and Reduce Toxicity in Mice. *Journal of Biological Chemistry*. 2017;292(9):3900-3908. doi:10.1074/jbc.M116.767749
23. van Elsas A, Hurwitz AA, Allison JP. Combination Immunotherapy of B16 Melanoma Using Anti-Cytotoxic T Lymphocyte-Associated Antigen 4 (Ctla-4) and Granulocyte/Macrophage Colony-Stimulating Factor (Gm-Csf)-Producing Vaccines Induces Rejection of Subcutaneous and Metastatic Tumors Accompanied by Autoimmune Depigmentation. *J Exp Med*. 1999;190(3):355-366.
24. Simpson TR, Li F, Montalvo-Ortiz W, et al. Fc-dependent depletion of tumor-infiltrating regulatory T cells co-defines the efficacy of anti-CTLA-4 therapy against melanoma. *J Exp Med*. 2013;210(9):1695-1710. doi:10.1084/jem.20130579
25. Dahan R, Segal E, Engelhardt J, Selby M, Korman AJ, Ravetch JV. FcγRs Modulate the Anti-tumor Activity of Antibodies Targeting the PD-1/PD-L1 Axis. *Cancer Cell*. 2015;28(3):285-295. doi:10.1016/j.ccell.2015.08.004
26. Gould HJ, Mackay GA, Karagiannis SN, et al. Comparison of IgE and IgG antibody-dependent cytotoxicity in vitro and in a SCID mouse xenograft model of ovarian

- carcinoma. *Eur J Immunol.* 1999;29(11):3527-3537. doi:10.1002/(SICI)1521-4141(199911)29:11<3527::AID-IMMU3527>3.0.CO;2-5
27. Leoh LS, Daniels-Wells TR, Penichet ML. IgE Immunotherapy Against Cancer. In: Lafaille JJ, Curotto de Lafaille MA, eds. *IgE Antibodies: Generation and Function*. Vol 388. Springer International Publishing; 2015:109-149. doi:10.1007/978-3-319-13725-4_6
 28. Adrienne Marie Rothschilds. *Engineering Protein-Based Modulators of Allergic, Temporal, and Checkpoint Blockade Anti-Cancer Immunity*. Massachusetts Institute of Technology; 2019. <https://dspace.mit.edu/handle/1721.1/123064>
 29. Carlini MJ, Dalurzo MCL, Lastiri JM, et al. Mast cell phenotypes and microvessels in non-small cell lung cancer and its prognostic significance. *Hum Pathol.* 2010;41(5):697-705. doi:10.1016/j.humpath.2009.04.029
 30. de Vries VC, Wasiuk A, Bennett KA, et al. Mast cell degranulation breaks peripheral tolerance. *Am J Transplant.* 2009;9(10). doi:10.1111/j.1600-6143.2009.02755.x



5

Generation and characterization of novel co-stimulatory anti-mouse TNFR2 antibodies

Aina Segués^{a,b,c}, Sander M.J. van Duijnhoven^a, Marc Parade^a, Lilian Driessen^a, Nataša Vukovic^d, Dietmar Zaiss^{d,e}, Alice J. A. M. Sijts^b, Pedro Berraondo^d, Andrea van Elsas^{a,*}

- a. *Aduro Biotech Europe, Oss, The Netherlands*
- b. *Faculty of Veterinary Medicine, Department of Infectious Diseases and Immunology, Utrecht University, Utrecht, The Netherlands*
- c. *Division of Immunology and Immunotherapy, CIMA Universidad de Navarra, Pamplona, Spain*
- d. *Institute of Immunology and Infection Research, School of Biological Sciences, University of Edinburgh, United Kingdom*
- e. *Institute of Immune Medicine, University Hospital Regensburg, Regensburg, Germany*

* *Corresponding author*

E-mail address: andrea.vanelas@gmail.com

Journal of Immunological Methods, Volume 499 (2021) 113173
<https://doi.org/10.1016/j.jim.2021.113173>

Contribution statement: *Aina Segués Cisteró conceived the original idea, designed, planned and carried out the experiments. She contributed to the interpretation of the results and to the writing of the manuscript.*

Abstract

Tumor necrosis factor receptor 2 (TNFR2) has gained much research interest in recent years because of its potential pivotal role in autoimmune disease and cancer. However, its function in regulating different immune cells is not well understood. There is a need for well-characterized reagents to selectively modulate TNFR2 function, thereby enabling definition of TNFR2-dependent biology in human and mouse surrogate models. Here, we describe the generation, production, purification, and characterization of a panel of novel antibodies targeting mouse TNFR2. The antibodies display functional differences in binding affinity and potency to block TNF α . Furthermore, epitope binding showed that the anti-mTNFR2 antibodies target different domains on the TNFR2 protein, associated with varying capacity to enhance CD8⁺ T-cell activation and costimulation. Moreover, the anti-TNFR2 antibodies demonstrate binding to isolated splenic mouse Tregs *ex vivo* and activated CD8⁺ cells, reinforcing their potential use to establish TNFR2-dependent immune modulation in translational models of autoimmunity and cancer.

Key words

TNFR2, antibody, epitope, Cysteine-Rich Domain, costimulation, Treg

Highlights

- We have generated a diverse library of anti-mouse TNFR2 antibodies
- Developed anti-mouse TNFR2 antibodies show binding to regulatory T cells (Tregs) and activated CD8⁺ cells
- Some anti-mouse TNFR2 antibodies costimulate CD8⁺ cells

Introduction

The immune system encodes multiple controls evolved to ensure a balance of immune homeostasis ready to fight infections and inhibit the development of cancer, but also aiming to prevent unwanted inflammation and autoimmunity. A disbalance in immune regulation can contribute to immune overreaction, as recently observed in severe Covid-19 cases¹, leading to autoimmune and infectious disease, inadequate tumor immunity, or even immune paralysis in sepsis. Blockade of immune checkpoint receptors such as programmed cell death protein 1 (PD-1) and cytotoxic T lymphocyte-associated protein 4 (CTLA-4) plays an important role in the treatment of cancer^{2,3}. In contrast, defects in or deliberate blockade of immune checkpoint pathways may result in the loss of peripheral tolerance and autoimmunity⁴. Enhancing the activity of immune checkpoint pathways potentially using agonistic agents may hold promise for the treatment of autoimmunity^{5,6}. In this context, tumor necrosis factor receptor 2 (TNFR2; TNFRSF1B; CD120b) might act as an immune checkpoint on T lymphocytes.

In the past decade, the interest to target the co-stimulatory tumor necrosis factor receptor superfamily (TNFRSF) for immunotherapy of cancer^{7,8} and autoimmune disease^{9,10} has increased significantly. Approximately 30 members of the TNFRSF have been identified. TNFRSF, together with its respective ligands, control cell survival, proliferation, differentiation, and effector function in different cell types, including immune cells¹¹. Some of these receptors have already been defined to play a crucial role in immune dysfunction, autoimmunity, and cancer. For example, the CD40L-CD40 interaction has been shown to be correlated with inflammatory and muscle wasting diseases^{12,13}. Furthermore, promotion of antitumor T cell activity has been achieved by using several agonistic anti-CD40 antibodies^{14,15}, and other examples include antibodies targeting CD27, 4-1BB, and OX40. However, these agonists are not yet a clinical success, likely due to promiscuous expression and function on other cells leading to safety concerns.

Tumor necrosis factor α (TNF α) is involved in several immune response pathways mediating its activity via TNF receptor 1 (TNFR1) and TNF receptor 2 (TNFR2). While TNFR1 is ubiquitously expressed on almost all cell types¹⁶,

TNFR2 expression is limited to certain subpopulations of immune cells. Beyond its expression on specific immune cell subpopulations, TNFR2 expression has also been described for several other cell types, such as oligodendrocytes, cardiomyocytes, mesenchymal stem cells and endothelial progenitor cell^{17–20}. TNF α is the principal ligand of TNFR1 and TNFR2. TNFR1 receptor signaling is activated through both soluble and membrane TNF- α , whereas TNFR2 is mainly activated by membrane TNF- α ²¹. However, while TNFR1 stimulation can trigger both a strong pro-inflammatory response as well as cell death through its death domains, TNFR2 stimulation has so far only be involved in cell survival, proliferation and differentiation as well as inducing a more anti-inflammatory response²².

Due to its inducible expression on regulatory T cells (Tregs), TNFR2 has been identified as an important target in autoimmune diseases and cancer²³. In mice, the highest TNFR2 expression is found on Tregs with potent immunosuppressive capacity, as well as on conventional T cells that resist Treg mediated immunosuppression. However, overall, in tumor-derived T cell populations, the suppressive effect appears to be dominant²⁴. In cancer cells, TNFR2 expression has been correlated with tumor growth²⁵ and its absence in CD8⁺ T cells with enhanced immune rejection²⁶. TNFR2 signaling in innate immune lymphocytes enhanced allergic lung inflammation²⁷. However, consistent with a role in Tregs, TNFR2 signaling suppressed autoimmunity in the central nervous system²⁸. Furthermore, the induction of Treg differentiation by specific cell types, such as mesenchymal stem cells, has also been shown to be TNFR2 dependent²⁹. Therefore, TNFR2 is an appealing target in both cancer and autoimmune disease. Although TNFR2 was recently considered an immune checkpoint, its role in different immune cells and diseases is not well understood and requires well-defined reagents.

Here, we generated and characterized the activity of a novel panel of 13 diverse rat anti-mouse TNFR2 antibodies. The panel contains antibodies that bind to different extracellular domains of TNFR2 and selectively display varying functional capacity. These novel antibodies have been sequenced and classified based on their binding and blocking activity, epitope binning with respect to binding of specific TNFR2 extracellular domains, and their

capacity to enhance costimulation of CD8⁺ T-cell activation. Furthermore, a subset of antibodies demonstrates potent binding to TNFR2 on the surface of mouse Tregs and activated C8⁺ cells. This diverse set of well-characterized antibodies may serve to explore further TNFR2 function in mouse models of health and disease.

Material and methods

Cell lines

All cell lines were maintained at 37 °C in a humidified 5% CO₂ incubator. CHO-K1 cells were cultured in DMEM/F12 (Gibco, 11320-074) supplemented with 100 U/mL Penicillin, 100 µg/mL Streptomycin (Gibco, 15140-122), and 5% NBCS (Biowest, S0750-500). Additionally, 0.8 mg/mL Geneticin (Gibco, 19131-027) was added to stable transfected CHO-K1.mTNFR2. B-cells were cultured in DMEM/F12 HAM medium (Sigma Aldrich, D6421) supplemented with 365 mg/L L-glutamine (Gibco, 25030), 0.5 mM Sodium pyruvate (Gibco, 11360-039), 50 µM 2-mercaptoethanol (Gibco, 31350-010), 100 U/mL Penicillin, 100 µg/mL Streptomycin (Gibco, 15140-122), and 10% BCS (Hyclone, SH30072.03) in the presence of 5 x 10⁵ cells/mL irradiated EL.4 B5 cells (feeder cells). SP2/0-Ag14 cells were cultured in DMEM/F12 (Gibco, 11320-074) supplemented with 100 U/mL Penicillin, 100 µg/mL Streptomycin (Gibco, 15140-122), 50 µM 2-mercaptoethanol (Gibco, 31350-010), and 10% FBS (Hyclone, SH30414.02). Hybridomas were selected in DMEM/F12 medium (Gibco, 11320-074) supplemented with 0.5 mM Sodium pyruvate (Gibco, 11360-039), 50 µM 2-mercaptoethanol (Gibco, 31350-010), 100 U/mL Penicillin, 100 µg/mL Streptomycin (Gibco, 15140-122), 10% FBS (Hyclone, SH30414.02), 1% T24 conditioned media, and 2% HAT supplement 50X (Gibco, 21060-017). Hybridomas were cultured in DMEM/F12 medium (Gibco, 11320-074) supplemented with 0.5 mM Sodium pyruvate (Gibco, 11360-039), 50 µM 2-mercaptoethanol (Gibco, 31350-010), 100 U/mL Penicillin, 100 µg/mL Streptomycin (Gibco, 15140-122), 10% NBCS (Biowest, S0750-500), 1% T24CM, and 1% HT supplement 100X (Gibco, 11067-030).

Generation of hybridomas producing monoclonal antibodies (mAbs)

Three 9-week-old female Sprague Dawley rats were immunized on the ears using mTNFR2 encoding DNA coated gold-carrier beads via gene gun. After 4 rounds of immunization, cells derived from lymph nodes, spleen, and bone marrow were harvested and TNFR2 specific B cells isolated following published procedures³⁰. Briefly, negative and positive panning strategies were performed to select TNFR2 specific B-cells. Culture plates with CHO-K1 and transiently transfected CHO-K1 with mouse TNFR1, or in parallel plates coated with mIgG and mTNFR1 recombinant protein were used for negative panning as cross-reactivity to mTNFR1 was non desired. TNFR2 expressed on cells or recombinant mTNFR2 protein were used for positive panning.

CHO-K1.mTNFR2 or mTNFR2 protein-bound lymphocytes were harvested with Trypsin-EDTA (Sigma Aldrich, T4174). Harvested B-cells were cultured, as described by Steenbakkers et al., 1994, Mol. Biol. Rep. 19: 125-134³¹. Briefly, selected B-cells were mixed with 10% (v/v) T-cell supernatant and 50,000 irradiated (25 Gray) EL-4 B5 feeder cells in a final volume of 200 μ L medium in 96-well flat-bottom tissue culture plates and were cultured at 37 °C and 95% humidity for 9 days.

Immunoreactivity to mouse TNFR2 and cross-reactivity to human TNFR2 was assessed by ELISA using recombinant mTNFR2/Fc-protein (R&D Systems, 9707-R2) and hTNFR2 (R&D Systems, 726-R2) as well as CHO-K1.mTNFR2 and CHO-K1.hTNFR2. 0.1 μ g/ml mTNFR2 and 0.2 μ g/ml hTNFR2 protein-coated 96-well plates were blocked in PBS/1% bovine serum albumin (BSA) (Sigma Aldrich, A7409) for 1 hour at room temperature (RT). Assay plates with B-cell conditioned medium were incubated for 1 hour at RT. Next, plates were washed with PBS-T and incubated for 1 hour at RT with goat-anti-rat IgG-HRP conjugate (Jackson Immuno Research, 112-035-167). Subsequently, wells were washed three times with PBS-T, and anti-mTNFR2 immunoreactivity was visualized with TMB Stabilized Chromogen (Invitrogen, SB02). Reactions were stopped with 0.5 M H₂SO₄, and absorbances were read at 420 and 620 nm.

B-cell clones that showed specific binding to mTNFR2 (with or without cross-reactivity toward hTNFR2) and no cross-reactivity to TNFR1 were immortalized by mini-electrofusion following published procedures (Steenbakkers *et al.*, 1992, *J. Immunol. Meth.* 152: 69-77; Steenbakkers *et al.*, 1994, *Mol. Biol. Rep.* 19:125-34)^{31,32} with some minor deviations.

Briefly, B-cells were mixed with 1×10^6 Sp2/O-Ag14 murine myeloma cells in Electrofusion Isomolar Buffer (Eppendorf). Electrofusions were performed in a 50 μ L fusion chamber by an alternating electric field of 15 s, 1 MHz, 23 Vrms AC followed by a square, high field DC pulse of 10 μ s, 180 Volt DC and again by an alternating electric field of 15 s, 1 MHz, 23 Vrms AC. Content of the chamber was transferred to hybridoma selective medium and plated in a 96-well plate under limiting dilution conditions. On day 10 following the electrofusion, hybridoma supernatants were screened for mTNFR2, hTNFR2, mTNFR1 binding activity by and ELISA, as described above. Hybridomas that secreted antibodies in the supernatant that specifically bound mTNFR2 and/or hTNFR2 were both frozen at -180 °C and subcloned by limited dilution to safeguard their clonal integrity and stability.

28 hybridomas clones producing different anti-mTNFR2 were obtained, and based on different characteristics, 13 candidates were selected to be further characterized, methods, and results shown in this manuscript. Generated antibodies were sent for sequencing, and sequences can be found attached in Supplementary Table 1. All antibodies were tested for their isotype using the Rat Monoclonal Antibody Isotyping Test Kit (Bio-Rad, RMT1) following manufacturer's instructions.

Production and purification of mAbs

13 hybridomas clones producing different anti-mTNFR2 antibodies were incubated in hybridoma serum-free medium (HSFM) (Gibco, 12045-076) supplemented with serum-free T24 CM and 100 U/mL Penicillin and 100 μ g/mL Streptomycin (Gibco, 15140-122) at a density of 5×10^5 cells/mL for 7 days at 37 °C in 8% CO₂ at 80 rpm. Cells were spun down, and the supernatant was filtered through a 0.22 μ m filter. All anti-mTNFR2 mAbs were purified by GammaBind Plus Sepharose (GE Healthcare, 17-0886-01)

followed by size exclusion chromatography (SEC) using a Waters BEH200 SEC column (4.6 x 300 mm, 1.7µm). mAbs were rebuffered in 10mM L-Histidine 0.1M NaCl pH 5.5.

Quality control

Monomericity of mAbs was tested via Size Exclusion Chromatography Ultra Performance Liquid Chromatography (SEC-UPLC) on a Waters BEH200 SEC column, 4.6 x 300 mm, 1.7 µm with an Agilent 1100 series HPLC system. Separation was carried out in 50mM phosphate 0.2M NaCl, pH 7.0. The monomericity was also tested following incubation and storage at different temperatures to assess protein stability. Two temperature studies were performed: (i) 10 freeze and thaw (F/T) cycles and (ii) incubation at 40 °C for one week. Based on the initial monomericity, the stability has been reported as the recovery percentage.

The purity of mAbs produced was tested by Capillary electrophoresis sodium dodecyl sulfate (CE-SDS) in non-reduced mode. CE-SDS analysis was carried out on a CE system PA800 Plus machine (Beckman Coulter). Non-reduced samples were diluted to 1 mg/mL with 10kDa internal standard and 15mM iodoacetamide in SDS-MW sample buffer and heated to 70 °C for 10 min. Reduced samples were diluted to 1 mg/mL with 10kDa internal standard and 2-mercaptoethanol (Sigma Aldrich, M3148) in SDS-MW sample buffer and heated to 70 °C for 10 min. 95 µL were transferred into sample vials and loaded into the machine. Separations were performed in a 30 cm bara-fused silica 50 µm I.D capillary at 22 °C. The capillary was flushed with 0.1 M HCl, NaOH, water, and running buffer before sample loading at 5kV for 20sec. Data acquisition was performed with the 32Karat software, but data processing was carried out with Empower software.

Flow cytometry: Cell binding and TNFα blocking assay

Binding potency of the anti-mTNFR2 mAbs on mTNFR2 CHO-K1 stable transfected cell line was assessed by flow cytometry. 1×10^5 cells were incubated with 3-fold increasing concentrations (max 10 µg/mL) of anti-mTNFR2 mAbs at 4 °C for 30 min, and binding was detected with anti-rat IgG PE (BD Biosciences, 550767). TNFR2 expression of the cell line was assessed

via hamster anti-mouse CD120b (TNF R Type II/p75) -PE (TR75-89) (Biolegend, 113405), and hamster IgG1 isotype control-PE (BD Biosciences, 553972) was used as a negative control.

For all anti-mTNFR2 mAbs, competitive binding in the presence of TNF α was assessed with CHO-K1.mTNFR2 stable transfected cell line by flow cytometry. 1×10^5 cells were incubated with 3-fold increasing concentrations (max 50 $\mu\text{g}/\text{mL}$) of anti-mTNFR2 mAbs at 4 °C for 30 min followed by TNF α -biotin (Sino Biological, 50349-MNAE-B) incubation at 4 °C for 30 min without wash step. Blocking activity was detected with Streptavidin-APC (BD Biosciences, 349024). Two benchmark hamster antibodies against mTNFR2 were taken as a reference: Purified anti-mouse CD120b (TNFR Type II/p75, clone TR75-54.7) (Biolegend, 113302) listed as anti-TNFR2 mAb with blocking activity and Purified anti-mouse CD120b (TNFR Type II/p75, clone TR75-89) (BD Biosciences, 559916) as a non-blocking anti-TNFR2 mAb. Furthermore, a benchmark rat anti-mTNFR2 clone HM102 (Abcam, ab7369) with unknown blocking activity was included together with a rat IgG2a mAb (clone EBR2a) (eBioscience, 14-4321-85) as a negative control. Each time that binding and blocking experiment was performed, a gating for TNFR2 expression for FACS signal was performed with unstained CHO-K1.mTNFR2 cell line (Fig. S1 A), and in parallel TNFR2 expression was assessed (Fig. S1; B and C). mTNFR1 expression was assessed by anti-mTNFR1 PE antibody (Biolegend, 113003) and only detected following transfection with the mTNFR1 construct (Fig. S1 D).

The stained cells were analysed on a FACS CantoTM II (BD) using the software program BD FACSDiva. Ten thousand events were counted. Further analysis was performed with FlowJo and shown results plotted in GraphPad.

Bio-Layer interferometry (BLI)

Antibody binding kinetics towards mouse TNFR2 were evaluated by bio-layer interferometry (BLI) using an Octet Red96 (Forte-Bio) in triplicates. First, the dissociation rate constant of 28 anti-mTNR2 antibodies derived from hybridoma supernatant was assessed (data not shown).

To assess mAbs kinetics, the affinity constant (K_D) toward recombinant mTNFR2 protein was determined. Rat anti-mTNFR2 purified antibodies were diluted (10 $\mu\text{g}/\text{mL}$) in 10mM acetate pH 5.0 and loaded on NHS/EDC activated Amine Reactive 2nd Generation (AR2G)(Forte-Bio, 18-5088). Thereafter, the antibody loaded biosensors were blocked with 1M ethanolamine (Forte-Bio, 18-1071). First, a single estimation screening of K_D value was performed with an expected saturating concentration of 100nM His tagged mTNFR2 (R&D Systems, 426-R2/CF) 100nM diluted in 10x Kinetics Buffer (KB) followed by a dissociation step. Based on the estimated K_D , the experiment was repeated three times per candidate starting with a recombinant mTNFR2 concentration 10 or 5 times above the single estimated K_D followed by 2-fold decreasing concentration dilution. Binding kinetics were measured by Octet system according to the manufacturer's instructions (ForteBio). Data was analysed using Data analysis software HT V10.0 (ForteBio).

Epitope mapping

Mouse-human TNFR2 chimeras were designed based on four different cysteine-rich domains (CRD) swap mutants: hTNFR2 (mCRD1), hTNFR2 (mCRD2), hTNFR2 (mCRD3), hTNFR2 (mCRD4), mTNFR2 (hCRD1), mTNFR2 (hCRD2), mTNFR2 (hCRD3) and mTNFR2 (hCRD4). mTNFR2, hTNFR2, and mTNFR1 were also included in the study. The N-terminal region for CRD1 and the C-terminal region following CRD4 was included as part of the respective domains. cDNA constructs were synthesized (GeneArt) and were subcloned with DH5 α competent cells (Invitrogen, 18265-017) and amplified with GenElute HP plasmid Midiprep Kit (Sigma Aldrich, NA0200). Each construct was expressed after transient transfection of CHO-K1 cells using Lipofectamine 2000 (Invitrogen, 11668-019). After 6h hours with incubation media, cells were detached, and 5×10^6 cells were seeded per 96-wells f-bottom plates (Thermo Scientific, 150350) in final volume of 50 μL per well. Cells were incubated at 37 $^\circ\text{C}$ with 5% CO_2 and 95% humidity for 16 hours. Afterwards, cells were incubated with 10-fold increasing concentrations (max 5 $\mu\text{g}/\text{mL}$) of anti-mTNFR2 mAbs diluted in CHO medium at 4 $^\circ\text{C}$ for 1 h and after 3 wash cycles with PBS 0,05% Tween-20 (VWR, 663684B), binding

was detected with anti-rat IgG HRP 1:5000 (Jackson Immuno Research, 112-035-167). After 3 wash cycles with PBS 0,05% Tween-20, TMB (Invitrogen) was added and after 15 min, reaction was stopped with 0.5M H₂SO₄. OD 450-620 was measured on Spectramax 340PC reader. Collected data was analysed in GraphPad Prism.

Treg staining

Binding of all anti-mTNFR2 mAbs was assessed on flow-sorted CD4⁺Foxp3/YFP⁺ cells from B6.129(Cg)-Foxp3tm4(YFP/cre)Ayr/J mice³³. Splens from FoxP3/YFP mice were homogenized and RBC lysed using the 1X RBC lysis buffer (Sigma Aldrich, R7757). Splenocytes were seeded at 2 x 10⁶ cells/ml per 96-wells u-bottom plates (Thermo Scientific, 163320) in final volume of 50 µL per well. Two different staining procedures were followed: (i) Treg staining with generated anti-mTNFR2 antibodies and (ii) Treg staining with generated anti-mTNFR2 antibodies competing with benchmark anti-mTNFR2 (clone TR75-89, TNFα non-blocking).

i) Splenocytes were washed once with PBS 1% BSA (Sigma Aldrich, A7409) (FACS buffer). Cells were incubated at 4 °C for 30 min with 20 µg/mL of anti-mTNFR2 mAbs diluted in FACS buffer. Commercial hamster anti-mTNFR2 direct labelled with PE (clone TR75-79)(Biolegend, 113405) and hamster isotype control direct labelled with PE (BD Biosciences, 553972) were included as controls following manufacturer's concentrations. After 3 wash steps, cells were incubated at 4 °C for 30 min with hamster 5 µg/mL of anti-CD3-PE/Cy7 (Clone 145-2C11)(Biolegend, 100320) and mTNFR2 binding was detected with goat 4 µg/mL of anti-rat IgG-AF647 (Invitrogen, A21247).

ii) Similarly, splenocytes were washed once with PBS 1% BSA (Sigma Aldrich, A7409) (FACS buffer). Cells were incubated at 4 °C for 30 min with 20 µg/mL of anti-mTNFR2 mAbs diluted in FACS buffer. After 3 wash step, cells were incubated at 4 °C for 30 min with hamster 5 µg/mL of anti-CD3-PE/Cy7 (Clone 145-2C11)(Biolegend, 100320) and 2,5 µg/mL of hamster anti-mouse CD120b (TNFR Type II/p75) -PE, (clone TR75-89) (Biolegend, 113405). Followed by 3 wash step, a third incubation at 4 °C for 30 min was performed to detect mTNFR2 binding with goat 4 µg/mL of anti-rat IgG AF647

(Invitrogen, A21247) assessing if both anti-mTNFR2 gave double positive signal.

Each replicate the gating strategy for TNFR2 expression obtained by FACS signal was performed with (i) rat isotype control (Fig. S2 A) and (ii) rat isotype control together with anti-mTNFR2-PE clone TR75-89. The stained cells were analysed on a FACS LSRFortessa (BD) using the software program BD FACSDiva. Further analysis was performed with FlowJo and shown results plotted in GraphPad.

CD8 staining

Binding of all anti-mTNFR2 mAbs was assessed on flow-sorted activated CD8⁺ cells from OT1 hom Rag1 KO mice, endogenously expressing mTNFR2 cells upon activation. Splens from OT1 home Rag1 KO mice were homogenized and RBC lysed using the 1X RBC lysis buffer (Sigma Aldrich, R7757). Splenocytes were activated with 1:1000 SIINFKEL peptide and seeded at $0,5 \times 10^6$ cells/ml per 12 wells plates (Corning, 353043) in final volume of 1ml per well with IMDM complete medium (Sigma, I3390). Cells were for incubated for 2 days at 37 °C in 8% CO₂. Cells were split 1:2 at day two and used at day 3.

Activated OT1 cells were washed once with PBS 1% BSA (Sigma Aldrich, A7409) (FACS buffer). Cells were incubated at 4 °C for 30 min with 20 µg/mL of anti-mTNFR2 mAbs diluted in FACS buffer. Commercial hamster anti-mTNFR2 direct labelled with PE (clone TR75-79)(Biolegend, 113405) and hamster isotype control direct labelled with PE (BD Biosciences, 553972) were included as controls following manufacturer's concentrations. After 3 wash steps, cells were incubated at 4 °C for 30 min with human 1 µg/mL of anti-CD8-PerCP-Vio700 (Clone REA793)(Miltenyi Biotec, 130-111-637) and mTNFR2 binding was detected with goat 1 µg/mL of anti-rat IgG-PE (BD Biosciences, 550767).

The gating strategy for TNFR2 expression obtained by FACS signal was performed with a rat isotype control (gating strategy not shown). The stained cells were analysed on a FACS Canto (BD) using the software program BD FACSDiva. Further analysis was performed with FlowJo.

In vitro CD8⁺ T lymphocyte costimulation assay

Mouse CD8⁺ T lymphocytes were isolated from total splenocytes of C57BL/6J mice with CD8⁺ T cell isolation kit (MACS Miltenyi Biotec, 130-104-075) following manufacturer's instructions. Afterward, CD8⁺ T cells were costimulated at 37 °C with 5% CO₂ and 95% humidity for 72 h with preincubated plate-bound at 4 °C for 48 hours with Purified anti-mouse CD3 antibody (0.5 µg/mL, clone 17A2)(BioLegend, 100314) and anti-TNFR2 (2-fold decreasing concentrations starting at 50 µg/mL, generated Abs) at 1 x 10⁶ cells/mL cultured in RPMI (Gibco, 61870-010) supplemented with 100 U/mL Penicillin, 100 µg/mL Streptomycin (Gibco, 15140-122), 50 µM 2-mercaptoethanol (Gibco, 31350-010), and 10% FBS (Life Technologies, 10270106). Costimulation with 0.5 µg/mL anti-CD3 antibody and 5 µg/mL purified anti-mouse CD28 antibody (clone E18)(Biolegend, 122004) was taken as a positive control. Single stimulation with 0.5 µg/mL anti-CD3e was taken as a reference control and isolated CD8⁺ T cells without any stimulation were considered as negative control. After 72 hours, IFN-γ present in media was measured via Mouse IFN-γ ELISA Set (BD Biosciences, 555138) to assess co-stimulatory capacity following manufacturer's instructions. Collected data of the experiment performed twice was analysed, where wells containing just media were considered as a blank. IFN_γ was calculated based on the standard curve after blank subtraction, and values derived per plate from anti-CD3 incubation were normalized as 0% value of costimulation and values derived from anti-CD3 + anti-CD28 incubation were considered as a 100% signal of costimulation.

Results

Generation of a panel of anti-mouse TNFR2 mAbs

Novel antibodies that bind specifically to murine TNFR2 were generated in rats by mTNFR2 gene gun immunization. Following anti-TNFR2 B-cell enrichment, B-cell expansion, and subsequent B-cell lead selection for mini-electrofusion led to a set of 13 hybridomas producing distinct anti-mTNFR2 mAbs. Isotyping results revealed that all the produced antibodies were rat IgG2a isotype (data not shown). In order to assess protein quality of each

anti-TNFR2 antibody, antibodies were purified and characterized using several analytical procedures. SEC-UPLC analysis showed good monomericity between 95.3% and 99.5% for each of the 13 selected candidates (Supplementary Table 2). While freeze and thaw cycles had no significant impact on protein monomericity with values higher than 98%, incubation at 40 °C for one week affected the quality of some candidates leading to aggregates formation with monomericities from 45.2% of candidate 16A to 93.8% of candidate 18A (Supplementary Table 2). Furthermore, CE-SDS analysis confirmed proper assembly of heavy and light chain the percentage of intact IgG being more than 90% in all samples (Supplementary Table 2, Fig. S3).

α -mTNFR2 mAbs present different cell binding and blocking activity

Mean binding activity was assessed on mTNFR2 stably transfected CHO-K1 cell line (Fig. 1 A, B). Benchmark rat anti-mTNFR2 was included as a positive control together with a rat IgG2a mAb isotype as a negative control. Based on the binding plateau (efficacy), mAbs candidates could be divided in two groups. While most of the candidates reach plateau around 7500 gMFI, candidates 5A, 10A, 14A, 18A and 26A present lower efficacy achieving approximately 2500 gMFI. Among those showing equal efficacy, monoclonal antibody candidates presented with different potency (mAb concentration at which 50% of maximum signal is observed (EC50)) ranging from 0.07 nM up to 3.75 nM. Candidate 14 with an EC50 of 16.41 nM is not represented by full S-shaped curve; mAb 8A is the most efficacious and potent, presenting the lowest EC50, 0.07 nM (Table 1). The affinity of purified anti-mTNFR2 antibodies for binding to recombinant monomeric mTNFR2 was quantified using bio-layer interferometry (BLI). Assessment of binding kinetics showed fast on-rate for most antibodies, resulting in K_D values ranging from 2.7 to 56.8 nM (Table 1). A fully characterization for binding kinetics from candidate 14A was not achieved, most likely because of technical limitations explained at least in part by its low binding efficiency.

Table 1. EC50, IC50 and binding kinetics. Summary of EC50 based on gMFI of binding and report of TNF α blocker or non-blocker antibodies showing which IC50 values for the blocker ones, based on gMFI. Binding kinetics based on Kon, Koff and KD. Values shown in nM result from the mean of three independent experiments \pm standard deviation. N.A., non- available. (*) Value obtained without full S-shaped curve reaching the maximum baseline.

anti-mTNFR2 mAbs	EC50 binding (nM \pm SD)	mTNF α blocker	IC50 blocking (nM \pm SD)	Kon average (1/Ms) \pm SD)	Koff average (1/s) \pm SD)	KD average (nM \pm SD)
5A	1,90 \pm 0,001	No	-	3,96E+05 \pm 9,22E+04	1,87E-02 \pm 1,74E-03	49,3 \pm 13,5
6A	0,39 \pm 0,061	No	-	2,34E+05 \pm 6,35E+04	1,14E-03 \pm 5,42E-04	4,8 \pm 1,7
8A	0,07 \pm 0,033	Yes	0,22 \pm 0,07	3,49E+05 \pm 8,22E+04	4,14E-03 \pm 6,72E-04	12,0 \pm 1,5
10A	0,92 \pm 0,104	No	-	4,95E+05 \pm 2,20E+04	2,81E-02 \pm 2,23E-03	56,8 \pm 3,8
12A	1,32 \pm 0,270	Yes	4,19 \pm 0,29	2,64E+05 \pm 6,11E+04	9,10E-04 \pm 7,01E-05	3,6 \pm 1,0
14A	16,41 \pm	No	-	N.A.	N.A.	N.A.
15A	1,06 \pm 0,157	No	-	4,71E+05 \pm 7,05E+04	8,79E-03 \pm 1,06E-03	18,7 \pm 0,9
16A	3,75 \pm 1,133	Yes	10,20 \pm 2,59	1,87E+05 \pm 3,13E+04	1,44E-03 \pm 1,38E-04	7,9 \pm 1,4
18A	0,50 \pm 0,003	No	-	4,15E+05 \pm 4,32E+04	1,44E-02 \pm 6,14E-04	35,1 \pm 5,4
25A	0,16 \pm 0,055	Yes	0,40 \pm 0,40	1,21E+05 \pm 5,95E+04	2,99E-04 \pm 1,09E-04	2,7 \pm 0,8
26A	0,42 \pm 0,217	No	-	5,11E+05 \pm 1,07E+05	2,26E-02 \pm 2,23E-03	45,7 \pm 11,5
29A	1,80 \pm 0,588	Yes	6,01 \pm 1,95	2,76E+05 \pm 3,00E+04	3,07E-03 \pm 3,42E-05	11,2 \pm 1,3
30A	0,25 \pm 0,020	No	-	1,72E+05 \pm 5,26E+04	6,23E-04 \pm 2,60E-05	3,8 \pm 1,0

Next, the blocking activity of the mAb candidates was evaluated by flow cytometry using recombinant biotinylated TNF α for binding to CHOK1.mTNFR2 cells. Purified clone TR75-54.7 listed as blocking and clone TR75-89 listed as a non-blocking anti-TNFR2 mAb were taken as a reference. Candidates 8A, 12A, 16A, 25A, and 29A were able to block TNF α binding either partially or completely (Fig. 1 C), with candidate 25A showing the most potent (0.40 nM) blocking activity, assessed by the IC50, (Fig. 1 C) compared to 2.59 nM for the blocking benchmark antibody (data not shown). Based on these results, candidates 8A, 16A, and 29A are considered partial blockers as all presented more than 50% reduction of signal (Fig. 1 C). Candidates that showed less than 25% of reduction of signal compared to the benchmark

hamster anti-mTNFR2 non-blocking antibody are considered non-blocking antibodies (Fig. S1 E).

In summary, a panel of thirteen novel anti-mTNFR2 antibodies with different biophysical properties, varying binding affinity to mTNFR2 and varying TNF α ligand blocking potency were identified.

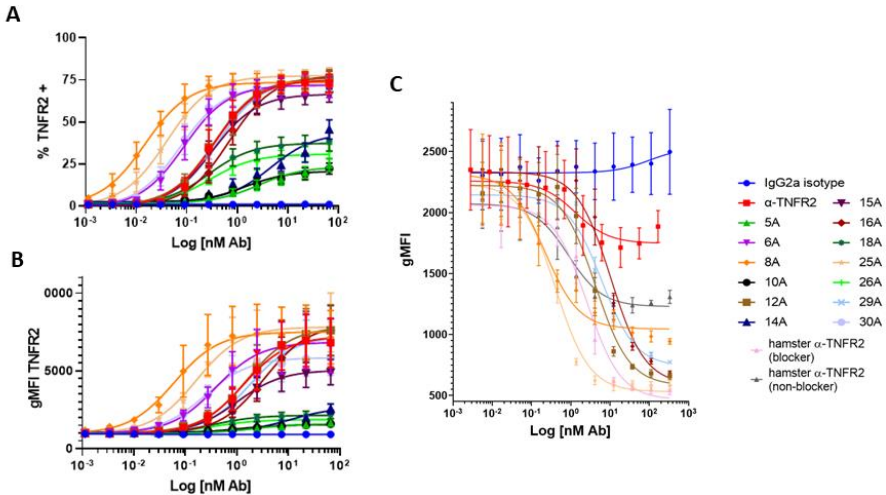


Figure 1. Characterization of anti-mouse TNFR2 antibodies in vitro. (A and B) mTNFR2 stable transfected CHO-K1 cells were incubated with 3-fold increasing concentrations of each rat IgG2a mAbs, and binding was detected by flow cytometry assessing TNFR2⁺ population percentage (A) and gMFI (B). (C) TNF α ligand competition with generated antibodies assessed by FACS. Data represented as a three-parameter gMFI dose-response curve fit of the blocker antibodies with appropriate controls incubations with 3-fold increasing concentrations. Two benchmark hamster-anti-mTNFR2 antibodies with known blocking activity were added as controls. All data based on mean and SEM is representative of three independent experiments.

Mapping of mTNFR2 binding domains

Cysteine-Rich Domains (CRDs) of human TNFR2 were replaced by their cognate mouse regions and vice versa and subsequently expressed on CHO cells (Fig. 2 A, Fig. S4 A). This reciprocal set-up allows to study the mCRD binding domains for each anti-TNFR2 antibody. CHO empty vector and mTNFR1 were also included (Fig S4 B).

Binding to mTNFR2 constructs with individual human CRD domains swapped in, respectively, was taken as a reference for each candidate (Fig. 2 B).

Candidate 14A was determined to be cross-reactive to human mTNFR2 (Fig. 2 B), it bound to all the constructs. Based on domain swapping, candidates 5A, 6A and 8A bound to mCRD1. The epitope of these mCRD1-binding candidates might include the N-terminal region, as this was included in the CRD1 swap mutants. Candidates 12A, 16A, 18A, 29A bound to mCRD2, similar to the benchmark rat anti-mTNFR2 clone HM102. Candidates 10A, 15A, 25A, 26A, and 30A were found to bind to mCRD3. None of the candidates bind to mCRD4 (most proximal to the cell membrane). The binding activity data for the reverse set-up (individual hCRD domains grafted in mTFR2) is shown in Fig. S4 B. By this analysis, the benchmark rat anti-mTNFR2 clone HM102 was shown to bind to a region containing parts of mCRD1 and mCRD2 (Fig. 2 B), and confirming the same binding region for all generated antibodies as observed in the previous set-up. None of the candidates presented cross-reactivity to mTNFR1 (Fig. S4 B). Rat IgG2a isotype control was taken as a negative control and presented no binding to any of the studied conditions (Fig. S4 C). The binding site of the novel rat anti-mouse TNFR2 antibodies was mapped to the extracellular CRDs as graphically displayed onto the human TNFR2:TNF α complex PDB structure (PDB ID: 3ALQ) summarized in Figure 2 C, with a sequence homology of 74% thought to be highly structurally similar.

Similarly to other TNFR superfamily members³⁴, CRD2 and CRD3 of mouse TNFR2 are the most important for ligand binding^{35,36}. Blocking antibodies 12A, 16A and 29A were able to block TNF α binding, which is consistent with their binding region overlapping with the ligand interface in CRD2. Along a similar line of reasoning, the most potent and efficacious blocking antibody was candidate 25A mapped to bind to CRD3. Candidate 18A, which presented binding to mCRD2, and candidates 10A, 15A, 26A, and 30A which presented binding to mCRD3, do not display blocking activity. Interestingly, candidate 8A presented TNF α blocking activity despite its binding to CRD1

which is outside of the ligand interface. Altogether, a diverse set of thirteen antibodies was identified targeting three mTNFR2 CRDs.

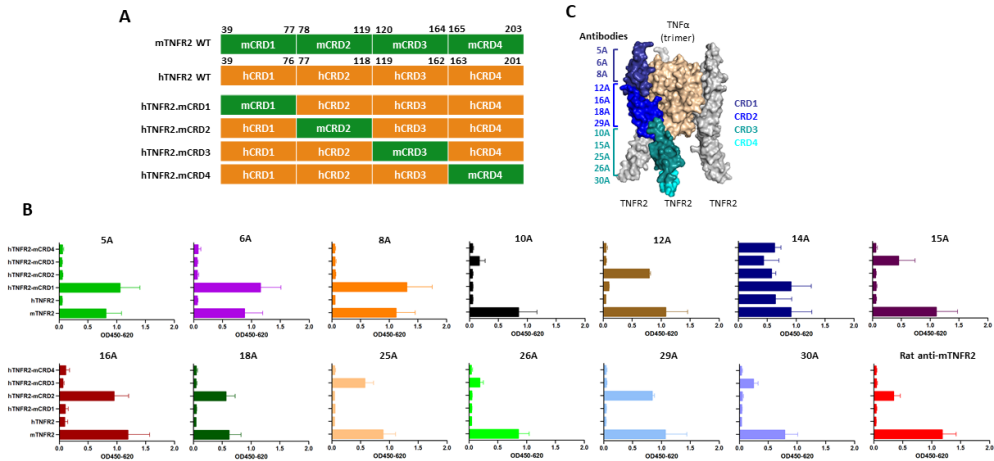


Figure 2. Characterization of anti-mTNFR2 mAbs targeting CRDs 1-4. (A) Schematic representation of the 6 mouse-human TNF2 chimeras CRD1-CRD4 (Cystein Rich Domain). (B) The targeting CRD of each mAb were determined by cell ELISA with mouse-human TNFR2 domain swap mutants. Data represented as a three-parameter OD450-620 detection based on mean and SD of three independent experiments. (C) The domain epitopes of the 13 mAbs are indicated on a hTNFR2-hTNFα trimer structure (PDB: 3ALQ), 74% similar to mouse TNFR2. The CRDs for one TNFR2 receptor are shown in indicated colors.

α-mTNFR2 mAbs stain mouse splenic Tregs and CD8+ cells

To verify whether this panel of anti-mTNFR2 antibodies is attractive to explore the role and activity of TNFR2 on immune cells *in vivo*, flow cytometry mAb staining on mouse Treg cells was assessed *ex vivo* using spleen-derived Tregs identified by YFP expression (FoxP3-YFP transgenic mice³³). All candidates were found to stain YFP⁺ mouse Tregs (Fig. 3 A) and activated CD8⁺ cells (Fig. 3B). While the most potent binders detected Tregs and activated CD8⁺ cells with a clear shift on the flow cytometer (up to ~95% TNFR2⁺), some candidates (5A, 10A, 18A and 26A) displayed a weaker signal (~10% TNFR2⁺) (gMFI for mTNFR2 Treg binding shown in Supplementary Table 3). Furthermore, competitive binding to TNFR2 was assessed using the hamster-anti-mTNFR2 clone TR75-89 known to stain mouse Tregs³⁷. In a



competitive flow cytometry assay using YFP⁺ mouse Tregs, two different staining profiles were observed as expected, exemplified by 8A that directly competed and suppressed the TR75-89 signal, whereas 25A displayed concurrent binding to mouse TNFR2 indicating a different epitope (Fig. 3 C). Antibodies 5A and 18A appeared to outcompete the benchmark antibody for binding to Tregs but did not generate a strong signal themselves, (Supplementary Table 3). Overall, all anti-rat TNFR2 antibodies characterized in this panel detected and stained splenic Treg cells *ex vivo*.

A selection of α -mTNFR2 antibodies shows capacity to costimulate CD8⁺ T-cells

In addition to CD28, several TNFRSF family members are able to generate an alternative co-stimulatory signal *in vivo*³⁸. Therefore, we explored the potential of our panel of antibodies for their capacity to costimulate CD8⁺ T-cells *ex vivo*. Using suboptimal anti-CD3 plus each anti-mTNFR2 antibody coated onto assay plates, the co-stimulatory activity of our antibody panel was assessed by reading out IFN γ production from freshly isolated splenic CD8⁺ T-cells.

Results were normalized against optimal costimulation achieved using anti-CD28 (set at 100%). Some of our anti-mTNFR2 antibodies displayed co-stimulatory capacity on CD8⁺ T-cells at a coating concentration of 50 μ g/mL (Fig. 3 D). Notably, 15A demonstrated reproducible co-stimulatory capacity in independent experiments and across individual mice. Similarly, 5A, 10A, 18A, 26A and 30A appear to display varying co-stimulatory activity, albeit only in some of the experiments. Antibodies 6A, 8A, 12A, 14A and 29A did not show co-stimulatory activity in three consecutive independent experiments.

Therefore, although most of the antibodies did not demonstrate robust activity towards mouse CD8⁺ T-cells, few candidates presented reproducible CD8⁺ T cell, highlighting candidate 15. Surprisingly, these were characterized to bind different CRDs on mouse TNFR2.

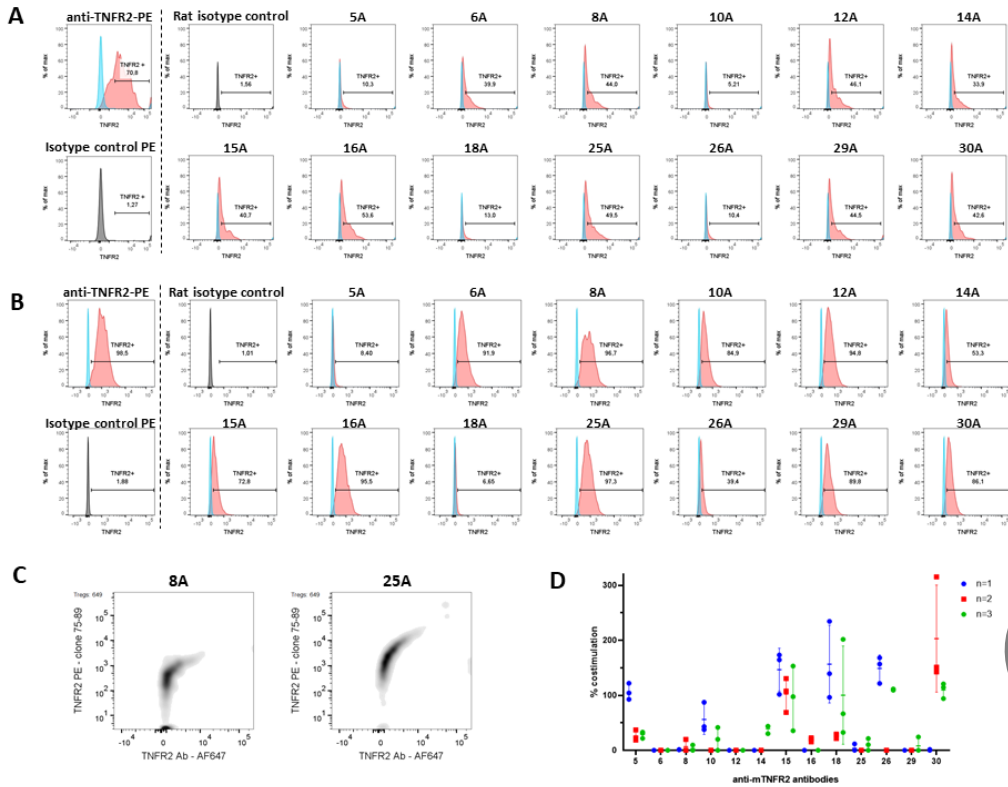


Figure 3. Characterization of anti-mouse TNFR2 antibodies with ex vivo material. (A) TNFR2 expression upon binding of anti-mTNFR2 antibodies to Treg cell population. Detection by commercial hamster anti-TNFR2 direct labeled with PE with the respective hamster-isotype control labeled with PE (left). Generated rat anti-mTNFR2 antibodies and a rat isotype control were detected by a secondary antibody anti-rat AF647 label (right). Gating strategy shown in (Fig. S2 A) The isotype control has been overlaid in each anti-mTNFR2 antibody histogram represented with % of max. Data representative of two independent experiments. (B) TNFR2 expression upon binding of anti-mTNFR2 antibodies to activated CD8⁺ cells. Detection by commercial hamster anti-TNFR2 direct labeled with PE with the respective hamster-isotype control labeled with PE (left). Generated rat anti-mTNFR2 antibodies and a rat isotype control were detected by a secondary antibody anti-rat PE label (right). Gating strategy not shown. Gating strategy for CD8⁺ population was done on unstained OT1 activated cells. First, OT1 cells were gated based on FSC-A / SSC-A properties. Next, single cells were gated based FSC-A / FSC-H. CD8⁺ population were gated as CD8-PerCP-Vio700 positive. Next to the CD8⁺ population, a mouse TNFR2⁺

gate was set with a rat isotype control via histogram. The isotype control has been overlaid in each anti-mTNFR2 antibody histogram represented with % of max. Data representative of single experiment out of two independent experiments. (C) TNFR2 expressing Treg cells co-staining, representation of candidates 18 and 25 with a benchmark antibody, clone TR75-89. Data representative of two independent experiments. (D) Costimulation of CD8⁺ T-cells with anti-TNFR2 antibodies. Assessment of *in vitro* CD8⁺ T-cell costimulation for different anti-TNFR2 antibodies (plate bound anti-CD3 at 0.5 $\mu\text{g}/\text{mL}$). Anti-TNFR2 antibodies were plate bound in 2-fold decreasing dilution starting at 50 $\mu\text{g}/\text{mL}$. Data representative of three independent experiments with $n=3$ biological replicates on the read out of IFN γ in supernatant at 50 $\mu\text{g}/\text{mL}$ per each candidate and mean of independent experiment. Blank was subtracted, IFN γ was calculated based on the standard curve and normalized based on single incubation of anti-CD3 antibodies as 0% costimulation and double incubation of anti-CD3 + anti-CD28 antibodies as a 100% costimulation.

Discussion

TNFR2 function affects multiple signaling pathways and cell states. However, it is still not entirely clear what critical activity TNFR2 has on different immune cells, and this may explain the substantial controversy that exists regarding the question as to how to target this receptor in disease^{39,40}.

The lack of well-characterized and available antibody reagents against mouse TNFR2 prompted us to generate a novel panel of thirteen rat anti-mouse TNFR2 antibodies to support more definitive exploration of TNFR2 in mouse models of disease.

These thirteen candidates can be classified based on their properties, all of them presenting distinct features. While all of them bind to mTNFR2, only candidate 14A has been shown to be cross-reactive to human TNFR2. However, this hallmark of 14A may be convoluted by a reduced potency and efficacy of mTNFR2 binding, rendering it difficult to explore further. Candidates 8A and 25A presented the highest efficacy of binding to CHO-K1.mTNFR2 based on absolute MFI, whereas mAbs 5A, 10A, 14A, 18A, and 26A were ranked with the lowest one. K_D values ranging from 2.7 to 56.8 nM presented 1-2 orders of magnitude lower EC50 of binding compared to EC50 determined of binding to native protein expressed on CHO-K1 cells, presumably because BLI experiments were set up to detect monovalent

binding (affinity) while binding experiments by flow cytometry included bivalent binding (avidity). With the exception of candidates 16A and 18A, antibodies with reduced K_D to recombinant protein also demonstrated reduced binding efficacy to TNFR2 expressed on cells, suggesting the latter could be a result of relative fast dissociation of the mAb.

Five candidates present TNF α blocking activity. For candidates 12A, 16A, 25A and 29A this result is consistent with epitope mapping to CRD2 or CRD3 (25A), whereas candidate 8A can compete with the ligand binding although it binds to different TNFR2 domain, CRD1, which is not known to interact with TNF α . Surprisingly, candidate 18A which presented binding to CRD2 does not present blocking activity. Blocking antibodies were found in all epitope bins, presumably because of steric hindrance or by conformational changes induced in the ligand binding domains in addition to direct blockade of ligand binding. An extensive study via protein modeling would help to understand these differences and the interaction of each antibody with the receptor.

The TNFR2 staining intensity on the Treg population marked by FoxP3 driven YFP expression and on activated CD8⁺ cells is proportional with antibody affinity. Their capacity to cause a clear shift in the flow cytometer largely correlated to binding on CHO-K1.mTNFR2: for instance 5A and 18A did not generate a high gMFI on CHO-K1.mTNFR2 and demonstrate weak binding to mouse Tregs at the concentrations used in flow cytometry. Similarly, weak mTNFR2 binding on activated CD8⁺ cells is observed with candidates 5A and 18A. Most of the anti-mTNFR2 candidates demonstrated staining of mouse Treg TNFR2 when coincubated with hamster-anti-mTNFR2 clone TR75-89 antibody, with the exception of 6A, 8A (epitopes mapped to CRD1) and 10A (CRD2/3) that might compete for the same epitope or affect binding otherwise (steric hindrance, conformational change).

Several of the generated antibodies reproducibly demonstrated costimulation of mouse CD8⁺ T-cells *in vitro*. Costimulatory anti-mTNFR2 antibodies were found to bind across multiple epitope bins (5A, 15A, 18A mapped to CRD1, CRD3, CRD2, respectively). Further study of protein structure by crystallography could potentially help explain which antibody

features might explain blocking or costimulatory activity towards mTNFR2. Despite the lack of this information, studying the biology triggered upon anti-TNFR2 binding on TNFR2 on cell surface is an interesting approach to be explored in cancer and autoimmune disease field. Using the antibody characteristics described in this study, it would make sense to explore whether they display the ability to modulate TNFR2-dependent pharmacology *in vitro* and *in vivo*. For example, in experimental autoimmune encephalomyelitis (EAE), TNFR2 stimulation was shown to promote oligodendrocyte differentiation and remyelination⁴¹ and increase numbers of Tregs which would reduce the number of pathogenic T conventional cells⁴². Therefore, it could be interesting to confirm activity of 15A in this model, and compare it to non-(co-) stimulatory candidates. Similarly, highlighting its crucial role in maintaining an immunosuppressive tumor microenvironment, blocking the TNF α -TNFR2 axis on Tregs and myeloid-derived suppressor cells, or depleting TNFR2 expressing cells appears to be a promising treatment in cancer. Consequently, for this purpose, it would be more convenient to select one of the TNF α blocking antibodies. Furthermore, as a potential strategy to enhance tumor immunity Fc-mediated depletion of TNFR2 expressing Tregs cells could be explored. However, since activated effector CD8 T cells also express TNFR2⁴³, this might require careful characterization of TNFR2 expression in tumor microenvironment to find a potential therapeutic window in time, enabling selective depletion of Tregs.

In conclusion, this novel anti-mouse TNFR2 antibody panel represents a useful tool to study TNFR2 biology *in vitro* and *in vivo* with potential applications in cancer and autoimmune diseases.

Study approval

The welfare of the mice was maintained in accordance with the general principles governing the use of animals in experiments of the European Communities (Directive 2010/63/EU) and Dutch legislation (The revised Experiments on Animals Act, 2014).

Funding details

This work was supported by the European Union's Horizon 2020 research and innovation programme under the Marie Skłodowska-Curie grant agreement [grant numbers 765394, 2018]. We thank T. Guyomard (Aduro Biotech Europe), J. Russo and D. Cuculescu (CIMA Universidad de Navarra) for their expert technical assistance.

Disclosure statement

The authors declare no competing interests.

Supplementary online material

Materials and Methods

Supplementary Table 1. Antibody sequences.

Supplementary Table 2. Overall quality control for monomericity and purity of anti-mTNFR2 mAbs purified.

Supplementary Table 3. Treg staining percentages and MFI.

Figure S1. Characterization of anti-mouse TNFR2 antibodies in vitro.

Figure S2. Characterization of anti-mouse TNFR2 antibodies with ex vivo material.

Figure S3. BLI representation, CE-SDS and SEC-HPLC.

Figure S4. Characterization of anti-mTNFR2 mAbs targeting CRDs 1-4.

Materials and Methods

Quality control tests report good purity and stability of generated antibodies

To assess the quality control (QC) from the generated antibodies the monomericity, purity and temperature stability was checked. Monomericity was checked in duplicate via SEC-UPLC. All candidates present more than 95% monomericity. F/T test had non-significant impact on protein characteristic as all candidates present the same monomericity after 10 F/T cycles, with a recovery around 100%. However, incubating samples at high temperature for one week drastically affects de quality of some of the candidates leading to aggregates formation, with a recovery range from 45 to 97%.

Purity was determined via CE-SDS. Under non-reducing conditions, the intact IgG purity shows some signs of fragmentation, although values are higher than 90%. Under reducing conditions, the total IgG content, sum of light chain and heavy chain purity, is above 95%.

In short, anti-mTNFR2 generated antibodies present good monomericity and purity output, and while all of them remain stable at freezing temperatures, high temperatures might affect the stability of some of them.

Modelling of mouse TNFR2 and TNF α complex

The human TNFR2 model, 74% similar to mouse TNFR2, was used to summarize the binding sites of generated anti-mTNFR2 antibodies. The crystal structure of hTNFR2-hTNF α trimer (PDB: 3ALQ), was uploaded into PyMol v2.3.3 (Schrodinger) software.

Supplementary Table 1. Antibody sequences. Sequences of constant and variable of heavy and light chains of novel generated rat anti-mTNFR2 IgG2a antibodies. Variable heavy (VH), constant heavy (CH), variable light (VL) and variable constant (CL).

Candidate 5A
Heavy chain protein sequence – Complete integrity
VH: EIQLVESGGGLVPGTSLKLSVCVASGFTFSDYWMTWVRQTPGKTMEWIGDIKNDGSFTNYSP SLKNRFTISRDNASTLYLQMSNLRSEDTATYSCTTSPQWAYWGQGLTVTVSS
CH: TETTAPSVYPLAPGTALKSNSMVTLGCLVKGYFPEPVTVTWNSGALSSGVHTFPAVLQSGLYTL TSSVTVPSSTWSSQAVTCNVAHPASSTKVDKKIVPRECNPCGCTGSEVSSVFIFPPKTKDVLITIL TPKVTCVVVDISQNDPEVRFVWFIDDEVHTAQTHAPEKQSNSTLRVSELPIVHRDWLNGKT FKCKVNSGAFPAPIEKISKPEGTPRGPQVYTMAPPKEEMTQSQVSITCMVKGFYPPDIYTEWK MNGQPQENYKNTPTMDTDGSYFLYSKLNKKETWQQGNTFTCSVLHEGLHNHHTEKLSLH SPGK
Light chain protein sequence – type Kappa – Complete integrity
VL: DIQMTQSPSSLPASLGDRVTITCRASQDIGNFLRWFLQRPKSPRLMIYGASNLAVGVPSRFSG SRSGSDYSLTISSEEDMADYYCLQSKESPFTFGSGTKVEIK
CL: RADAAPTVSIFPPSMEQLTSGGATVVCVFNFFPRDISVKWKIDGSEQRDGLDSDVTDQDSKD STYSMSSTLSLTKVEYERHNLTYCEVHKTSSSPVVKSFNRNEC
Candidate 6A
Heavy chain protein sequence – Complete integrity
VH: EVQLVESGGGLVQPGRSLKLSVCVASGFTFSNYGIHWFRQAPTKGLEWVASISPSGDTTYRDSV KGRFTISRDNAKNTLYLQMSLRSSEDTATYYCATAPLSAYWGQGLTVTVSS
CH: AETTAPSVYPLAPGTALKSNSMVTLGCLVKGYFPEPVTVTWNSGALSSGVHTFPAVLQSGLYTL TSSVTVPSSTWSSQAVTCNVAHPASSTKVDKKIVPRECNPCGCTGSEVSSVFIFPPKTKDVLITIL TPKVTCVVVDISQNDPEVRFVWFIDDEVHTAQTHAPEKQSNSTLRVSELPIVHRDWLNGKT FKCKVNSGAFPAPIEKISKPEGTPRGPQVYTMAPPKEEMTQSQVSITCMVKGFYPPDIYTEWK MNGQPQENYKNTPTMDTDGSYFLYSKLNKKETWQQGNTFTCSVLHEGLHNHHTEKLSLH SPGK
Light chain protein sequence – type Kappa – Complete integrity
VL:

<p>DIQMTQSPSSMSASLGDRVITTCQASQDIGNNLIWFQQKPGKSPRPMIYYVTNLAKGVPSRFS GSRSGSDYSLTISSLESEDMADYHCLQYKQYPLAFGSGTKLEIK CL: RADAAPTVSIFPPSMEQLTSGGATVVCVFNFFYPRDISVKWKIDGSEQRDGLDSDVTDQDSKD STYSMSSTLSLTKVEYERHNLTYCEVVHKTSSSPVVKSFNRNEC</p>
Candidate 8A
Heavy chain protein sequence – Complete integrity
<p>VH: EVQLQQSGPEVGRPGSSVKISCKASGYFTDYFMNWLKQSPGQGLEWIGWIDPEYGSTDYAE KFKKKATLTADTSSSTAYIQLSSLTSEDATYFCARGMYGTDYYNNWFPCWGQGLTVTVSS CH: AETTAPSVYPLAPGTALKSNSMVTLGCLVKGYFPEPVTVTWNSGALSSGVHTFPAVLQSGLYTL TSSVTVPSSWSSQAVTCNVAHPASSTKVDKIVPRECNPGCTGSEVSSVFIFPPKTKDVLITIL TPKVTCVVVDISQNDPEVRFWSFIDDEVHTAQTHAPEKQSNSTLRVSELPVHRDWLNGKT FKCKVNSGAFPAPIEKISISKEGTPRGQPQYTMAPPKEEMTQSQVSITCMVKGFYPPDIYTEWK MNGQPQENYKNTPTMDTDGSYFLYSKLNVKKETWQQGNTFTCSVLHEGLHNHHTKSLSH SPGK</p>
Light chain protein sequence – type Kappa – Complete integrity
<p>VL: DIVMTQSPSSLAVSAGETVTLNCKSSQLLSSGNQRNYLAWFHQKPGQSPKLLIYLASTRESGV PDRFIGSGSGTDFLTISTMQAEDLAVYFCQQHYDTPFTFGPGTKLELK CL: RADAAPTVSIFPPSMEQLTSGGATVVCVFNFFYPRDISVKWKIDGSEQRDGLDSDVTDQDSKD STYSMSSTLSLTKVEYERHNLTYCEVVHKTSSSPVVKSFNRNEC</p>
Candidate 10A
Heavy chain protein sequence – Complete integrity
<p>VH: EVQLVETGGGLVRPGSSLLKSCATSGFTFSNTWMNWRQAPGKGLEWVALIKDKYDNYEAN YAESVKGKRFITSRDSSKSRVYLQMNTLRVQDTATYYCTRQLNWFAYWGQGLTVTVSS CH: AETTAPSVYPLAPGTALKSNSMVTLGCLVKGYFPEPVTVTWNSGALSSGVHTFPAVLQSGLYTL TSSVTVPSSWSSQAVTCNVAHPASSTKVDKIVPRECNPGCTGSEVSSVFIFPPKTKDVLITIL TPKVTCVVVDISQNDPEVRFWSFIDDEVHTAQTHAPEKQSNSTLRVSELPVHRDWLNGKT FKCKVNSGAFPAPIEKISISKEGTPRGQPQYTMAPPKEEMTQSQVSITCMVKGFYPPDIYTEWK MNGQPQENYKNTPTMDTDGSYFLYSKLNVKKETWQQGNTFTCSVLHEGLHNHHTKSLSH SPGK</p>
Light chain protein sequence – type Kappa – Complete integrity



<p>VL: EIVLTQSPTTMTASPGEKVTITCRASSSVSYMHWYQQKPGASPKPWIYETSKLASGVPDRFSGS GSGTSYSLTINMEAEADAATYYCQQWNPWTFGGGTKLELK</p> <p>CL: RADAAPTVISIFPPSMEQLTSGGATVVCVFNFFYPRDISVKWKIDGSEQRDGLDSVTDQDSKD STYSMSSTLSLTKVEYERHNLTYCEVVHKTSSSPVVKSFNRNEC</p>
Candidate 12A
Heavy chain protein sequence – Partial integrity
<p>VH: EVQLVESGGGLVQPGKSLKLSCEASGFTFSDYHMAWVRQAPKKGLEWVATIVFDGSRTYYRD SVKGRFTISRYSKSTLYLQMDSLRSEDATYYCATQETGSSDYWGQGMVTVSS</p> <p>CH: AETTAPSVYPLAPGTALKSNSMVTLGCLVKGYFPEPVTVTWNSGALSSGVHTFPAVLQSGLYTL TSSVTVPSSTWSSQAVTCNVAHPASSTKVDKIVPRECNPGCTGSEVSSVFIFPPKTKDVLITIL TPKVTCVVVDISQNDPEVRFVWFIDDEVHTAQTHAPEKQSNSTLRVSELPVHRDWLNGKT FKCKVNSGAFPAPIEKISISKEGTPRGPQVYTMAPPKEEMTQSQVSITCMVKGFYPPDIYTEWK MNGQPQENYKNTPPTMDTDGSYFLYSKLNVKKTETWQQGNTFTCSVLHERSEEHTSELQSPA ISYAVFCLKRGGGGGGG</p>
Light chain protein sequence – type Kappa – Complete integrity
<p>VL: DIQMTQSPSSLPASLGERVTISCRASQGISKLNWYQQKPDGTINPLIYYTSLNLFQVPSRFSGS GSGTDYSLTSSLEPEDFAMYYCQQDASFPTFGGGTKLELK</p> <p>CL: RADAAPTVISIFPPSMEQLTSGGATVVCVFNFFYPRDISVKWKIDGSEQRDGLDSVTDQDSKD STYSMSSTLSLTKVEYERHNLTYCEVVHKTSSSPVVKSFNRNEC</p>
Candidate 14A
Heavy chain protein sequence – Complete integrity
<p>VH: EVQLQESGPGLVKPSQSLTCSVTGYSITSTYRWNWIRKFPGNKLEWNGYINSAGTTNYPNS LKSRIISITRETSKNQFFLQVNSVTTEDATYYCARDYDGYLNIFYFDYWGQGMVTVSS</p> <p>CH: AETTAPSVYPLAPGTALKSNSMVTLGCLVKGYFPEPVTVTWNSGALSSGVHTFPAVLQSGLYTL TSSVTVPSSTWSSQAVTCNVAHPASSTKVDKIVPRECNPGCTGSEVSSVFIFPPKTKDVLITIL TPKVTCVVVDISQNDPEVRFVWFIDDEVHTAQTHAPEKQSNSTLRVSELPVHRDWLNGKT FKCKVNSGAFPAPIEKISISKEGTPRGPQVYTMAPPKEEMTQSQVSITCMVKGFYPPDIYTEWK MNGQPQENYKNTPPTMDTDGSYFLYSKLNVKKTETWQQGNTFTCSVLHEGLHNHHTKSLSH SPGK</p>
Light chain protein sequence – type lambda – Complete integrity
VL:

<p>QVVLTPKSVSTSLSTVKLSCKLNSGNISSYMHWYQQHEGRSPTNMIYRDDKRPDGVDR FSGSIDSSNSAFLTINNVQTEDEAIYFCHSYDSSINIFGGGTKLTVLG CL: QPKSTPTLTVFPPSTEELQGNKATLVCLISDFYPSDVEVAWKANGAPISQGVDTANPTKQGNKY IASSFLRLTAEQWRSRNSFTCQVTHEGNTVEKSLSPAECV</p>
<p>Candidate 15A</p>
<p>Heavy chain protein sequence – Complete integrity</p>
<p>VH: EVQLVESGGGLVQPSSSLKLSVSGFTFSNYGMNWIRQAPKKGLEWIAMIYFDSSNKYYADS VKGRFTISRDNSKNTLYLEMNSLRSEDAMYYCARYYYDGTYYDYFDYWGQGVMVTVSS CH: AETTAPSVYPLAPGTALKSNSMVTLGCLVKGYFPEPVTVTWNSGALSSGVHTFPAVLQSGLYTL TSSVTVPSSTWSSQAVTCNVAHPASSTKVDKIVPRECNPGCTGSEVSSVFIFPPKTKDVLITL TPKVTCVVVDISQNDPEVRFWSFIDDEVHTAQTHAPEKQSNSTLRSVSELPVHRDWLNGKT FKCKVNSGAFPAPIEKSISKPEGTPRGPQVYTMAPPKEEMTQSQVSITCMVKGFPDIYTEWK MNGQPQENYKNTPTMDTDGSYFLYSKLNVKKETWQQGNTFTCSVLHEGLHNNHTEKLSLH SPGK</p>
<p>Light chain protein sequence – type Kappa – Complete integrity</p>
<p>VL: EIVLTQSPTAMAASPGEKVTLICLASSSVTCMNWYQQKSGASPKLWIYGTNSLASGVPNRFSG SGGSTYSYSLTIISMEAEDVATYYCLQLSSYPPTWTFGGGTKLELK CL: RADAAPTVISIFPPSMEQLTSGGATVVCVFNFFPRDISVKWKIDGSEQRDGLDSVTDQDSKD STYSMSSTLSLTKVEYERHNLTYCEVVHKTSSSPVVKSFNRNEC</p>
<p>Candidate 16A</p>
<p>Heavy chain protein sequence – Complete integrity</p>
<p>VH: EVKLVESGGGLVQGRSLKLSVASGFTFNNYWMTWIRQAPKKGLEWVTSITN TDGNTYYPDSVKGRFTVSRDNAKTTLYLQLNSLRSEDATYYCTRGGDGTYYYGV MDAWGQGASVTVSS CH: AETTAPSVYPLAPGTALKSNSMVTLGCLVKGYFPEPVTVTWNSGALSSGVHTFPA VLQSGLYTLTSSVTVPSSTWSSQAVTCNVAHPASSTKVDKIVPRECNPGCTGS EVSSVFIFPPKTKDVLITLTPKVTCVVVDISQNDPEVRFWSFIDDEVHTAQTHA PEKQSNSTLRSVSELPVHRDWLNGKTFKCKVNSGAFPAPIEKSISKPEGTPRGPQ VYTMAPPKEEMTQSQVSITCMVKGFPDIYTEWK MNGQPQENYKNTPTMD TDGSYFLYSKLNVKKETWQQGNTFTCSVLHEGLHNNHTEKLSLHSPGK</p>



Light chain protein sequence – type Kappa – Complete integrity
VL: NIQLTQSPSLLSASVGDVRTLSCKGSQNINNYLAWYQQKLGAEAPKLLIYNTNSLQT GFPSRFGSGSGTDYTLTITSLQPEDVATYFCYEYNNGYAFGPGTKLELK
CL: RADAAPTVSIFPPSMEQLTSGGATVVCVNNFYPRDISVKWKIDGSEQRDGVLD SVTDQDQSKDSTYSMSSTLSLTKVEYERHNLYTCEVVHKTSSSPVVKSFNRNEC
Candidate 18A
Heavy chain protein sequence – Complete integrity
VH: EVQLVESGGGLVQPGRSLKLSAASGFTFSNFGMHWIRQAPTKGLEWVASISPS GGNTYYRDSVKGRLTISRDNASTLYLQLDSLRS EDTATYYCARGETTGIQDWFA YWGQGLTVTVSS
CH: AETTAPSVYPLAPGTALKSNSMVTLGCLVKGYFPEPVTVTWNSGALSSGVHTFPA VLQSGLYTLTSSVTPSSTWSSQAVTCNVAHPASSTKVDKKIVPRECNPCGCTGS EVSSVFIKPKTKDVLITLTPKVTQVVDISQNDPEVRFVWFIDDEVEVHTAQTHA PEKQSNSTLRVSELPVHRDWLNGKTFKCKVNSGAFPAPIEKISIKPEGTPRGPQ VYTMAPPKEEMTQSQVSITCMVKGFPDIYEWKMNGQPQENYKNTPTMD TDGSYFLYSKLNKKETWQQGNTFTCSVLHEGLHNNHTEKLSLHSPGK
Light chain protein sequence – type Kappa – Complete integrity
VL: DIQMTQSPSFLSASVGERVTLSCRASQININRYLDWYQQKLGGETPKLLMYNTINLH TGIPSRFSGSGTDYTLTITSLQPEDVATYFCLQRNSWPNTFGAGTKLELK
CL: RADAAPTVSIFPPSMEQLTSGGATVVCVNNFYPRDISVKWKIDGSEQRDGVLD SVTDQDQSKDSTYSMSSTLSLTKVEYERHNLYTCEVVHKTSSSPVVKSFNRNEC
Candidate 25A
Heavy chain protein sequence – Complete integrity
VH: EVQLVESGGGLVQPGRSLKVSCTVSGFTFSYDMDMAWVRQTPMKGLEWVASIST GGGNTYYRDSVKGRFTISRDNAKNIQYLQMDSLRSEDTATYYCATNYGGYSESDF FDYWGGQGMVTVSS
CH:

<p>AETTAPSVYPLAPGTALKSNSMVTLGCLVKGYFPEPVTVTWNSGALSSGVHTFPA VLQSGLYTLTSSVTPSSTWSSQAVTCNVAHPASSTKVDKKIVPRECNPCGCTGS EVSSVFIFPPKTKDVLITLTPKVTCVVVDISQNDPEVRFSWFIDDVEVHTAQTHA PEKQSNSTLRVSSELPIVHRDWLNGKTFKCKVNSGAFPAPIEKSISKPEGTPRGPQ VYTMAPPKEEMTQSQVSITCMVKGFYPPDIYTEWKMNQPPQENYKNTPTMD TDGSYFLYKLNKKETWQQGNTFTCSVLHEGLHNNHTEKSLSHSPGK</p>
<p>Light chain protein sequence – type Kappa – Complete integrity</p>
<p>VL: DIQMTQSPSSLPSSLGERVTISCRASQGISNNLNWYQQKPDGTIKPLIYYTSNLQS GVPSRFGSGSGTGYSLTISLEPEDFAMYYCQQDAIFPNTFGAGTKLELK CL: RADAAPTVSIFPPSMEQLTSGGATVVCVNNFYPRDISVKWKIDGSEQRDGVLD SVTDQDSKDYSTYSMSSTLSLTKVEYERHNLTYCEVVHKTSSSPVVKSFNRNEC</p>
<p>Candidate 26A</p>
<p>Heavy chain protein sequence – Complete integrity</p>
<p>VH: EVQLVETGGGLVRPGSSKLSCVTSGFTFSNTWMNWVRQAPGKGLEWVALIKD KYDNYEANYAESVKGRFTISRDDSKSRVYLQMNTLRDQDTATYYCTRQLNWFAY WGQGTLLTVSS CH: AETTAPSVYPLAPGTALKSNSMVTLGCLVKGYFPEPVTVTWNSGALSSGVHTFPA VLQSGLYTLTSSVTPSSTWSSQAVTCNVAHPASSTKVDKKIVPRECNPCGCTGS EVSSVFIFPPKTKDVLITLTPKVTCVVVDISQNDPEVRFSWFIDDVEVHTAQTHA PEKQSNSTLRVSSELPIVHRDWLNGKTFKCKVNSGAFPAPIEKSISKPEGTPRGPQ VYTMAPPKEEMTQSQVSITCMVKGFYPPDIYTEWKMNQPPQENYKNTPTMD TDGSYFLYKLNKKETWQQGNTFTCSVLHEGLHNNHTEKSLSHSPGK</p>
<p>Light chain protein sequence – type Kappa – Complete integrity</p>
<p>VL: EIVLTQSPTTMTASPGKVTITCRASVSVMHWYQQKAGASPKPIWYETSKLAS GVPDRFSGSGSGTYSLTINMEAEADAATYYCQQWNPWTFGGGKLELK CL: RADAAPTVSIFPPSMEQLTSGGATVVCVNNFYPRDISVKWKIDGSEQRDGVLD SVTDQDSKDYSTYSMSSTLSLTKVEYERHNLTYCEVVHKTSSSPVVKSFNRNEC</p>



Candidate 29A
Heavy chain protein sequence – Complete integrity
VH: EVQLVESGGGLEQPGRSLKLSVCASGFTFSDYHMAWVRQAPKKGLEWVATIIYD GSRYYRDSVKGRFTISRDNASTLYLQMDSLRSEDATYYCATQGTGSSDYWG QGVMVTVSS CH: AETTAPSVYPLAPGTALKSNSMVTLGCLVKGYFPEPVTVTWNSGALSSGVHTFPA VLQSGLYTLTSSVTVPSSTWSSQAVTCNVAHPASSTKVDKKIVPRECNPCGCTGS EVSSVFIFPPKTKDVLITLTPKVTQVVDISQNDPEVRFVWFIDDEVEVHTAQTHA PEKQSNSTLRVSELPVHRDWLNGKTFKCKVNSGAFPAPIEKISIKPEGTPRGPQ VYTMAPPKEEMTQSQVSITCMVKGFYPPDIYTEWKMNGQPQENYKNTPTMD TDGSYFLYSKLNKKETWQQGNTFTCSVLHEGLHNHHTEKSLSHSPGK
Light chain protein sequence – N.A.
Candidate 30A
Heavy chain protein sequence – Complete integrity
VH: EVQLVETGGGLVRPGSSLKLSCATSGFTFSNTWMNWVRQAPGKLEWVALVK DEYNDYEANYAESVKGRFTISRDDSKSRVYLQMNTLRDQDTATYYCTRATYYGLF PYWGQGS�VTVSS CH: AETTAPSVYPLAPGTALKSNSMVTLGCLVKGYFPEPVTVTWNSGALSSGVHTFPA VLQSGLYTLTSSVTVPSSTWSSQAVTCNVAHPASSTKVDKKIVPRECNPCGCTGS EVSSVFIFPPKTKDVLITLTPKVTQVVDISQNDPEVRFVWFIDDEVEVHTAQTHA PEKQSNSTLRVSELPVHRDWLNGKTFKCKVNSGAFPAPIEKISIKPEGTPRGPQ VYTMAPPKEEMTQSQVSITCMVKGFYPPDIYTEWKMNGQPQENYKNTPTMD TDGSYFLYSKLNKKETWQQGNTFTCSVLHEGLHNHHTEKSLSHSPGK
Light chain protein sequence – Incomplete integrity
VL: DIQMTQSPASLSSSLGETVTIECRASEDIYSNLAWYQQKPGNSPQLLIFDANTLAD GVPSRFGSGSGPQYSLHINSLSQSEDVASYFCQQYNNYPLTFGSGTRLEIK CL: RADAAPTVSIFPPSMEQLTSGGATVVCVNNFYPRDISVKWKIDGSEQRDGVLD SVTDQDSKDYMSSTLSLTKVEYERHNLTYCEVHKTSSSPVVKSFNRNEC

Supplementary Table 2. Overall quality control for monomericity and purity of anti-mTNFR2 mAbs purified. Monomericity data represented as mean and SD of antibodies produced of two independent experiments (n=2). Monomericity was checked to test the temperature stability: after 10 cycles of freeze-and-thaw (F/T) and after 1 week incubation at 40 °C in a single independent experiment. Purity was assessed via CE-SDS non-reduced (NR) and reduced (R).

Anti-TNFR2 mAbs	Concentration (mg/ml)	Monomer average (% ± SD)	Stability test		NR	R
			Monomer (%) post 10 cycles F/T	Monomer (%) post 1 week incubation 40 °C	CE-SDS Intact IgG (%)	CE-SDS LC+HC (%)
5A	2,08	98,80 ± 0,14	99,70	67,90	90,90	98,40
6A	1,18	95,64 ± 0,20	96,10	92,50	N.A.	97,70
8A	0,77	95,30 ± 0,14	95,70	85,20	95,10	98,60
10A	1,47	98,70 ± 0,14	98,90	89,70	90,50	99,60
12A	0,99	99,02 ± 0,16	99,20	72,00	93,00	99,50
14A	1,53	98,81 ± 0,30	98,90	71,50	91,00	99,40
15A	1,16	99,12 ± 0,54	99,50	64,00	93,50	98,70
16A	1,52	99,18 ± 0,03	99,40	45,20	93,80	98,70
18A	2,31	98,69 ± 0,40	98,70	93,80	92,10	99,40
25A	2,16	99,13 ± 0,18	99,10	78,30	93,20	99,10
26A	2,12	98,55 ± 0,21	98,70	89,40	92,40	99,20
29A	1,76	98,32 ± 0,17	98,10	71,80	91,60	99,10
30A	1,80	99,52 ± 0,31	99,50	85,50	90,60	99,20

Supplementary Table 3. Treg staining percentages and MFI. Percentage of TNFR2⁻ and TNFR2⁺ Tregs stained either with hamster-anti-TNFR2 PE antibody (clone TR75-89), rat-anti-TNFR2 antibody or both. gMFI for TNFR2 signal detected by AF647 signal. Data representative of single experiment out of two independent experiments.

Abs	% Tregs TNFR2⁻	% Tregs TNFR2⁺ (PE⁺)	% Tregs TNFR2⁺ (PE⁺ and AF647⁺)	% Tregs TNFR2⁺ (AF647⁺)	gMFI AF647 signal in CD3⁺ YFP⁺
5A	61,45	33,10	2,68	2,77	442
6A	73,15	0,11	3,80	22,95	1118
8A	66,90	0,11	1,97	31,05	1267
10A	71,25	10,15	6,40	12,21	401
12A	53,95	1,63	23,55	20,88	1344
14A	70,95	1,93	18,15	8,97	1019
15A	64,25	0,50	13,30	21,98	1169
16A	55,35	0,97	23,90	19,78	1504
18A	63,15	30,45	4,50	1,90	471
25A	52,75	0,90	21,25	25,16	1466
26A	66,55	19,97	10,35	3,16	485
29A	62,95	2,39	21,45	13,22	1357
30A	48,05	0,06	17,65	34,15	1154
rat	56,00	32,95	3,45	2,64	346

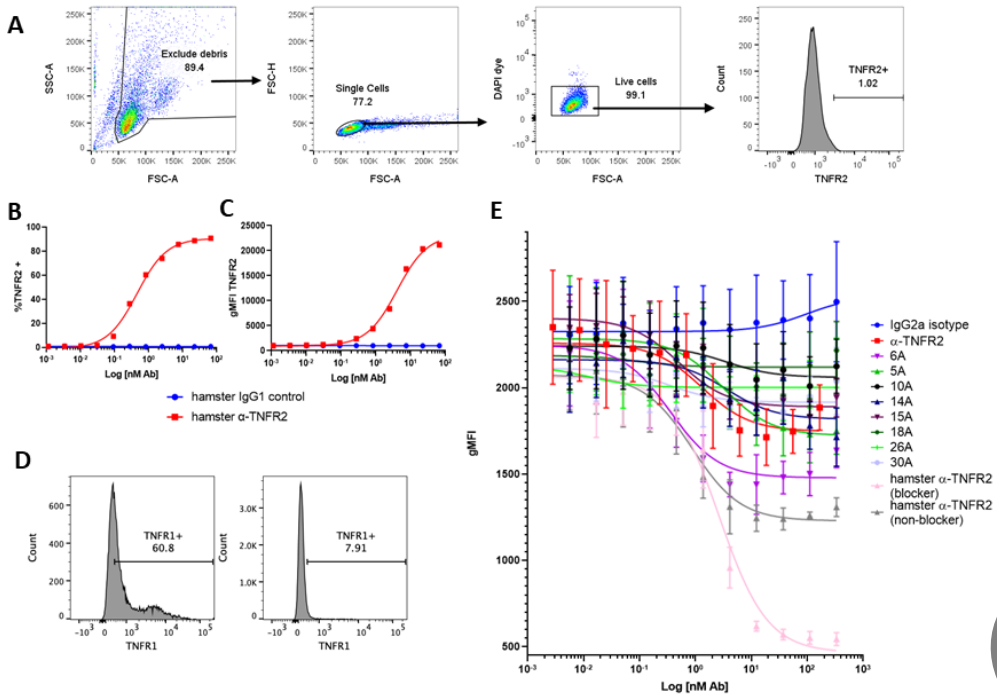


Figure S1. Characterization of anti-mouse TNFR2 antibodies in vitro. (A) Gating strategy followed. Gating was done on unstained CHO-K1.mTNFR2 cells. First, cell debris was excluded based on FSC-A / SSC-A properties. Next, single cells were gated based on FSC-A / FSC-H. Live cells were gated based on FSC-A / DAPI properties. Next to the live unstained single cell population, a mouseTNFR2⁺ gate was set based on TNFR2 histogram. Data representative of single experiment out of three independent experiments. (B and C) mTNFR2 expression was checked in stable transfected CHO-K1 cells which were incubated with 3-fold increasing concentrations of each rat IgG2a mAb TNFR2 expression in stable transfected CHO-K1 via direct staining. Expression levels was detected by flow cytometry assessing TNFR2⁺ population percentage (B) and gMFI (C). Data representative of single experiment out of three independent experiments. (D) TNFR1 expression was tested on parental CHO-K1 (right) and transiently transfected CHO-K1 cells (left). TNFR1 gating was done on unstained CHO-K1 cells, similar as shown in (A). (E) TNF competition FACS of antibodies. Data represented as a three-parameter gMFI dose-response curve fit based on mean and SEM of three independent experiments of the non-blocker antibodies with appropriate controls incubations with 3-fold increasing concentrations. Two benchmark hamster-anti-mTNFR2 antibodies with known blocking activity were added as controls.



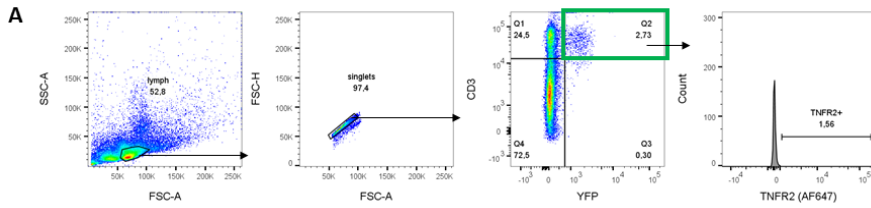


Figure S2. Characterization of anti-mouse TNFR2 antibodies with ex vivo material. (A) Treg gating strategy followed. Gating was done on unstained freshly isolated splenocytes. First, lymphocytes were gated based on FSC-A / SSC-A properties. Next, single cells were gated based FSC-A / FSC-H. Treg population were gated as CD3 positive and FoxP3-YFP positive. Next to the Treg population, a mouse TNFR2⁺ gate was set with a rat isotype control via histogram. Data representative of single experiment out of two independent experiments.

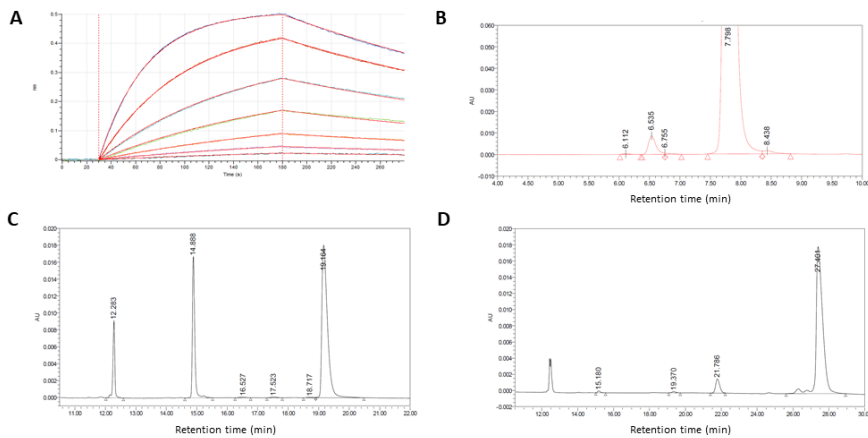


Figure S3. BLI representation, CE-SDS and SEC-HPLC. (A) BLI analysis of candidate for binding to recombinant mTNFR2. The mAb association at 10 $\mu\text{g/ml}$ to recombinant mTNFR2 protein loaded biosensors is displayed with 5-fold decreasing concentrations starting at 95 nM. Data representative of three independent experiments. (B) Auto-scaled SEC-HPLC profile of anti-mTNFR2 antibody. (C and D) Purity of mAb evaluated by CE-SDS. 10 kDa standard marker (~ 12.3 mins) was used for the calibration of retention time for each trace, reduced (C) and non-reduced (D). Numbers represent the retention time. Data representative of a single mAb anti-mTNFR2, candidate 29; (B, C and D) data representative of a single independent experiment.

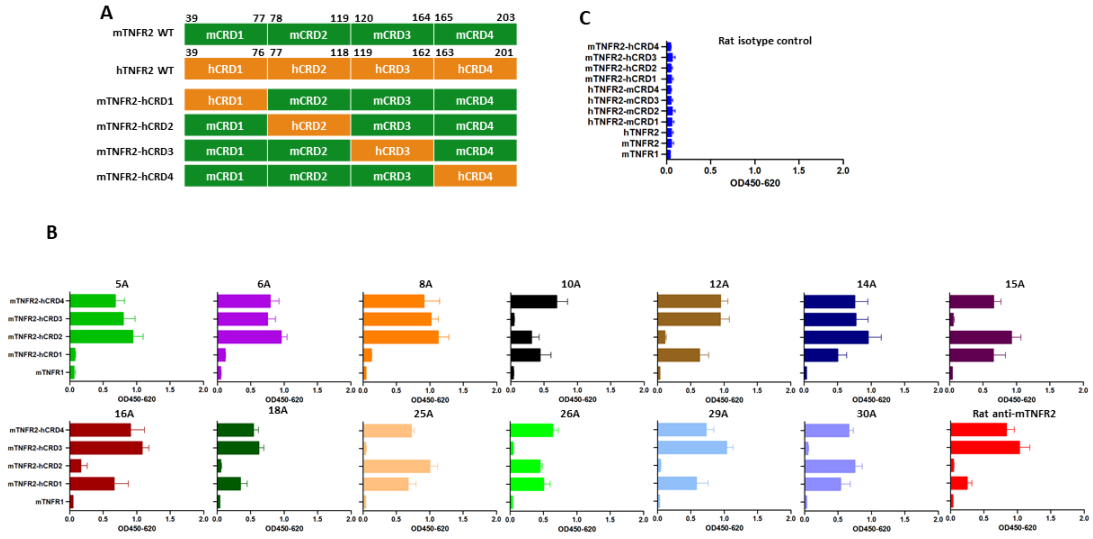


Figure S4. Characterization of anti-mTNFR2 mAbs targeting CRDs 1-4. (A) Schematic representation of the 6 mouse-human TNF2 chimeras CRD1-CRD4 (Cystein Rich Domain). (B) The targeting CRD of each mAb were determined by cell ELISA with mouse-human TNFR2 domain swap mutants. mTNFR1 and CHO-empty vector targeting was included too. (C) Targeting of rat isotype control included in all assays. All data represented as a three-parameter OD450-620 detection based on mean and SD of three independent experiments.



References

1. Kalfaoglu B, Almeida-Santos J, Tye CA, Satou Y, Ono M. T-Cell Hyperactivation and Paralysis in Severe COVID-19 Infection Revealed by Single-Cell Analysis. *Front Immunol.* 2020 Oct 8. doi: 10.3389/fimmu.2020.589380. PMID: 33178221
2. Callahan MK, Postow MA, Wolchok JD. Targeting T Cell Co-receptors for Cancer Therapy. *Immunity.* 2016 May 17. doi: 10.1016/j.immuni.2016.04.023. PMID: 27192570
3. Sade-Feldman M, Yizhak K, Bjorgaard SL, Ray JP, de Boer CG, Jenkins RW, et al. Defining T Cell States Associated with Response to Checkpoint Immunotherapy in Melanoma. *Cell.* 2019 Jan 10. doi: 10.1016/j.cell.2018.12.034 PMID: 30633907
4. Ramos-Casals M, Brahmer JR, Callahan MK, Flores-Chávez A, Keegan N, Khamashta MA, et al. Immune-related adverse events of checkpoint inhibitors. *Nat Rev Dis Primer.* 2020 May 7. doi: 10.1038/s41572-020-0160-6. PMID: 32382051
5. Paluch C, Santos AM, Anzilotti C, Cornall RJ, Davis SJ. Immune Checkpoints as Therapeutic Targets in Autoimmunity. *Front Immunol.* 2018 Oct 8. doi: 10.3389/fimmu.2018.02306. PMID: 30349540
6. Zhang Q, Vignali DAA. Co-stimulatory and co-inhibitory pathways in autoimmunity. *Immunity.* 2016 May 17. doi: 10.1016/j.immuni.2016.04.017. PMID: 27192568
7. Mayes PA, Hance KW, Hoos A. The promise and challenges of immune agonist antibody development in cancer. *Nat Rev Drug Discov.* 2018 Jul. doi: 10.1038/nrd.2018.75. PMID: 29904196
8. Eskiocak U, Guzman W, Wolf B, Cummings C, Milling L, Wu H-J, et al. Differentiated agonistic antibody targeting CD137 eradicates large tumors without hepatotoxicity. *JCI Insight.* 2020 Mar 12. doi: 10.1172/jci.insight.133647. PMID: 32161196
9. Liu Z, Davidson A. BAFF inhibition: a new class of drugs for the treatment of autoimmunity. *Exp Cell Res.* 2011 May 15. doi: 10.1016/j.yexcr.2011.02.005. PMID: 21333645
10. Sonar S, Lal G. Role of Tumor Necrosis Factor Superfamily in Neuroinflammation and Autoimmunity. *Front Immunol.* 2015 Jul 20. doi: 10.3389/fimmu.2015.00364. PMID: 26257732
11. Ward-Kavanagh LK, Lin WW, Šedý JR, Ware CF. The TNF Receptor Superfamily in Co-stimulating and Co-inhibitory Responses. *Immunity.* 2016 May 17. doi: 10.1016/j.immuni.2016.04.019. PMID: 27192566
12. Poggi M, Jager J, Paulmyer-Lacroix O, Peiretti F, Gremeaux T, Verdier M, et al. The inflammatory receptor CD40 is expressed on human adipocytes: contribution to crosstalk between lymphocytes and adipocytes. *Diabetologia.* 2009 Jun. doi: 10.1007/s00125-009-1267-1. PMID: 19183933

13. Lincecum JM, Vieira FG, Wang MZ, Thompson K, De Zutter GS, Kidd J, et al. From transcriptome analysis to therapeutic anti-CD40L treatment in the SOD1 model of amyotrophic lateral sclerosis. *Nat Genet.* 2010 May. doi: 10.1038/ng.557. PMID: 20348957
14. van Mierlo GJD, den Boer AT, Medema JP, van der Voort EIH, Franssen MF, Offringa R, et al. CD40 stimulation leads to effective therapy of CD40- tumors through induction of strong systemic cytotoxic T lymphocyte immunity. *Proc Natl Acad Sci.* 2002 Apr 16. doi: 10.1073/pnas.082107699. PMID: 11929985
15. Sandin LC, Orlova A, Gustafsson E, Ellmark P, Tolmachev V, Totterman TH, et al. Locally Delivered CD40 Agonist Antibody Accumulates in Secondary Lymphoid Organs and Eradicates Experimental Disseminated Bladder Cancer. *Cancer Immunol Res.* 2014 Jan 1. doi: 10.1158/2326-6066. PMID: 24778163
16. Schling P, Rudolph C, Heimerl S, Fruth S, Schmitz G. Expression of tumor necrosis factor alpha and its receptors during cellular differentiation. *Cytokine.* 2006 Mar 7. doi: 10.1016/j.cyto.2006.02.007. PMID: 16580225
17. Arnett HA, Mason J, Marino M, Suzuki K, Matsushima GK, Ting JP-Y. TNF α promotes proliferation of oligodendrocyte progenitors and remyelination. *Nat Neurosci.* 2001 Nov. doi: 10.1038/nn738. PMID: 11600888
18. Irwin MW, Mak S, Mann DL, Qu R, Penninger JM, Yan A, et al. Tissue Expression and Immunolocalization of Tumor Necrosis Factor- α in Postinfarction Dysfunctional Myocardium. *Circulation.* 1999 Mar 23. doi: 10.1161/01.cir.99.11.1492. PMID: 10086975.
19. Naserian S, Abdelgawad ME, Afshar Bakshloo M, Ha G, Arouche N, Cohen JL, et al. The TNF/TNFR2 signaling pathway is a key regulatory factor in endothelial progenitor cell immunosuppressive effect. *Cell Commun Signal CCS.* 2020 Jun 16. DOI: 10.1186/s12964-020-00564-3. PMID: 32546175.
20. Beldi G, Khosravi M, Abdelgawad ME, Salomon BL, Uzan G, Haouas H, et al. TNF α /TNFR2 signaling pathway: an active immune checkpoint for mesenchymal stem cell immunoregulatory function. *Stem Cell Res Ther.* 2020 Jul 16. DOI: 10.1186/s13287-020-01740-5 PMID: 32669116
21. Ware CF, Crowe P, Vanarsdale TL, Andrews JL, Grayson MH, Smith CA, et al. Tumor necrosis factor (TNF) receptor expression in T lymphocytes. Differential regulation of the type I TNF receptor during activation of resting and effector T cells. *J Immunol.* 1991 Dec 15. PMID: 1661312
22. Brenner D, Blaser H, Mak TW. Regulation of tumour necrosis factor signalling: live or let die. *Nat Rev Immunol.* 2015 Jun. DOI: 10.1038/nri3834 . PMID: 26008591
23. He J, Li R, Chen Y, Hu Y, Chen X. TNFR2-expressing CD4⁺Foxp3⁺ regulatory T cells in cancer immunology and immunotherapy. *Prog Mol Biol Transl Sci.* 2019 Apr 10. doi: 10.1016/bs.pmbts.2019.03.010. PMID: 31383403

24. Chen X, Subleski JJ, Hamano R, Howard OMZ, Wiltrout RH, Oppenheim JJ. Co-expression of TNFR2 and CD25 identifies more of the functional CD4 + FOXP3 + regulatory T cells in human peripheral blood: Immunomodulation. *Eur J Immunol*. 2010 Apr 14. doi: 10.1002/eji.200940022. PMID: 20127680
25. Zhao T, Li H, Liu Z. Tumor necrosis factor receptor 2 promotes growth of colorectal cancer via the PI3K/AKT signaling pathway. *Oncol Lett*. 2017 Jan. doi: 10.3892/ol.2016.5403. PMID: 28123565
26. Kim EY, Teh S-J, Yang J, Chow MT, Teh H-S. TNFR2-Deficient Memory CD8 T Cells Provide Superior Protection against Tumor Cell Growth. *J Immunol*. 2009 Nov 15. doi: 10.4049/jimmunol.0803482. PMID: 19841176
27. Hurrell BP, Galle-Treger L, Jahani PS, Howard E, Helou DG, Banie H, et al. TNFR2 Signaling Enhances ILC2 Survival, Function, and Induction of Airway Hyperreactivity. *Cell Rep*. 2019 Dec 24. doi: 10.1016/j.celrep.2019.11.102. PMID: 31875557
28. Atretkhany K-SN, Mufazalov IA, Dunst J, Kuchmiy A, Gogoleva VS, Andruszewski D, et al. Intrinsic TNFR2 signaling in T regulatory cells provides protection in CNS autoimmunity. *Proc Natl Acad Sci*. 2018 Dec 18. doi: 10.1073/pnas.1807499115. PMID: 30498033
29. Naserian S, Shamdani S, Arouche N, Uzan G. Regulatory T cell induction by mesenchymal stem cells depends on the expression of TNFR2 by T cells. *Stem Cell Res Ther*. 2020 Dec 10. DOI: 10.1186/s13287-020-02057-z. PMID: 33303019
30. Voets E, Paradé M, Lutje Hulsik D, Spijkers S, Janssen W, Rens J, et al. Functional characterization of the selective pan-allele anti-SIRP α antibody ADU-1805 that blocks the SIRP α -CD47 innate immune checkpoint. *J Immunother Cancer*. 2019 Dec 4. doi: 10.1186/s40425-019-0772-0. PMID: 31801627
31. Steenbakkers PGA, Hubers HAJM, Rijnders AWM. Efficient generation of monoclonal antibodies from preselected antigenspecific B cells. *Mol Biol Rep*. 1994 Mar 1. doi: 10.1007/BF00997158. PMID: 8072493
32. Steenbakkers PGA, van Meel FCM, Olijve W. A new approach to the generation of human or murine antibody producing hybridomas. *J Immunol Methods*. 1992 Jul 31. doi: 10.1016/0022-1759(92)90090-G
33. Williams LM, Rudensky AY. Maintenance of the Foxp3-dependent developmental program in mature regulatory T cells requires continued expression of Foxp3. *Nat Immunol*. 2007 Jan 14. doi: 10.1038/ni1437. PMID:17220892
34. Locksley RM, Killeen N, Lenardo MJ. The TNF and TNF receptor superfamilies: integrating mammalian biology. *Cell*. 2001 Feb 23. doi: 10.1016/s0092-8674(01)00237-9. PMID: 11239407.
35. Banner DW, D'Arcy A, Janes W, Gentz R, Schoenfeld HJ, Broger C, et al. Crystal structure of the soluble human 55 kd TNF receptor-human TNF beta complex:

- implications for TNF receptor activation. *Cell*. 1993 May 7. doi: 10.1016/0092-8674(93)90132-a. PMID: 8387891
36. Mukai Y, Nakamura T, Yoshikawa M, Yoshioka Y, Tsunoda S, Nakagawa S, Yamagata Y, Tsutsumi Y. Solution of the structure of the TNF-TNFR2 complex. *Sci Signal*. 2010 Nov 16. doi: 10.1126/scisignal.2000954. PMID: 21081755.
 37. Williams GS, Mistry B, Guillard S, Ulrichsen JC, Sandercock AM, Wang J, et al. Phenotypic screening reveals TNFR2 as a promising target for cancer immunotherapy. *Oncotarget*. 2016 Oct 18. doi: 10.18632/oncotarget.11943. PMID: 27626702.
 38. Teijeira A, Labiano S, Garasa S, Etxeberria I, Santamaría E, Rouzaut A, et al. Mitochondrial Morphological and Functional Reprogramming Following CD137 (4-1BB) Costimulation. *Cancer Immunol Res*. 2018 Jul. doi: 10.1158/2326-6066.CIR-17-0767. PMID: 29678874.
 39. Medler J, Wajant H. Tumor necrosis factor receptor-2 (TNFR2): an overview of an emerging drug target. *Expert Opin Ther Targets*. 2019 Apr 3. doi: 10.1080/14728222.2019.1586886. PMID: 30856027
 40. Fischer R, Kontermann RE, Pfizenmaier K. Selective Targeting of TNF Receptors as a Novel Therapeutic Approach. *Front Cell Dev Biol*. 2020 May 26. doi: 10.3389/fcell.2020.00401. PMID: 32528961
 41. Madsen PM, Motti D, Karmally S, Szymkowski DE, Lambertsen KL, Bethea JR, et al. Oligodendroglial TNFR2 Mediates Membrane TNF-Dependent Repair in Experimental Autoimmune Encephalomyelitis by Promoting Oligodendrocyte Differentiation and Remyelination. *J Neurosci*. 2016 May 4. doi: 10.1523/JNEUROSCI.0211-16.2016. PMID: 27147664
 42. Ronin E, Pouchy C, Khosravi M, Hilaire M, Grégoire S, Casrouge A, et al. Tissue-restricted control of established central nervous system autoimmunity by TNF receptor 2-expressing Treg cells. *Proc Natl Acad Sci*. 2021 Mar 30. doi: 10.1073/pnas.2014043118. PMID: 33766913
 43. Calzascia T, Pellegrini M, Hall H, Sabbagh L, Ono N, Elford AR, et al. TNF- α is critical for antitumor but not antiviral T cell immunity in mice. *J Clin Invest*. 2007 Nov 8. doi: 10.1172/JCI32567. PMID: 17992258



6

TNFR2 antibodies target Tregs and CD4⁺ T effector cells *in vivo*

Aina Segués^{1,2}, Martin Waterfall¹, Alice J. A. M. Sijts² and Dietmar M. Zaiss^{1,3,4,5*}

¹ *Institute of Immunology and Infection Research, School of Biological Sciences, University of Edinburgh, Edinburgh EH9 3FL, UK*

² *Faculty of Veterinary Medicine, Department of Infectious Diseases and Immunology, Utrecht University, 3584 CS Utrecht, The Netherlands;*

³ *Department of Immune Medicine, University Regensburg, 93053 Regensburg, Germany*

⁴ *Institute of Clinical Chemistry and Laboratory Medicine, University Hospital Regensburg, 93053 Regensburg, Germany*

⁵ *Institute of Pathology, University Regensburg, 93053 Regensburg, Germany*

* *Correspondence: dietmar.zaiss@ukr.de*

Unpublished data

Contribution statement: *Aina Segués Cisteró conceived the presented idea, designed, planned and carried out the experiments. She contributed to the interpretation of the results and took the lead in writing the manuscript.*

Abstract

T regulatory cells (Tregs) are a subset of CD4⁺ T cells characterized by an immunosuppressive activity. They play a key role in maintaining immune homeostasis and are, therefore, crucial for understanding autoimmune, chronic and cancer diseases. Although Treg importance has been recognized, targeting them to either promote or revert the immunosuppressive environment in disease conditions still poses certain challenges, due to the lack of a unique Treg surface marker.

Tumor necrosis factor receptor 2 (TNFR2) has been described to be expressed on the Treg surface and its expression correlates with higher immunosuppressive activity. In this study we assessed the immunomodulatory capacity of two novel anti-mTNFR2 antibodies (mAbs) in *in vitro*, *ex vivo* and *in vivo* experiments. One of the mAbs blocks mouse TNFR2 (candidate 25), the other is a non-blocking mAb (candidate 30). Both mAbs were equipped with an active or silent mouse IgG2a Fc tail and recombinantly expressed. As expected, both mAbs still bound mTNFR2. Purified mAb with an active Fc tail depleted TNFR2⁺ cells in a complement-dependent-cytotoxicity (CDC) assay, while mAbs carrying a silent Fc tail failed to do so, confirming that the Fc regions of both mAbs induce CDC. We hypothesized that anti-mTNFR2 antibodies would block and/or deplete Tregs also in an *in vivo* set up, leading to enhanced naïve CD4 proliferation, which we tested in a Rag 1 KO T cell transfer mice model. However, in these *in vivo* experiments, anti-mTNFR2 antibody 25 diminished Treg numbers irregardless of Fc tail activity while both mAbs prevented effector CD4⁺ T cell expansion. Thus, the two mAbs function both *in vitro* and *in vivo* but are not selective for the Treg subpopulation of CD4⁺ T cells.

Introduction

T regulatory cells (Tregs) represent an immunosuppressive subpopulation of CD4⁺ T cell that regulates immunological homeostasis. Tregs dampen overactive immune responses by inhibiting the proliferation and generation of effector T cells (Teff)^{1,2}. On one hand, this immunosuppressive activity prevents the development of autoimmune disorders, tissue destruction and chronic inflammatory diseases^{3,4}. On the other hand, the recruitment and accumulation of Tregs in tumor tissues leads to immune evasion by cancer cells. As a result of the immunosuppressive tumor microenvironment (TME), the T effector response is suppressed and tumor progression is promoted⁵. Hence, targeting tumor-infiltrating Tregs and consequently activating Teff cells in the TME are appealing approaches for boosting cancer immunotherapy.

Tumor necrosis factor (TNF) has been reported to play an important role in regulating Treg activity⁶. TNF-alpha (TNF α) is a cytokine which is involved in immune response, cell growth and proliferation, and tumor progression. The binding of TNF α to TNF receptors, such as tumor necrosis factor receptor 2 (TNFR2)⁷, it is a known mechanism which promotes Treg proliferation and immunosuppression mediated by PI3K/Akt and NK- κ B signalling pathway⁸. Several types of cancer, such as colon cancer, multiple myeloma and renal cell carcinoma, have been reported to express high levels of TNF in the TME⁹⁻¹¹.

TNF α main receptors are TNFR1 and TNFR2. While TNFR1 is widely expressed by different cell types, in humans and mice, TNFR2 is predominantly expressed on Tregs. High level of TNFR2 expression is correlated with greater suppressive activity of Tregs¹²⁻¹⁴. TNFR2 with more limited cell expression is also found on myeloid-derived suppressing cells and in different types of tumors and malignant cells¹⁵.

Since TNFR2 is highly expressed on tumor-infiltrating Tregs and its expression is correlated to a higher immunosuppressive activity^{16,17}, antagonistic TNFR2 antibodies or TNFR2 blocking agents could be an

interesting tool for antitumor therapy. An earlier study found that blocking TNFR2 with antagonistic antibodies decreased the tumor growth and tumor-associated Tregs, demonstrating the therapeutic potential of anti-TNFR2 antibodies in cancer immunotherapy¹⁸.

In this work, we further explored Treg targeting with newly generated anti-TNFR2 monoclonal antibodies (mAbs). The main objective was to assess the impact of mouse TNFR2-targeting with a blocking (candidate 25) or a non-blocking mAb (candidate 30). In addition, we also assessed the importance of the downstream effector function of the Fc portion of tested mAbs, by using either active or silent Fc. This allowed us to test if binding to TNFR2 alone was sufficient to obtain a biological effect (Fab-mediated), or additional Fc-mediated destruction of target cells was needed. For this purpose, mIgG2a was selected as the most active isotype^{19,20}, while mIgG2a with L234A/L235A/P329G mutations that abrogate FcγR and complement binding was used as a silent Fc^{21,22}.

TNFR2-targeting mAb candidates 25 and 30 were selected based on the previously published work²³, where both candidates presented ~3nM K_D and high efficacy binding to TNFR2 receptor. Here, they were expressed with mouse Fc, and further characterized by (1) *in vitro* binding assay which confirmed binding to TNFR2-expressing cells, (2) *ex vivo* CDC assay which revealed Fc-dependent complement activation, and (3) *in vivo* activity assessment. To test the effect *in vivo*, naïve CD4 cells and Tregs were transferred into recipient mice which were then treated with anti-TNFR2 antibodies. Proliferation of naïve CD4 cells was used as a readout for TNFR2-mediated Treg targeting. The results indicate that tested anti-TNFR2 antibodies successfully target Treg population, but also T effector CD4⁺.

Results

Expression of different anti-TNFR2 antibodies with active and silent Fc-isotypes

We previously described 13 TNFR2-specific antibodies²³, of which two (candidate 25 and 30) were selected to assess their effects on Treg function.

Candidate 25 was considered as a TNF α blocker and candidate 30 as a TNF α non-blocker. Both candidates were expressed with an active Fc (mIgG2a) and a silent Fc (mIgG2a.LALA-PG), resulting in four antibodies in total (Fig. 1A).

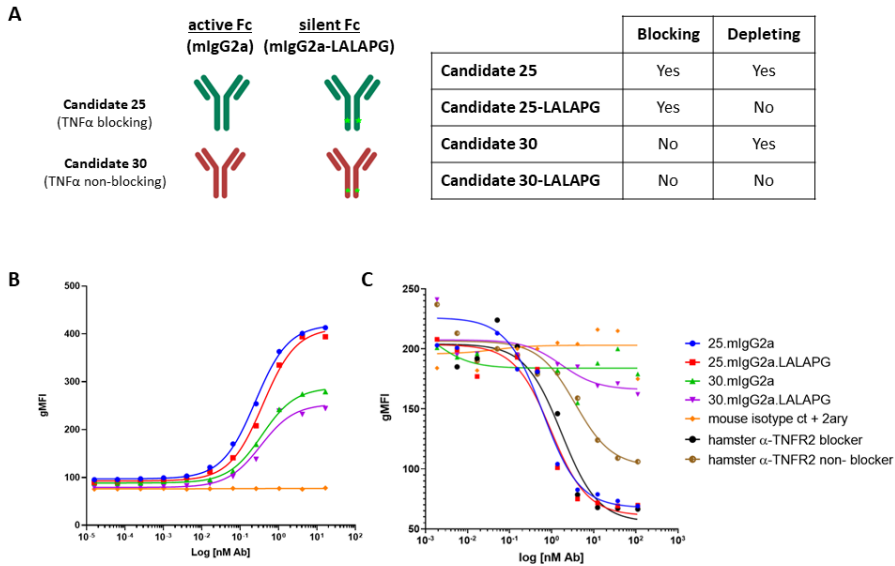


Figure 1. Mouse anti-mTNFR2 antibodies show similar binding profile regardless of the isotype. (A) Schematic representation of used mTNFR2 antibodies, which differ in their blocking activity (Fab-dependent) and depleting activity (Fc-dependent). (B) mTNFR2 stable transfected CHO-K1 cells were incubated with 3-fold increasing concentrations of each mouse anti-mTNFR2 mAbs, and binding was detected by flow cytometry assessing gMFI. (C) TNF α ligand competition with generated antibodies assessed by FACS. Data represented as gMFI dose-response curve fit of the blocker antibodies with appropriate controls incubations with 3-fold increasing concentrations. Two benchmark hamster-anti-mTNFR2 antibodies with known blocking activity were added as controls. (B and C) Representative biological replicate of $n=2$ biological replicates. *Green star indicates introduction of LALA-PG mutations.

All antibodies were produced recombinantly and purified using MabSelect SuRe LX resin. SDS-PAGE was performed to confirm the correct molecular weights and purity of antibodies. The analysis under non-reducing conditions confirmed the expected molecular weights and indicated that a high purity (>90%) was reached in all samples (Fig. S1). Furthermore, only

heavy chain (HC) and light chain (LC) were observed under reducing conditions, confirming the correct antibody composition (Fig. S1).

Since for this study we switched the isotype of candidates 25 and 30 from rat, as used previously, to mouse IgG2a, the binding activity to mTNFR2 and TNF α blocking activity were reassessed²³. FACS analysis showed that both mAbs stained TNFR2-expressing CHO cells (Fig. 1B) confirming that antigen binding was preserved. Furthermore, the higher affinity of candidate 25 compared to candidate 30 is maintained after isotype switching from rat to mouse. In parallel, blocking activity was checked through a competition assay consisting of TNFR2-expressing CHO cells bound to TNFR2 antibodies in a first incubation step followed by a second incubation step with biotinylated TNF α and detected with streptavidin-APC. Similarly, candidate 25 preserved TNF α blocking activity and candidate 30 remained TNF α non-blocker, regardless of the mouse Fc used (Fig. 1C).

Taken together, the produced antibodies complied with high-quality standards regarding monomericity and purity. Rat to mouse isotype switch did not alter the binding and blocking features.

mTNFR2 antibodies mediate Fc-dependent CDC against Tregs

Monoclonal antibodies can mediate their effects by a variety of mechanisms, including interference with cell signalling resulting in cell cycle arrest, direct induction of apoptosis, sensitization to cytotoxic drugs, CDC, antibody-dependent phagocytosis (ADPC), and ADCC. In the present study, the role of the complement activity of the different candidates was assessed *in vitro* and *ex vivo*.

In order to detect on-target CDC killing, CHO-K1.mTNFR2 target cells and CHO-K1 control cells were labelled with different dyes and mixed in 1:1 ratio. Next, the antibody-mediated complement activation was induced and the changes in target:control cell ratio were assessed by FACS. The gating strategy is shown in Fig. 2A. A significantly lower target:control cell ratio was observed after complement activation with anti-TNFR2 antibodies with active Fc (IgG2a) compared to isotype control or complement alone (Fig. 2A). Therefore both anti-TNFR2 candidates successfully induced CDC against

CHO-K1.mTNFR2 target cells. As expected, the introduction of LALA-PG mutations into IgG2 isotype abrogated the CDC effect (Fig. 2B).

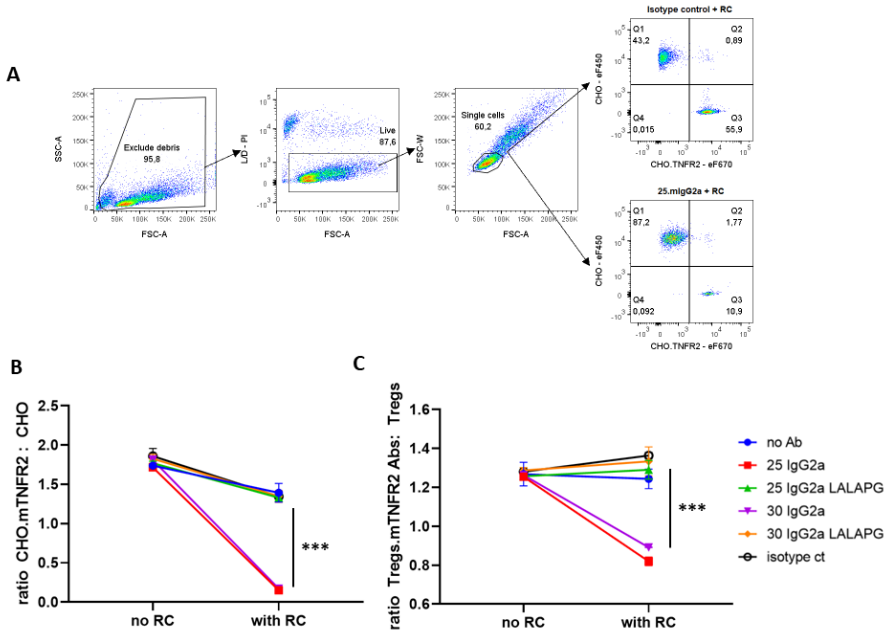


Figure 2. CDC profiles of anti-TNFR2 constructs targeting CHO-K1.mTNFR2 and Tregs. (A) Representative plots used to calculate CHO-K1.mTNFR2:CHO-K1 ratio. First, CHO-K1 cells were gated based on FSC-A / SSC-A properties. Next, Live cells were based on FSC-A/ PI staining. Live cells were gated for single cells based FSC-A / FSC-W. Target cells CHO-K1.mTNFR2 are found in Q3 as eF670⁺ and CHO-K1 are found as Q1 as eF450⁺. Data representative from samples incubated isotype control or 25.IgG2a and with RC. (B) CHO-K1.mTNFR2 target cells and CHO-K1 control cells were previously stained, then co-incubated with anti-TNFR2 antibodies followed by RC incubation Cells were analysed by FACS and CHO-K1.mTNFR2:CHO-K1 ratio was calculated. (C) Similarly, Tregs expanded ex vivo for 5 days. At day 5, Tregs incubated with anti-TNFR2 antibodies previously stained with eF670 and Tregs without antibody incubation stained with eF450. After antibody incubation, cells were mixed 1:1 and incubated with RC. Cells were analysed by FACS and Tregs.mTNFR2 Abs:Tregs ratio was calculated. Mean + SD of duplicates are shown of a representative biological replicate out of n=2 biological replicates. (Statistics: CDC assay – one-way ANOVA on subtracted values (no RC – with RC), ***P<0.0005).

Furthermore, we tested if anti-TNFR2 antibodies were able to induce CDC against Tregs in an ex vivo assay. Harvested splenocytes were sorted as CD4⁺

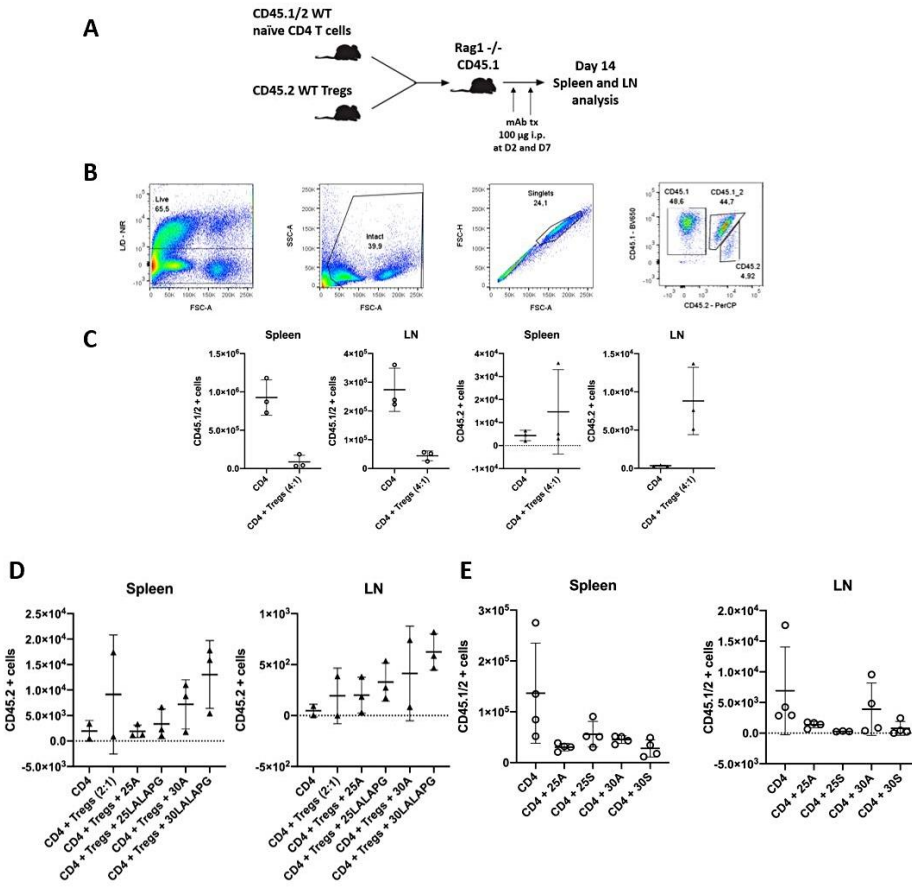
CD45RB^{low} CD25^{high} and were 5-day expanded with anti-CD3/CD28 dynabeads (1:1 ratio) plus recombinant mouse IL2 (20 ng/ml) in 96 round-bottom plates (4×10^5 cells/well). Treg depletion was driven by complement-dependent toxicity with the active isotype antibodies, and this was abrogated by the Fc silencing LALA-PG mutation (Fig. 2C). CDC activity was also tested on freshly sorted naïve CD4 T cells and after 5-day expansion. On day 0, naïve CD4 did not express TNFR2 (data not shown). Although CD4 T cells upregulated TNFR2 expression after 5-day expansion (Fig. S2A), they were not susceptible to anti-TNFR2-mediated CDC (Fig. S2 B).

In summary, the expressed anti-TNFR2 antibodies of IgG2a isotype successfully mediated CDC against CHO-K1.mTNFR2 and Tregs, but not against naïve CD4 cells expanded for 5 days. CDC activity was lost after the introduction of Fc-silencing LALA-PG mutations.

TNFR2 antibodies target Treg and effector CD4⁺ T cell populations in vivo

To further assess the potential use of anti-TNFR2 antibodies for Treg targeting, we tested whether the anti-TNFR2 treatment could modulate the suppressive capacity of Tregs in vivo. Naïve wild-type CD4⁺ T cells (CD45.1/2⁺) were mixed with or without Tregs (CD45.2⁺) in the indicated ratios and injected intravenously into Rag1^{-/-} (CD45.1⁺) recipient mice. At day 2 and 7, indicated groups received 100µg of anti-TNFR2 antibody intraperitoneally. After 14 days, splenocytes and lymph nodes were analysed for the presence of CD45.1/2 and CD45.2 cells (Fig. 3 A). The gating strategy is shown in Fig. 3 B.

When naïve cells (CD45.1/2⁺) were co-transferred with Tregs (CD45.2⁺) without antibody treatment, lower numbers of naïve cells were observed in spleen and lymph nodes (Fig. 3C, left) compared to the group that received only naïve CD4 T cell transfer. Thus, the results indicate that Tregs suppressed the expansion and proliferation of naïve CD4 T cells. As expected, CD45.2⁺ cells were only observed in the group who received Treg transfer (Fig. 3C, right).



6

Figure 3. Tregs and effector CD4 T cells are targeted in vivo by anti-mTNFR2 mAbs. (A) Scheme of the *in vivo* setup. WT naive CD45.1/2⁺ CD4⁺ CD25⁻ CD45RB^{high} cells (4×10^5) were injected alone or together with WT CD45.2⁺ CD4⁺ CD25⁺ Tregs ($1-2 \times 10^5$) intravenously into Rag1 KO recipients in 2:1 or 4:1 ratio as indicated. After 14 days, spleens and lymph nodes (mix of brachial, axillar and inguinal) were assessed by flow cytometry for their proportions and absolute numbers of CD45.1/2⁺ and CD45.2⁺ Tregs. (B) Representative plots used at day 14 to analyse cell numbers. First, live splenocytes or cells derived from lymph nodes (LN) were gated based on FSC-A / NIR staining. Cell debris was excluded based on FSC-A / SSC-A properties. Next, CD45.1 and CD45.2 populations were gated. Data representative for spleen samples from mice injected with naïve and Tregs 2:1. (C) Control results of naïve CD4 T cells injected with or without Tregs (4:1) into Rag 1 KO recipient mice. Absolute numbers of CD45.1/2⁺ cells are shown on the left side (spleen and lymph node) and CD45.2⁺

cells on the right side. (D) Absolute numbers of CD45.2⁺ Tregs in spleen and inguinal lymph nodes (iLN) of mice injected with naïve CD4 T cells, Tregs (2:1) and anti-TNFR2 antibody treatment. (E) Absolute numbers of CD45.1/2 cells in spleen and inguinal lymph nodes (iLN) of mice injected with naïve CD4 T cells and anti-TNFR2 mAbs. (D and E). Mice received 100µg of mAb per group diluted in 250µl PBS intraperitoneally administered at day 2 and day 7. Each symbol represents an individual mouse. Data are representative of one individual experiment. Bars represent mean±SD.

Upon addition of anti-mTNFR2 treatment, the number of recovered Tregs were dependent on anti-mTNFR2 candidate that was used (Fig. 3 D). Treg numbers (CD45.2) were reduced in the presence of TNFR2-blocking candidate 25. No difference was observed between candidate 25 with mIgG2a or mIgG2a.LALA-PG. On the other hand, the candidate 30 did not reduce Treg numbers, irrespective of the Fc backbone (active or silent).

Finally, the number of CD45.1/2 cells (naïve CD4 T cells) was assessed, as their higher proliferation would be indicative of diminished Treg-mediated suppression. Although a reduction in Treg number was observed in the group treated with TNFR2-blocking candidate 25, this did not lead to an increase in CD45.1/2 T cell numbers (naïve CD4 T cells) (Fig. S3A).

Since we failed to observe an increase in CD4 T cell numbers, despite reduction of Treg numbers by anti-TNFR2 treatment, and we detected TNFR2 expression on CD4 T cells (Fig. S2A), we hypothesized that the anti-TNFR2 mAbs may also target the CD4 effector T cells *in vivo*. Therefore, injection of naïve CD4 T cells alone (without Tregs) was tested together with anti-TNFR2 mAbs treatment. The control group that received CD4 T cells alone and no antibody treatment presented higher numbers of CD45.1/2⁺ cells, compared to the group that received CD4 T cell transfer and anti-TNFR2 antibodies. (Fig.3 E). All tested anti-TNFR2 mAbs, regardless of the candidate and Fc backbone, reduced the numbers of CD45.1/2⁺ cells.

These data demonstrate that anti-mTNFR2 antibodies target both Tregs and effector CD4⁺ T cells *in vivo*, and thus fail to achieve Treg-exclusive cell targeting.

Discussion

Cancer immunotherapy aiming to target Tregs has been unsuccessful in the recent years, as different strategies failed during different stages of clinical trials. In this study, we used two novel antibodies against mTNFR2 with different binding properties (TNF blocking or non-blocking) and Fc activity (active or silent) to target Tregs. These antibodies have been tested *in vitro* in CHO-K1.mTNFR2, *ex vivo* with sorted and expanded Tregs and naïve CD4 cells, and *in vivo*, were Rag1 KO CD45.1⁺ mice received naïve CD4⁺ CD45.1/2⁺ cells, with or without Tregs CD45.2⁺ and anti-mTNFR2 treatment. Our results show that in this setting, active anti-mTNFR2 antibodies are able to mediate *in vitro* CDC activity against CHO-K1.mTNFR2 cells and Tregs, but not *ex vivo* expanded CD4 T cells that also express TNFR2. *In vivo*, however, it seems that anti-TNFR2 antibodies target both Tregs and T effector CD4⁺ cells.

Among the thirteen candidates presented previously²³, two candidates were selected for further characterization. The first selection criteria was a good target binding efficacy. Secondly, we wanted to compare a blocking and a non-blocking antibody, to assess the impact of ligand competition with TNF α on Treg activity. From antibody production and purification perspective, antibody sequences propense to increase aggregation and potential post-translational modifications were excluded. To this end, candidate 25 was selected as a blocking anti-TNFR2 mAb and candidate 30 was selected as a non-blocking anti-TNFR2 mAb. In our previously published work, these antibodies were of rat isotype²³. Here, they were expressed with a mouse Fc, as they were tested in mouse models *in vivo*. In addition, we used both an active Fc (IgG2a) and a silent Fc (IgG2a with silencing mutations) in order to assess the importance of Fc-mediated depletion in addition to Fab-mediated TNFR2 blocking.

As expected, isotype switch did not affect the binding to mTNFR2 expressed on CHO-K1 stably transfected cell line, nor the TNF α blocking properties. Cytotoxicity mediated by the two selected antibodies with active and silent Fc was assessed by CDC and ADCC. CHO-K1.mTNFR2 as target cells were only significantly reduced when active mIgG2a isotype was used, suggesting that only the mIgG2a isotype successfully mediated CDC against target cells. The

introduction of the Fc silencing LALA-PG mutations into mIgG2a isotype abrogated the complement-mediated cell depletion. A similar trend was observed with sorted Tregs that were expanded for 5 days *ex vivo*. However, the decrease was less drastic. 1 hour incubation should be enough to observe CDC assay^{24,25}, but cell biology and expansion *ex vivo* might affect the cell viability. Surprisingly, the CDC activity was not observed when complement was incubated with sorted naïve CD4 cells expanded for 5 days. The culture at day 5 was 95% pure for CD4 cells, where more than 65% were TNFR2⁺, therefore, CDC can be expected. The results might indicate different TNFR2 expression patterns on the surface of CD4⁺ effector cells and Tregs, which can lead to differences in antibody-mediated cross-linking and, hence, downstream complement effect.

While ADCC assays have been broadly described in literature²⁶⁻²⁸, no ADCC experiment has been reported aiming to target TNFR2-expressing cells yet. This might be indicative of the challenges of setting up such an ADCC assay. Commonly used effector cells for ADCC are NK cells²⁹. However, it has been previously reported that NK cells express TNFR2³⁰, which we also confirmed (Fig. S2C). Nevertheless, we tried to minimize the unwanted binding of our anti-TNFR2 mAbs to NK cells by incubating the mAbs with CHO-K1.mTNFR2 target cells first, washing the unbound antibodies and adding the NK cells in the end. Unfortunately, the results were inconclusive for both ADCC assay setups that we tested: i) via lactate dehydrogenase, which is a cytosolic enzyme that is released into the cell culture medium upon damage of the plasma membrane, and (ii) via release of a cell dye and FACS analysis after inducing ADCC. We believe that the constant association and dissociation of the antibodies to their targets could potentially explain the readout failure³¹. Thus, upon NK cell addition, the anti-TNFR2 antibodies could dissociate from target cells and bind to NK cells instead, limiting in such way the target cell killing. Macrophages could have also been tested as effector cell population, but TNFR2 expression on their surface wouldn't have allowed to establish a better setup³². These results confirm the difficulties in optimizing ADCC assay against TNFR2-expressing cells.

Several models have been described to assess the suppressive capacity of Tregs *in vivo*^{33,34}. Here, Treg targeting with anti-mTNFR2 antibodies was assessed after Treg and naïve CD4 T cell co-transfer into Rag 1 KO mice.

Three different CD45 background mice were used to track the cells. We hypothesised that the Treg-mediated suppression of naïve CD4 T cell proliferation would be reverted if anti-mTNFR2 antibodies successfully blocked Treg activity. Tregs could be either depleted by anti-mTNFR2 mAbs with an active Fc, or suppressed but not depleted with the TNF α -blocking but Fc-silent anti-mTNFR2 antibody (candidate 25 with LALA-PG mutations).

The control group used in this mouse model revealed that CD45.1/2 cell numbers (derived from injected naïve CD4 T cells) are reduced upon Treg injection. Upon TNFR2 treatment, it seems that the number of Tregs was dependent on the used antibody candidate (Fig. 3D). Candidate 25, a blocking antibody, reduced Treg numbers regardless of the isotype. Candidate 30, a non-blocking antibody, slightly reduced Treg numbers with the active isotype but not when the Fc was silent. However, the observed effect on the number of Tregs had no impact on CD45.1/2 cell proliferation, as CD45.1/2 cell numbers were similar to the control group that received naïve CD4 T cells only (Fig. S3A). The main limitation here was that the number of CD45.1/2 cells in control group where naïve CD4 and Tregs were injected was higher than in the control group with naïve cells alone, contrary to previous experiment in Fig. 3C. This suggests that the experiment might not have worked accurately, most likely because the injected naïve CD4 cells were not pure enough. Furthermore, only 2 or 3 mice were included per group which makes data less robust. To further confirm if naïve CD4 cells are also targeted by TNFR2 treatment, Tregs were excluded in the next experiment. Here, Figure 3E, the control groups were as expected; the data showed a reduction of CD45.1/2 T cell populations upon all TNFR2-targeted treatments.

Nevertheless, in an *in vivo* setting, the TNFR2⁺ NK cell-mediated cellular lysis may be of considerably greater importance —an aspect that has been discussed with extensive details for the clinical application of RituxiMab³⁵ — which would make presented data still technically correct. The available complement in the blood is thought to be rapidly depleted inside the body. In lymphoma studies, it is known that NK cells can lyse rituximab-coated transformed B cells. Thus, the *in vivo* experiments could potentially be explained by an even better NK-cell depletion of Tregs as well as Tregs cells since NK-cell mediated lysis *in vitro* was unable to be examined.

In summary, our data show that the two novel anti-mTNFR2 antibodies were able to target different TNFR2-expressing cells, including Tregs and effector CD4 T cells *in vivo*. *Ex vivo* data proved that effector-mediated CDC against Tregs and CHO-K1 cells were isotype-dependent, as LALA-PG mutations abrogated CDC activity. However, isotype became less relevant upon *in vivo* injection. Furthermore, *in vivo* data suggests that TNFR2 blocking mAb are more effective in reducing Treg numbers *in vivo*, compared to non-blocking mAb.

Material and methods

Cloning and antibody production: Generation of anti-TNFR2 antibodies with mouse isotypes

Variable amino acid sequences of all anti-TNFR2 antibodies were provided in our previous research²³ (supplementary Table 1). In short, the starting point were anti-TNFR2 hybridomas which were sequenced in order to obtain heavy and light chain variable domain sequences (VH, VL); candidates 25 and 30 were selected. Next, we designed chimeric anti-TNFR2 mIgG2a-LALA-PG heavy chains by combining the VH with the known sequences of the constant domains of murine IgG2a-LALA-PG (CH). Just between VH and CH domains, a unique restriction site (AfeI) was introduced, allowing us to change the isotypes by cloning. The mIgG2a HC were cloned using standard cloning techniques from plasmids available in house (anti-OVA) into the pcDNA3.1 (+) encoding for anti-TNFR2 (Fig. 1A). Correct clones were confirmed by Sanger sequencing (GENEWIZ). The plasmids encoding for the anti-TNFR2 light chains were *de novo* synthesized (GeneArt).

Production and purification of mAbs

Candidates 15 and 30 targeting mTNFR2 with mIgG2a and mIgG2a-LALA-PG were produced in FreeStyle293 cells. Briefly, cells were transfected with pcDNA3.1.(+) expression vectors encoding corresponding heavy and light chains (1:1 ratio), using 293fectin reagent (Invitrogen) according to the manufacturer's recommendation. The cells were incubated for 7 days at 37 °C, 8% CO₂ at 120 rpm. On day 7 post-transfection, the cell suspension was

collected and centrifuged for 15 min at 2500 g. The supernatants were filtered over a 0.22 µm filter and stored at 4 °C.

The supernatants were mixed with a pre-determined amount of MabSelect SuRe LX resin (GE Lifesciences) and rotated overnight at 4 °C. Following overnight capturing, the bound antibody was purified from the resin by affinity chromatography using Pierce™ Centrifuge Columns (ThermoFisher Scientific) and re-buffered to PBS using PD-10 Desalting Columns (GE healthcare) according to the manufacturer's instructions. Quality control consisting of SDS-PAGE was performed.

Cell lines

CHO-K1 (ATCC) and CHO-K1.mTNFR2 stably transfected were cultured in heat-inactivated Fetal Bovine Serum (Gibco), 1% penicillin/streptomycin (Gibco), 2mM L-glutamine (Gibco).

Mice

Ly5.1 het CD45.1/2 mice on a C57BL/6 background were obtained internally from University of Edinburgh. Rag1 KO CD45.1 mice on a C57BL/6 background were bred in the animal facility at the University of Edinburgh. Experiments were carried out under the project license PPL: PP7488818. All animal experiments were approved by The University of Edinburgh.

Flow cytometry

TNFR2 binding and TNFα blocking assay assessed on CHO-K1.mTNFR2 has been done as described before²³. Briefly, 1×10^5 cells were incubated with 4-fold increasing concentrations (max. 50 µg/ mL) of anti-mTNFR2 mAbs at 4 °C for 30 min, and binding was detected with anti-mouse IgG PE (BD Biosciences). To assess blocking activity, TNFα-biotin (Sino Biological) was co-incubated with CHO-K1.mTNFR2 cells after antibody incubation and its signal was detected by APC-streptavidin (BD Biosciences). Results are shown as geometric Mean Fluorescence Intensity. Two benchmark hamster antibodies against mTNFR2 were taken as a reference: Purified anti-mouse CD120b (TNFR Type II/p75, clone TR75-54.7) (Biolegend) listed as anti-TNFR2 mAb with blocking activity and Purified anti-mouse CD120b (TNFR Type

II/p75, clone TR75-89) (BD Biosciences) as a non-blocking anti-TNFR2 mAb. The stained cells were analysed on a FACS Canto™ II (BD) using the software program BD FACSDiva. Ten thousand events were counted. Further analysis was performed with FlowJo and shown results plotted in GraphPad.

Complement-dependent cytotoxicity (CDC) assay

Complement activity was tested on the TNFR2 antibodies with active and silent isotypes. CHO-K1 and CHO-K1.mTNFR2 cells were detached with 2mM EDTA (Gibco) and were pre-stained with eF450 and eF670 (eBioscience) respectively, following manufacturers' instructions. Cells were mixed 2:1 after staining in 96-round well plate, with a total concentration of 5e5 cells per well. Cells were washed three times with FACS buffer (1% FBS PBS) at 400g for 3' at 4 °C and incubated with 50 µl of each antibody at 50 µg/ml for 30' at 4 °C in the dark. After three wash steps, cells were incubated with pre-warmed Rabbit Complement (RC) (Cedarlane) at 1:8 diluted in IMDM complete media. 50 µl of RC dilution were added to each well and cells were incubated for 1 hour at 37 °C. Cells were washed 3 times and DNase (Promega) was added to FACS buffer at 1 U/µl. Cells were resuspended in 150 µl FACS buffer with 1 mg/ml Propidium iodide (PI) (Sigma Aldrich). 100 µl of the stained cells were analysed on a FACS LSRFortessa (BD) using the software program BD FACSDiva. Further analysis was performed with FlowJo and shown results plotted in GraphPad (one-way ANOVA statistics applied). For CDC assay on Tregs and naïve CD4 at day 5 of expansion *ex vivo*, similar procedure was followed with the following variations mentioned below. Cells were first stained, followed by antibody incubation, and after three wash steps with FACS buffer, cells were mixed 1:1 and incubated with pre-warmed RC at 1:15 in RPMI complete media for 1 hour at 37 °C. Then, the same protocol mentioned above was followed for detection and analysis.

Generation of NK cells

Spleens from Rag1 KO mice were homogenized and submitted to red blood cell lysis using the RBC lysis buffer (Sigma Aldrich). The splenocytes were seeded at 2×10^6 cells/ml in 24-wells plates with RPMI (Sigma) supplemented with 10% heat-inactivated Fetal Bovine Serum (Gibco), 1%

penicillin/streptomycin (Gibco), 2mM L-glutamine (Gibco), 50 μM 2-mercaptoethanol (Gibco), 20 ng/ml of IL-2 (BD Pharmingen) and 20 ng/ml of IL-15 (Peprotech). Cells were used at day 5 when ~95% of intact cell population was identified as NK cells based on the expression of NKp46 (eBioscience) and NK1.1 (eBioscience) and lack of expression of CD3 (BD Pharmingen) by flow cytometry (CD3⁻ NKp46⁺ NK1.1⁺) using FACS LSRFortessa (BD). TNFR2 expression of the cell population was assessed via hamster anti-mouse CD120b (TNF R Type II/ p75) – BV421 (TR75–89) (Biolegend).

Antibody-dependent cell cytotoxicity (ADCC) assay

CHO-K1 and CHO-K1.mTNFR2 target cells were detached with 2mM EDTA (Gibco) and added to 96-well round bottom plates at 1 x 10⁴ cells/well. Anti-mTNFR2 mAbs were added at 10 μg/ml per well in FACS buffer and incubated for 30min at 4 °C, followed by two washing steps with FACS buffer at 400g for 3min at 4 °C. The effector NK cells were then added in pre-warmed media at 3-fold decreasing concentrations starting at 9:1 effector:target ratio. The cells were centrifuged at 400g for 2min to concentrate them at the bottom of the wells and ADCC assay was run for 4 hours at 37 °C. After 4 hours of incubation, the cells were centrifuged at 300g for 5min, and the supernatant was used to assess the cell toxicity with CytoTox 96® Non-Radioactive Cytotoxicity Assay LDH cytotoxicity Assay kit (Promega) following manufacturer's instructions. The LDH activity of medium alone was subtracted from the LDH activity of test conditions to obtain the corrected values. These corrected values were then used to calculate the percentage of cellular cytotoxicity using the following formula: percentage specific lysis = $\frac{(E+T+mAb)-(E+T)}{T \max \text{ lysis} - T} \times 100$, where E are the effector cells, T are the target cells and Tmax the lysed target cells alone.

Naïve CD4 and Treg purification

Naïve CD4 T cells were isolated from single-cell suspension from Ly5 het CD45.1/2 mice spleens by sorting stained cells with anti-CD4 AF700 (Biolegend), anti-CD45RB PE (BD Pharmingen), anti-CD25 APC (Biolegend). The sorted population was defined as CD4⁺ CD45RB^{high} and CD25^{low}. Treg

cells were isolated from single-cell suspension from a C57B/L6 CD45.2 mice spleens by sorting stained cells with anti-CD4 AF700 (Biolegend), anti-CD45RB PE (BD Pharmingen), anti-CD25 APC (Biolegend). The sorted population was defined as CD4⁺ CD45RB^{low} CD25^{high}.

Expansion ex vivo

For the bead-based expansion, naïve CD4 or Tregs were incubated in RPMI media supplemented with anti-CD3/CD28 dynabeads (Thermo Fisher) (1:1 ratio) plus recombinant mouse IL2 (BD Pharmingen) (20 ng/ml) in 96 round-bottom plates (4 x 10⁵ cells/well). Media was refreshed at day two and cells were used at day 5. Cells were used at day 5 and receptor expression was reassessed by flow cytometry using FACS LSRFortessa (BD). TNFR2 expression at day 5 was assessed via hamster anti-mouse CD120b (TNFR Type II/ p75) -BV421 (TR75–89) (Biolegend).

Cells at day 5 were used for the complement assay following the protocol mentioned above, where cells were pre-stained and half of them incubated with the different antibodies and after 3 wash steps, cells were mixed and incubated with 1:15 RC.

Adoptive cell transfer

To analyse the potential role of anti-mTNFR2 treatment on naïve CD4 proliferation and Treg function *in vivo*, purified populations of naïve CD45.1/2⁺ (5 x 10⁵ cells) with or without CD45.2⁺ Tregs (2.5x 10⁵ cells) (2:1 ratio) were injected intravenously into Rag1^{-/-} CD45.1⁺ recipient mice and analysed after 14 days. At day 2 and day 7, 100µg of anti-TNFR2 treatment diluted in 250µl PBS was administered intraperitoneally. At day 14, fresh spleens and brachial, axillar and inguinal LN from Rag1^{-/-} CD45.1⁺ recipient mice were used for cell isolation. The spleens and LN were mashed through a 70 µm cell strainer, after which the Red Blood Cell Lysing Buffer (Hybri-Max, Sigma) was used to remove any erythrocytes from splenocytes. Live cells derived from each cells suspension were counted with CASY Cell counter and Analyzer (BIOKÉ). 0.5-1 x 10⁶ cells were first stained with NIR (1:2000) (Life Technologies) followed by CD45.1-BV650 (Biolegend) and CD45.2-PerCP-Cy5.5 (Biolegend) and analysed on a FACS LSRFortessa (BD)

using the software program BD FACSDiva. Further analysis was performed with FlowJo and shown results plotted in GraphPad.

Acknowledgements

We thank Nicola Logan (University of Edinburgh) for her technical assistance in animal experiments.

Funding

This work was supported by the European Union's Horizon 2020 research and innovation programme under the Marie Skłodowska-Curie grant agreement [grant numbers 765394, 2018].

Disclosure statement

The authors declare no competing interests.

Supplementary material

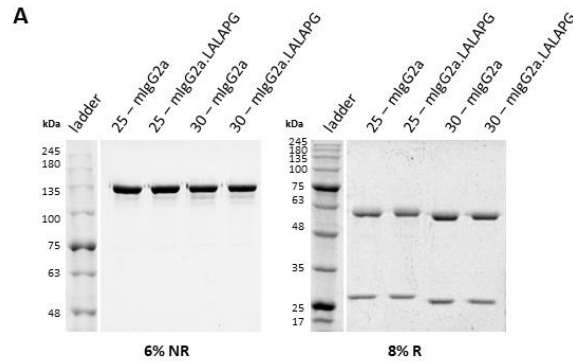


Figure S1. Quality control of anti-mTNFR2 antibodies. (A) CE-SDS under non-reducing conditions (left) and under reducing conditions (right). NR: non-reducing, R: reducing.

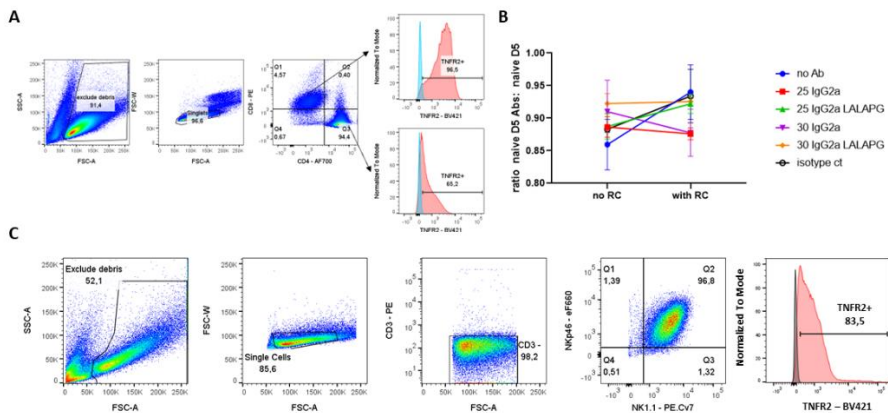


Figure S2. Flow cytometry data and analysis. (A) Characterization of CD4 population at day 5 derived from ex vivo material. Gating was done on FSC-A / SSC-A properties to exclude cell debris. Next, single cells were gated based FSC-A / FSC-W. Cells were gated as CD4 or CD8 cell populations. Next, TNFR2 expression was assessed in each cell population. In blue, FMO and in red, TNFR2⁺ cells, expressed in percentage. (B) At day 5 of naïve cells expansion, part of the cells were incubated with 50 µg/mL of anti-TNFR2 antibodies at 4 °C for 30 min were previously stained with eF670 and in parallel, cells without antibody incubation stained with eF450. After antibody incubation, cells were mixed 1:1 and incubated with RC for 1h at 37 °C. Cells were analysed by FACS and naïve D5 mTNFR2 Abs: naïve D5 was calculated. Mean + SD of triplicates are shown of a representative biological replicate out of n=2 biological

replicates. No significant differences were observed. (Statistics: CDC assay – one-way ANOVA on subtracted values (no RC – with RC)). (C) Characterization of NK population at day 5 derived from ex vivo material. Gating was done on unstained splenocytes at day 5 and its respective fluorescence-minus-one sample. First, NK cells were gated based on FSC-A / SSC-A properties. Next, single cells were gated based FSC-A / FSC-W. NK population were gated as CD3⁻ population, NK population are found at NKp46⁺ NK1.1⁺ gate. TNFR2 expression was assessed on NKp46⁺ NK1.1⁺ cells. In grey, FMO and in red, TNFR2⁺ cells, expressed in percentage.

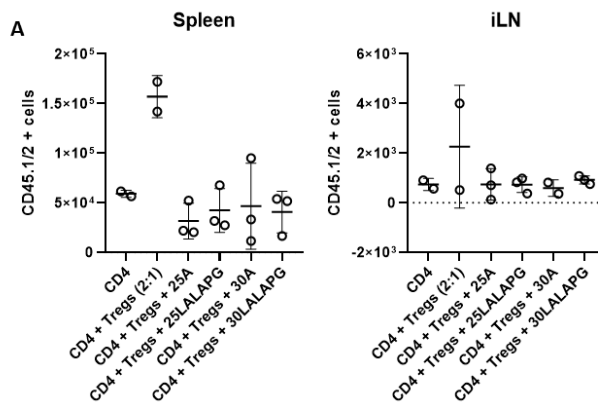


Figure S3. Poor proliferation of CD45.1/2⁺ cells upon anti-mTNFR2 mAbs treatment. (A) Absolute numbers of CD45.1/2⁺ cells in spleen and inguinal lymph nodes (iLN) of mice injected with naïve, naïve and Tregs (2:1) and antibody treatment of mAbs anti-TNFR2. Mice received 100µg of mAb per group diluted in 250µl PBS intraperitoneally administered at day 2 and day 7. Each symbol represents an individual mouse. Data are representative of one individual experiment. Bars represent SD. Control groups (naïve CD4⁺ T cells alone and naïve CD4⁺ T cells + Tregs) indicate assay failure since absolute CD45.1/2⁺ numbers were expected to be the highest in the naïve CD4⁺ T cells alone group.



References

1. Yang S, Wang J, Brand DD, Zheng SG. Role of TNF–TNF Receptor 2 Signal in Regulatory T Cells and Its Therapeutic Implications. *Front Immunol* [Internet]. 2018 Apr 19 [cited 2019 May 8];9. Available from: <http://journal.frontiersin.org/article/10.3389/fimmu.2018.00784/full>
2. Sakaguchi S, Yamaguchi T, Nomura T, Ono M. Regulatory T Cells and Immune Tolerance. *Cell*. 2008 May;133(5):775–87.
3. Coombes JL, Robinson NJ, Maloy KJ, Uhlig HH, Powrie F. Regulatory T cells and intestinal homeostasis. *Immunol Rev*. 2005;204(1):184–94.
4. Xystrakis E, Kusumakar S, Boswell S, Peek E, Urry Z, Richards DF, et al. Reversing the defective induction of IL-10-secreting regulatory T cells in glucocorticoid-resistant asthma patients. *J Clin Invest*. 2006 Jan;116(1):146–55.
5. Woo EY, Chu CS, Goletz TJ, Schlienger K, Yeh H, Coukos G, et al. Regulatory CD4+CD25+ T Cells in Tumors from Patients with Early-Stage Non-Small Cell Lung Cancer and Late-Stage Ovarian Cancer1. *Cancer Res*. 2001 Jun 1;61(12):4766–72.
6. Valencia X, Stephens G, Goldbach-Mansky R, Wilson M, Shevach EM, Lipsky PE. TNF downmodulates the function of human CD4+CD25hi T-regulatory cells. *Blood*. 2006 Jul 1;108(1):253–61.
7. Santee SM, Owen-Schaub LB. Human tumor necrosis factor receptor p75/80 (CD120b) gene structure and promoter characterization. *J Biol Chem*. 1996 Aug 30;271(35):21151–9.
8. Vanamee ÉS, Faustman DL. TNFR2: A Novel Target for Cancer Immunotherapy. *Trends Mol Med*. 2017 Nov;23(11):1037–46.
9. Uhlén M, Björling E, Agaton C, Szigartyo CAK, Amini B, Andersen E, et al. A human protein atlas for normal and cancer tissues based on antibody proteomics. *Mol Cell Proteomics MCP*. 2005 Dec;4(12):1920–32.
10. Rauert H, Stühmer T, Bargou R, Wajant H, Siegmund D. TNFR1 and TNFR2 regulate the extrinsic apoptotic pathway in myeloma cells by multiple mechanisms. *Cell Death Dis*. 2011 Aug;2(8):e194–e194.
11. Nakayama S, Yokote T, Hirata Y, Akioka T, Miyoshi T, Hiraoka N, et al. TNF- α expression in tumor cells as a novel prognostic marker for diffuse large B-cell lymphoma, not otherwise specified. *Am J Surg Pathol*. 2014 Feb;38(2):228–34.
12. Chen X, Subleski JJ, Kopf H, Howard OMZ, Mannel DN, Oppenheim JJ. Cutting Edge: Expression of TNFR2 Defines a Maximally Suppressive Subset of Mouse CD4+CD25+FoxP3+ T Regulatory Cells: Applicability to Tumor-Infiltrating T Regulatory Cells. *J Immunol*. 2008 May 15;180(10):6467–71.
13. Chen X, Subleski JJ, Hamano R, Howard OMZ, Wiltrout RH, Oppenheim JJ. Co-expression of TNFR2 and CD25 identifies more of the functional CD4 + FOXP3 + regulatory T cells in human peripheral blood: Immunomodulation. *Eur J Immunol*. 2010 Apr;40(4):1099–106.
14. Chen X, Wu X, Zhou Q, Howard OMZ, Netea MG, Oppenheim JJ. TNFR2 Is Critical for the Stabilization of the CD4 + Foxp3 + Regulatory T Cell Phenotype in the Inflammatory Environment. *J Immunol*. 2013 Feb 1;190(3):1076–84.

15. Diaz-Montero CM, Finke J, Montero AJ. Myeloid derived suppressor cells in cancer: therapeutic, predictive, and prognostic implications. *Semin Oncol*. 2014 Apr;41(2):174–84.
16. Chen X, Oppenheim JJ. Targeting TNFR2, an immune checkpoint stimulator and oncoprotein, is a promising treatment for cancer. *Sci Signal*. 2017 Jan 17;10(462):eaal2328.
17. Zhao T, Li H, Liu Z. Tumor necrosis factor receptor 2 promotes growth of colorectal cancer via the PI3K/AKT signaling pathway. *Oncol Lett*. 2017 Jan;13(1):342–6.
18. Torrey H, Butterworth J, Mera T, Okubo Y, Wang L, Baum D, et al. Targeting TNFR2 with antagonistic antibodies inhibits proliferation of ovarian cancer cells and tumor-associated T_{regs}. *Sci Signal*. 2017 Jan 17;10(462):eaaf8608.
19. Rosales C, Uribe-Querol E. Fc receptors: Cell activators of antibody functions. *Adv Biosci Biotechnol*. 2013;04(04):21–33.
20. Vukovic N, van Elsas A, Verbeek JS, Zaiss DMW. Isotype selection for antibody-based cancer therapy. *Clin Exp Immunol*. 2021 Mar;203(3):351–65.
21. Schlothauer T, Herter S, Koller CF, Grau-Richards S, Steinhart V, Spick C, et al. Novel human IgG1 and IgG4 Fc-engineered antibodies with completely abolished immune effector functions. *Protein Eng Des Sel PEDS*. 2016 Oct;29(10):457–66.
22. Lo M, Kim HS, Tong RK, Bainbridge TW, Vernes JM, Zhang Y, et al. Effector-attenuating Substitutions That Maintain Antibody Stability and Reduce Toxicity in Mice. *J Biol Chem*. 2017 Mar;292(9):3900–8.
23. Segués A, van Duijnhoven SMJ, Parade M, Driessen L, Vukovic N, Zaiss D, et al. Generation and characterization of novel co-stimulatory anti-mouse TNFR2 antibodies. *J Immunol Methods*. 2021 Dec;499:113173.
24. Saito PK, Yamakawa RH, da Silva Pereira LCM, da Silva Junior WV, Borelli SD. Complement-Dependent Cytotoxicity (CDC) to Detect Anti-HLA Antibodies: Old but Gold. *J Clin Lab Anal*. 2014 Feb 27;28(4):275–80.
25. Larson B, Banks P, Dhawan S, Wadwani S, Rothenberg M. A Semi-Automated, Non-Radioactive Assay for the Detection of Antibody-Based Complement-Dependent Cytotoxicity. :6.
26. Zhang M, Wen B, Anton OM, Yao Z, Dubois S, Ju W, et al. IL-15 enhanced antibody-dependent cellular cytotoxicity mediated by NK cells and macrophages. *Proc Natl Acad Sci [Internet]*. 2018 Nov 13 [cited 2022 Oct 31];115(46). Available from: <https://pnas.org/doi/full/10.1073/pnas.1811615115>
27. Wang G, Yu G, Wang D, Guo S, Shan F. Comparison of the purity and vitality of natural killer cells with different isolation kits. *Exp Ther Med*. 2017 May;13(5):1875–83.
28. Gasteiger G, Hemmers S, Firth MA, Le Floc’h A, Huse M, Sun JC, et al. IL-2-dependent tuning of NK cell sensitivity for target cells is controlled by regulatory T cells. *J Exp Med*. 2013 Jun 3;210(6):1167–78.
29. Vukovic N, Segués A, Huang S, Waterfall M, Sijts AJAM, Zaiss DM. Mouse IgG2a isotype therapeutic antibodies elicit superior tumor growth control compared to mIgG1 or mIgE. *Cancer Res Commun*. 2023 Jan 6;CRC-22-0356.
30. Xu J, Chakrabarti AK, Tan JL, Ge L, Gambotto A, Vujanovic NL. Essential role of the TNF-TNFR2 cognate interaction in mouse dendritic cell–natural killer cell crosstalk. *Blood*. 2007 Apr 15;109(8):3333–41.

31. Jarmoskaite I, ALSadhan I, Vaidyanathan PP, Herschlag D. How to measure and evaluate binding affinities. *eLife*. 2020 Aug 6;9:e57264.
32. Ruspi G, Schmidt EM, McCann F, Feldmann M, Williams RO, Stoop AA, et al. TNFR2 increases the sensitivity of ligand-induced activation of the p38 MAPK and NF- κ B pathways and signals TRAF2 protein degradation in macrophages. *Cell Signal*. 2014 Apr;26(4):683–90.
33. Collison LW, Workman CJ, Kuo TT, Boyd K, Wang Y, Vignali KM, et al. The inhibitory cytokine IL-35 contributes to regulatory T-cell function. *Nature*. 2007 Nov;450(7169):566–9.
34. Brownlie RJ, Miosge LA, Vassilakos D, Svensson LM, Cope A, Zamoyska R. Lack of the Phosphatase PTPN22 Increases Adhesion of Murine Regulatory T Cells to Improve Their Immunosuppressive Function. *Sci Signal*. 2012 Nov 27;5(252):ra87–ra87.
35. Merkt W, Lorenz HM, Watzl C. Rituximab induces phenotypical and functional changes of NK cells in a non-malignant experimental setting. *Arthritis Res Ther*. 2016;18:206.



7

General discussion

General discussion

mAbs have shown a great potential in immunotherapeutic treatments such as in cancer and autoimmune disease¹. While some mAbs have been approved to target malignant antigens such as Rituximab against CD20 in non-Hodgkin's lymphoma² or Ofatumumab for MS³, substantial interest in mAbs is currently focused on targeting immune checkpoints. Checkpoint inhibitors block receptors expressed by the immune system which prevent the immune system attacking tumoral cells. In 2020, the worldwide immune checkpoint inhibitors market was valued at \$29,803.71 million and is expected to surpass around \$140 billion by 2030.

The immune checkpoints most well-explored are cytotoxic T lymphocyte associated protein 4 (CTLA-4) and programmed cell death protein (PD-1) among with its ligand PD-L1 applied in different types of cancer such as lung cancer, bladder cancer, melanoma, Hodgkin lymphoma among others^{4,5}. Ipilimumab, an anti-CTLA4 mAb was the first immune checkpoint approved by the FDA for advanced melanoma in 2011⁶. Anti-PD1 drugs (nivolumab, pembrolizumab) and anti-PD-L1 drugs (atezolizumab, avelumab, durvalumab) were later approved⁷. However, a growing number of other co-stimulatory receptors has emerged in recent years aiming to be targeted such as receptors belonging to tumor necrosis factor receptor superfamily (TNFRsf) – OX40, 41BB, ICOS, GITR, CD27⁸⁻¹¹, LAG3^{12,13}, CD40¹⁴, TIGIT¹⁵, TIM3¹⁶.

Despite the clinical successes obtained with immune checkpoint inhibiting mAbs and the overall improved treatment outcome, these therapeutics are beneficial only for a small proportion of patients. Cold tumors are characterized by an immunosuppressive TME thus preventing effector cells from attacking tumor cells. mAbs have appeared to be poorly effective in cold tumors and tumor relapse after mAb treatment has been described^{17,18}. Furthermore, as a result of the checkpoint inhibitor-induced increase in effector responses, autoimmune toxicities have been observed¹⁹. Hence, an optimization of current immunotherapeutic treatments or novel approaches are indispensable.

BsAbs and a novel suggested approach for BsAb optimized treatment

To overcome the limitations associated with mAbs, in **Chapter 2**, we focused on the therapeutic potential and application of BsAbs. Upon their application, BsAbs can redirect immune cells to cancerous cells improving the killing activity.

BsAbs can dually target two different receptors which perform unique or overlapping functions and thereby reduce the drug resistance potential. Furthermore, BsAbs present higher specificity, targetability and less toxic side-effects. BsAb's structure and mechanism of action (MOA) might potentially reduce the costs of treatment, as they may be more efficacious and less costly to develop²⁰.

The study on BsAbs binding, compared to mAbs, results in the capability to target cells either in a *cis*- or in a *trans*-binding orientation increasing target selectivity. Consequently, they can respectively bridge two different cells by recognizing two different antigens expressed on two different cell populations or dually target by recognizing two different antigens expressed on the very same cell.

Since the first BsAb was described, technical challenges have emerged during the production and manufacturing of the constructs. To this end, a variety of technical approaches were explored to reliably produce BsAbs with high purity and stability. The available approaches and production platforms for BsAb generation differentiate between IgG-like and non-IgG-like BsAbs. The three BsAbs which are currently available in the market were reviewed in this chapter:

- Emicizumab: It is used to treat hemophilia A disease. It consists of a humanized modified asymmetric BsAb IgG4 antibody which binds to blood clotting factor IXa and factor X. Its generation is based on the Art-Ig IgG-like platform²¹.
- Blinatumomab: It is used to treat relapsed B-precursor acute lymphoblastic leukemia (ALL). It is a fragment-based BsAb, lacking an Fc region, that targets CD19 and CD3 in trans-binding^{22,23}.

- Amivantamab: It is indicated for the treatment of advanced or metastatic NSCLC harboring EGFR exon 20 insertion mutations. It is a fully-humanized IgG1-based BsAb targeting both epidermal growth factor receptor (EGFR) and mesenchymal-epithelial transition factor (MET). Its generation is based on the Duobody IgG-like platform²⁴.

In addition, one of the most commonly used constructs which have achieved late-stages in the clinical development pipeline are T cell redirecting bispecific antibodies (TbsAbs)²⁵. TbsAbs became a popular therapeutic approach with FDA approval for Blinatumomab, a CD19-directed T cell engager (see above), in 2018²⁶. These reagents are used to bridge tumor and immune cells. The most common TbsAbs redirect and activate CD3-expressing T cells to target and attack cancerous cells expressing specific antigens.

Despite the progress achieved with TbsAbs constructs, further optimization is required. TbsAbs can be classified as IgG-like TbsAbs and non-IgG-like TbsAbs. Blinatumomab, as an example of non-IgG-like TRBA, belongs to the bispecific T-cell engager (BiTE) format which is produced by recombinant expression of two cross-linked different variable fragments with linkers binding simultaneously CD3 and CD19. BiTEs like Blinatumomab present a trivial drawback: a short serum half-life (~2.11 h) due to the lack of Fc-portion. Consequently, patients require continuous intravenous infusion²⁷. Furthermore, while the lack of Fc-portion promotes a highly effective and specific killing, it also prevents the Fc-mediated effector functions.

Regarding IgG-like TbsAbs, the presence of the Fc enables TbsAbs to exhibit a similar half-life comparable to mAbs, roughly 10-21 days²⁸. However, full-length TbsAbs exhibit formation of undesirable homodimers and mis-paired molecules limiting the production, stability and/or biological activity. To this end, an optimized format is suggested in **Chapter 3**. A TbsAb consisting of Fab x sdAb-Fc is evaluated targeting mEGFR on tumor cells and mCD3 on T cells. To optimize the previously reported novel bispecific format by Huang *et al.*²⁹, different hinge designs of the sdAb arm of the BsAb were tested.

According to our research, a TbsAb with a shorter hinge of 23 amino acids (TbsAb.short) significantly outperforms a TbsAb with a longer hinge of 39 amino acids (TbsAb.long), the common length for an antibody hinge, in T cell redirected tumor killing. Additionally, the comparison of both constructs revealed that TbsAb.short format induced greater T cell and tumor cell aggregation. These data are also supported by increased expression levels of the CD69 and CD25 activation markers on T cells. These findings suggest that minor modifications to the hinge design of TbsAbs can be an appealing approach to optimize TbsAb application, enabling a better anti-tumor activity.

Currently, early clinical data reveal that treatments with TbsAbs have a promising favourable outcome for hematopoietic malignancies as well as solid tumors³¹⁻³⁴. However, there are still many patients who are unresponsive to TbsAbs therapy. Recent studies have shown that the main causes of treatment failure are loss of antigenicity and the presence of immunosuppressive factors, in particular, increased expression of inhibitory immune checkpoint molecules. Furthermore, due to high toxicity of the treatment, some clinical trials had to be discontinued, such as those with duvortuxizumab (NCT02743546) and AFM11 (NCT02848911 and NCT02106091), developed for B-cell malignancies^{35,36}. The approach proposed in Chapter 3 reveals a strategy to obtain a TbsAb with higher efficacy and specificity, linking T cells to tumor cells, which might become a successful technique to improve TbsAbs results in preclinical and clinical studies.

The importance of correct antibody isotype for treatment efficacy in a cancer model

Another key factor playing a role in the successful clinical outcome of mAb immunotherapy is isotype selection. Different mechanisms are involved in mAb-mediated anti-tumor effects, such as complement and cell-mediated tumor cell lysis, blockage of tumor-specific receptors promoting tumor growth, or immune inhibitory receptors. Thus, the effectiveness of many mAbs depends on the Fc-mediated effector response. Immune responses triggered by different Ig isotypes vary because of differential binding

capacities to immune cell Fc receptors. The desired MOA of therapeutic mAbs hence determines the isotype selection. Given that a positive clinical outcome of mAb candidates is observed in a low percentage of patients only, an adjusted (proper) isotype selection may be crucial to improve treatment efficacy. Accordingly, in **Chapter 4** we explored and compared the efficacy of IgG2a, IgG1 and IgE against a surface tumor antigen (Thy1.1) in the B16-OVA-Thy1.1 model.

Currently, the majority of mAbs approved on the market for tumor therapy belong to the IgG isotype. IgG1 has been traditionally used as the most active human isotype, i.e. showing the highest activating-to-inhibitory (A/I) ratio, to achieve higher anti-tumor activity^{36,37}. The mouse analogue of human IgG1 is mIgG2a³⁸.

It was previously reported that a better preclinical outcome was achieved by targeting a tumor associated antigen (TAA) with a mAb with mIgG2a than with mIgG1 isotype³⁹. However, this was studied in a B16 lung metastasis model and the treatment was administered prophylactically, followed by several mAb injections after tumor inoculation. In Chapter 4, the different mAbs were tested in a therapeutic set up, and administered at day 7, 13, 17 and 24 after tumor cell injection. Our results demonstrate that only mIgG2a is able to successfully prevent tumor growth. The lack of an active Fc-portion due to introduction of the LALA-PG mutation in the mIgG2a Fc backbone confirmed that the anti-tumor effect observed was Fc-mediated. The results further suggest that an IgE antibody, with the same Fab as the mIgG2a antibody, is not effective to prevent tumor growth in this set-up and unable to mediate IgE mast cell degranulation and histamine release⁴⁰. This finding would correlate with the lack of mast cells previously described in the tumor microenvironment²⁵. Furthermore, similar results were observed in tumor rejection when the tested antibody isotypes were combined with OT-1 adoptive cell transfer (ACT). Thus, none of the IgG2a, IgG1 or IgE treatments synergized with OT-1 ACT treatment.

Despite the better outcomes and increased survival with the introduction of mAbs to treat several types of cancer, a significant portion of patients does not respond to tumor-targeting antibody strategies. The work presented in

Chapter 4 underlines the importance of the right isotype selection, in this case a IgG2a for a cancer therapeutic setting. This work emphasizes the need for further optimisation of antibody-based strategies, in which isotype selection is relevant to improve the MOA of the therapeutic applications.

Generation of novel anti-TNFR2 antibodies aiming to target Tregs

As previously introduced in Chapter 2, there is a lack of compounds successfully targeting Tregs. This cell population plays a pivotal role maintaining an immune balance between self-tolerance and effector responses⁴². However, a distinctive Treg cell surface marker has not been identified thus far. Clinically successful BsAbs currently available on the market highlight BsAbs as a promising approach and opportunity to target Tregs, with special interest in TME. To date, there are three compounds at late preclinical phase or at phase 1 in clinical trials: ATOR-1015⁴³, ATOR-1144⁴⁴ and KY1055⁴⁵.

In parallel, in recent years, an interest in the detected TNFR2 expression on the Treg surface has increased and TNFR2 is aimed to be targeted. Some compounds against mTNFR2 have been characterized and applied in pre-clinical studies. Unfortunately, antibody sequences of the available compounds against mTNFR2 are not accessible, such as, M861 anti-mTNFR2-blocking antibody⁴⁶ or TY101 anti-mTNFR2 antagonistic antibody⁴⁷.

To this end, and due to the lack of available accessible open data of anti-TNFR2 reagents, we designed, generated and developed a strategy for the induction of novel anti-mTNFR2 antibodies. In **Chapter 5**, we present data obtained through the characterization of thirteen novel anti-mTNFR2. Among all candidates, only one candidate, 14A, presents cross-reactivity to human TNFR2. However, this candidate presents a reduced potency and efficacy of mTNFR2 binding. Among the different candidates identified a wide range of efficacy binding mTNFR2 is covered. Furthermore, TNF α blocking and non-blocking activity was achieved. TNFR2 binding not only is observable with *in vivo* assays but also with *ex vivo* material as Tregs or CD8⁺ T-cells, with all candidates showing capacity to bind.

The panel of antibodies presented in this study represents a useful tool to explore TNFR2 biology with potential different applications such as cancer or an autoimmune disease. For example, an increased number of Tregs correlates with a reduced number of autoreactive T cells in a model of experimental autoimmune disease⁴⁸. To this end, a TNFR2 costimulatory candidate aiming to stimulate Tregs would be a suitable treatment, and candidates 5A, 15A and 18A would become possible strategies since they demonstrated costimulatory activity on CD8⁺ T-cells *in vitro*. On the other side, blocking or depleting TNFR2⁺ Tregs in tumor microenvironment would be a promising treatment. Therefore, candidates 8A, 12A, 16A, 25A, and 29A which presented TNF α blocking activity could be tested.

Confirming the rising interest in TNFR2, in parallel to this work and once the mAb discovery campaign was already ongoing, the variable heavy and light chains sequence of five different mAbs was published as supplementary data in one study⁴⁹. Obtained sequences of the novel thirteen antibodies maintain approximately 50% identity compared to the published available sequences.

In order to assess the potential therapeutic window of the novel generated antibodies, two of these novel anti-mTNFR2 candidates were selected to examine further its application in more translationally relevant experiments. Thus, in **Chapter 6**, candidate 25A and 30A were studied in different *in vitro*, *ex vivo* and *in vivo* conditions.

The main objective was to evaluate and compare the effects of targeting mouse TNFR2 with either a blocking (candidate 25) or a non-blocking mAb (candidate 30). Additionally, by using either active or silent Fc, the significance of the downstream effector function of the Fc region of the tested mAbs was assessed. Consequently, studying whether biological effects could be obtained by binding to TNFR2 alone (Fab-mediated) or whether additional Fc-mediated apoptosis of target cells was required. To this end, mIgG2a isotype was selected and L234A/L235A/P329G mutations were introduced to mIgG2a backbone using it as a silent Fc³⁹.

As expected, rat isotype switch to mouse isotype either active or silent didn't alter the ligand binding and the TNF α blocking activity since both are mediated via Fab region. Complement dependent cytotoxicity was assessed and observed with both active anti-mTNFR2 candidates, either targeting CHO-K1.mTNFR2 or expanded Tregs, but not against *ex vivo* expanded T effector CD4⁺ cells.

In contrast, the *in vivo* set up revealed that naïve CD4⁺ cells proliferation could not be assessed since both anti-mTNFR2 antibodies targeted Treg as well as T effector CD4⁺ cells.

Blocking TNFR2 has become a highly effective strategy for treating cancer because it is overexpressed in some tumor cells and plays a crucial role in immunosuppressive cells, particularly on Tregs. However, there is evidence revealing that therapies activating TNFR2 can also be effective inhibiting tumor growth.

The rising interest in targeting TNFR2 is reflected by the emergence of several new immunotherapeutic approaches. However, most of the novel constructs are still in early phases of development and related data is still not published, exclusively found in conferences' abstracts or company media release.

Currently, two anti-TNFR2 antibodies with antagonistic activity have reached phase 1 in clinical trials: BI-1808^{51,52} and LBL-019⁵³. In addition, several antagonistic candidates are in preclinical development such as B1TR2101⁵⁴, APX601^{52,53}, AN3025⁵⁷, SIM0235⁵⁸ and NBL-020⁵⁹. The most common reported mechanisms are either intra-tumor TNFR2⁺ immunosuppressive cell depletion, particularly Tregs, CD8⁺ T-cell expansion and TNFR2⁺ tumor cell killing. In parallel, TNFR2 agonistic antibodies have also reached preclinical phase studies, including BI-1910⁶⁰, HFB200301⁵⁸ and MM-401^{62,63}. In this instance, the most indicated mechanisms are activation and expansion of CD4⁺ and CD8⁺ T cells and enhanced pro-inflammatory cytokine production. Thus, both strategies could reduce tumor loads.

In terms of either inhibiting or activating TNFR2 in the tumor, it is still unknown how these two contradictory compounds get the same antitumor

outcome. Tumor inhibition by Treg elimination and CD8⁺ T cells activation both have resulted in tumor inhibition in pre-clinical studies^{49,64,65}. Since TNFR2 is widely described for its role in promoting cell survival and proliferation, TNFR2⁺ tumor cells are expected to benefit from this property⁶⁶. However, different cell types in the TME can express relatively high levels of TNFR2, while certain cancers express TNFR2 at much lower levels than healthy tissues⁶⁷. Each component of the TME is a unique, interconnected, and complex system; as a result, they can all influence one another and respond differently to various TNFR2 treatments. Thus, TNFR2 expression on tumors should be considered in the design of TNFR2-targeting approaches.

The characterization of novel anti-mTNFR2 antibodies described in Chapter 5 and further exploration of two candidates in Chapter 6 have established these candidates as attractive tools to study the effects of anti-TNFR2 strategies in various scenarios, such as cancer and autoimmune disease, at a preclinical stage. Thus, these reagents would allow one to assess whether for a specific condition, TNFR2 blocking or non-blocking mAbs would be more appropriate, with further consideration of whether Fc-mediated effector functions or a silent Fc would be more suitable.

To conclude, despite the great advances in antibody-based immunotherapies, optimization for selection of BsAbs targets, isotype and antibody platform designs are crucial, as pointed out in this thesis. Our studies are relevant to understand how antibody design and selection modulate treatment outcome and generated data may be useful to develop and test new strategies for future immunotherapies.

References

1. Zahavi D, Weiner L. Monoclonal Antibodies in Cancer Therapy. *Antibodies*. 2020;9(3):34. doi:10.3390/antib9030034
2. Maloney DG, Smith B, Rose A. Rituximab: Mechanism of action and resistance. *Semin Oncol*. 2002;29(1, Supplement 2):2-9. doi:10.1053/sonc.2002.30156
3. Bar-Or A, Grove RA, Austin DJ, et al. Subcutaneous ofatumumab in patients with relapsing-remitting multiple sclerosis: The MIRROR study. *Neurology*. 2018;90(20):e1805-e1814. doi:10.1212/WNL.0000000000005516
4. Snyder A, Makarov V, Merghoub T, et al. Genetic basis for clinical response to CTLA-4 blockade in melanoma. *N Engl J Med*. 2014;371(23):2189-2199. doi:10.1056/NEJMoa1406498
5. Rizvi NA, Hellmann MD, Snyder A, et al. Mutational landscape determines sensitivity to PD-1 blockade in non-small cell lung cancer. *Science*. 2015;348(6230):124-128. doi:10.1126/science.aaa1348
6. Ledford H. Melanoma drug wins US approval. *Nature*. 2011;471(7340):561. doi:10.1038/471561a
7. Wei SC, Duffy CR, Allison JP. Fundamental Mechanisms of Immune Checkpoint Blockade Therapy. *Cancer Discov*. 2018;8(9):1069-1086. doi:10.1158/2159-8290.CD-18-0367
8. Weinberg AD, Rivera MM, Prell R, et al. Engagement of the OX-40 Receptor In Vivo Enhances Antitumor Immunity. *J Immunol*. 2000;164(4):2160-2169. doi:10.4049/jimmunol.164.4.2160
9. Thomas LJ, He LZ, Marsh H, Keler T. Targeting human CD27 with an agonist antibody stimulates T-cell activation and antitumor immunity. *Oncoimmunology*. 2014;3(1):e27255. doi:10.4161/onci.27255
10. Chester C, Sanmamed MF, Wang J, Melero I. Immunotherapy targeting 4-1BB: mechanistic rationale, clinical results, and future strategies. *Blood*. 2018;131(1):49-57. doi:10.1182/blood-2017-06-741041
11. Lim M, Ye X, Piotrowski AF, et al. Updated phase I trial of anti-LAG-3 or anti-CD137 alone and in combination with anti-PD-1 in patients with recurrent GBM. *J Clin Oncol*. 2019;37(15_suppl):2017-2017. doi:10.1200/JCO.2019.37.15_suppl.2017
12. Papadopoulos KP, Lakhani NJ, Johnson ML, et al. First-in-human study of REGN3767 (R3767), a human LAG-3 monoclonal antibody (mAb), ± cemiplimab in patients (pts) with advanced malignancies. *J Clin Oncol*. 2019;37(15_suppl):2508-2508. doi:10.1200/JCO.2019.37.15_suppl.2508
13. Hong DS, Schoffski P, Calvo A, et al. Phase I/II study of LAG525 ± spartalizumab (PDR001) in patients (pts) with advanced malignancies. *J Clin Oncol*. 2018;36(15_suppl):3012-3012. doi:10.1200/JCO.2018.36.15_suppl.3012
14. Vitale LA, Thomas LJ, He LZ, et al. Development of CDX-1140, an agonist CD40 antibody for cancer immunotherapy. *Cancer Immunol Immunother*. 2019;68(2):233-245. doi:10.1007/s00262-018-2267-0
15. D H, Y X, X Z, et al. A novel human anti-TIGIT monoclonal antibody with excellent function in eliciting NK cell-mediated antitumor immunity. *Biochem Biophys Res Commun*. 2021;534. doi:10.1016/j.bbrc.2020.12.013

16. Curigliano G, Gelderblom H, Mach N, et al. Phase I/Ib Clinical Trial of Sabatolimab, an Anti-TIM-3 Antibody, Alone and in Combination with Spaltalizumab, an Anti-PD-1 Antibody, in Advanced Solid Tumors. *Clin Cancer Res*. 2021;27(13):3620-3629. doi:10.1158/1078-0432.CCR-20-4746
17. Feng Y, Roy A, Masson E, Chen TT, Humphrey R, Weber JS. Exposure-response relationships of the efficacy and safety of ipilimumab in patients with advanced melanoma. *Clin Cancer Res Off J Am Assoc Cancer Res*. 2013;19(14):3977-3986. doi:10.1158/1078-0432.CCR-12-3243
18. Bonaventura P, Shekarian T, Alcazer V, et al. Cold Tumors: A Therapeutic Challenge for Immunotherapy. *Front Immunol*. 2019;10:168. doi:10.3389/fimmu.2019.00168
19. Postow MA, Sidlow R, Hellmann MD. Immune-Related Adverse Events Associated with Immune Checkpoint Blockade. *N Engl J Med*. Published online January 10, 2018. doi:10.1056/NEJMra1703481
20. Dhimolea E, Reichert JM. World Bispecific Antibody Summit, September 27–28, 2011, Boston, MA. *mAbs*. 2012;4(1):4-13. doi:10.4161/mabs.4.1.18821
21. Kitazawa T, Esaki K, Tachibana T, et al. Factor VIIIa-mimetic cofactor activity of a bispecific antibody to factors IX/IXa and X/Xa, emicizumab, depends on its ability to bridge the antigens. *Thromb Haemost*. 2017;117(07):1348-1357. doi:10.1160/TH17-01-0030
22. Goebeler ME, Bargou R. Blinatumomab: a CD19/CD3 bispecific T cell engager (BiTE) with unique anti-tumor efficacy. *Leuk Lymphoma*. 2016;57(5):1021-1032. doi:10.3109/10428194.2016.1161185
23. Löffler A, Kufer P, Lutterbüse R, et al. A recombinant bispecific single-chain antibody, CD19 × CD3, induces rapid and high lymphoma-directed cytotoxicity by unstimulated T lymphocytes. *Blood*. 2000;95(6):2098-2103. doi:10.1182/blood.V95.6.2098
24. Vijayaraghavan S, Lipfert L, Chevalier K, et al. Amivantamab (JNJ-61186372), an Fc Enhanced EGFR/cMet Bispecific Antibody, Induces Receptor Downmodulation and Antitumor Activity by Monocyte/Macrophage Trophocytosis. *Mol Cancer Ther*. 2020;19(10):2044-2056. doi:10.1158/1535-7163.MCT-20-0071
25. Huang S, van Duijnhoven SMJ, Sijts AJAM, van Elsas A. Bispecific antibodies targeting dual tumor-associated antigens in cancer therapy. *J Cancer Res Clin Oncol*. 2020;146(12):3111-3122. doi:10.1007/s00432-020-03404-6
26. Kantarjian H, Stein A, Gökbuget N, et al. Blinatumomab versus Chemotherapy for Advanced Acute Lymphoblastic Leukemia. *N Engl J Med*. 2017;376(9):836-847. doi:10.1056/NEJMoa1609783
27. Yuraszek T, Kasichayanula S, Benjamin JE. Translation and Clinical Development of Bispecific T-cell Engaging Antibodies for Cancer Treatment. *Clin Pharmacol Ther*. 2017;101(5):634-645. doi:10.1002/cpt.651
28. Mankarious S, Lee M, Fischer S, et al. The half-lives of IgG subclasses and specific antibodies in patients with primary immunodeficiency who are receiving intravenously administered immunoglobulin. *J Lab Clin Med*. 1988;112(5):634-640.
29. Huang S, Segué A, Hulsik DL, et al. A novel efficient bispecific antibody format, combining a conventional antigen-binding fragment with a single domain antibody, avoids potential heavy-light chain mis-pairing. *J Immunol Methods*. 2020;483:112811. doi:10.1016/j.jim.2020.112811

30. Malik H, Buelow B, Rangaswamy U, et al. TNB-486, a Novel Fully Human Bispecific CD19 x CD3 Antibody That Kills CD19-Positive Tumor Cells with Minimal Cytokine Secretion. *Blood*. 2019;134:4070. doi:10.1182/blood-2019-123226
31. Izhak L, Cullen DE, Elgawly M, et al. Abstract 3636: Potent antitumor activity of duvortuxizumab, a CD19 x CD3 DART® molecule, in lymphoma models. *Cancer Res*. 2017;77(13_Supplement):3636. doi:10.1158/1538-7445.AM2017-3636
32. Hummel HD, Kufer P, Grüllich C, et al. Phase I study of pasotuxizumab (AMG 212/BAY 2010112), a PSMA-targeting BiTE (Bispecific T-cell Engager) immune therapy for metastatic castration-resistant prostate cancer (mCRPC). *J Clin Oncol*. 2020;38(6_suppl):124-124. doi:10.1200/JCO.2020.38.6_suppl.124
33. Tran B, Horvath L, Dorff T, et al. 609O Results from a phase I study of AMG 160, a half-life extended (HLE), PSMA-targeted, bispecific T-cell engager (BiTE®) immune therapy for metastatic castration-resistant prostate cancer (mCRPC). *Ann Oncol*. 2020;31:S507. doi:10.1016/j.annonc.2020.08.869
34. Liu L, Lam CYK, Long V, et al. MGD011, A CD19 x CD3 Dual-Affinity Retargeting Bispecific Molecule Incorporating Extended Circulating Half-life for the Treatment of B-Cell Malignancies. *Clin Cancer Res*. 2017;23(6):1506-1518. doi:10.1158/1078-0432.CCR-16-0666
35. Reusch U, Duell J, Ellwanger K, et al. A tetravalent bispecific TandAb (CD19/CD3), AFM11, efficiently recruits T cells for the potent lysis of CD19+ tumor cells. *mAbs*. 2015;7(3):584-604. doi:10.1080/19420862.2015.1029216
36. Nordstrom JL, Gorlatov S, Zhang W, et al. Anti-tumor activity and toxicokinetics analysis of MGAH22, an anti-HER2 monoclonal antibody with enhanced Fc receptor binding properties. *Breast Cancer Res BCR*. 2011;13(6):R123. doi:10.1186/bcr3069
37. Jefferis R. Antibody therapeutics: *Expert Opin Biol Ther*. 2007;7(9):1401-1413. doi:10.1517/14712598.7.9.1401
38. Nimmerjahn F, Ravetch JV. Divergent Immunoglobulin G Subclass Activity Through Selective Fc Receptor Binding. *Science*. 2005;310(5753):1510-1512. doi:10.1126/science.1118948
39. Nimmerjahn F. Divergent Immunoglobulin G Subclass Activity Through Selective Fc Receptor Binding. *Science*. 2005;310(5753):1510-1512. doi:10.1126/science.1118948
40. De Vries VC, Wasiuk A, Bennett KA, et al. Mast Cell Degranulation Breaks Peripheral Tolerance. *Am J Transplant*. 2009;9(10):2270-2280. doi:10.1111/j.1600-6143.2009.02755.x
41. Carlini MJ, Dalurzo MCL, Lastiri JM, et al. Mast cell phenotypes and microvessels in non-small cell lung cancer and its prognostic significance. *Hum Pathol*. 2010;41(5):697-705. doi:10.1016/j.humpath.2009.04.029
42. Sakaguchi S, Miyara M, Costantino CM, Hafler DA. FOXP3+ regulatory T cells in the human immune system. *Nat Rev Immunol*. 2010;10(7):490-500. doi:10.1038/nri2785
43. Kvarnhammar AM, Veitonmäki N, Hägerbrand K, et al. The CTLA-4 x OX40 bispecific antibody ATOR-1015 induces anti-tumor effects through tumor-directed immune activation. *J Immunother Cancer*. 2019;7(1):103. doi:10.1186/s40425-019-0570-8

44. Fritzell S, Levin M, Dahlman A, et al. ATOR-1144 is a tumor-directed CTLA-4 x GITR bispecific antibody that acts by depleting Tregs and activating effector T cells and NK cells. :1.
45. Sainson RC, Parveen N, Borhis G, et al. Abstract LB-153: KY1055, a novel ICOS-PD-L1 bispecific antibody, efficiently enhances T cell activation and delivers a potent anti-tumour response in vivo. *Cancer Res.* 2018;78(13 Supplement):LB-LB-153. doi:10.1158/1538-7445.AM2018-LB-153
46. Nie Y, He J, Shirota H, et al. Blockade of TNFR2 signaling enhances the immunotherapeutic effect of CpG ODN in a mouse model of colon cancer. *Sci Signal.* 2018;11(511):eaan0790. doi:10.1126/scisignal.aan0790
47. Case K, Tran L, Yang M, Zheng H, Kuhlreiber WM, Faustman DL. TNFR2 blockade alone or in combination with PD-1 blockade shows therapeutic efficacy in murine cancer models. *J Leukoc Biol.* 2020;107(6):981-991. doi:10.1002/JLB.5MA0420-375RRRRR
48. Ronin E, Pouchy C, Khosravi M, et al. Tissue-restricted control of established central nervous system autoimmunity by TNF receptor 2–expressing Treg cells. *Proc Natl Acad Sci.* 2021;118(13):e2014043118. doi:10.1073/pnas.2014043118
49. Tam EM, Fulton RB, Sampson JF, et al. Antibody-mediated targeting of TNFR2 activates CD8⁺ T cells in mice and promotes antitumor immunity. *Sci Transl Med.* 2019;11(512):eaax0720. doi:10.1126/scitranslmed.aax0720
50. Schlothauer T, Herter S, Koller CF, et al. Novel human IgG1 and IgG4 Fc-engineered antibodies with completely abolished immune effector functions. *Protein Eng Des Sel PEDS.* 2016;29(10):457-466. doi:10.1093/protein/gzw040
51. Biolnvent International AB. *Phase 1/2a Open-Label, Dose-Escalation, Multicenter, FIH, Consecutive-Cohort, Clinical Trial of BI-1808, a Monoclonal Antibody to TNFR 2 as a Single Agent and in Combination With Pembrolizumab (MK-3475) in Subjects With Advanced Malignancies (Keynote-D20).* clinicaltrials.gov; 2022. Accessed December 18, 2022. <https://clinicaltrials.gov/ct2/show/NCT04752826>
52. Mårtensson L, Kovacek M, Holmkvist P, et al. 725 Pre-clinical development of TNFR2 ligand-blocking BI-1808 for cancer immunotherapy. In: *Regular and Young Investigator Award Abstracts.* BMJ Publishing Group Ltd; 2020:A434.1-A434. doi:10.1136/jitc-2020-SITC2020.0725
53. Project and pipeline - R & D line - Nanjing Leads Biolabs Co.,Ltd. Accessed December 19, 2022. <https://en.leadsbiolabs.com/R-D-pipeline.html>
54. An agreement to advance BITR2101. Drug Discovery News. Accessed December 19, 2022. <https://www.drugdiscoverynews.com/an-agreement-to-advance-bitr2101-15058>
55. Filbert E, Krishnan S, Alvarado R, Huang G, Bahjat F, Yang X. 693 APX601, a Novel TNFR2 antagonist antibody for cancer immunotherapy. *J Immunother Cancer.* 2020;8(Suppl 3):A417-A417. doi:10.1136/jitc-2020-SITC2020.0693
56. Krishnan S, Alvarado R, Huang G, Yang X, Filbert EL. Abstract LB175: APX601, a Potent TNFR2 Antagonist as a Novel and Promising Approach to Reverse Tumor Immune Suppression. *Cancer Res.* 2021;81(13_Supplement):LB175. doi:10.1158/1538-7445.AM2021-LB175

57. Chen Y, Jia M, Xu S, et al. Abstract 1451: AN3025: A novel anti-human TNFR2 antibody that exhibits immune activation and strong anti-tumor activity in vivo. *Cancer Res.* 2021;81(13_Supplement):1451. doi:10.1158/1538-7445.AM2021-1451
58. Simcere. Accessed December 19, 2022. <https://en.simcere.com/news/detail.aspx?mtt=170>
59. Sum CS, Danton M, hu Q, et al. Abstract 1869: Novel TNFR2 antibodies to overcome T cell exhaustion and suppressive tumor microenvironment. *Cancer Res.* 2021;81(13_Supplement):1869. doi:10.1158/1538-7445.AM2021-1869
60. Mårtensson L, Cleary K, Semmrich M, et al. Targeting TNFR2 for Cancer Immunotherapy - Ligand blocking depletors versus receptor agonists.
61. Wei S, Fulton R, Lu YY, et al. Abstract 1883: Mechanism of action and biomarker strategy for HFB200301, an anti-TNFR2 agonist antibody for the treatment of cancer. *Cancer Res.* 2021;81(13_Supplement):1883. doi:10.1158/1538-7445.AM2021-1883
62. Richards J, Wong C, Koshkaryev A, et al. MM-401, a novel anti-TNFR2 antibody that induces T cell co-stimulation, robust anti-tumor activity and immune memory.
63. Sampson J, Kurella V, Paragas V, et al. *Abstract 555: A Novel Human TNFR2 Antibody (MM-401) Modulates T Cell Responses in Anti-Cancer Immunity.*; 2019:555. doi:10.1158/1538-7445.SABCS18-555
64. Torrey H, Khodadoust M, Tran L, et al. Targeted killing of TNFR2-expressing tumor cells and Tregs by TNFR2 antagonistic antibodies in advanced Sézary syndrome. *Leukemia.* 2019;33(5):1206-1218. doi:10.1038/s41375-018-0292-9
65. Torrey H, Butterworth J, Mera T, et al. Targeting TNFR2 with antagonistic antibodies inhibits proliferation of ovarian cancer cells and tumor-associated T_{regs}. *Sci Signal.* 2017;10(462):eaaf8608. doi:10.1126/scisignal.aaf8608
66. Naudé PJW, den Boer JA, Luiten PGM, Eisel ULM. Tumor necrosis factor receptor cross-talk. *FEBS J.* 2011;278(6):888-898. doi:10.1111/j.1742-4658.2011.08017.x
67. Tang Z, Li C, Kang B, Gao G, Li C, Zhang Z. GEPIA: a web server for cancer and normal gene expression profiling and interactive analyses. *Nucleic Acids Res.* 2017;45(W1):W98-W102. doi:10.1093/nar/gkx247



8

Summary in English

Summary

In context of an increasing interest in immunotherapeutic treatments, the work described in this thesis expands the current knowledge of several potential antibody-based therapeutic approaches. A new development is the use of bispecific antibodies (BsAb). To introduce BsAb, **chapter 2** describes the different platforms currently used to generate IgG-like and non-IgG-like BsAbs, as well as the strategies to gain clinical approval for the different BsAbs. A highly selective binding, as can be achieved with BsAbs, could be beneficial to 'target' certain cell populations, such as Tregs, against which current treatments appear to be insufficiently specific. Focusing on BsAb-based therapeutic approaches, in **chapter 3** we investigate a novel strategy to optimize a T-cell redirecting bispecific antibody. Two Fab x sdAb-Fc, directed against CD3 and EGFR, with different lengths of the hinge region, were compared. The results show that a shorter hinge design improves BsAb-induced anti-tumor activity, induces more effector cell/target cell clustering and activates T cells more efficiently. In addition, we show (**chapter 4**) how important it is to select the right isotype antibody. In a mouse tumor model, only IgG2a antibodies were found to exert anti-tumor function, achieving a survival rate of approximately 50%. None of the isotypes tested showed a synergistic effect with adoptive T-cell therapy. An increasing interest in the costimulatory receptor TNFR2 in cancer has prompted us to design, generate and produce novel anti-mTNFR2 antibodies (**chapter 5**). The characterization and different features of these antibodies are described in this chapter, and they could be used as tools in follow-up studies to further investigate i) the role of TNFR2 in cancer, and ii) how TNFR2 targeting with different antibody candidates that either block or activate this receptor could improve immunotherapy. In **chapter 6**, two anti-mTNFR2 antibodies were selected for assessment of their application *in vitro*, *ex vivo* and *in vivo*, which revealed their capacity to bind to Tregs but also to CD4⁺ effector T cells.

Taken together, the results presented in this thesis highlight the progress achieved in immunotherapy approaches, with focus on BsAbs and novel strategies to improve cancer treatments. Furthermore, novel anti-mTNFR2

antibodies were developed and featured as useful tools to unravel the role of this receptor in tumor growth.

Nederlandse Samenvatting

Samenvatting

In context van een toenemende belangstelling voor immunotherapeutische behandelingen, vergroot het werk beschreven in dit proefschrift de huidige kennis van verschillende potentiële, op antilichamen- gebaseerde, therapeutische benaderingen. Een nieuwe ontwikkeling is de inzetbaarheid van bispecifieke antilichamen (BsAb). Om BsAb te introduceren beschrijft **hoofdstuk 2** de verschillende platforms die momenteel worden gebruikt om 'IgG-like' en 'non-IgG-like' BsAbs te genereren, alsmede de strategieën ter verkrijging van klinische goedkeuring voor de verschillende BsAbs. Een zeer selectieve binding zoals met BsAbs bereikt kan worden, zou gunstig kunnen zijn om bepaalde celpopulaties te 'targeten', zoals Tregs, waartegen huidige behandelingen onvoldoende specifiek blijken. Focuserend op BsAb-gebaseerde therapeutische benaderingen, onderzoeken we in **hoofdstuk 3** een nieuwe strategie om een T-cel 'redirecting' bispecifiek antilichaam te optimaliseren. Twee Fab x sdAb-Fc, gericht tegen CD3 en EGFR met verschillende lengte van de 'hinge region', werden vergeleken. De resultaten tonen aan dat een kortere 'hinge' de BsAb-geïnduceerde tumordodende activiteit verbetert, meer effectorcel/doelcel clustering induceert en T-cellen efficiënter activeert. Daarnaast laten we zien (**hoofdstuk 4**) hoe belangrijk het is om het juiste isotype antilichaam te selecteren. In een muizentumormodel bleek alleen IgG2a antitumoractiviteit uit te oefenen, waarmee een overlevingspercentage van ongeveer 50% bereikt. Geen van de geteste isotypes vertoonde een synergetisch effect met adoptieve T-cel-therapie. Een toenemende interesse in de co-stimulerende receptor TNFR2 in kanker heeft ons ertoe aangezet om nieuwe anti-mTNFR2-antilichamen te ontwerpen, genereren en produceren (**hoofdstuk 5**). De karakterisering en de verschillende kenmerken van deze antilichamen zijn beschreven in dit hoofdstuk, en zouden in vervolgstudies kunnen helpen om i) de rol van TNFR2 bij kanker verder te onderzoeken, en ii) hoe TNFR2 'targeting' met verschillende antilichaamkandidaten die deze receptor blokkeren of juist activeren de immunotherapie zouden kunnen verbeteren. In **hoofdstuk 6** hebben we twee anti-mTNFR2-antilichamen geselecteerd en hun toepassing in vitro, ex vivo en in vivo, bepaald. Hierbij bleek dat zij zowel aan Tregs als ook aan CD4+ effector T-cellen.

Concluderend beschrijft dit proefschrift de recente vooruitgang op het gebied van immunotherapie, met focus op BsAbs en strategieën om huidige behandelingen hiermee te verbeteren. Daarnaast hebben wij nieuwe anti-mTNFR2-antilichamen ontwikkeld die ingezet kunnen worden om de rol van deze receptor in tumorontwikkeling te onderzoeken.

Appendix

Acknowledgements

Curriculum Vitae

List of publications

Acknowledgements

Along my PhD odyssey, I had the great opportunity to meet amazing people who have made me grow professionally and personally, and also be accompanied by lifelong people who helped me become the person and arrive where I am right now. I am forever grateful to:

My supervisor **Andrea van Elsas** for all your initial guidance in the first stage of my project. To adopt us in Aduro Biotech Europe, showing us how to work in a different environment from academia, to give us the chance to learn how important and great is making science next to an amazing, organized, united and well-built team. For all your brilliant knowledge, not only in cancer immunotherapy and antibody production, but also on how to circumvent all the challenges, going step by step. I am very grateful to have had the chance to meet such an extraordinary and charming supervisor.

My supervisor **Dietmar Zaiss** to embrace my project during an uncertain period of my PhD and to guide me through the second stage of my project at Edinburgh University. To all your encouraging feedback and knowledge. Thanks to organise the journal club and the chance to learn from other immunology topics differing from our projects; sometimes I am still surprised how you can remember a specific figure and experiment from a paper published 20 years ago. It has been very satisfying to work with you and grow as a scientific researcher.

My promoters, **Alice Sijts** and **Femke Broere** for all your support and encouragement during my PhD. I am very grateful to have met such a patient people always willing to help, giving their wise advice. Thanks to share and encourage your passion and your positive attitude.

My initial co-supervisor, **Sander**. God bless your patience. Thanks for your daily supervision and support, for all your guidance and all your knowledge. We had a saying: Have a Sander in your life! And honestly, I am still wondering how I would have survived the first stage of my project without you and your help. I know with my sentimental temperament I was also a challenge to yourself, but I hope I was also a good practice for your leadership. Thanks for all the science but also for all the management within the situation, thank you to be so kind.

To the rest of **Aduro team**, especially: **Paul Vink** for his immunology classes and push our scientific thoughts go further (I hope you learnt my name), **Lilian** helping me with the antibody discovery campaign and always being so kind to help and give advice, **Mark Parade** for all his technical advices and his patience, always smiling, **Thomas** for his help with the quality control, **Maurice, Erik** and **Peter** providing a cheerful atmosphere, **Tu-Anh**, for all her advice and nice chats and being careful about our uncertain future, **Joost** for your sympathy, thanks to help us at the very beginning and at the last minute with the house, **Mary** for helping us furnish our house and sharing your knowledge with the multicolor flow cytometry panel experiment, **Daniëlle** for all the bureaucratic work and support, **Marc Snippert, Jos, Ingeborg, Inge, Maarten, Teun** and everybody else for excellent work atmosphere and always making me feel like a member of the team.

The **European Commission** for funding all the project and the support received from all the Tumor Treg Targeting ITN network: **Nacho** for his exceptional mind and his advice to apply for this position, **Kepa** for his guidance specially during my stay in his lab, **Belén** and **Itziar** for her administrative and organization support, and the rest of students – **Natasa, Shuyu, Claudia** and **Susy**.

***Natasa**, GRACIAS y siempre me quedaré corta. Empezar agradeciendo la primera noche en Oss, compartiendo habitación con una extraña llena de dudas. Y desde ese momento gracias por todo lo que ha venido, que no ha sido poco. Gracias por aguantarme simplemente, sé que no es fácil. Por todos estos momentos de frustración compartidos, pero por todas esas aventuras descubriendo Oss y sus alrededores, las salidas en bicicleta sin acabar al suelo, todas las excursiones en tren, los momentos cocinillas empezando con una simple kettle de un hotel y que se convirtieron en tradición en Edimburgo, por las borracheras – nunca olvidaremos ese King’s Day en Utrecht, por todos los viajes que hemos hecho y los que quedan, por cebarme en mi estancia a Belgrado, por el Raki – bendito descubrimiento, por todas las mudanzas y papeleo, por todos los planes improvisados, y una infinita lista, que se puede resumir en gracias por hacer las cosas tan fáciles. Gracias por ser como eres y acogerme en tu “mafia”. Si existiese más gente como tú, el mundo sería mejor. A cada despedida contigo, sí, me he emocionado, pero*

creo que también forma parte de la emoción para la siguiente aventura que nos depara el futuro. Has dejado huella para siempre.

Shuyu, oh Shuyusito. We are polar opposites, but it's been a great pleasure to share this sinking boat experience with you. All the struggle we have been through has made us stronger, we can introduce resilience in our CV. Thanks to be always so calm and patient, for all your scientific passion and lab efficiency, and productivity. Thanks for all your technical advice, you are definitely not the director of tea. Thanks for introducing me to your culture which was quite unknown to me, you have been a great teacher!, thanks for making my horizons become wider, making me try new dishes, and realizing how spicy some people can eat and how much someone can sleep on a road trip. I know a great future holds for you. We are looking forward to receiving an invitation to your official wedding party in Shanghai, hope by then you have learned how to swim if the event is held in a boat. If you learn it, a red envelope is ensured – it's a deal! Best luck, you deserve it.

***Claudia**, tú siempre contagiando tu alegría. Ha sido una suerte coincidir contigo y un placer cada encuentro. Por el apoyo científico y por esas inyecciones i.v. una tarde muy tarde de julio. Gracias por ofrecerme un hogar en Pamplona y acogerme en el Manneken Beer. Siempre nos vamos a reír de ese “buenos días” de San Fermín Txikito, de tu habilidad bajando las escaleras en Oss, la aventura en Ámsterdam con la cena más surrealista del mundo... Hemos compartido un periodo de incertidumbre juntas con el cierre de la empresa y por si no fuese poco, llegó el maldito virus, y real que lo que no te mata te hace más fuerte, esa cena antes del confinamiento entre llantos y comprando vuelos y empaquetando TODO es una de las situaciones más alucinante que hemos vivido y viviremos. Ahora bien, nos llevamos de recuerdo uno de los mejores carnavales en Den Bosch y todas las aventuras, ya sea en la Trappe, Mainz o Madrid. Porque da igual donde esté, si es contigo. ¡¡Kalimera, kalimera!!*

My co-supervisor at Edinburgh University, **Rose Zamoyska**, thanks to adopt us in your group, for being as approachable always open to discuss the project with critical thought and advice. To the rest of Zamoyska lab: **Nicola**, for her crucial help with the *in vivo* work and its processing, and for all her leisure suggestions, **Alex** for all their help and support, to be there when I needed to discuss about science and to share joys and sorrows having lunch,

Patricia *gracias por cuidar de mí, por los consejos y la paciencia, por ser tan atenta y darme cobijo, el mundo necesita más gente con tu carisma, David Wright* for his technical support. To them and everybody else for making me feel welcome in the **Zamoyska team** and selflessly sharing their knowledge and expertise with me.

Martin Waterfall for making me lose the fear to be alone in the flow cytometry room. For teaching me how to compensate, for all the multi panel discussions, to come earlier to start a long sorting, to all your FACS expertise and advice. It's been a pleasure to hear all your anecdotes.

To the Ash5 Animal Unit staff, especially **Richard, Laraine, David** and **Craig**, for training me and making sure the *in vivo* experiments run smoothly.

Jim for making the journal club more entertaining with his valuable insights. I know I will always learn something listening to you.

Elaine to be so kind and teaching me the correct procedure on how to irradiate mice.

Nila and **Neelakshi** and to share joys and sorrows in the lab or having lunch. You are such a great company. Also, **Domi**, and I definitely think you should have moved in earlier, since you came, I feel like home.

The rest of **Ashworth scientists** for sharing their equipment and reagents. You are one great community!

Doina and **Joan** for their technical help in Pamplona when it was impossible to me to be there in person.

A la meva família per creure en mi, pel seu suport incondicional i intentar entendre què he estat fent durant aquest temps. Per escurçar la distància, per ser una prioritat a la vostra agenda, per poder compartir vermut i sopars com si fos a casa, per tots els cafès que hem substituït mitjançant videotrucada, per fer dels dies més grisos, una mica més lluminosos, per fer-ho tot més fàcil. Als follets anaclets per ser-hi sempre, ensenyar-me que l'amistat és un regal que no tothom té i fer que no es noti el pas del temps, com un bon whisky, envellim bé! En especial als que m'han pogut visitar durant aquesta odissea, aquestes aventures són les que deixen més petjada. No discutir-nos en cap moment i omplir de riures els pocs metres quadrats

*d'una furgoneta ha estat un plaer. A l'**Aida**, per demostrar-me la definició d'amistat i la seva santa paciència a escoltar-me. Per aquestes persones pilar: les infinites videotrucades amb la **Mireia** i fer-me sempre lloc a la seva agenda ni que sigui per una abraçada de veritat; i a l'**Ot**, per aguantar els atacs de verborrea i mantenir-nos mútuament la fe. A la **Cèlia**, l'**Andrea** i la **Marina** per compartir penes i glòries, per fer extraordinària la rutina, per ser i estar, per fer inexistent la distància i el pas del temps. A tota aquella gent que he tingut la sort de conèixer durant aquesta odissea. A l'**Anna** i la **Maria**, per donar sentit a la vida vivint a Oss. A la **Núria**, per fer-ho tot senzill, pels bons monòlegs, riures, powerpoints, mapes i teràpies, com agraeixo aquestes connexions. A la **Marta**, per saber com congelar el temps i mantenir l'essència. A la **Carla**, per ser llar (amiga i mami), per entretenir-me (essencial a Edimburg), una amistat pura i porca que costa de trobar en aquesta etapa. **Laura** for all our shared disconnections and for being such a good listener. Vull agrair també sentir-se com a casa amb la **Colla Castellera d'Edinburgh** i totes aquelles personetes que ho han fet possible, poc m'esperava crear els vincles que s'han creat. A l'**Àlex**, per la seva energia 24/7 que dona menys sentit al nihilisme, emets vida. Al **Javi** por su facilidad en organizar y planificar las mejores desconexiones, gracias por ser profundo. A l'**Emma** per la companyia que m'ha donat a tants dinars. Al **Llorenç** per ser-hi, per la fàcil complicitat, per estar sempre al peu del canó (per burxar i portar la contrària, però també pel seu 6è sentit), a la **Laia** pel seu entusiasme i fer-ho tot més fàcil, he descobert una versió millorada amb capacitat organitzativa i motivació!, al **Xavi**, pels seus debats, la música i ser sempre tan catalanament correcte, tens un cor molt molt gran, i al **Max** per totes les seves bromes molt elementals i tots els riures que ens han acompanyat.*

Entre tots em sento molt afortunada, podria dir que he estat en una muntanya russa, que he tingut l'oportunitat de poder-me embarcar en aquesta aventura, la sort de trencar la rutina en diferents països (amb tots els maldecaps que comporta la burocràcia), però que acompanyada de les persones adequades, tot és més senzill. Un trosset de mi romandrà sempre a Noord-Brabant i la captivadora ciutat d'Edimburg i les seves terres. He après també que no és fàcil quadrar agendes, especialment vivint fora i apareixent caps de setmana esporàdics, però així he descobert que per sort, tinc persones al meu voltant que mourien cel i terra per fer-ho possible. Crec que he crescut professionalment, i de ben segur, he crescut personalment.

Curriculum Vitae

Aina Segués Cisteró was born on December 29th, 1995 in Sant Ramon (Lleida), Catalunya. She grew up and finished primary, middle, and high school in Guissona. From September 2013 to July 2017, she studied Biomedical Sciences at *Universitat de Lleida*. Each summer break during the degree she had short internships in different institutions and different departments: IDIBAPS - Gastroenterology department, Hospital Clínic - Anatomical Pathology, IRB Lleida - Experimental Neuro-muscular Pathology. At her last academic year, she received Erasmus Plus funding to do an internship at Karolinska Institute where she wrote her bachelor thesis about reactivating p53 gene under supervision of Prof. Galina Selivanova. In September of 2017, she started her master in Drug research, control and development in *Universitat de Barcelona*. She did an 8-month internship at Leitat Technological Centre establishing 3D-skin models with microorganisms under the supervision of Dra. Elisabet Fernández. After receiving her master's degree in 2018 she worked as a junior researcher following up her master's thesis. In March of 2019, she had the opportunity to join the "Tumor-Tregs-Targeting" Innovative Training Network with H2020 - Marie Skłodowska-Curie grant agreement. She started her PhD project "Antibody-based approaches to modulate immune response" under the promotion of Dr. Alice Sijts. Her project was developed between a company and academic institutes: she started her project in Aduro Biotech Europe under the supervision of Dr. Andrea van Elsas, she did a short internship at CIMA (*Universidad de Navarra*) under the supervision of Dr. Pedro Berraondo and Dr. Ignacio Melero and she completed her project at University of Edinburgh under the supervision of Dr. Dietmar Zaiss. The research results of this project are described in this thesis.

A

List of publications

- Huang, S., **Segués, A.**, Hulsik, D. L., Zaiss, D. M., Sijts, A., van Duijnhoven, S., & van Elsas, A. (2020). A novel efficient bispecific antibody format, combining a conventional antigen-binding fragment with a single domain antibody, avoids potential heavy-light chain mis-pairing. *Journal of immunological methods*, 483, 112811.
- **Segués, A.**, van Duijnhoven, S., Parade, M., Driessen, L., Vukovic, N., Zaiss, D., Sijts, A., Berraondo, P., & van Elsas, A. (2021). Generation and characterization of novel co-stimulatory anti-mouse TNFR2 antibodies. *Journal of immunological methods*, 499, 113173.
- Di Trani, C. A., Fernandez-Sendin, M., Cirella, A., **Segués, A.**, Olivera, I., Bolaños, E., Melero, I., & Berraondo, P. (2022). Advances in mRNA-based drug discovery in cancer immunotherapy. *Expert opinion on drug discovery*, 17(1), 41–53.
- **Segués, A.**, Huang, S., Sijts, A., Berraondo, P., & Zaiss, D. M. (2022). Opportunities and challenges of bi-specific antibodies. *International review of cell and molecular biology*, 369, 45–70.
- Huang S, **Segués A**, Waterfall M, Wright D, Vayssiere C, van Duijnhoven SMJ, van Elsas A, Sijts AJAM, Zaiss DM. Shortened Hinge Design of Fab x sdAb-Fc Bispecific Antibodies Enhances Redirected T-Cell Killing of Tumor Cells. *Biomolecules*. 2022; 12(10):1331.
- Vukovic N, **Segués A**, Huang S, Waterfall M, Sijts AJAM, Zaiss DM. Mouse IgG2a isotype therapeutic antibodies elicit superior tumor growth control compared to mIgG1 or mIgE. *Cancer Res Commun*. 2023 Jan 6;CRC-22-03 .